FIREURISK - DEVELOPING A HOLISTIC, RISK-WISE STRATEGY FOR EUROPEAN WILDFIRE MANAGEMENT

Grant Agreement Number: 101003890 **Call identifier:** H2020-LC-CLA-2018-2019-2020	
Topic:	LC-CLA-15-2020 Forest Fires risk reduction: towards an integrated fire management approach in the E.U.
Instrument:	RIA

D1.1 – Report on methodological frameworks for each Danger modelling process

Deliverable Identifier:	D1.1
Deliverable Due Date:	31/03/2023
Deliverable Submission Date:	07/07/2023
Deliverable Version:	v.1
Lead partner:	UDL
Authors:	Fermín Alcasena, Elena Aragoneses, Vadim Bogomolov, Marin Bugarić, David Caballero, Emilio Chuvieco, Àngel Cunill Camprubí, Mariano García, Pere Joan Gelabert, Adrián Jimenez-Ruano, Ana Miranda, Diogo Lopes, Viktor Myroniuk, Clara Ochoa Velez, Nadia Politi, Carlos Prado, Michele Salis, Victor Resco de Dios, Luis Mario Ribeiro, Marcos Rodrigues, Ángela Rivera, Thanasis Sfetsos, Darko Stipaničev, Luis Torres, Mandy Vlachogianni, Sergiy Zibtsev, Cristina Vega-Garcia.
Work Package:	WP1 – Fire risk assessment to improve prevention
Task:	Task 1.1 –Fire Danger Assessment
Dissemination Level:	☒ PU: Public ☐ CO: Confidential, only for members of the Consortium (including the Commission Services)

This project has received funding from the European Union's Horizon 2020 research and innovation programme under grant agreement No 101003890.

Revision History

Version	Date	Edited by	Description
v.0.1	3/03/2023	UDL	Document Content outline / structure
v.0.2	30/03/2023	UDL, CNR, NCSRD, FESB, REEFMC, MTO, ADAI, UAH	Draft version
v.0.3	31/03/2023	UDL, CNR, NCSRD, FESB, REEFMC, MTO, ADAI, UAH	Complete version formatted according to template
v.0.4	24/05/2023	UDL	Complete version with Annexes
v.0.5	28/05/2023	UDL	Complete draft review by WP1 Leader
v.0.6	22/06/2022	TUD, SU	Internal approval review by the QRB
v.0.7	07/07/2023	UDL, MTG, SIA	Internal review of the Complete version
v.1.0	07/07/2023	UDL	Final version submitted

Quality Control

Type	Date	Reviewed by	Approved/Comment
Internal	02-06-2023	Schmidt, Luisa (TUD)	Approved
Internal/QRB	22-06-2023	Stefan Doerr (SU)	Approved

Copyright © FirEUrisk Consortium. All rights reserved.

Executive Summary

Fire danger is defined as the likelihood that a fire ignites and propagates, following the terminology usually accepted in the fire management community. The assessment of fire danger requires the estimation and combination of many meteorological, fuel, topographic and socioeconomic variables in predictive/explanatory models. Such an assessment for current conditions is developed here with technical and methodological specifications, at different temporal and spatial scales linked to the European Territory and the Pilot Sites of the project.

Copyright © FirEUrisk Consortium. All rights reserved.

Disclaimer

The content of the publication herein is the sole responsibility of the publishers and it does not necessarily represent the views expressed by the European Commission or its services.

While the information contained in the documents is believed to be accurate, the authors(s) or any other participant in the FirEURisk consortium make no warranty of any kind with regard to this material including, but not limited to the implied warranties of merchantability and fitness for a particular purpose.

Neither the FirEurisk Consortium nor any of its members, their officers, employees or agents shall be responsible or liable in negligence or otherwise howsoever in respect of any inaccuracy or omission herein.

Without derogating from the generality of the foregoing neither the FirEurisk Consortium nor any of its members, their officers, employees or agents shall be liable for any direct or indirect or consequential loss or damage caused by or arising from any information advice or inaccuracy or omission herein.

Copyright message

© FirEURisk Consortium, 2021-2025. This deliverable contains original unpublished work except where clearly indicated otherwise. Acknowledgement of previously published material and of the work of others has been made through appropriate citation, quotation or both. Reproduction is authorised provided the source is acknowledged.

Table of Contents

1 Introduction 15
1.1 Purpose of the document 15
1.2 Structure of the Document 15
2 Fire weather and fuel status prevention 15
2.1 Weather variables 15
2.2 Fuel Moisture 17
2.2.1 Calculation of dead fuel moisture content: theoretical basis 17
2.2.1.1 Fine fraction (1HR) 18
2.2.1.2 Medium fraction (10HR) and thick fraction (100HR) 22
2.2.1.3 Downscaling procedures conducted for each variable. 23
2.2.2 Product Description: European Dead Fuel Moisture map (ET) 24
2.2.3 Product Description: Pilot site Dead Fuel Moisture map (PS) 24
2.3 Calculation of live fuel moisture content: Theoretical basis 24
2.3.1 Radiative Transfer Models 25
2.3.2 Model Variables and LFMC 26
2.3.3 Global Sensitivity Analysis of PROSPECT + SAIL 27
2.3.3.1 PROSPECT + SAIL 27
2.3.4 Global Sensitivity Analysis of PROSPECT + SAIL + GEO 32
2.3.4.1 Vegetation Modeling Strategy 37
2.3.5 Model Inversion Strategy 37
2.3.6 Optimal Inversion Parameters 39
2.3.7 Dataset 1: Lousa, Portugal (ADAI) 40
2.3.8 Dataset 2: Capo Caccia, Sardinia, Italy (CNR) 40
2.3.9 Extraction of the Optimal Inversion Parameters 42
2.3.9.1 Amount of Spectral Information 42
2.3.9.2 Cost Function 43
2.3.9.3 Number of Selected Solutions 43
2.3.9.4 Measures of Central Tendency 43
2.3.9.5 Final Inversion Parameters 44
2.3.10 Validation 44
2.3.10.1 Lousa Dataset 44
2.3.10.2 Capo Caccia Dataset 45
2.3.11 Product Description: Live fuel moisture content map (ET) 47
2.3.12 Product Description: Live fuel moisture content map (PS) 47

Copyright © FirEURisk Consortium. All rights reserved.

2.4 Fire weather danger rating indices 48
2.4.1 Rationale 48
2.4.2 Approach and Methods 49
2.4.2.1 Results 49
2.4.3 Fire Danger weather estimations at PS Greece 51
2.4.3.1 Fire Weather Assessment under climate change – Methodology of NCSRD 51
2.4.3.2 Description of the model 52
2.4.3.3 Calculation of fire weather indices 53
2.4.3.4 Application in PS5: Attica region 53
2.4.4 Product Description: Daily Fire Danger Index (DFDI) (ET) 58
2.4.5 Product Description: Fire Danger weather estimations at PS Greece (PS5) 59
3 Natural fire ignitions: Lightning 60
3.1 Modelling lightning at ET scale 60
3.2 Modelling lightning at Pilot Site scale 60
4 Human ignition drivers & Public participation in fire prevention and preparedness 62
4.1 Product description: Human ignition probability map (ET) 65
4.2 Product description: Fire ignition data and driver variables (PS) 65
5 Risk wise landscape and fuel models development 66
5.1 Fuel models development 66
5.2 Landscape fuel map and custom fuels at PS scale 68
5.2.1 Product Description: Fuel types (ET) 68
5.2.2 Product Description: Fuel types (PS) 68
6 Analysis of fire propagation, fuel consumption and smoke emission as risk factors 69
6.1 Propagation potential for European Territory (ET) 69
6.1.1 Methodology for propagation potential estimation at ET scale 69
6.1.2 Surface fire behaviour modelling at ET scale 72
6.1.2.1 Preparation of static data – Fuel Map 77
6.1.2.2 Preparation of static data – Slope Map 84
6.1.2.3 Preparation of fire dynamic data 86
6.1.2.4 Preparation of dynamic data – Fuel Moisture 86
6.1.2.5 Calculation of final Moisture Content Mf 88
6.1.2.6 Preparation of dynamic data – Wind Speed 91
6.1.3 Verification of direct implementation of Rothermel equations for cell-based wildland landscape surface fire growth simulations 93
6.1.4 Results – surface propagation potential maps for EU territory 95
6.1.5 Crown fire behaviour modelling at ET scale 111

Copyright © FirEURisk Consortium. All rights reserved.

6.1.5.1 Inputs for calculation crown fire indicators 113
6.1.5.2 Calculation of crown fire indicators 120
6.1.5.3 Crown fire models in BehavePlus and FlamMap 121
6.1.6 Results – crown propagation potential maps for EU territory 135
6.1.7 Product Description: Fire propagation (ET) 144
6.2 Fire propagation modelling at PS scale 145
6.2.1 Procedure for propagation potential calculation using FlamMap 146
6.2.2 Procedure for propagation potential calculation using FlamMap 147
6.2.3 Preparation of input data for FlamMap simulations 149
6.2.4. FlamMap simulations and preparation of final outputs 151
6.2.4 Availability of input data for propagation potential calculation for Pilot Site using FlamMap 154
6.2.5 Outputs of wildfire propagation potential calculation 159
6.2.5.1 Rate of Spread 160
6.2.5.2 Heat per Unit Area 163
6.2.5.3 Flame Length 167
6.2.5.4 Fireline Intensity 171
6.2.5.5 Crown Fraction Burned 175
6.2.5.6 Crown Fire Activity 179
6.2.6 Burn probability (dynamic run) 183
6.2.7 Product description: Fire propagation (PS) 186
7 Smoke potential emissions 187
8 Appendix I: Fire danger index classification for Chornobyl Exclusion Zone 188
8.1 Data used 188
8.2 Methodology 190
8.3 Software implementation 191
8.4 Results 192
8.4.1 Product Description: Fire danger index classification for Chernobyl Exclusion Zone 202
9. References 203

Copyright © FirEUrisk Consortium. All rights reserved.

List of Figures

Figure 1: Coupling scheme of PROSPECT and SAIL 26
Figure 2: PROSPECT + SAIL GSA in the entire portion of the spectrum supported by PROSPECT 27
Figure 3: PROSPECT + SAIL GSA in the Sentinel-3 SYNERGY OLCI Channels 29
Figure 4: PROSPECT + SAIL GSA in the Sentinel-3 SYNERGY SLSTR Channels 30
Figure 5: PROSPECT + SAIL GSA in the Sentinel-2 MSI channels 31
Figure 6: PROSPECT + SAIL + GEO GSA in the entire portion of the spectrum supported by PROSPECT 33
Figure 7: PROSPECT + SAIL + GEO GSA in the Sentinel-3 SYNERGY OLCI Channels 34
Figure 8: PROSPECT + SAIL + GEO GSA in the Sentinel-3 SYNERGY SLSTR Channels 35
Figure 9: PROSPECT + SAIL + GEO GSA in the Sentinel-2 MSI channels 36
Figure 10: S3A-OLCI (left) and SLSTR (right) spectral response functions. 38
Figure 11: Sentinel-2A MSI spectral response functions 38
Figure 12: Bing Satellite map of the Lousa sampling site, roughly delimited by the blue rectangle. The red dots mark the Sentinel-2 pixels used for the validation, and the associated value represents the coefficient of determination of the estimated timeseries with respect to the average dataset. 40
Figure 13: Bing Satellite map of the Capo Caccia sampling site, roughly delimited by the blue rectangle. The red dots mark the Sentinel-3 pixels used for the validation, and the associated value represents the coefficient of determination of the estimated timeseries with respect to the average dataset. 42
Figure 14: average of the 7-day rolling mean timeseries of the Sentinel-2 points shown in figure 9 (orange) and ADAI pinus pinaster measurements (blue). 45
Figure 15: average of the 7-day rolling mean timeseries of the Sentinel-2 points shown in figure 10 (orange) and CNR average species measurements (blue). 46
Figure 16: average of the 7-day rolling mean timeseries of the Sentinel-3 points shown in figure 11 (orange) and CNR average species measurements (blue). 46
Figure 17: Example of product output on PS3 (Portugal) on January 17th and August 12th. 48
Figure 18: Relationship between the Hot-Dry-Unstable (HDU) index and cumulative burned area for all the fires occurring between 2001-2021 and registered in the database GlobFire. A segmented regression was fitted to the data and significant breakpoints are indicated by the red circles. Biomes 5, 6, 8, 4 and 12 indicate temperate grasslands, boreal forests, temperate conifer forests, temperate broadleaf and mixed forests and Mediterranean forests, respectively. 50
Figure 19: Modelling Domains: d01 refers to the outermost domain of 20 km and d02 to the nested domain of 5 km (region of Greece). This figure is obtained by Politi et al 2022. 53
Figure 20: PS5 in orange color for the Attica region. 54
Figure 21: FWI threshold value of the 90th percentile for the historical and future periods for each emission scenario for PS5. 54
Figure 22: The number of days above 90th percentile (threshold value is set as 90th percentile of the historical period for the specific cell for all time periods) under the future emission scenarios in the near and far future periods for PS5. 55
Figure 23: The maximum number with consecutive days above 90th percentile (threshold value is 90th percentile of the historical period for the specific cell) for historical period and RCP4.5 and RCP8.5 for the near and far future periods for PS5. 56

Copyright © FirEURisk Consortium. All rights reserved.

Figure 24: The mean value of Initial Spread Index for the historical period (top map) and future changes under RCP4.5 and RCP8.5 (in %) for the near and far future periods with respect to the historical period (middle and bottom maps) for PS5. 57
Figure 25: DFDI maps in DA5 (Sardinia) on May 1st (left) and July 1st (right) 2022 59
Figure 26: Human ignition probability map 63
Figure 27: Fuel type map of the ET area. Classes codes correspond to the FirEUrisk classification system (source: Aragoneses et al., 2023) 67
Figure 28: Conceptual integration of fire risk components within the FirEUrisk project (Chuvieco, Viegas, Eftychidis; 2022) 69
Figure 29: Procedure for cell based (pixel based) calculation of propagation potential variables on EU territory. Instead of temperature, relative and cloud cover (not shown in picture) weather input maps could be fuel moisture map for at least 10-h dead fuel and wind speed map at 10 m height. 77
Figure 30: New FirEURisk EU fuel model map adapting the Fuel types to the Scott and Burgan fuel models (Aragoneses et al. 2023) - https://essd.copernicus.org/preprints/essd-2022-184/ 78
Figure 31: Conversion table between new FirEURisk EU fuel categories and Scott-Burgan FBFM categories - Aragoneses et al. 2022c- https://essd.copernicus.org/preprints/essd-2022-184/ 79
Figure 32: New FirEURisk EU fuel map used for propagation potential calculation (Map was part of material for 1st FirEUrisk workshop: Prof. Emilio Chuvieco and Elena Aragoneses, University of Alcalá (Spain), FirEUrisk training event online, focusing on "The FirEUrisk fuel classification system and the European fuel map", Feb 2nd, 2023, adapted for propagation potential calculation.) 80
Figure 33: EU slope map 85
Figure 34: Map of average (50th percentile) 10h dead fuel moisture content in %, calculated by MeteoGRID from past fires on EU territory 89
Figure 35: Map of extreme (5th percentile) 10h dead fuel moisture content in %, calculated by MeteoGRID from past fires on EU territory 90
Figure 36: Map of average (50th percentile) wind speed in [m/s] calculated by MeteoGRID from past fires on EU territory 92
Figure 37: Map of extreme (95th percentile) wind speed in [m/s] calculated by MeteoGRID from past fires on EU territory 93
Figure 38: Map of Rate of Spread (ROS) [m/s] for extreme 95th percentile wind speed and 5th percentile fuel moisture 97
Figure 39: Map of Reaction Intensity (RI) [kJ/(m^2 s)] for extreme 95th percentile wind speed and 5th percentile fuel moisture 98
Figure 40: Map of Fireline Intensity (FI) [kW/m^2] for extreme 95th percentile wind speed and 5th percentile fuel moisture 99
Figure 41: Map of Flame Length (FL) [m] for extreme 95th percentile wind speed and 5th percentile fuel moisture 100
Figure 42: Map of Rate of Spread [m/s] for average 50th percentile wind speed and 50th percentile fuel moisture 102
Figure 43: Map of Reaction Intensity [kJ/(m^2 s)] for average 50th percentile wind speed and 50th percentile fuel moisture 103
Figure 44: Map of Fireline Intensity [kW/m^2] for average 50th percentile wind speed and 50th percentile fuel moisture 104

Copyright © FirEURisk Consortium. All rights reserved.

Figure 45: Map of Flame Length [m] for average 50th percentile wind speed and 50th percentile fuel moisture .. 105
Figure 46: Comparison of Rate of Spread (ROS) [m/s] for extreme and average wind speed and fuel moisture (left – extreme, right – average) 107
Figure 47: Comparison of Reaction Intensity (RI) [kJ/(m^2 s)] for extreme and average wind speed and fuel moisture (left – extreme, right – average)..... 107
Figure 48: Comparison of Fireline Intensity (FI) [kW/m^2)] for extreme and average wind speed and fuel moisture(left – extreme, right – average) 108
Figure 49: Comparison of Rate of Spread (ROS) [m/s] for extreme weather conditions and weighting factors f_{ij} and g_{ij} calculated (left) or derived from tables (right)..... 109
Figure 50: Comparison of Fireline Intensity (FI) [kW/m^2)] for weighting factors f_{ij} and g_{ij} calculated (left) or derived from tables (right) 110
Figure 51: Comparison of Flame Length (FL) [m] for extreme and average wind speed and fuel moisture (left – extreme, right – average) 110
Figure 52: Input data for FlamMap simulations - source: FlamMap 3 instruction manual - https://wfdss.usgs.gov/wfdss/pdfs/intro_flammap3_(desktop).pdf. 146
Figure 53: Nodes of meteorological data 189
Figure 54: Fires inside demonstration area for the period since 2010 to 2020 years 189
Figure 55: Map of UDFHI in DA-15 for June 13th, 2015 192
Figure 56 Comparison of UDFHI for the whole demonstration area and on burned areas over seasons during 11 year period. 200
Figure 57: Distribution of the UDFHI on the entire area (left) and on burned areas (right) over seasons during 11 year period. 200
Figure 58: Map of UDFHI for April 25th, 2015 overlaid by fires during the following 5 days 201
Figure 59: Distribution of the UDFHI on the entire area (left) and on burned areas (right) for the period from April 26 to 30, 2015. 201

Copyright © FirEURisk Consortium. All rights reserved.

List of tables

Table 1: List of Acronyms 13
Table 2: Moisture content of forest fuels 18
Table 3: Basic moisture of dead fine fuel. Day: from 8.00 a.m. to 8:00 p.m. 18
Table 4: Adding corrector of the moisture content of the fuel. (May June July) 19
Table 5: Adding a corrective for the moisture content of the fuel (February-March-April-August-September-October) Day: From 08:00 a.m. to 08:00 p.m. (solar) 19
Table 6: Adding a corrective for the moisture content of the fuel (November-December-January) Day: from 08:00 a.m. To 08:00 p.m. (solar) 20
Table 7: Fuel moisture. Night: From 8:00 p.m. to 8:00 a.m. (solar) 21
Table 8: Probability of ignition increases under different precipitation thresholds 21
Table 9: Effect of number of days since last precipitation 22
Table 1: Parameter bounds used for the GSA of PROSPECT-D + 4SAIL 32
Table 2: Parameter bounds used for the GSA of PROSPECT-D + 4SAIL + GEO 37
Table 3: list of the best performing channels of the Sentinel-2 S2MSI2A and Sentinel-3 SY _2_SYN for the inversion of the LFMC 43
Table 4: LFMC retrieval performance with different cost functions on the ADAI and CNR dataset 43
Table 5: LFMC retrieval performance with an increasing number of selected solutions. The N selected solutions are those that minimize the chosen cost function 43
Table 6: LFMC retrieval performance using different measures of central tendency to harmonize the selected solutions 44
Table 7: inversion parameters used to generate the LFMC estimates 44
Table 10: Variation in fire size (ha) at different percentiles under the different HDU breakpoints (see Figure 2) for the European Territory and the different biomes. Biome names as in Figure 2. 51
Table 11: The classification of values for the FWI and its sub-component ISI 52
Table 14: Names of pilot sites, country where is located or regions that contain, dates availability and total number of human-caused fires. 64
Table 15: AUC values and the top four fire drivers more relevant in RF models for each pilot site. 65
Table 16: Equations for the basic fire spread model for heterogeneous fuel (Andrews, 2018, p.19) 73
Table 17: Equations of related models implemented in BehavePlus (Andrews, 2018, p.27) 74
Table 18: Input parameters for the basic fire spread model (Andrews, 2018, p.16) 74
Table 19: FirEURisk hierarchical fuel classification system present on EU territory – adapted from (Aragoneses et al. 2022a) 78
Table 20: Scott-Burgan standard FBFM fuel model parameters for categories presented on EU territory (Aragoneses et al. 2022c) - https://essd.copernicus.org/preprints/essd-2022-184/ with corrections 81
Table 21: Calculation of weighting factors g_{ij} (Andrews, 2018, Table 6a, p.17). 82
Table 22: Weighting factors according to table 21 83
Table 23: Calculation of weighting factors g_{ij} (Andrews, 2018, Table 6a, p.17) 84
Table 24: weighting factors for static and dynamic standard FBFM fuel models 84
Table 25: Fuel Moisture Scenarios (Pettinari & Chuvieco, 2017) 87
Table 26: Static fuel model SH8 weighting factors 91
Table 27: Wind Adjustment Factor (WAF) for standard fuel models (Scott, 2007) 91

Copyright © FirEURisk Consortium. All rights reserved.

Table 28: Comparison of final and intermediate propagation potential variables calculated by direct implementation of Rothermel equations for cell-based wildland landscape fire growth simulations and BehavePlus 6.0.0 for fuel model SH8 (High load, humid climate shrub) 94
Table 29: Comparison of propagation potential variables for all fuel models calculated by direct implementation of Rothermel equations for cell-based wildland landscape fire growth simulations (model) and BehavePlus 6.0.0 (BP) 95
Table 30: Comparison of statistical property of propagation potential indicator variables (ROS – Rate of Spread, RI – Reaction Intensity, FI – Fireline Intensity, FL – Flame Length for average and extreme weather conditions 108
Table 31: Comparison of statistical property of propagation potential indicator variables (ROS – Rate of Spread, RI – Reaction Intensity, FI – Fireline Intensity, FL – Flame Length for calculated weighting factors f_{ij} and g_{ij} (Calculated) and weighting factors derived from tables 110
Table 12: Statistics of UDFHI on days with fires 193
Table 13: Ranges of UDFHI 200

Copyright © FirEUrisk Consortium. All rights reserved.

List of Acronyms

Table 1: List of Acronyms

List of Acronyms	
Acronym	**Description**
AEMET	Spanish Meteorological Agency
AIC	Akaike Information Criterion
AUC	Area Under the Curve
BA	Burned Area
BFB	Basic Fire Behavior
CLC	Corine Land Cover
CRC	Coordinate Reference System
DC	Drought Code
DECIF	Dispositivo Especial de Combate a Incêndios Florestais (Special Device for Forest Fire Fighting)
DFDI	Daily Fire Danger Index
DFHI	Daily Fire Hazard Index
dFMC	Daily Dead Fuel Moisture Content
DGVM	Dynamic Global Vegetation Models
DMC	Dry Matter Content
ECMWF	European Centre for Midrange Weather Forecast
EGIF	Estadística General de Incendios Forestales (Spanish General Statistics of Forest Fires)
EPSG	European Petroleum Survey Group
ET	European Territory
ET	European Territory
ETRS89	European Terrestrial Reference System 1989
EU	European Union
EUROSTAT	Statistical Office of the European Union
EWT	Equivalent Water Thickness
FBFM	Fire Behavior Fuel Models
FCCS	Fuel Class Classification System
FFM	Fire Forecasting Model
FFT	Fuel and Fire Tools
FI	Fireline Intensity
FirEUrisk	European Forest Fire Information System
FL	Flame Length
FMC	Fuel Moisture Content
FMI	Finnish Meteorological Institute
FPI	Fire Potential Index
FRP	Fire Radiative Power
GDAL	Geospatial Data Abstraction Library
GEDI	Global Ecosystem Dynamics Investigation
GeoTiff	Georeferenced Tagged Image File Format
GRIP	Global Roads Inventory Project
GSA	Global Sensitivity Analysis

Copyright © FirEUrisk Consortium. All rights reserved.

ha	hectares
IS4FIRES	Integrated System for Fire Management and Decision Support
kJ	kilojoule
kJ/m2	kilojoules per square meter
km	kilometer
kW	kilowatt
kW/m2	kilowatts per square meter
kWh	kilowatt hour
LAEA	Lambert Azimuthal Equal Area
LBP	Landscape Burn Probability
LFMC	Live Fuel Moisture Content
LFMC	Live Fuel Moisture Content
LiDAR	Light Detection and Ranging
LUT	LookUp Tables
m	meter
MODIS	Moderate Resolution Imaging Spectroradiometer
MTT	Minimum Travel Time
NASADEM	NASA's Global Digital Elevation Model
NDVI	Normalized Difference Vegetation Index
NDVI	Normalized Difference Vegetation Index
NWP	Numerical Weather Prediction
PS	Pilot Site
PSI	pounds per square inch
PUM	Product User Manual
RS	Rate of Spread
RF	Random Forest
RI	Reaction Intensity
RMSE	Root Mean Square Error
ROS	Rate of Spread
RTM	Radiative Transfer Models
s	second
SYNERGY	Sentinel3 Synergy
UAH	Universidad de Alcalá
VPD	Vapour Pressure Deficit
WAI	WildlandUrban Interface
WGI	WildlandGrassland Interface
WP	Work Package
WUI	WildlandUrban Interface

Copyright © FirEUrisk Consortium. All rights reserved.

1 Introduction

This report describes the methodologies developed within WP1-Task 1.1 for the assessment of Fire Danger in current conditions, as part of the work needed to produce all risk-life-cycle variables, models, and methodological schemes required for state-of-the art risk assessment in current conditions, at different temporal and spatial scales. Danger is defined as the likelihood that a fire ignites and propagates, following the terminology usually accepted in the fire management community (i.e. US National Fire Danger Rating System (NFDRS), Canadian Forest Fire Danger Rating System (CFFDRS)). As a Risk assessment component, it is the first that needs to be estimated to ultimately determine Exposure and Vulnerability of individuals, communities, infrastructures, assets, or systems (incl. ecosystems) to be adversely affected.

1.1 Purpose of the document

The purpose of this document is to provide the technical and methodological specifications for fire danger assessment: the development of variables, models and outputs required to estimate the potential for ignition and propagation of unwanted fires at the Pilot Site (PS) and European Territory (ET) scales.

1.2 Structure of the Document

The document follows a similar structure as the activities in WP1-Task 1.1, which are as follows:

A1.1.1 Fire weather and fuel status prevention
A1.1.2 Natural fire ignitions: Lightning
A1.1.3 Human ignition drivers & Public participation in fire prevention and preparedness
A1.1.4 Risk-wise landscape and fuel models development
A1.1.5 Analysis of fire propagation, fuel consumption and smoke emission as risk factors

These activities, and the Report, are structured in agreement with the physical development of any fire, starting with an analysis of fire weather effects on fuels, analysis of ignition points caused by lightning or people, depending on weather effects on dead fuels, and propagating in the landscape, also as a function of weather and fuel conditions (dead and alive).

2 Fire weather and fuel status prevention

2.1 Weather variables

Weather variables commonly used in wildfire risk assessment indicate those atmospheric variables that affect ignition or propagation (temperature, relative humidity, precipitation, wind speed and direction, etc.). They can refer to current (instantaneous), aggregated (last days-weeks) atmospheric conditions, or even historical conditions (past scenarios). These variables are obtained from meteorological observations or short-term weather forecasts based on climate models. Additionally, adaptation to future wildfire conditions requires understanding future weather patterns, which is done through Climate and Dynamic Global Vegetation Models (DGVM) to represent

Copyright © FirEUrisk Consortium. All rights reserved.

future values of meteorological danger indices, but also to estimate future fire occurrence by linking DGVM with fire models.

Weather variables are a critical element and widely used in existing wildfire risk assessment systems, which generally address only the fire danger component. Weather plays a key role in the ignition and propagation of wildfires. Temperature, atmospheric humidity (relative humidity and vapor pressure deficit), precipitation, wind speed and direction are the common meteorological inputs to danger rating systems. Fire weather extremes also drive large and at times catastrophic wildfires. These events have been increasing over much of the globe, and indicate that our fire climate is already changing.

In addition to weather or short-term atmospheric conditions, climate patterns are relevant to fire occurrence, particularly for the build-up of vegetation fuels. Climate plays a role in determining the fuel available to burn, the length of the fire season as well as the presence of lightning, which is the most common natural source of ignition. Climate including long-term averages has been used to explain the spatial variation in fire regimes. Additionally, climate variability helps explain the global interannual variability in areas burned, especially forested areas. Many studies describe climate-fire relationships along a continuum, ranging from fuel limited to fire weather limited systems. Fire weather limited systems are largely driven by extreme fire weather and fuel moisture, whereas fuel limited regions are positively related to precipitation prior to the fire season that promotes vegetation growth and subsequent biomass for combustion during the fire season. Lastly, and perhaps most importantly, human-caused climate change is causing profound modifications in global fire regimes through changes in fire season length, fuel moisture, fire intensity and fire severity.

Weather patterns also affect natural ignitions, both directly to the convergence of lightning and drought, as well as the characteristics of strikes and thunderstorms. Lightning strikes are one of the most common natural causes of wildfires, accounting for around 10–15% of all wildfires worldwide. Lightning-induced wildfires are particularly prevalent in regions with a high incidence of thunderstorms and dry vegetation. While lightning strikes can occur at any time, they are most common during the summer months when hot and dry conditions make it easier for fires to start and spread. One of the significant challenges in identifying lightning-induced wildfires is the prolonged latent phase, known as the holdover time, between ignition and fire detection. Typically, lightning-caused fires start as smoldering in the organic matter surrounding the base of the tree struck by lightning. This smoldering phase can last from several minutes to one or three days or even several weeks in rare cases, making it difficult to accurately identify the lightning that caused the fire. This phenomenon poses a great challenge to the development of predictive methods that can establish a cause-effect relationship, which is currently limited to specific regions. A robust association between lightning and wildfires can aid in understanding the natural fire regime, such as estimating holdover duration, identifying igniting lightning characteristics, and modelling lightning fire occurrence. The principal possibility of building such a model was demonstrated by Wotton and Martell from Ontario, Canada. Unfortunately, there are currently no global datasets that unambiguously link igniting lightning to its corresponding wildfires. However, improvements in lightning location systems (LLSs) and fire databases have facilitated the identification of possible igniting lightning, and numerous methodologies have been developed to match wildfires and related lightning. Consequently, identifying the igniting lightning of a wildfire by searching the lightning dataset remains challenging, making predicting single lightning-ignition events difficult. However, utilizing a statistical approach that incorporates lightning data from Numerical Weather Prediction (NWP) models and other environmental factors occurring when a fire is observed may offer a potential solution. The target variables for prediction could be widely available satellite products, such as Fire Radiative Power (FRP) or Burned Area (BA).

Copyright © FirEUrisk Consortium. All rights reserved.

Weather parameters were computed from ERA5-Land global reanalysis data (https://cds.climate.copernicus.eu/cdsapp#!/dataset/reanalysis-era5-land?tab=overview, accessed on 30 March 2023). A topography-based transfer function was applied to the 9 km-resolution time series of the hourly ERA5-Land reanalysis data (https://cds.climate.copernicus.eu/cdsapp#!/dataset/reanalysis-era5-land?tab=overview, accessed on 30 March 2023) for the following variables: Temperature, Dew Point Temperature, Relative Humidity, Wind and Daily Precipitation. Particularly, for each climate variable simulated by the reanalysis, the statistical downscaling was based on three steps: (1) For all the variables and for each time step (with 0.073° × 0.073° resolution), a purely geo-statistical approach was performed to a 1km×1km grid by using AIC-based stepwise regression [334] with topological and geographical parameters (altitude above sea level, latitude, longitude and distance to the Atlantic Ocean and Mediterranean Sea). Finally, a bilinear model was applied to the residual errors obtained by comparison of the geo-statistical approach and the original ERA5Land grid point values. In other words, for each hour of the target days, a stepwise regression is used to obtain the interpolation function of ERA5Land data to a 1 km^2 grid using as selection method the likelihood function as described in Akaike, using the R stat package. The interpolated data are subsequently compared with the original ERA5Land ones in order to obtain the residual errors that are then interpolated with a bilinear model to obtain the final values for the target grid.
In addition, altitude was taken into consideration in the case of temperature. (2) Similarly, for each targeted time step, residual errors of the AIC-based stepwise regression were interpolated from the original grid (0.073° × 0.073°) to the final 1 km^2 grid by using a bilinear model. (3) Finally, the projected value for each time step was obtained by adding the result of Step (1) and Step (2), obtaining climate scenarios in a 1 km × 1 km grid at an hourly timescale (daily in case of precipitation).

2.2 Fuel Moisture

2.2.1 Calculation of dead fuel moisture content: theoretical basis

It is commonly used to classify the particles of dead plant material that make up the complex forest fuel into three types: fine, medium and coarse. This classification has been made based on the size of the particles, which has a direct relationship with the capacity to absorb and eliminate moisture from and to the atmosphere. Of these, dead fine particles are generally a key factor for fire ignition and propagation, therefore they are of special importance in the elaboration of indices and for models of fire propagation.
Since the dead fine fuel particles are in equilibrium with the humidity of the air immediately around them, the following definitions are adopted:

1. Fine dead fuel (1HR): they take 1 hour to acquire 2/3 of the equilibrium humidity with the air (smaller dimension is < 6 mm)
2. Medium dead fuel (10HR): it takes 10 hours to acquire 2/3 of the equilibrium humidity with the air (minor dimension is >= 6 mm and < 20 mm)
3. Large dead fuel (100HR): it takes 100 hours to acquire 2/3 of the equilibrium humidity with the air (minor dimension >=20 mm).

Given that fine particles (1HR) react relatively quickly to changes in air humidity, it can be estimated that these are instantaneous, and therefore the humidity of fine particles can be obtained from the temperature and relative humidity of the air by means of the application of tables and subsequent corrections for the effect of precipitation, as proposed in BEHAVE and which is applied in this case.
For the medium (10HR) and large (100HR) particles, a slower variation is taken into account (it explains a daily variation for the medium and weekly for the large ones) and that is related to the oscillations (daily, weekly) of the

Copyright © FirEURisk Consortium. All rights reserved.

air temperature and relative humidity. The estimation of these two temperatures is carried out by applying a physical model (theoretical approximation) on the behavior of the loss and gain of humidity of a wooden rod of equivalent dimensions under constant conditions (Nelson, 2000). The theoretical basis on which the calculations of the offered maps are based is described in more detail below.

2.2.1.1 Fine fraction (1HR)

It is expressed as a percentage relative to the dry weight in the oven and is normally between 2 and 30%. To calculate this value, a table is applied (based on Bradshaw et al. 1983) that relates the readings of the meteorological variables air temperature according to the dry bulb and relative humidity. The value obtained is corrected based on sun exposure according to local conditions of cloud cover, slope, and orientation for an hour and time of year. The procedure is empirical, so it requires a calibration and obtaining the degree of error committed after a series of field observations of the real moisture of the dead fine fuel. This is obtained by weighing, drying in an oven at 100ºC for 24 hours and new weighing of samples taken at significant points in the region where the index is applied. Nevertheless, given that all the involved processes are mechanicistic, the procedure could be potentially applied to any part of the world without too many changes in the tables or none at all.

Table 2: Moisture content of forest fuels

Moisture content of forest fuels
The humidity of the dead fuel does not exceed 30% and can drop to values below 5%, always in hygroscopic equilibrium with the air (Table II.1). The humidity of the dead fine fuel is determined for the hours of the day with Table II.1, adding the corrective sum obtained in Tables II.2, II.3 or II.4, as appropriate. Table II.5 will be used for the night.

Table 3: Basic moisture of dead fine fuel. Day: from 8.00 a.m. to 8:00 p.m.

BASIC MOISTURE OF DEAD FINE FUEL. Day: From 8:00 a.m. to 8:00 p.m. (solar)																				
Temp. Thermometer Dry Bulb (ºC)	AIR RELATIVE HUMIDITY (percentage)																			
	0-4	5-9	10-14	15-19	20-24	25-29	30-34	35-39	40-44	45-49	50-54	55-59	60-64	65-69	70-74	75-79	80-84	85-89	90-94	95-99	100
<0	1	2	2	3	4	5	5	6	7	8	8	8	9	9	10	11	12	12	13	13	14
0-9	1	2	2	3	4	5	5	6	7	7	7	8	9	9	10	11	11	12	13	13	14
10-20	1	2	2	3	4	5	5	6	6	7	7	8	8	9	10	11	11	11	11	13	13
21-31	1	1	2	2	3	4	5	5	6	7	7	8	8	8	09	10	11	12	13	13	13
32-42	1	1	2	2	3	4	4	5	6	7	7	8	8	8	99	10	11	12	13	13	13
>42	1	1	2	2	3	4	4	5	6	7	7	8	8	8	99	10	10	11	12	12	13

Copyright © FirEURisk Consortium. All rights reserved.

															10 10	10 11	11 11	12 11	12 12	13 12
Add the corrective addend that corresponds according to Tables II.2, II.3 or II.4.																					

Table 4: Adding corrector of the moisture content of the fuel. (May June July)

Day: from 08:00 a.m. To 08:00 p.m. (solar)

ADDING CORRECTOR OF THE MOISTURE CONTENT OF THE FUEL. (May June July) Day: From 08:00 a.m. to 08:00 p.m. (solar)								
		Exposed. Less than 50% of shade fuels						
		Hour						
Exposure	Slope	08:00	10:00	12:00	14:00	16:00	18:00	20:00
N	0-30% >30%	3 4	1 2	0 1	0 1	1 2	3 4	
E	0-30% >30%	2 2	1 0	0 0	0 1	1 3	4 5	
S	0-30% >30%	3 3	1 1	0 1	0 1	1 1	3 3	
W	0-30% >30%	3 5	1 3	0 1	0 0	1 0	3 2	
Shading. More than 50% of fuels in shade or cloudy								
N	0% +	5	4	3	3	4	5	
E	0% +	4	4	3	4	4	5	
S	0% +	4	4	3	3	4	5	
W	0% +	5	4	3	3	4	4	
Flat terrain = South exposure								

Table 5: Adding a corrective for the moisture content of the fuel (February-March-April-August-September-October) Day: From 08:00 a.m. to 08:00 p.m. (solar)

ADDING A CORRECTIVE FOR THE MOISTURE CONTENT OF THE FUEL (February-March-April-August-September-October) Day: From 08:00 a.m. to 08:00 p.m. (solar)								
		Exposed. Less than 50% of fuels in shade.						
		Hour						
Exposure	Slope	08:00	10:00	12:00	14:00	16:00	18:00	20:00
N	0-30% >30%	4 4	2 3	1 3	1 3	2 3	4 4	
E	0-30% >30%	4 3	2 1	1 1	1 2	2 4	4 5	
S	0-30%	4	2	1	1	2	4	

Copyright © FirEURisk Consortium. All rights reserved.

	>30%	4	2	1	1	2	4	
W	0-30% >30%	4 5	2 4	1 2	1 1	2 1	4 3	
Shading. More than 50% of fuels in shade or cloudy.								
N	0% +	5	5	4	4	5	5	
E	0% +	5	4	4	4	5	5	
S	0% +	5	4	4	4	4	5	
W	0% +	5	5	4	4	4	5	
Flat terrain = South Exposure.								

Table 6: Adding a corrective for the moisture content of the fuel (November-December-January) Day: from 08:00 a.m. To 08:00 p.m. (solar)

ADDING A CORRECTIVE FOR THE MOISTURE CONTENT OF THE FUEL (November-December-January) Day: From 08:00 a.m. to 08:00 p.m. (solar)								
		Exposed. Less than 50% of fuels in shade.						
		Hour						
Exposure	Slope	08:00	10:00	12:00	14:00	16:00	18:00	20:00
N	0-30% >30%	5 5	4 5	3 5	3 5	4 5	5 5	
E	0-30% >30%	5 5	4 4	3 3	3 2	4 5	5 5	
S	0-30% >30%	5 5	4 3	3 1	2 1	4 3	5 5	
w	0-30% >30%	5 5	4 5	3 4	3 2	4 3	5 5	
Shading. More than 50% of fuels in shade or cloudy.								
All exposures and slopes		5	5	5	5	5	5	
Flat terrain = South Exposure.								

Copyright © FirEURisk Consortium. All rights reserved.

Table 7: Fuel moisture. Night: From 8:00 p.m. to 8:00 a.m. (solar)

FUEL MOISTURE. Night: From 8:00 p.m. to 8:00 a.m. (solar)																				
	AIR RELATIVE HUMIDITY (percentage)																			
Temp. Thermometer Dry Bulb (ºC)	0-4	5-9	10-14	15-19	20-24	25-29	30-34	35-39	40-44	45-49	50-54	55-59	60-64	65-69	70-74	75-79	80-84	85-89	90-94	95-99	100
0-9	1	2	3	4	5	6	7	8	9	9	1	1	1	1	1	1	1	2	2	25	25
10-20	1	2	3	4	5	6	6	8	8	9	1	1	2	3	4	6	8	1	4	+	+
21-31	1	2	3	4	4	5	6	7	8	9	1	1	1	1	1	1	1	2	2	25	25
32-42	1	2	3	3	4	5	6	7	8	9	0	1	1	2	4	6	7	0	3	+	+
>42	1	2	3	3	4	5	6	6	9	9	1	1	1	1	1	1	1	2	2	25	25
											0	0	1	2	3	5	7	0	3	+	+
											9	1	1	1	1	1	1	1	2	25	25
												0	0	1	3	4	6	9	2	24	+
												9	1	1	1	1	1	1	2		25
													0	1	2	4	6	9	1		+
Does not require correction.																					

Weather exposure is estimated taking into account, on the one hand, the tree cover of each fuel model and, on the other, the cloud cover that has been observed or predicted for the calculation horizon. Both effects are considered simultaneously, having a summative effect when there is both tree cover and cloudiness.

Likewise, it is important to emphasize that in the estimation of the humidity of the dead fine fuel, those models that correspond to grasses and other plant species that, given their high humidity of living fuel, behave seasonally as incombustible (winter and spring months) or as fuels (models 1 and 2, for example, some pastures in summer). In this way, both the humidity of the fuel and the indices that depend on it carry this non-combustibility condition, thus avoiding an overestimation of the characteristics of the potential fire developed in winter and spring. This condition is estimated from the data offered by the NDVI index based on remote sensing products.

Correction for precipitation

The calculation of the humidity of the fine fuels takes into account the effect of the precipitation of the last days, according to the studies carried out in Andalusia on this aspect (Rodríguez and Silva, 2001). The implemented method performs a reduction in the ignition probability, beginning the calculation in the ignition probability of the day before the precipitation occurred:

Table 8: Probability of ignition increases under different precipitation thresholds

Precipitation (mm)	Probability Increase (%)
< 5	+5

Copyright © FirEURisk Consortium. All rights reserved.

5 - 15	+10
15 - 35	+20
> 35	+30

Subsequently, the effect of the days that pass after the day of the last precipitation is collected and estimated, by considering the amount of precipitation corresponding to the number of days elapsed, the total precipitation fallen and the time of year for which the calculations are made.

Table 9: Effect of number of days since last precipitation

Number of days since last precipitation	Pp < 5mm		Pp 5-15mm		Pp 15-35mm		Pp >35mm	
	apr-oct	nov-mar	apr-oct	nov-mar	apr-oct	nov-mar	apr-oct	nov-mar
1	R	R	R	R	R	R	R	R
2	R	R	5	R	15	R	35	R
3	0	R	1	R	5	R	15	35
4	0	R	0	R	1	15	5	15
5	0	1	0	5	0	5	1	5
6	0	0	0	1	0	1	0	1
7	0	0	0	0	0	0	0	0

0 0 0 0

where R is the rainfall in mm.

Subsequently, the humidity increase factor is estimated as a percentage according to the relationship between the humidity of the fine dead fuel and the probability of ignition under the same circumstances, by means of linear interpolation between the probability values obtained.

2.2.1.2 Medium fraction (10HR) and thick fraction (100HR)

In calculating the moisture values of medium and large particles (expressed as % of the dry weight in the oven), this physical approximation is used, simplified for its practical application in a polynomial expression that takes into account the value of dead fine fuel (for the calculation of 10HR) and the half-dead fuel (for the calculation of 100HR) as well as the expected variation of both relative humidity and air temperature. This variation, for each day and for the calculation of the means, is estimated based on the readings at 6 a.m. and 3 p.m. of both variables and applying an interpolation between them, namely:

$$HR10_{15} = HR01_{15} + (0.4142 \cdot (HR01_{6} - HR01_{15})) + 0.5$$

$$HR10_{6} = HR01_{6} + (0.5571 \cdot (HR01_{6} - HR01_{15})) + 0.5$$

In the same way, the moisture calculation for the 100HR coarse particles is estimated from the value obtained for the 10HR medium particles in the previous step and then applying an interpolation between them:

Copyright © FirEURisk Consortium. All rights reserved.

$$HR100_{15} = HR10_{15} + (0.4142 \cdot (HR10_6 - HR10_{15})) + 0.5$$

$$HR100_6 = HR10_6 + (0.5571 \cdot (HR10_6 - HR10_{15})) + 0.5$$

The generation of the European dead fuel moisture map has been done combining several resources and data:

1. The European combustible specifically created for FirEURisk.
2. An European slope map created for the FirEURisk project.
3. An European aspect map created for the FirEURisk project.
4. Meteorological variables from Copernicus ERA5Land comprising Temperature, Dew Point, Wind and Precipitation.
5. Additionally, the Cloud Cover was obtained from Copernicus Era5.

2.2.1.3 Downscaling procedures conducted for each variable.

The generation of the fuel maps needed a set of inputs with the correct format, resolution, sizes and projections in all of them. For this purpose, the initial step of the calculation process was to reproject, resample and resize the input rasters mentioned above to the desired conditions. This was achieved using several Python libraries (SciPy, Rasterio, Geopandas or Fiona) along with GDAL. Additionally, it was needed to calculate the humidity and wind direction and speed based on the variables already mentioned. To obtain humidity both temperature and dew point were required and to calculate wind direction and module, the two components of wind (u and v components of wind at 10 m) from ERA5Land were employed.

Weather parameters for the target days were computed from ERA5-Land global reanalysis data (https://cds.climate.copernicus.eu/cdsapp#!/dataset/reanalysis-era5-land?tab=overview). A topography-based transfer function (1) has been applied to the 9 km-resolution time series of the hourly ERA5-Land reanalysis data (https://cds.climate.copernicus.eu/cdsapp#!/dataset/reanalysis-era5-land?tab=overview) for the following variables: Temperature, Dew Point Temperature, Wind components and daily Precipitation.

Once all the input data was processed the dead fuel moisture was calculated for every hour of each of the days selected with the objective of having data to perform direct statistical analysis. Two sets of calculations were performed to better evaluate the results. One set of calculations was done without taking into account the precipitation and the other one considering its effects.

One final calculation needed was that of the percentiles and mode of some of the variables obtained. As most of the variables, except for precipitation, are hourly, it was determined that the best cases would be to consider the values for 12H and 18H and obtain the percentiles at these times. As such the calculations performed were done for:

1. Percentiles 5 and 50 of the Relative Humidity at 12H and 18H.
2. Percentiles 50 and 95 of Wind Speed at 12H and 18H.
3. Percentiles 5 and 50 of the Fine Dead Fuel Moisture at 12H and 18H.
4. Percentiles 5 and 50 of the Medium Dead Fuel Moisture at 12H and 18H.
5. Mode of Wind Direction at 12H.

Copyright © FirEURisk Consortium. All rights reserved.

2.2.2 Product Description: European Dead Fuel Moisture map (ET)

- **Format:** The Europe fuel moisture map is provided in GeoTIFF format in one single-band categorical raster layer with 1 km pixel resolution. The file is named: FirEUrisk_Europe_fuel_map.tif
- **Spatial resolution:** 1 km.
- **Spatial projection:** ETRS89 Lambert Azimuthal Equal Area (EPSG: 3035).
- **Access:** Data can be accessed by direct download from:
- https://drive.google.com/drive/folders/1VlnPn1KPUtggVpn3pgWV371SrBTtLSR1?usp=share_link
- **Description:** The Europe fuel moisture map was generated from ERA5Land data for the days in which a fire larger than 2000 hectares occurred in the ET territory (a total of 403 days from 2001 to 2020). The procedure has been described on this document: Dead fuel moisture calculation.
- **Contact:** In case of doubts and/or suggestions, forward an email to Luis Torres (luis@meteogrid.com) and David Caballero (david@meteogrid.com).

2.2.3 Product Description: Pilot site Dead Fuel Moisture map (PS)

No applicable

2.3 Calculation of live fuel moisture content: Theoretical basis

This product aims to provide Live Fuel Moisture Content (LFMC) estimates based on Sentinel-3 and Sentinel-2 satellite imagery. In particular, due to the computing resources needed to download and process Sentinel-2 imagery on a scale other than that of a DA (Demonstration Area), the Sentinel-3 product will be the only one regularly provided and updated on the FirEUrisk internal platform. The Sentinel-2 product will be used for the validation of the LUT (Look Up Table) creation and inversion algorithm, and *ad-hoc* Sentinel-2 based LFMC datasets will be provided to FirEUrisk users on demand.

In the scientific literature, Radiative Transfer Models (RTMs) have been extensively used to estimate reflected radiation associated to different combinations of biophysical variables to reflected radiation. However, oftentimes it is more interesting to proceed in the opposite way, i.e., reconstruct the combination of biophysical variables that generated the radiation captured by a certain instrument, such as for instance a sensor installed on a satellite. To this end, a number of Inversion Methods (IMs) of varying mathematical complexity have been developed and tested, with different results in terms of performance.

Therefore, we aim to provide LFMC estimates using an inversion procedure based on RTM (Radiative Transfer Models) and Sentinel imagery. The product will be validated using field samples collected by the FirEUrisk partners and freely available LFMC datasets where applicable.

Copyright © FirEUrisk Consortium. All rights reserved.

2.3.1 Radiative Transfer Models

In the specific case of Live Fuel Moisture Content estimation, the most established and widely used RTMs belong to the PROSPECT+SAIL family.

SAIL (Scattering by Arbitrarily Inclined Leaves) is one of the most widely used canopy reflectance models and was developed as an extension of the one-dimensional non-lambertian directional reflectance model developed by Suits in 1972. Suits himself had extended the functionality of previously existing models by implementing the capability to reproduce the effect of the viewing angle on the directional reflectance, and to trace back these effects to a specific class of canopy components. Suit's canopy model corresponded to a finite number of infinitely extended horizontal layers, each layer containing homogeneously mixed, but randomly distributed components. In 1984, Verhoef, proposed a new solution of Suit's equations in order to improve the model performance related to changing viewing angles. According to Verhoef, the simplifications adopted by the previous model resulted in unrealistic spectra for certain view angle distributions. By introducing the Leaf Area Index (LAI) and the Leaf Inclination Distribution Function (LIDF) in the calculation of the extinction coefficients, SAIL was able to model canopies with leaves of arbitrary inclination, hence the name.

PROSPECT is a radiative transfer model based on Allen's generalized plate model, which was capable of describing the reflectance and transmittance of monocotyledon and dicotyledon leaves by introducing a void area index to model the different internal structure of different leaf species. In 1990, Jacquemoud and Beret introduced PROSPECT to improve upon Allen's foundation, but at the same time to keep the number of model parameters to a minimum in order to facilitate model inversion. This first version of PROSPECT was based on three parameters representing the leaf internal structure, pigment concentration parameter and water content.

The inversion of PROSPECT is relatively easy, but from a remote sensing point of view, inverting the reflectance spectra of a singular leaf has limited applicability. On the other hand, SAIL provides a description of a leaf canopy, but is inversion from satellite data can be feasible only when several measurements from different viewing angles are available, which is almost never the case. To solve this issue, the two models were coupled into PROSAIL since the early nineties, and their parallel evolution allowed different versions to be coupled together to create different joint.

Finally, in 2001 Huemmrich [4] combined SAIL and the Jasinski geometric model to create **GeoSail**, in order to model discontinuous vegetation by weighting the reflectance and transmittance in terms of how modelled trees with very simple shapes (e.g. cylinders, cones) equally scattered onto a plane surface interacted with the incoming radiation.

Copyright © FirEURisk Consortium. All rights reserved.

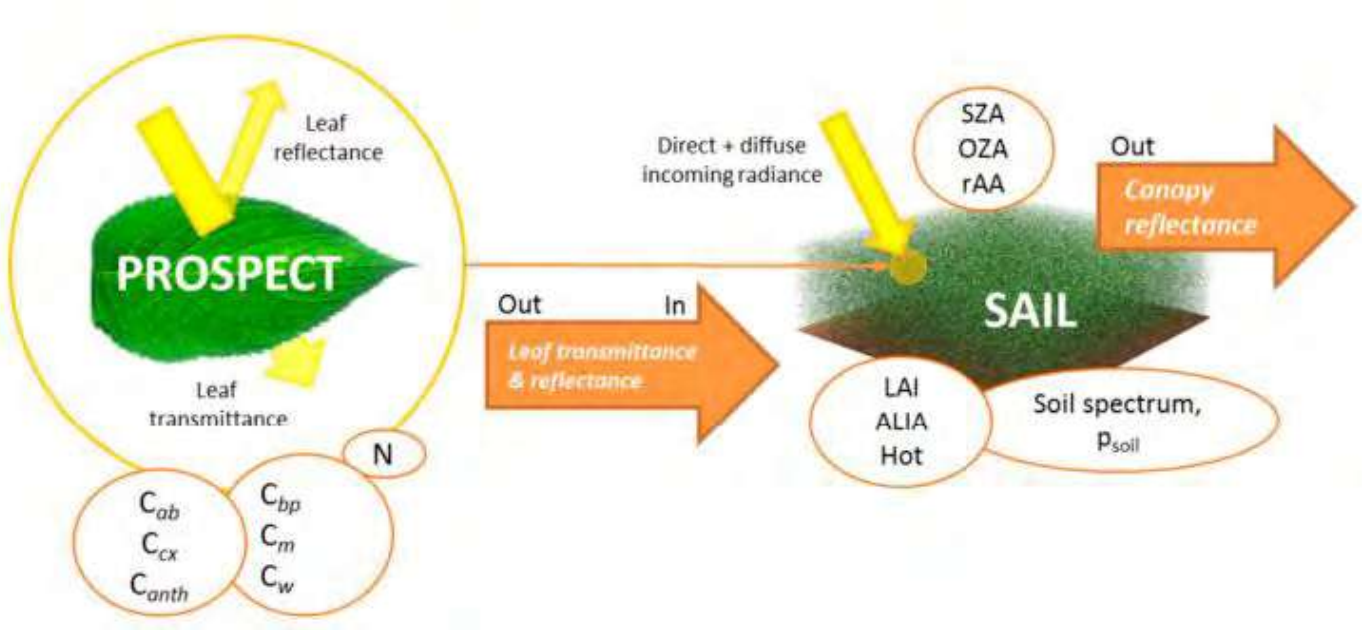


Figure 1: Coupling scheme of PROSPECT and SAIL

2.3.2 Model Variables and LFMC

Among the PROSPECT model variables are the water concentration C_w and the leaf dry matter content C_{dm}. C_w represents the leaf water per unit area in $\mu g/cm^2$, and is sometimes confused with the equivalent water thickness EWT, which represents the height in cm that the leaf water would reach if it were evenly spread on a layer with a surface equal to the leaf surface:

$$C_w \left[\frac{g}{cm^2}\right] = EWT\,[cm] * \rho_w \left[\frac{g}{cm^3}\right]$$

If we assume a water density $\rho_w = 1\ g/cm^2$, the two variables have the exact same value, justifying their confusion.

The LFMC can be calculated by dividing these two biophysical variables. Let us denote the leaf dry weight as DW, and the water weight as WW. By definition, the LFMC is the mass ratio of water contained in the leaf to the leaf dry weight:

$$LFMC = 100 * \frac{WW}{DW}$$

By dividing both numerator and denominator by the leaf area A, we obtain the definitions of the two aforementioned parameters:

$$LFMC = 100 * \frac{\frac{WW}{A}}{\frac{DW}{A}} = 100 * \frac{C_w}{C_{dm}}$$

This implies that, in principle, the LFMC can be estimated inverting the PROSPECT model. Nevertheless, in order to make sure that these variables have a significant impact on the model output, i.e. that their variation has a significant role in determining the intensity of the measured radiation, we must conduct a sensitivity analysis.

Copyright © FirEURisk Consortium. All rights reserved.

2.3.3 Global Sensitivity Analysis of PROSPECT + SAIL

In order to conduct the Global Sensitivity Analysis (GSA) of the different model combinations, we used the SALib Python library, which allows to easily create Sobol sequences to properly combine the model inputs and different functions to analyse the model outputs. The results will be presented in terms of **Total Order Sensitivity Indices**, which represent the percentage contribution of a given model parameter on the model output taking into account both the first order effects and the higher order interactions with the other variables. The results will be presented mostly for the model output along the entire spectrum supported by PROSPECT, and then in the Sentinel-3 SYNERGY bands. As done in Prikaziuk et al. (2019) [3], we assume a significance threshold of 5%.
The angular variables will be neglected in this analysis, since their value is provided alongside the satellite measurements and therefore does not need to be estimated.

Parts of these results were already discussed in the conference paper Pampanoni et al. (2021a) [2].

2.3.3.1 PROSPECT + SAIL

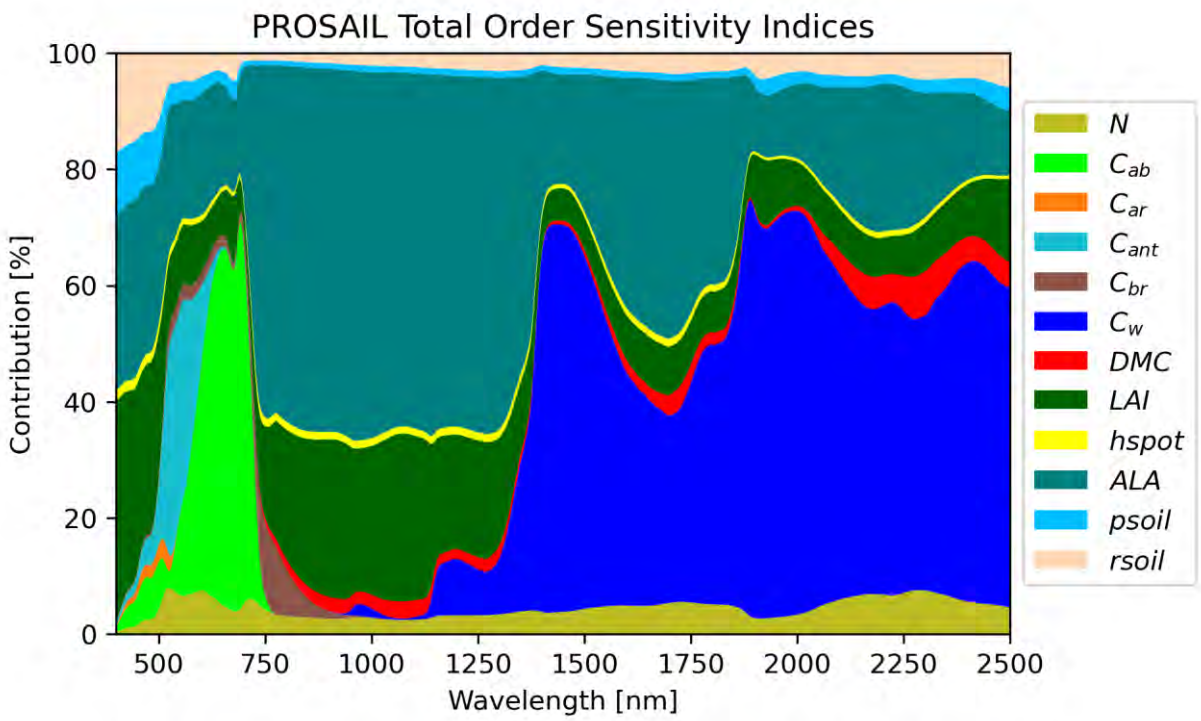


Figure 2: PROSPECT + SAIL GSA in the entire portion of the spectrum supported by PROSPECT

In the violet-blue wavelengths, the soil brightness and dryness parameters reach their highest significance values, with the LAI and ALA (Average Leaf inclination Angle) making up most of the reflectance. In the visible spectrum, the anthocyanin concentration C_{ant} and the chlorophyll a and b concentration C_{ab} take the lead, with the former being the highest significance parameter in the blue-green wavelengths (500-600 nm) and the latter becoming prominent in the red wavelengths (>600 nm). The LAI and ALA make up most of the output reflectance in the NIR (750-1200 mm), until we reach the SWIR (> 1200 nm) and the water thickness C_w takes on the majority of the significance. Finally, in the longer SWIR wavelengths (> 2100 nm), the dry matter content C_{dm} reaches its highest significance values, even though most of the reflectance is still traceable to C_w and ALA variations. The brown

Copyright © FirEURisk Consortium. All rights reserved.

pigment C_b is most significant in the shorter NIR wavelenghts, while the leaf structure parameter N contributes relatively consistently across the whole spectrum.

The graph in Figure 3 shows 15 out of the 16 OLCI bands included in the Sentinel-3 SYNERGY product. The OLCI Oa01 channel was disregarded since it does not completely fall into the portion of the electromagnetic spectrum covered by PROSAIL. The LAI and the ALA are the most significant variables in the blue channels, while the anthocyanin content plays a prominent role as we transition into the green channels Oa05 and Oa06. The chlorophyll content takes over from channel Oa07 onwards. The OLCI NIR channels (Oa11 and following) are mostly dominated by the ALA, but the brown pigment and the LAI also contribute to a significant portion of the reflectance. The other model parameters such as dry matter content, leaf structure parameter, and soil parameters are generally of low significance.

The SYNERGY product contains all the SLSTR Sun-reflective bands except for band S4. Channels S1 and S2 fall in the green and red respectively, and show very similar results to the overlapping OLCI bands Oa06 and Oa08. The same can be said for channel S3, which falls in the NIR and encompasses OLCI Oa17. Unsurprisingly, SWIR channels S5 and S6 show very significant water thickness contribution. Furthermore, S6 is also the SYNERGY channel where the dry matter content contribution is most significant. Consequently, successful inversion of the LFMC cannot disregard these two channels.

Figure 5 contains the total order sensitivity indices of the Sentinel-2 MSI bands. Unsurprisingly, the results align very well with the equivalent OLCI and SLSTR bands. It should be noted that band 10 is used only for aerosol processing purposes, and is not distributed with the S2MSI2A product as it does not contain any surface reflectance information.

Copyright © FirEURisk Consortium. All rights reserved.

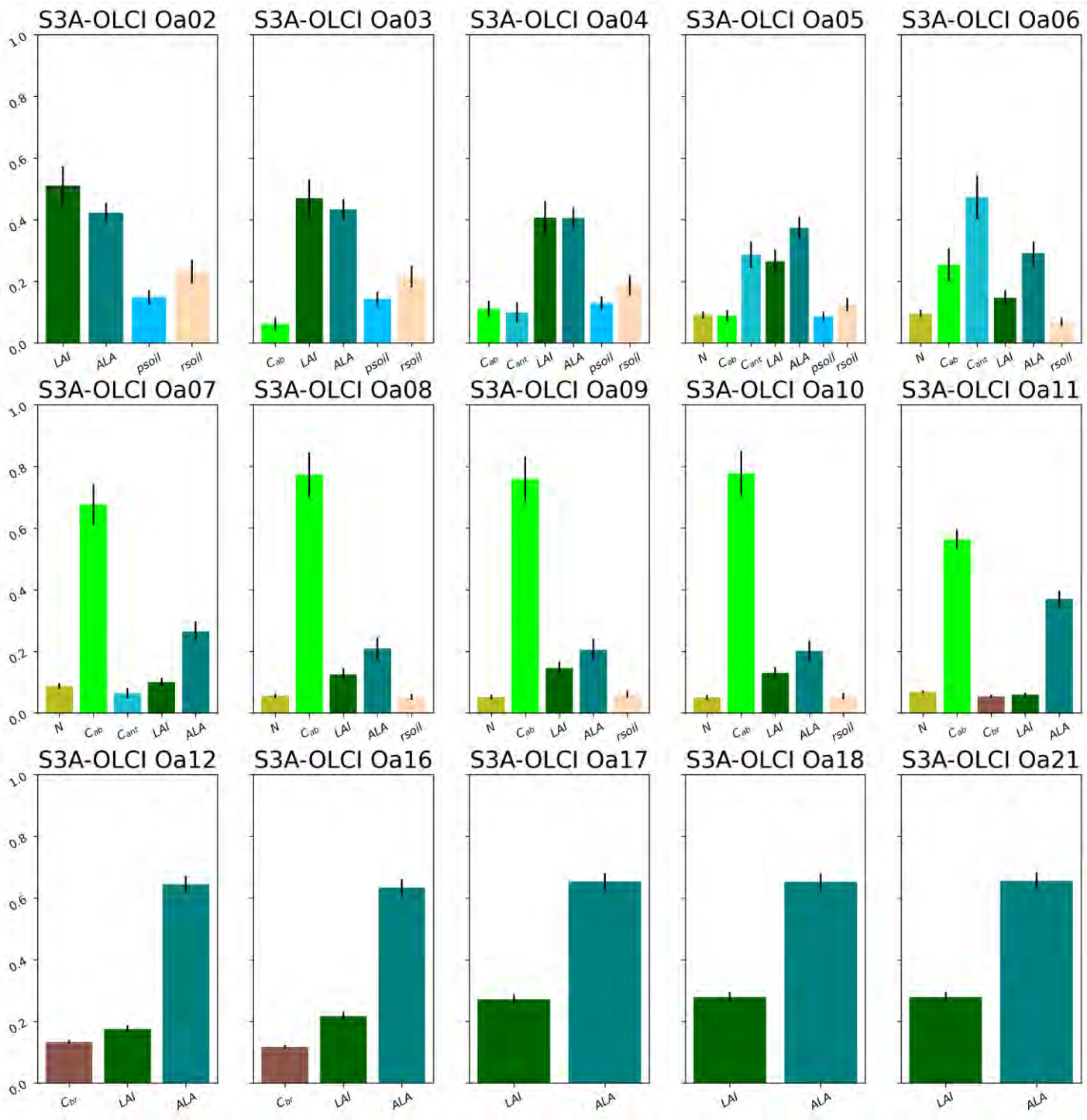


Figure 3: PROSPECT + SAIL GSA in the Sentinel-3 SYNERGY OLCI Channels

Copyright © FirEURisk Consortium. All rights reserved.

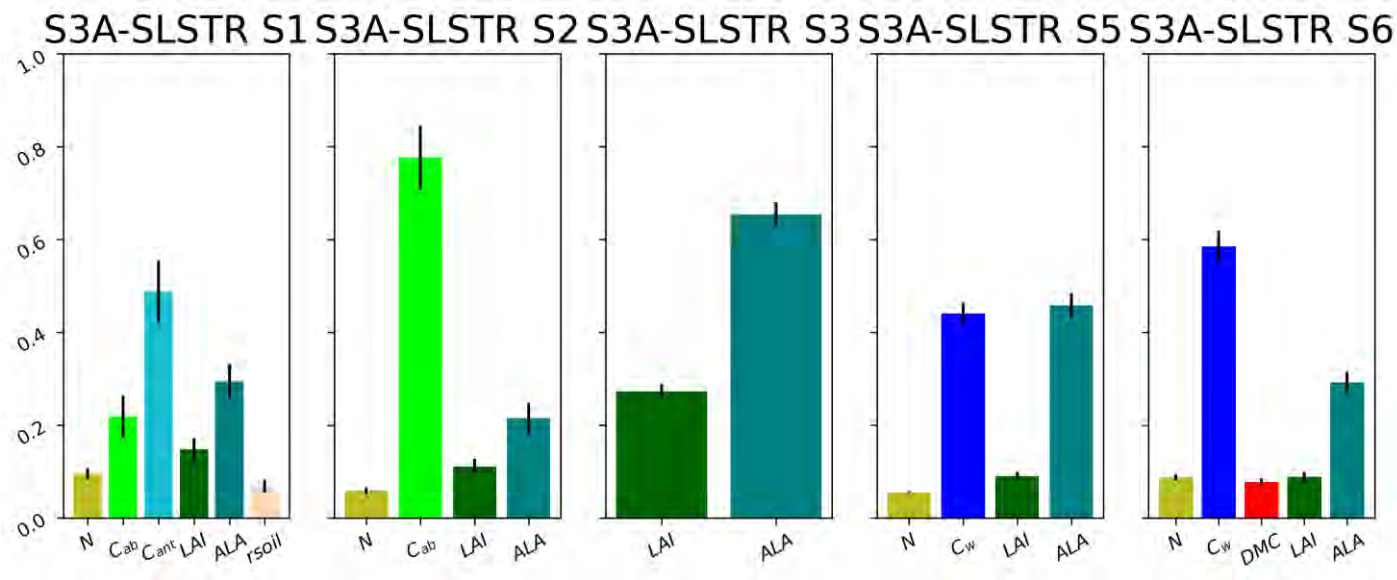


Figure 4: PROSPECT + SAIL GSA in the Sentinel-3 SYNERGY SLSTR Channels

Copyright © FirEURisk Consortium. All rights reserved.

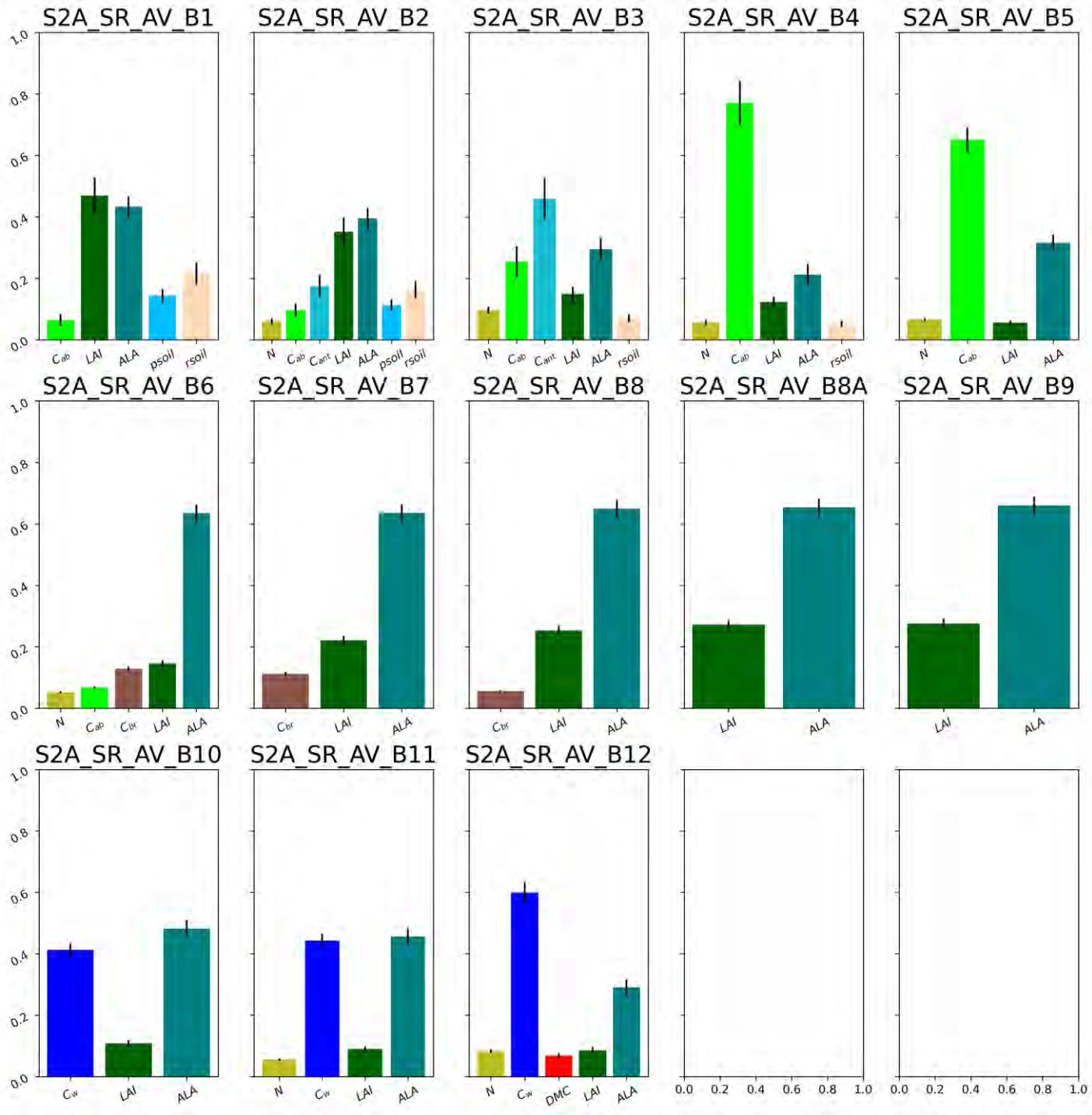


Figure 5: PROSPECT + SAIL GSA in the Sentinel-2 MSI channels

The inversion of the leaf dry matter content is significantly harder than that of the water content due to its lower sensitivity index across the most of the spectrum and in the SYNERGY and MSI channels. This is consistent with the results found in the related scientific literature, which implies that successful inversion of these parameters relies on proper parametrization of the model [1].

Copyright © FirEURisk Consortium. All rights reserved.

The boundaries of the model parameters used for the GSA can be found in table 1.

Symbol	Quantity	Unit	Min-Max	Type
PROSPECT-D				
N	Leaf structure parameter	–	$[1 - 3.0]$	float
C_w	Water concentration	g/cm^2	$[0.0001 - 0.0360]$	float
C_{dm}	Dry matter content	g/cm^2	$[0.0017 - 0.096]$	float
C_{ab}	Chlorophyll concentration	$\mu g/cm^2$	$[0 - 100]$	float
C_{ar}	Carotenoid concentration	$\mu g/cm^2$	$[0 - 10]$	float
C_{ant}	Anthocyanin concentration	$\mu g/cm^2$	$[0 - 40]$	float
C_{bp}	Brown Pigment	–	$[0 - 1]$	float
4SAIL				
LAI	Leaf Area Index	m^2/m^2	$[0.5 - 7.0]$	float
$lidfa$	Average leaf angle	deg	$[0 - 90]$	float
p_{soil}	Soil wetness parameter	–	$[0 - 1]$	float
r_{soil}	Soil brightness parameter	–	$[0 - 1]$	float
Hot	Hotspot parameter	–	$[0.01 - 0.40]$	float

Table 10: Parameter bounds used for the GSA of PROSPECT-D + 4SAIL

2.3.4 Global Sensitivity Analysis of PROSPECT + SAIL + GEO

While the SZA (Sun Zenith Angle) was not included in the sensitivity analysis for the same reasons stated in the PROSAIL case, the VZA (View Zenith Angle) and RAA (Relative Azimuth Angle) have been set to zero, since GEO only supports a nadir viewing geometry. Furthermore, the GSA was conducted for a cylinder shaped crown. For this reason, the additional variables compared to the PROSAIL case will be the crown height-to-width ratio chw and the crown coverage $ccov$. In addition, given the important role of the soil reflectance in this model, we set the soil brightness parameter $rsoil$ to a constant value of 0.3. This allowed us to obtain more useful results from the GSA, since otherwise the soil reflectance would dominate the output, especially in the visible portion of the spectrum.

As expected, the crown coverage $ccov$ has a prominent role in determining the output reflectance, because it directly controls the proportion of radiation that will be associated to the canopy and to the soil. The other additional variable, i.e. the crown height-to-width ratio, is not significant across most of the NIR and SWIR spectrum, and reaches its highest significance values in the visible spectrum in general and in the blue wavelengths in particular. Qualitatively, the considerations made in the previous section regarding the importance of the leaf biochemical parameters still apply here with no significant change, but quantitatively their role is significantly reduced by that of the crown coverage. Another major difference with the previous model combination is the role of the ALA, previously very important in the NIR-SWIR, now insignificant across the entire spectrum due to the prominence of the the crown coverage.

With respect to the PROSAIL case, the LAI has much less influence in the output of the OLCI visible channels, with most of the reflectance being associated to variations in the soil dryness parameter and in the crown coverage. The crown height-to-width ratio is also significant from Oa02 to Oa04. The anthocyanins and chlorophyll concentration take up their usual roles in the blue and green-red wavelengths respectively, while the brown pigment and LAI rise up in importance in the NIR channels.

Copyright © FirEURisk Consortium. All rights reserved.

The SLSTR channels show the usual water thickness prominence in the SWIR channels S5 and S6, but the crown coverage has a strong effect in both channels. In S5 it reaches a higher total sensitivity index than the water thickness itself. Compared to the PROSAIL case, the dry matter content maintains generally higher sensitivity index values.

Similar results can be observed in the Sentinel-2A S2MSI2A channels, where the dry matter content shows up among the significant parameters even in the NIR band B9.

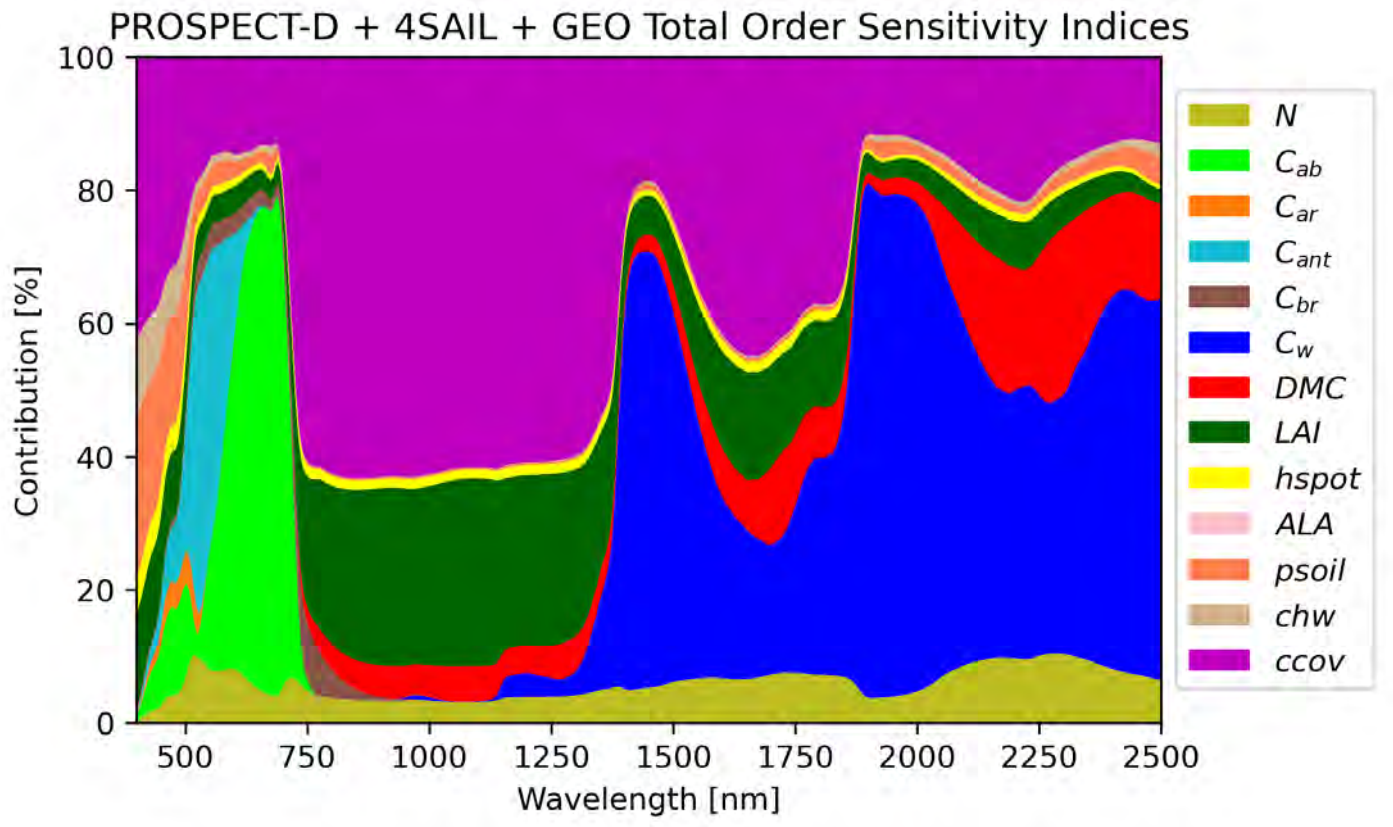


Figure 6: PROSPECT + SAIL + GEO GSA in the entire portion of the spectrum supported by PROSPECT

Copyright © FirEURisk Consortium. All rights reserved.

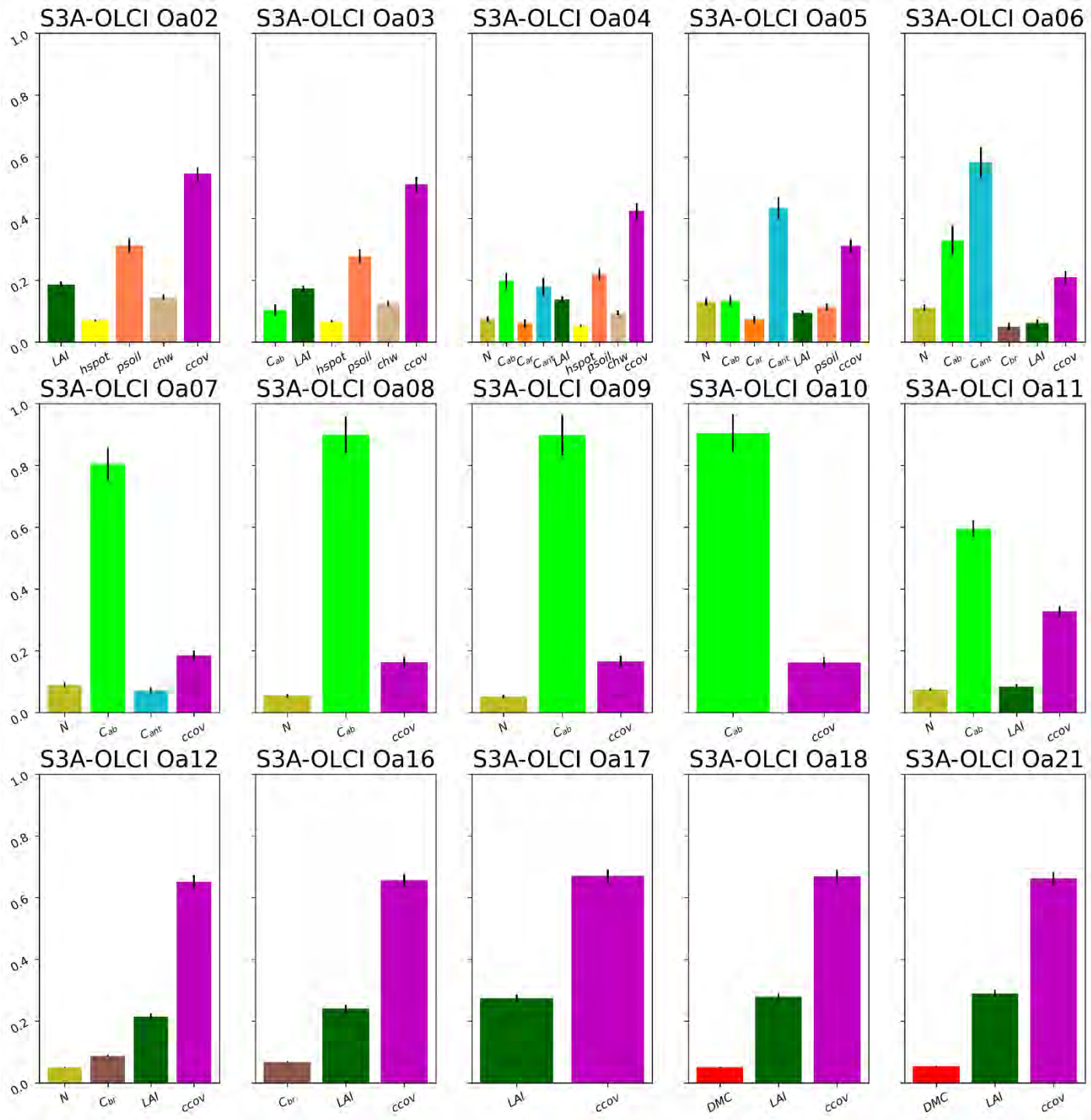


Figure 7: PROSPECT + SAIL + GEO GSA in the Sentinel-3 SYNERGY OLCI Channels

Copyright © FirEURisk Consortium. All rights reserved.

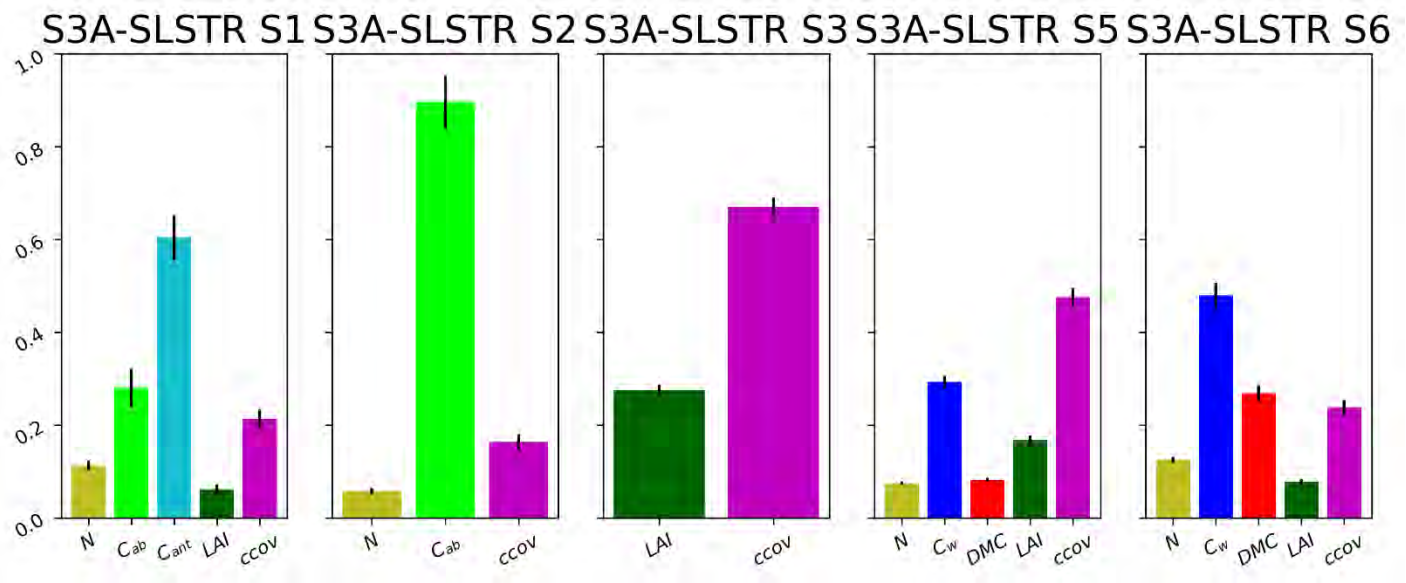


Figure 8: PROSPECT + SAIL + GEO GSA in the Sentinel-3 SYNERGY SLSTR Channels

Copyright © FirEURisk Consortium. All rights reserved.

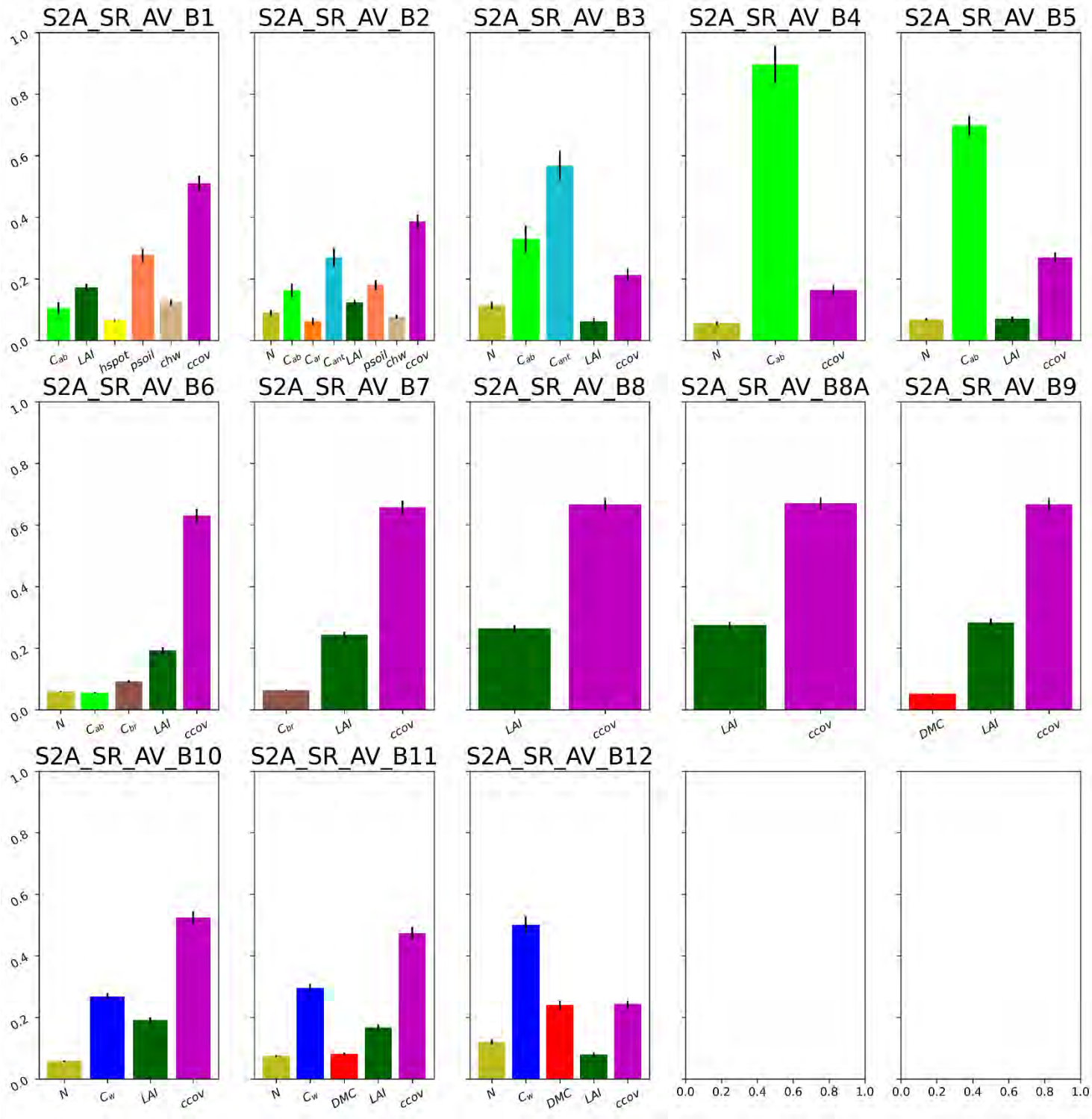


Figure 9: PROSPECT + SAIL + GEO GSA in the Sentinel-2 MSI channels

Copyright © FirEURisk Consortium. All rights reserved.

The parameter boundaries used for this GSA can be consulted in table 2.

Symbol	Quantity	Unit	Min-Max	Type
PROSPECT-D				
N	Leaf structure parameter	–	$[1 - 3.0]$	float
C_w	Water concentration	g/cm^2	$[0.0001 - 0.0360]$	float
C_{dm}	Dry matter content	g/cm^2	$[0.0017 - 0.096]$	float
C_{ab}	Chlorophyll concentration	$\mu g/cm^2$	$[0 - 100]$	float
C_{ar}	Carotenoid concentration	$\mu g/cm^2$	$[0 - 10]$	float
C_{ant}	Anthocyanin concentration	$\mu g/cm^2$	$[0 - 40]$	float
C_{bp}	Brown Pigment	–	$[0 - 1]$	float
4SAIL				
LAI	Leaf Area Index	m^2/m^2	$[0.5 - 7.0]$	float
$lidfa$	Average leaf angle	deg	$[0 - 90]$	float
p_{soil}	Soil wetness parameter	–	$[0 - 1]$	float
r_{soil}	Soil brightness parameter	–	$[0.3]$	float
Hot	Hotspot parameter	–	$[0.01 - 0.40]$	float
GEO				
chw	Crown height-to-width ratio	–	$[1 - 3]$	float
$ccov$	Crown coverage	–	$[0.2 - 1.0]$	float
$cshp$	Crown shape	–	$['cone', 'cylinder']$	float

Table 11: Parameter bounds used for the GSA of PROSPECT-D + 4SAIL + GEO

2.3.4.1 Vegetation Modeling Strategy

The modelling strategy is very similar to that found in Quan, Yebra (2021) [1]: the combination of the PROSPECT+SAIL model has been applied to grassland and shrubland land cover types, while the GEO module, which descends from the Jasinski geometric model, has been applied on top of the two models for the forest land cover types in order to properly describe discontinuous or scattered vegetation. Differently than [1], no grassy understory layer has been included in the forest land cover model. In all three cases, the soil model consists in a mix of a dry and a wet soil spectrum.

The software used to run the simulations is based on the jgomezdans/prosail Python bindings. However, since there existed no Python bindings for the Jasinski geometric model, this repository has been forked and the related functionality has been implemented *ex novo* by porting the relevant portions of the Geosail FORTRAN code. The forked repository can be consulted at valpamp/progeosail and freely cloned and edited.

2.3.5 Model Inversion Strategy

Among the many possible inversion methods, those based on LUTs are often cited as the most straightforward and mathematically simple. Assuming that the observation space is sufficiently sampled, they guarantee to avoid converging to local minima. Nevertheless, it is well known that the inversion of the PROSAIL family of models is ill-posed and under-determined: different combinations of variables may lead to relatively similar spectra, confusing the inversion process. Therefore, it is of paramount importance to avoid combining the model parameters into unrealistic scenarios, that may result in a valid spectrum, but will not naturally occur in the target environment and will only worsen the inversion results. For this purpose, we applied the ecological rules proposed by Quan, Yebra (2021) [1] to discard unrealistic parameter combinations. Once the target number of spectra is set, the LUT compilation algorithm randomly aggregates variables and checks them using the ecological rules. The combinations

Copyright © FirEURisk Consortium. All rights reserved.

that pass all the checks are then saved into the LUT and later used to calculate the reflectance spectra, while the ones that do not are discarded. This process is repeated until the target sample number is reached.
Finally, the resulting LUT spectra are convolved into the sensor Spectral Response Functions (SRFs) to simulate the measurements that would be acquired by that specific sensor if it were to point at the modelled vegetation. In the Sentinel-3 case, the SRFs can be found on the Copernicus website both for OLCI and SLSTR, and for each of the satellites of the constellation.

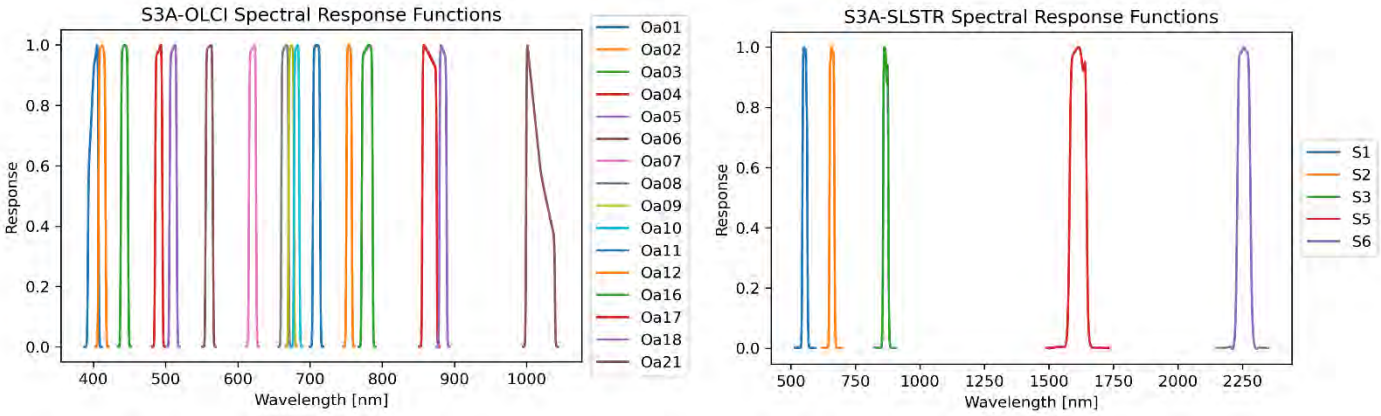


Figure 10: S3A-OLCI (left) and SLSTR (right) spectral response functions.

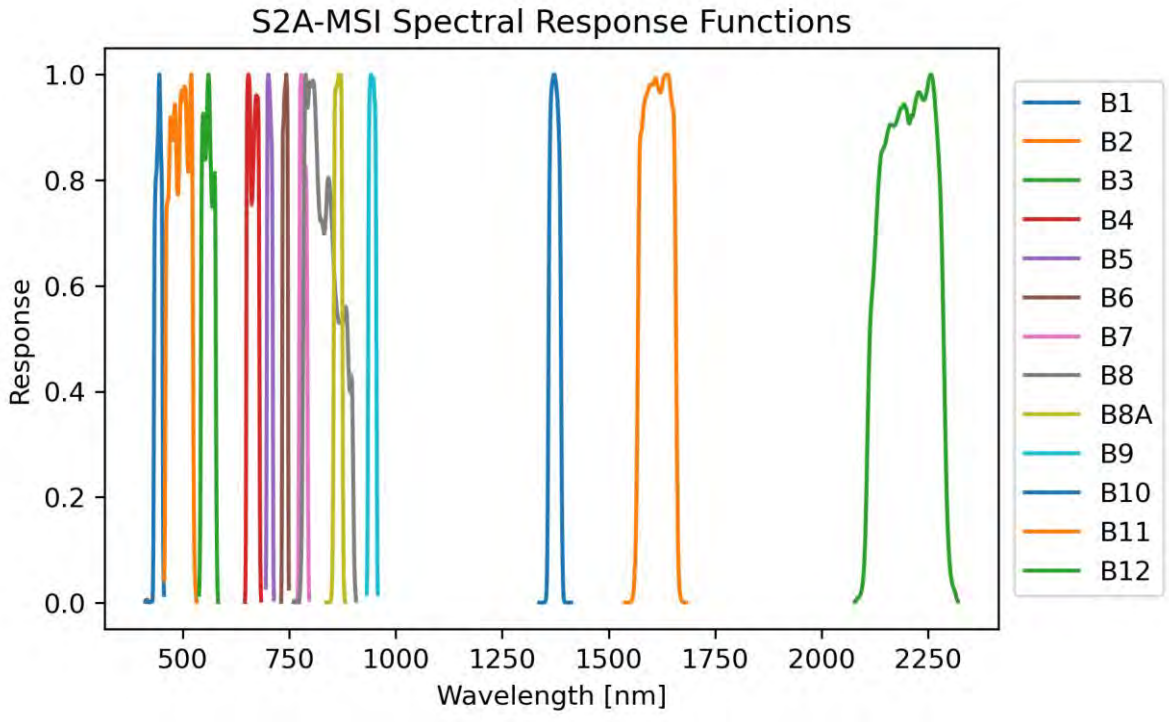


Figure 11: Sentinel-2A MSI spectral response functions

In addition to the procedure described in [1], the LUTs are re-calculated at each satellite passage depending on the average SZA of the passage. In the Sentinel-3 case, the SZA varies about 8 degrees around the mean value. For this reason, each LUT associated to the mean SZA will be generated using an uniform distribution centred around the mean SZA and varying between $SZA - 8°$ and $SZA + 8°$.

Copyright © FirEURisk Consortium. All rights reserved.

In the Sentinel-2 case, the mean SZA declared in the product XML is used to generate the LUT.

2.3.6 Optimal Inversion Parameters

The solution, which consists in a tuple of biophysical parameters which is assumed to be the best possible candidate to generate the measured spectrum according to the LUT, can be determined by a number of different inversion parameters. Quan, Yebra (2021) [1] contains an extensive analysis of the following inversion parameters:

- **Amount of spectral information**: number of spectral channels or vegetation indices used to compare the measured spectra to the LUT spectra.
- **Cost function**: different cost functions can be used to extract an arbitrary amount of spectra closest to the measured one.
- **Percentage of selected solutions**: the LFMC value resulting from the LUT inversion can be extracted by weighing a certain amount of closest spectra.
- **Measures of central tendency**: once a certain amount of closest spectra has been isolated, different measures of central tendency can be used to determine the optimal solution.

For each of the four inversion parameters, we proceeded by setting to a fixed value all the other three, inverted the LFMC values and compared the results with the field data provided by ADAI and CNR. This procedure relies on the assumptions that the four inversion parameters are independent of each other in determining the solution.

It should be noted that this procedure was applied previously to simulated data to obtain the results shown in Pampanoni et al. (2021a) [2]. The results obtained with the simulated data largely translated to the ones obtained with the field data, which we will show in the following paragraphs. Since the runs on PROSPECT + 4SAIL and PROSPECT + 4SAIL + GEO resulted in the same conclusions, we will only present the results on the PROSPECT + 4SAIL in this document for the sake of brevity.

LFMC data for the validation has been provided by ADAI, CNR and TUD. The TUD measurement campaign started in 2022, and therefore the number of data points was not sufficient to build a dataset large enough for the purposes of a validation. Hereafter we will show the results of the inversion on the Portuguese Lousa site, with data gathered by ADAI from 2018 to April 2022, and CNR data from the same period over the Capo Caccia site.

In both cases, the measured LFMC timeseries were compared with the Sentinel-2 and Sentinel-3 based estimates. The estimated and measured timeseries are aligned using the Pandas aligning tool in order to obtain daily values for both timeseries, since in both cases we do not necessarily have a daily sampling frequency.

Firstly, the estimated timeseries were used as is, and then they were smoothed using a rolling average algorithm with varying window size. In general, using the rolling mean of the estimated timeseries improves the correlation significantly. The improvement is noticeable from a window size of 3 measurements onwards, and improves up until around a window size of 7. Increasing the window size past 7 seems to bring no further improvement, until past the 10 mark the correlation starts to worsen.

The LFMC values and the graphs shown in the following paragraphs were all post-processed using this methodology.

Copyright © FirEURisk Consortium. All rights reserved.

2.3.7 Dataset 1: Lousa, Portugal (ADAI)

The ADAI dataset contains daily LFMC values for two tree species (*pinus pinaster* and *eucalyptus globulus*), and two shrub species (*calluna vulgaris* and *chamaespartium tridentatum*). The measurement campaign started in 1996 and continued uninterrupted until today. The measurements are gathered with different frequency depending on the time of the year: less frequently in the winter, and more frequently - even daily - during the fire season. In our case, we used the portion of this dataset that started on October 2018 and ended on April 2022.

The sampling area corresponds to a singular Sentinel-3 pixel, which is cut roughly in the middle by a road. This implies that the pixel is not perfectly homogeneous. In addition, at the moment our model is not capable of mixing spectra of trees and shrubs. Nevertheless, since both the Corine Land Cover and the ESA WorldCover classified this area as forested, we decided to focus on the two tree species.

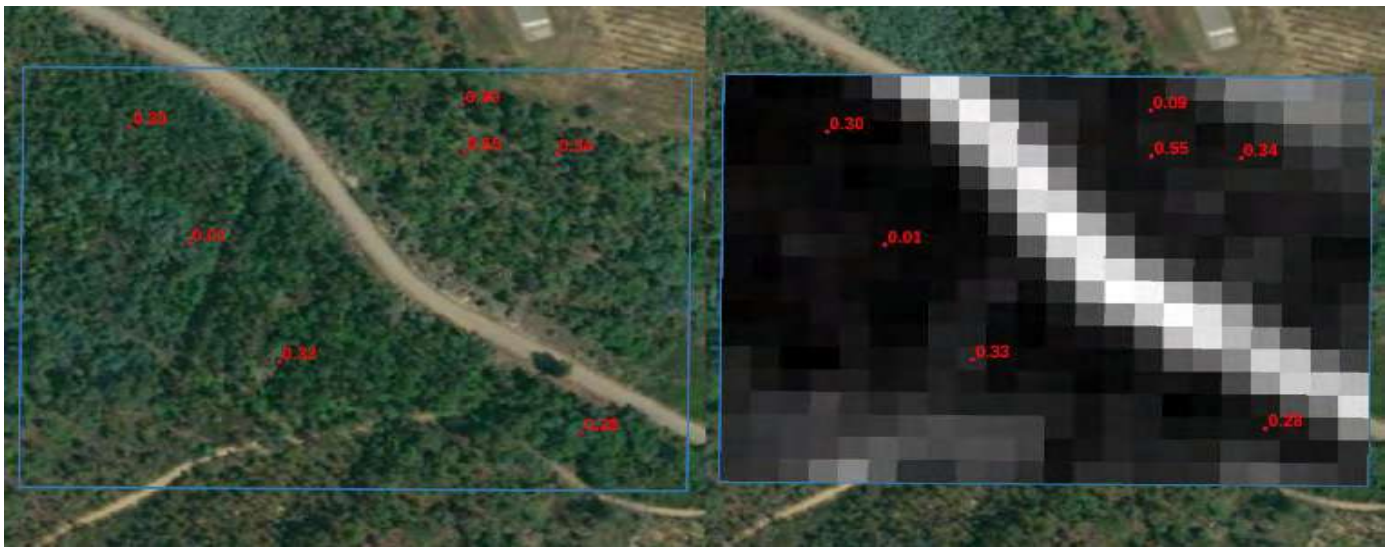


Figure 12: Bing Satellite map of the Lousa sampling site, roughly delimited by the blue rectangle. The red dots mark the Sentinel-2 pixels used for the validation, and the associated value represents the coefficient of determination of the estimated timeseries with respect to the average dataset.

After comparing a few estimated LFMC timeseries with the measurements, it became apparent that our estimates progression matched more closely the *pinus pinaster* measurements than the *eucalyptus globulus*. Even averaging the two measured timeseries, the correlation proved to be significantly worse than that with the sole *pinus pinaster*. Therefore, we will only show the results pertaining to this species. The right side of Figure 9 shows the Sentinel-2 pixels used for this validation and the associated coefficient of determination R^2, calculated by comparing the "predicted" LFMC values estimated with our procedure and the "true" values measured with by ADAI. For the sake of brevity, only the final results will be reported hereafter.

2.3.8 Dataset 2: Capo Caccia, Sardinia, Italy (CNR)

Capo Caccia is located in the North-Western part of Sardinia, and the sampling site shown in Figure 11 has been used by CNR since the early 2010s, with weekly or bi-weekly measurement campaigns. The local vegetation is dominated by *juniperus phoenicea*, with a smaller but significant presence of *pistacia lentiscus* and *phillyrea*

Copyright © FirEURisk Consortium. All rights reserved.

angustifolia. Other species worth mentioning are *cistus monspeliensis* and *rosmarinus officinalis*, which are more sensitive to seasonal changes, especially during the summer.
The dataset provided by CNR contains the raw measurements of the dominant species, i.e. the *juniperus*, and a timeseries of the average of all the aforementioned species, *juniperus* included.

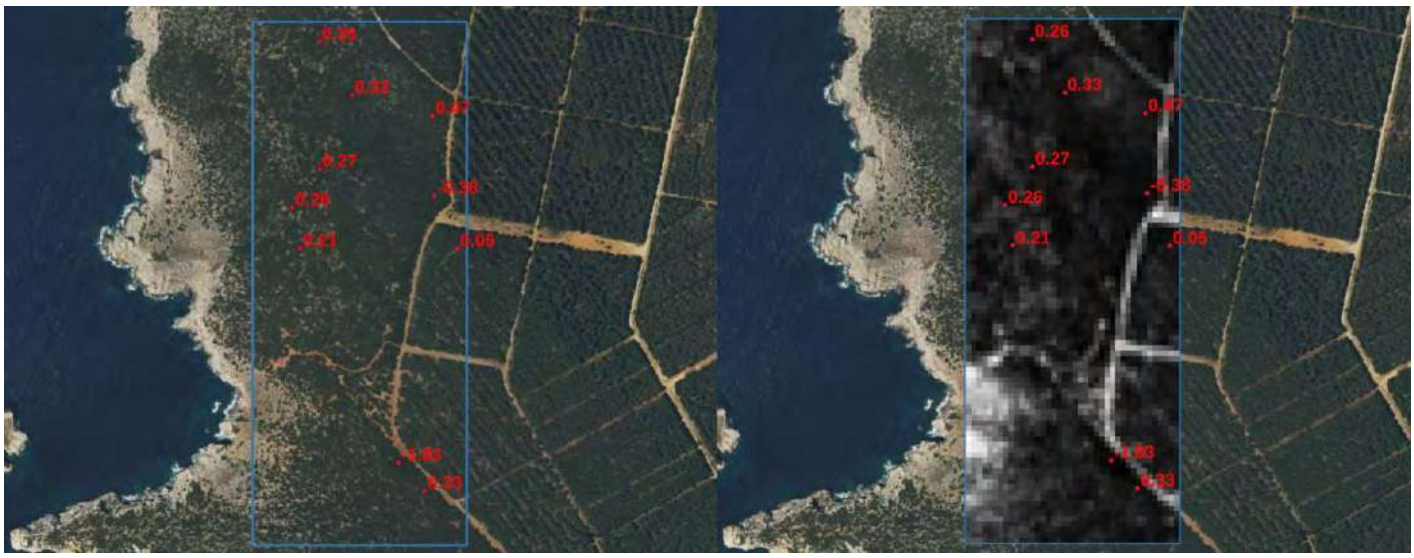


Figure 10: Bing Satellite map of the Capo Caccia sampling site, roughly delimited by the blue rectangle. The red dots mark the Sentinel-2 pixels used for the validation, and the associated value represents the coefficient of determination of the estimated timeseries with respect to the average dataset.

Copyright © FirEURisk Consortium. All rights reserved.



Figure 13: Bing Satellite map of the Capo Caccia sampling site, roughly delimited by the blue rectangle. The red dots mark the Sentinel-3 pixels used for the validation, and the associated value represents the coefficient of determination of the estimated timeseries with respect to the average dataset.

2.3.9 Extraction of the Optimal Inversion Parameters

2.3.9.1 Amount of Spectral Information

Quan, Yebra (2021) [1] shows clearly how using all the spectral channels for the inversion, while being certainly more performant than using any singular channel, is not the optimal in terms of the LFMC inversion due to the well-known ill-posedness of the inversion problem. While in Quan, Yebra (2021) [1] 12 different vegetation indices were ranked alongside the individual channels, in our case we made use of the results of the GSA, to rank the channels most sensitive to the water content C_w and the dry matter content C_{dm}. We started with at least two channels, and then added spectral information and verified whether or not the coefficient of determination r^2 between the estimated and real C_w , C_{dm} and LFMC values increased or decreased. In case it increased, the spectral information was kept in the inversion procedure, otherwise it was excluded. This procedure was used to determine the best performing Sentinel-2 and Sentinel-3 bands. Unsurprisingly, the largest boost in performance comes from using the SWIR bands, which are most sensitive to the leaf water content C_w but also tend to be the most sensitive to the dry matter content C_{dm}. For the sake of brevity, we will only report the best performing channel list for the two surface reflectance products:

Product	Channels
Sentinel-2 S2MSI2A	2, 8, 11, 12
Sentinel-3 SY_2_SYN	Oa06/SYN06, S3N/SYN19, S5N/SYN20, S6N/SYN21

Copyright © FirEURisk Consortium. All rights reserved.

Table 12: list of the best performing channels of the Sentinel-2 S2MSI2A and Sentinel-3 SY _2_SYN for the inversion of the LFMC

The product names in table 3 contain hyperlinks to the respective product spectral resolution specifications on the ESA Copernicus website.

2.3.9.2 Cost Function

Among the many cost functions tested in Quan, Yebra (2021) [1], we only compared the performance of the Root Mean Square Error function ($RMSE_f$), the exponential function, and the Bhattacharya Divergence.

Cost Function	Formula	R^2 Lousa	R^2 Capo Caccia
RMSE	$\sqrt{\sum_{i=1}^{n}\frac{(v_i - x_i)^2}{n}}$	0.47	0.76
Bhattacharya Divergence	$-\ln\left\{1+\sum_{i=1}^{n}\left(\sqrt{v_i w_i - \frac{v_i + w_i}{2}}\right)\right\}$	0.19	0.74
Exponential	$\sum_{i=1}^{n}\left\lvert w_i\left(\exp\left\{-\frac{v_i - w_i}{v_i}\right\}\right)\right\rvert$	0.53	0.74

Table 13: LFMC retrieval performance with different cost functions on the ADAI and CNR dataset

Where we denote the measured reflectances as v_i, the LUT stored reflectances as w_i and the number of involved channels as n. The RMSE and the Bhattacharya show very similar performance, while the exponential function performs slightly worse in Capo Caccia and slightly better in Lousa. Even on a point-by-point basis, the exponential function and RMSE tend to give rather similar results, making it difficult to identify a best performer. This is not surprising, since even in Quan, Yebra (2021) [1] the two functions show comparable performance.

2.3.9.3 Number of Selected Solutions

N	R^2 Lousa	R^2 Capo Caccia
20	0.55	0.76
50	0.55	0.76
100	0.48	0.75

Table 14: LFMC retrieval performance with an increasing number of selected solutions. The N selected solutions are those that minimize the chosen cost function

The performance of the inversion worsens after the 30-40 mark, while the optimum seems to always be located between 15 and 25 closest spectra.

2.3.9.4 Measures of Central Tendency

Compared to Quan, Yebra (2021) [1], only the arithmetic mean and median have been tested. In the referenced article, the performance differences between the six tested functions are marginal for grasslands, and more significant for shrublands and forests. The median seems to work best overall, and in particular for forests and shrublands. Our tests, summarized in table 6 confirm result.

Function	R^2 Lousa	R^2 Capo Caccia

Copyright © FirEURisk Consortium. All rights reserved.

mean	0.27	0.55
median	0.48	0.76

Table 15: LFMC retrieval performance using different measures of central tendency to harmonize the selected solutions

In general, on a point-by-point basis, changing the measure of central tendency may improve or worsen the results, but on average the results seem to improve consistently by using the median.

2.3.9.5 Final Inversion Parameters

After these tests, the following parameters have been set and used to generate all the project datasets:

Inversion Parameter	Value
Number of Selected Solutions	20
Cost Function	RMSE
Measure of Central Tendency	median

Table 16: inversion parameters used to generate the LFMC estimates

2.3.10 Validation

In this paragraph we will show the results of the validation using the optimal inversion parameters identified in 3.4.5. We reiterate that the estimated timeseries extracted using Sentinel-2 or Sentinel-3 data are then smoothed using a moving average algorithm with a 7-sample window.

2.3.10.1 Lousa Dataset

As mentioned in 3.2, the estimated timeseries follow rather closely the *pinus pinaster* measurements, while a significant bias persists if we compare the estimated timeseries to the *eucalyptus globulus* measurements and to a lesser extent to the average of *pinus* and *eucalyptus* measurements. Therefore, we used the *pinus pinaster* both for identifying the optimal inversion parameters and the validation. The 7 Sentinel-2 points used for the validation are shown in Figure 9, and were selected to avoid road pixels and mixed pixels and privileging more densely tree-covered areas in order to minimize spurious contributions to the reflectance.

If we compare the individual pixel timeseries with the *pinus pinaster* measurements the best performing pixel reaches a coefficient of determination R^2 of 0.55, while the worse performing shows an R^2 of 0.01.

If we average the timeseries of the seven pixels, i.e. if we generate another timeseries by aggregating the daily mean of the LFMC estimates, we obtain the result shown in Figure 11, with a satisfying R^2 of 0.47: this value, while not higher than the 0.55 of the individual best performer, is significantly higher than all the other six measurement points.

Copyright © FirEURisk Consortium. All rights reserved.

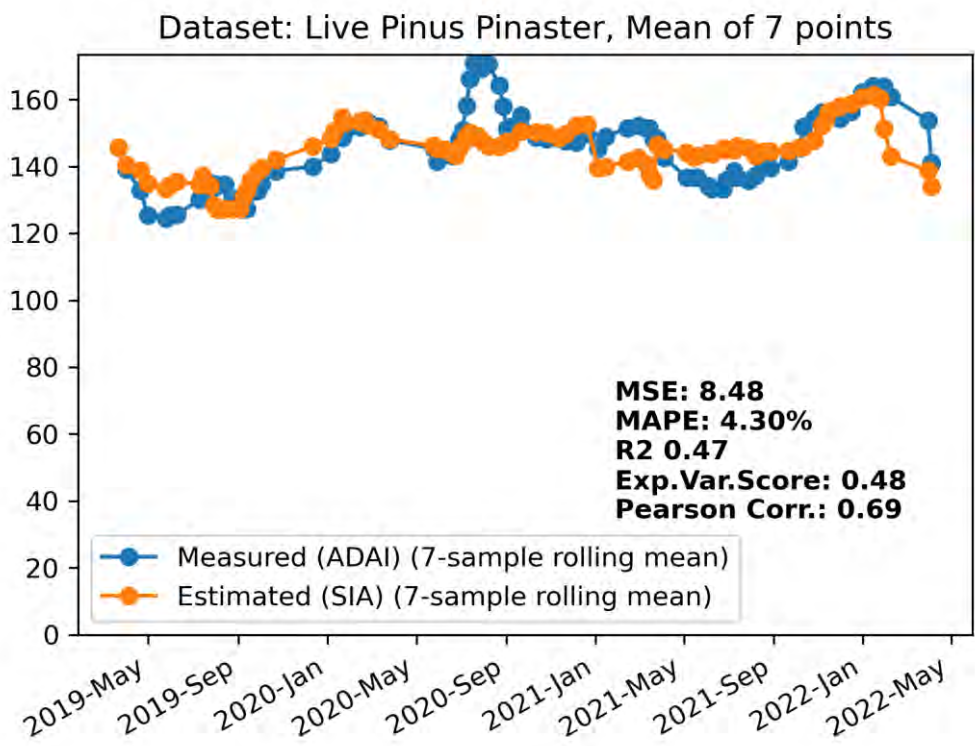


Figure 14: average of the 7-day rolling mean timeseries of the Sentinel-2 points shown in figure 9 (orange) and ADAI pinus pinaster measurements (blue).

2.3.10.2 Capo Caccia Dataset

In this case, the LFMC estimated timeseries follows more closely the measured dataset of the average of all the sampled species. The higher homogeneity and larger size of the sample site compared to the Lousa one allowed us to obtain an extremely high coefficient of determination with respect to the values usually found in the literature.

Figure 12 shows the progression of the average of the estimated timeseries of the ten Sentinel-2 points shown in Figure 10. The coefficient of determination is much higher than that of the individual point timeseries, reaching a value of 0.76.

The homogeneity and size of this site allowed us to obtain good correlation even with the 300 meter Sentinel-3 pixel size: if we compare the average timeseries extracted from the four Sentinel-3 pixels that overlap the sampling area, we obtain an R^2 of 0.42. This value, and the RMSE shown in Figure 16 are comparable with the ones found in Quan, Yebra (2021) [1] for the shrubland land cover.

Copyright © FirEURisk Consortium. All rights reserved.

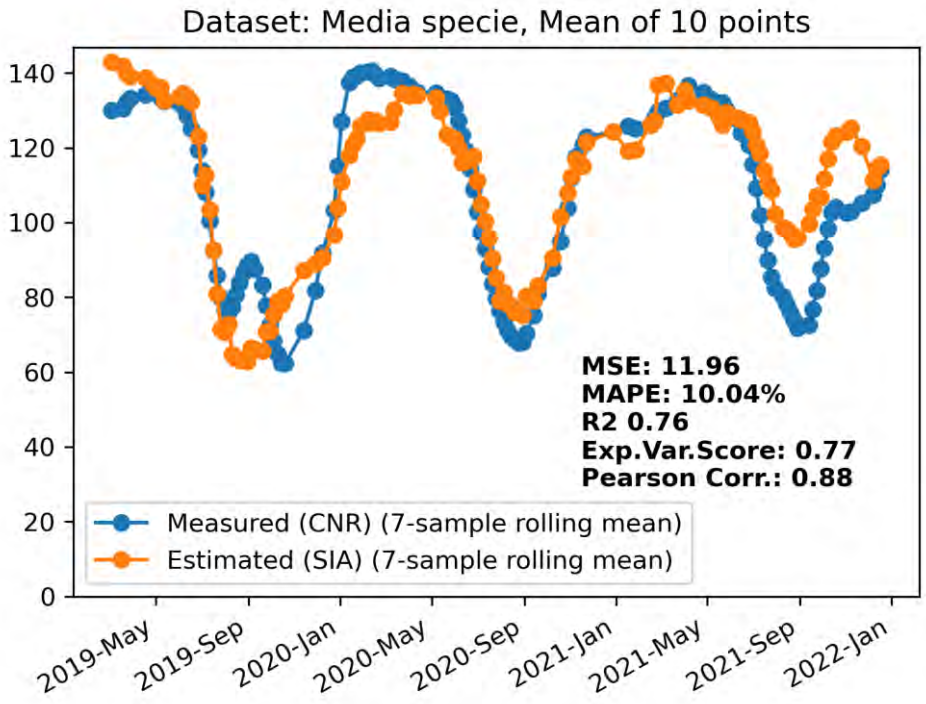


Figure 15: average of the 7-day rolling mean timeseries of the Sentinel-2 points shown in figure 10 (orange) and CNR average species measurements (blue).

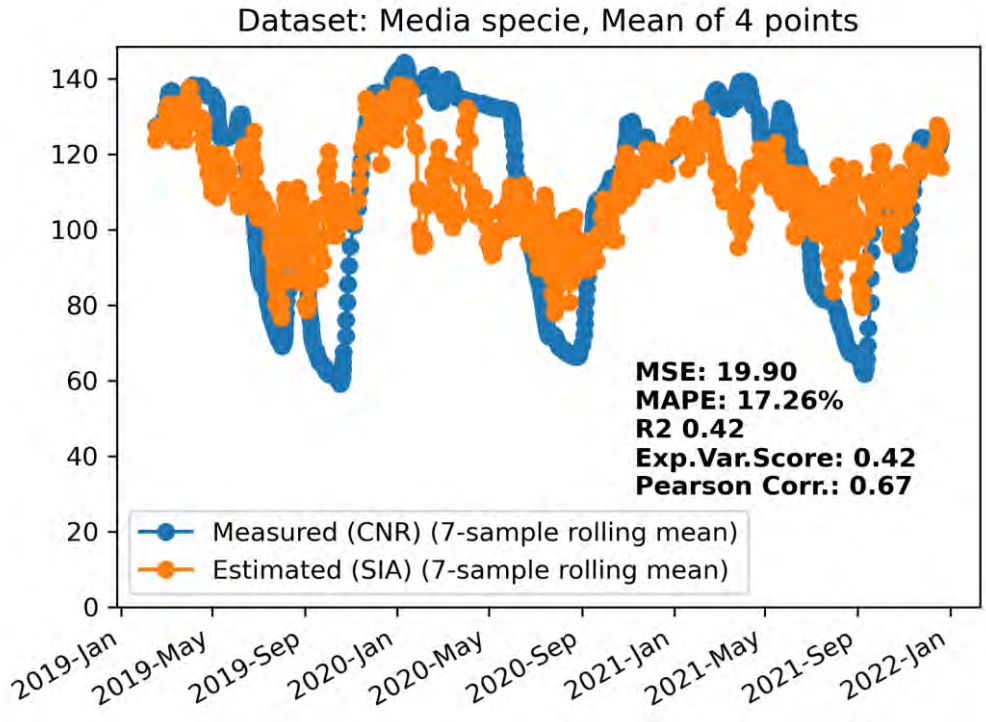


Figure 16: average of the 7-day rolling mean timeseries of the Sentinel-3 points shown in figure 11 (orange) and CNR average species measurements (blue).

Copyright © FirEURisk Consortium. All rights reserved.

2.3.11 Product Description: Live fuel moisture content map (ET)

- **Format:** Live-fuel moisture content climate archive is a geospatial product in .nc format and in percentage units at European Territory scale. The temporal coverages are from 1988 to 2020.
- **Resolution:** 0,25º.
- **Access:** Data can be accessed by direct download from:
- https://fireurisk.satways.net/datasets/62d5272ce4b0b33bb117af5c
- **Projection:** ETRS89-extended / LAEA Europe
- **Description:** The product allows to investigate the long-term coarse-scale live-fuel moisture content derived from integrating passive microwave satellite observations of vegetation optical depth with in-situ measurements for the European territory. The final output – geospatial netCDF dataset with the daily time step (scale: %) and spatial resolution of 0.25°. Developer: Technische Universitaet Dresden. The product developed within the Activity "A1.1.1 Fire weather and fuel status prevention". The product interprets LFMC as a weighted combination of vegetation optical depth estimated from passive microwave satellite observations and leaf area index within a logistic regression. The derived dataset is calibrated with the Globe-LFMC database and validated with the Globe-LFMC database as well as the MODIS LFMC based on the approach by Yebra et al. (2018). The accuracy of the global product is estimated with a RMSE of ca. 49%. The relative uncertainty of each pixel can be estimated from the provided variables LFMC_max and LFMC_min which represent the maximum and the minimum LFMC estimation of the model per grid cell and time step. Detailed description of algorithm of calculation and data sources available here: https://hess.copernicus.org/preprints/hess-2022-121/.

Contact: In case of doubts and/or suggestions, forward an email to Luisa Schmidt (luisa.schmid1@tu-dresden.de).

2.3.12 Product Description: Live fuel moisture content map (PS)

This product is based on the inversion of Look-Up Tables (LUT) created using a combination of the PROSPECT-D, 4SAIL Radiative Transfer Models (RTM) and a modified version of Huemmrich's GeoSail, and convolving the calculated reflectances in the Sentinel-3 SYNERGY channels. The LUTs used change depending on the land cover type: PROSPECT-D and 4SAIL are used for grasslands and shrublands, while for forests the 4SAIL output is fed into the Geo component to simulate discontinuous vegetation. The LUT compilation and inversion procedure is very similar to the one described in the following papers:

In addition, the LUTs are calculated at each satellite overpass depending on the Sun Zenith Angle interval. A GSA of the RTM used for the inversion and a partial validation on simulated observations is available in (Papmpanoni et al., 2022)

Copyright © FirEURisk Consortium. All rights reserved.

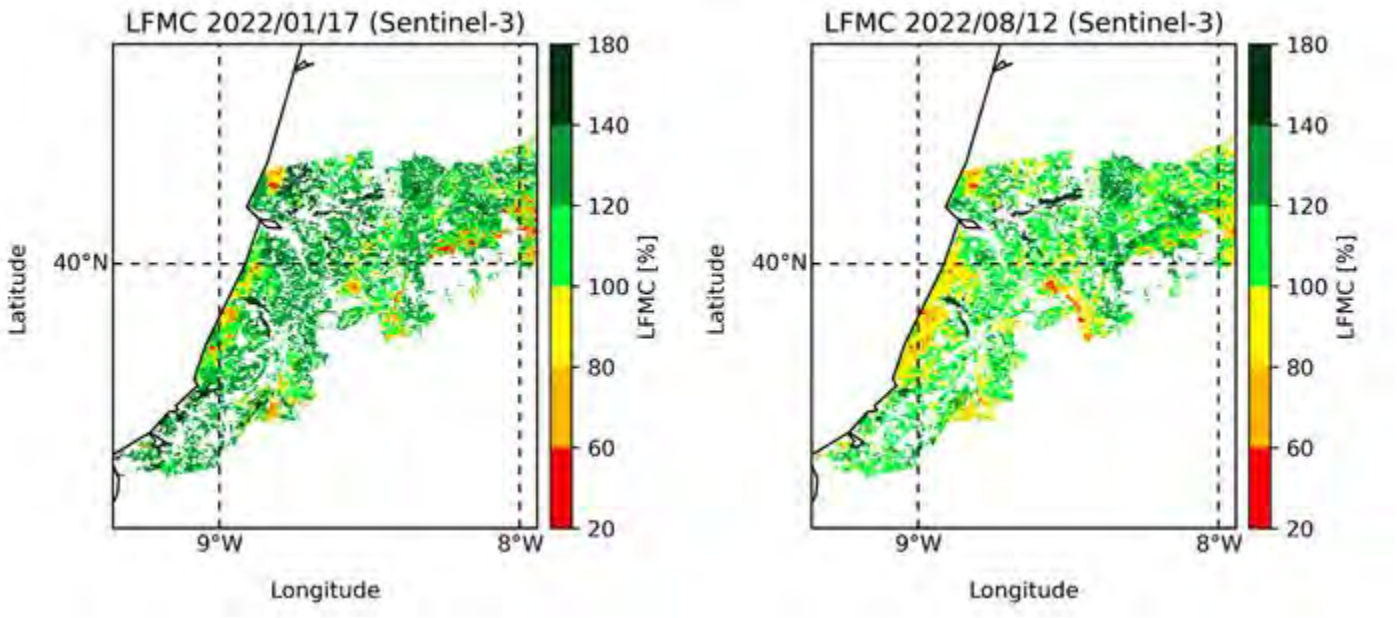


Figure 17: Example of product output on PS3 (Portugal) on January 17th and August 12th.

- **Format:** Live Fuel Moisture Content is a geospatial product in two different formats (.tiff and .nc), and it represents the moisture content in percentage (%). The update frequency is daily (depending on the availability of satellite observations). The temporal coverage is from October 2018 till the today.
- **Resolution:** 300 m.
- **Projection:** ETRS89-extended / LAEA Europe
- **Access:** Data can be accessed by direct download from: **PS Live Fuel Moisture Content:** https://fireurisk.satways.net/collection/6319b707e4b0b33bb11986d4
- **Description:** Live Fuel Moisture Content estimates derived from the Sentinel-3 SYNERGY product using the PROSAIL and PROGEOSAIL models.
  The SYNERGY SY_2_SYN____ product has a 300 meter resolution, and this collection means to cover the entire time series offered by ESA Sentinel API, which starts in October 2018. The SYNERGY product masks bad pixels and cloudy pixels, and the resulting imagery is cropped onto a land cover in order to include only grassland, shrubland and forest pixels.
  This collection covers all the project Pilot Sites, and is updated monthly using the latest Sentinel-3 SYNERGY observations. Two separate files are provided for each of the Sentinel-3 satellites S3A and S3B for each PS dataset.
- **Contact:** In case of doubts and/or suggestions, forward an email to Giovanni Laneve (Giovanni.laneve@uniroma1.it) and Valerio Pampanoni (valerio.pampanoni@uniroma1.it).

2.4 Fire weather danger rating indices

2.4.1 Rationale

The goal was to develop a novel fire danger metric that jointly captures dead fuel moisture content and atmospheric instability. Current fire danger metrics do not often include atmospheric instability as a component. At the same time, studies focused on surface properties often report vapor pressure deficit and/or indicators of dead fine fuel

Copyright © FirEURisk Consortium. All rights reserved.

moisture as the best indicators of fire danger. Here we seek to combine both approaches: predictions of dead fine fuel moisture and atmospheric instability. The analysis of the 2022 extreme fire season in SW Europe has shown that currently used indices, like HDW or C-Haines were not always at very high values during the mega-fires (>5,000ha) of the last season (Rodrigues et al. 2023). We argue this was because surface hot conditions do not always indicate high atmospheric instability or wind. Consequently, here we move beyond previous approaches by jointly addressing surface conditions and atmospheric instability.

2.4.2 Approach and Methods

Previous research has shown that vapor pressure deficit is a key indicator of dead fuel moisture content (Resco de Dios et al. 2015). At the same time, atmospheric instability can be measured as a first approximation from the difference in temperature at 700 and 850hPa (Haines 1988).

We thus developed the Hot-Dry-Unstable Index (HDI), which as two components:

1) VPD: vapor pressure deficit (kPa) as an indicator of dead fuel moisture content.
2) Atmospheric Component (AC): the difference in temperature (ºC) between 700 and 850hPa

The HDU (kPa ºC) is thus defined as:

HDU = VPD + AC/2

The range of variation in AC (~ 16ºC) was twice that of VPD (~8 kPa). We thus divided AC by 2, in order to place equal weight to AC and VPD. We tried different formulations (not shown) and the summation between AC/2 and VPD yielded best results. It is worth clarifying that we did not seek to transform VPD into dead fuel moisture content (DFMC). In the current formulation of the HDU index, increasing VPD and increasing AC both indicate increasing fire weather. If we had used DFMC instead, then we would hav had to apply some re-scaling to the data which was considered negative because that hinders data interpretation. That is, higher DFMC indicates less fire danger, while higher AC indicates worst fire danger, and re-scaling would have been necessary.

We assessed the performance of HDU at the whole European territory. The analysis was performed individually for forest fires (>20% of burned area in semi-natural landscapes excluding crops and urban areas) within the different biomes occurring in Europe (https://ecoregions.appspot.com). Burned area came from the GlobFire dataset (Artés et al. 2019), which is based on MODIS (MOD64A1 burned area product) and meteorological data from ERA5 (Hersbach et al. 2020). The study period ranged from 2001-2021.

Non-linear relationships between burned area and HDU were assessed through segmented regression, to identify critical break points. We first examined the quantile of fire size at different HDU intervals pre-defined in the segmented regression for the whole European Territory. We then performed a more detailed analysis at biome level, for each of the different biomes within the EU. We excluded the tundra biome from the biome analyses given the paucity of fires in that area (8 fires in the study period).

2.4.2.1 Results

We observed that there was a clear association between HDU and fire size at European scale, with increasingly large fires occurring at larger HDU values. There was a non-linear relationship between cumulative burned area and HDU, with different break points occurring at HDU values of 5.5kPaºC and 11.2 kPaºC, respectively (Fig. 1). The median, 0.75 and 0.95 quantiles in fire size for fires occurring with HDU <5.5kPaºC were 86, 215 and 838 ha, respectively (Table 17). These values raised to 150, 365 and 1525, respectively for fires occurring under HDU between 5.5-11.2kPaªC. And when HDU was above 11.2kPa, the values of fire size at 0.5,0.75 and 0.95 quantiles were 279, 752 and 4126 ha, respectively.

Copyright © FirEURisk Consortium. All rights reserved.

We then examined variation across the different biomes and we similarly observed that the 0.5, 0.75 and the 0.95 quantiles of fire size increased at each of the different HDU break points (Table 17). There were, however, some exceptions. In particular, in biomes 5 (temperate conifer forests) and 8 (temperate grasslands), there was no clear association between different HDU threshold values and fire size.

There are different reasons explaining why HDU could be of limited value at these biomes. In the case of the conifer biome, it is worth noting this is a cold limited ecosystem with the smallest area burned within Europe. In this case, VPD reached a maximum value of about 3 (Figure 18), while AC reached maximum value of 8 (Figure 18). Consequently, HDU minimizes the influence of VPD and maximizes that of AC, and this likely created the problem we have documented.

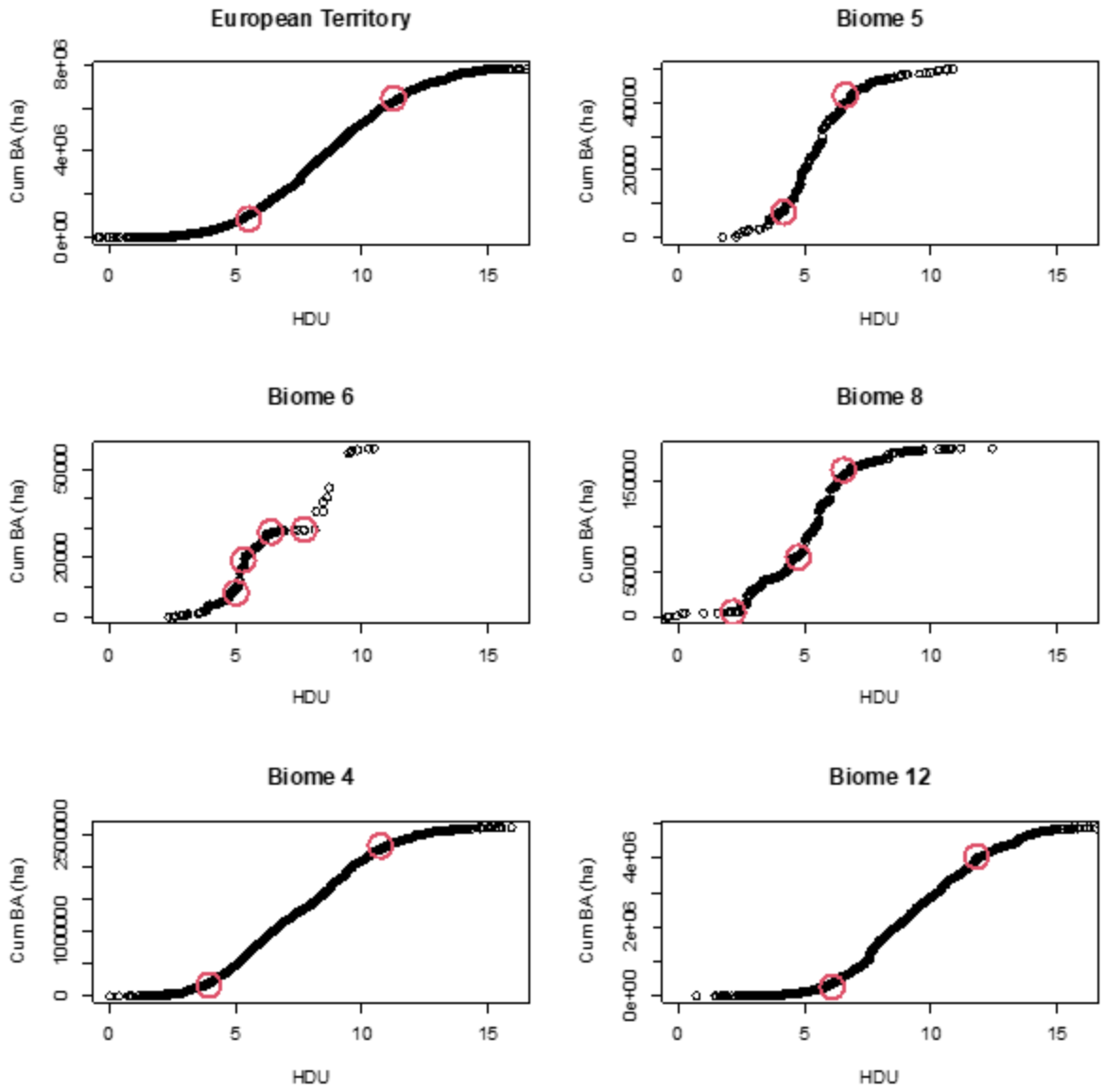


Figure 18: Relationship between the Hot-Dry-Unstable (HDU) index and cumulative burned area for all the fires occurring between 2001-2021 and registered in the database GlobFire. A segmented regression was fitted to the data and significant breakpoints are indicated by the red circles. Biomes 5, 6, 8, 4 and 12 indicate temperate

Copyright © FirEURisk Consortium. All rights reserved.

grasslands, boreal forests, temperate conifer forests, temperate broadleaf and mixed forests and Mediterranean forests, respectively.

Table 17: Variation in fire size (ha) at different percentiles under the different HDU breakpoints (see Figure 18) for the European Territory and the different biomes. Biome names as in Figure 18.

	European Territory			Biome 5			Biome 6			Biome 8		
Quantile	low HDU	mid HDU	high HDU	low HDU	mid HDU	high HDU	low HDU	mid HDU	high HDU	low HDU	mid HDU	high HDU
0.5	86	150	279	65	75	65	65	43	367	86	86	86
0.75	215	365	752	172	194	129	108	173	2344	280	215	204
0.95	839	1526	4126	796	857	403	410	593	7848	1747	1549	624

	Biome 4			Biome 12		
Quantile	low HDU	mid HDU	high HDU	low HDU	mid HDU	high HDU
0.5	86	108	215	107	193	387
0.75	215	258	516	258	473	1053
0.95	989	1011	1870	1034	1956	6929

2.4.3 Fire Danger weather estimations at PS Greece

According to the Hellenic National Meteorological Service (HNMS Climatology), the climate in Greece is characterized as predominantly Mediterranean, with hot and dry summers, wet and moderate winters and extended periods of sunshine through-out most of the year. Consequently, the wildfire activity in the country is regulated by the weather and climatic conditions. Unfortunately, during the last few decades, Greece has experienced significant and numerous wildfires with great impact not only on ecosystems, archaeological sites, infrastructures, etc. but also on loss of lives (Eftychidis et al 2007, Diakakis et al. 2016, Copernicus EMS, Mati wildfire, North Evia wildfire).

2.4.3.1 Fire Weather Assessment under climate change – Methodology of NCSRD

In the context of fire weather assessment, we applied the following methodology to investigate the projected changes in fire weather conditions in specific regions in Greece. The application of this methodology includes the description of the overall model setup to produce climate gridded datasets in the historical and future period in the high resolution of 5 km and their use for the calculation of the fire weather index. The Canadian Fire Weather Index (FWI, van Wagner 1985) values for the future fire weather were calculated using data derived from regional climate simulations for the area of interest, under two emission scenarios (RCP4.5 and RCP8.5) (Van Vuuren et al 2011, Riahi et al 2011). For the historical period 1980-2004, simulations were produced to provide a reference period for the FWI projection. The higher the FWI is, the more favorable the meteorological conditions to trigger a wildfire. At the final step, the analysis is performed to determine spatially the climate change signal of fire weather conditions on high resolution.

Taking into consideration the complex topography of the country with a significant variety of environmental conditions, the current analysis aimed at overcoming certain limitations that arise from using fixed FWI thresholds, proposed by the European Forest Fire Information System (EFFIS, https://effis.jrc.ec.europa.eu/) network, see also

Copyright © FirEURisk Consortium. All rights reserved.

Table 18. These thresholds can lead to systematic overestimation or underestimation of Fire Danger for certain regions pointed out Varela et al. 2018. For this reason, more specifically, the applied method is based on Percentiles Indices, proposed by Varela et al. 2018, that provides suitably varying FWI boundaries of classes which take into account the specific physical characteristics of the study area at high resolution. Thus, the use of high spatial resolution climate data with a combination of a novel approach to FWI classification established in this methodology provides a clear benefit to the derivation of fire danger patterns under a changing climate in Greece.

Table 18: The classification of values for the FWI and its sub-component ISI

FWI classes by EFFIS	FWI Percentiles by Varela et al. (2018)	ISI classes BY EFFIS
Very low (<5.2)	-	Very low <3.2
Low (5.2-11.2)	Low 25th percentiles	Low 3.2-5
Moderate (11.2-21.3)	Moderate 50th percentiles	Moderate 5-7.5
High (21.3-38)	High 75th percentiles	High 7.5-13.4
Very high (38-50)		Very high 13.4-30
Extreme (>=50)	Extreme 90tth percentiles	Extreme >30

2.4.3.2 Description of the model

The dynamical downscaling technique was applied through the non-hydrostatic Weather Research and Forecasting (WRF-ARW) model in version 3.6.1 (Skamarock et al 2008). The spatial configuration of the model was composed of two nested grids (Figure 19). The European outer domain (d01) was centered in the Mediterranean basin at 42.5 N and 16.00E of 20 km horizontal resolution and the high-resolution nested domain for the area of Greece was set up at 5 km (d02) of horizontal grid spacing. The physics parameterizations are described in detail in Politi et al 2021. The initial and boundary conditions for the climate change assessment were derived from EC-Earth global model (Hazeleger et al. 2010) climate simulations for RCP4.5 and RCP8.5 scenarios and encompassed time slices representative of the historical or reference period (1980–2004), near future (2025–2049), and end of century as far future (2075–2099) periods. For the future projections, the equivalent-CO2 concentration was updated every year in the WRF simulations according to the emission scenario. The description of this methodology is also included in the D3.1 “Downscaled CMIP5 and CMIP6 climate scenarios for selected PS and DA” that describe the methods and results concerning the climate projections generated under the Task 3.1.1 from NCSRD.

Copyright © FirEURisk Consortium. All rights reserved.

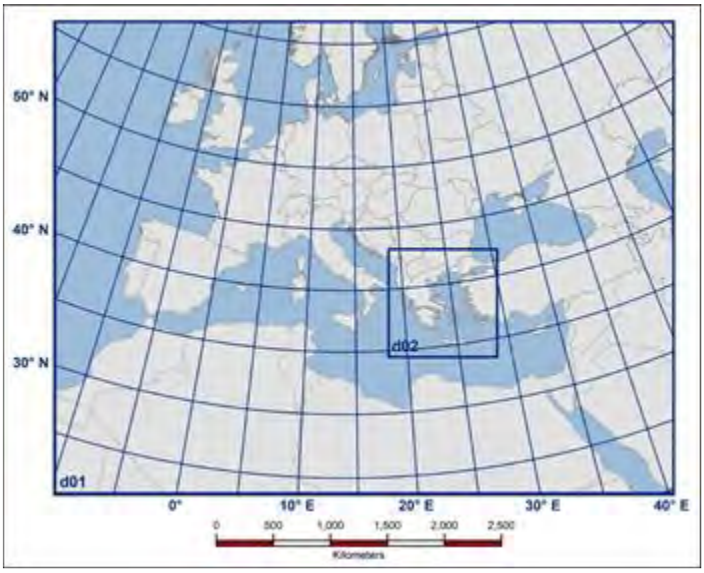


Figure 19: Modelling Domains: d01 refers to the outermost domain of 20 km and d02 to the nested domain of 5 km (region of Greece). This figure is obtained by Politi et al 2022.

2.4.3.3 Calculation of fire weather indices

For fire weather assessment, apart from the production of the existing codes of the FWI system, three more indices were calculated altogether. These were the 90th percentile of the FWI (representing the extreme class), the number of days with FWI above the 90th percentile (as extreme fire weather) and the maximum consecutive days above the 90th percentile. The calculation of the values of the Canadian FWI was performed using the package CFFDRS (https://r-forge.r-project.org/projects/cffdrs/) of R statistical computing software using as input four weather variables at 12:00 hours: the temperature at 2m, relative humidity, wind speed at 10m, and daily (total) precipitation. In addition, the maximum wind speed was decided to be used instead of the value at noon for considering an extreme case scenario in the FWI and ISI calculations.

For the calculation of FWI, the fire season has a duration from April to October (included), for each year. Moreover, the simulations were initialized one month in advance (in March) in order to equilibrate the model and minimize the effect of errors in the initial conditions used in the FWI calculation. The FWI is calculated over the land grid cells, for each grid point and for each time period. After calculating the daily values of the FWI system for each emission (RCP) scenario and fire season, the mean values over the 25-year periods were computed for FWI, ISI and for the additional indicators.

2.4.3.4 Application in PS5: Attica region

Future Fire weather assessment is applied in the PS5 area of Attica region (see Figure 20), as a case study of this methodology, examined in the framework of FirEUrisk. Moreover, the spatial analysis of the fire weather assessment for each index is presented in the following figures (Figure 21-Figure 23). Finally, the concluding remarks are described in bullets.

Copyright © FirEUrisk Consortium. All rights reserved.



Figure 20: PS5 in orange color for the Attica region.

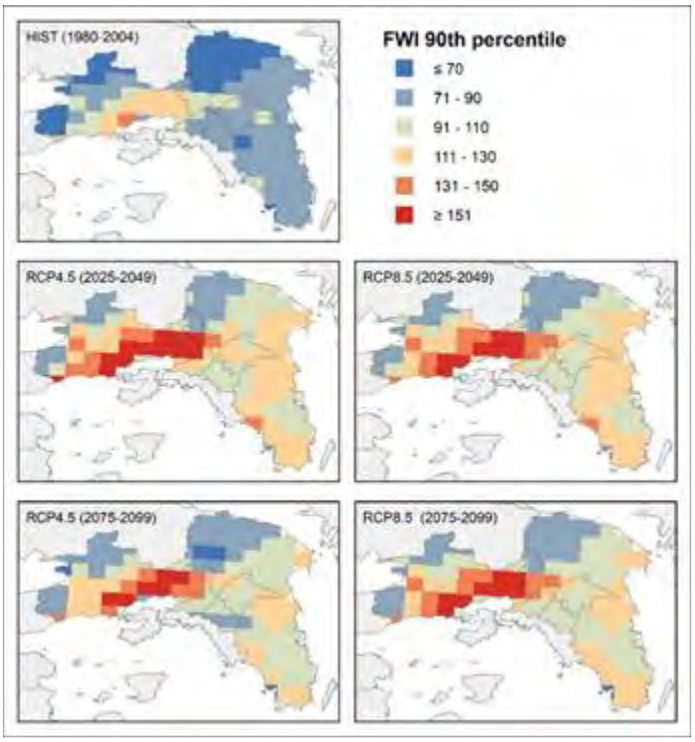


Figure 21: FWI threshold value of the 90th percentile for the historical and future periods for each emission scenario for PS5.

Copyright © FirEURisk Consortium. All rights reserved.

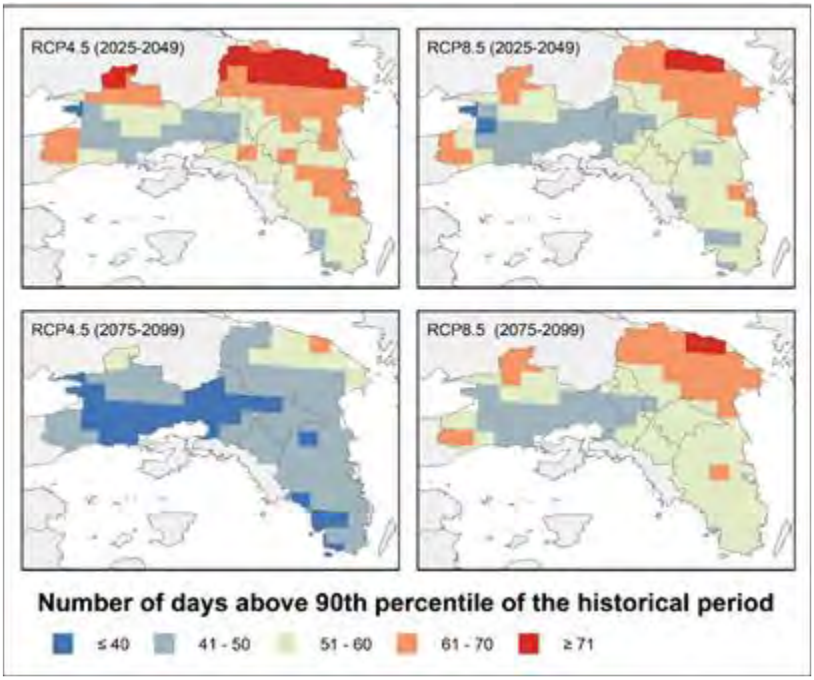


Figure 22: The number of days above 90th percentile (threshold value is set as 90th percentile of the historical period for the specific cell for all time periods) under the future emission scenarios in the near and far future periods for PS5.

Copyright © FirEURisk Consortium. All rights reserved.

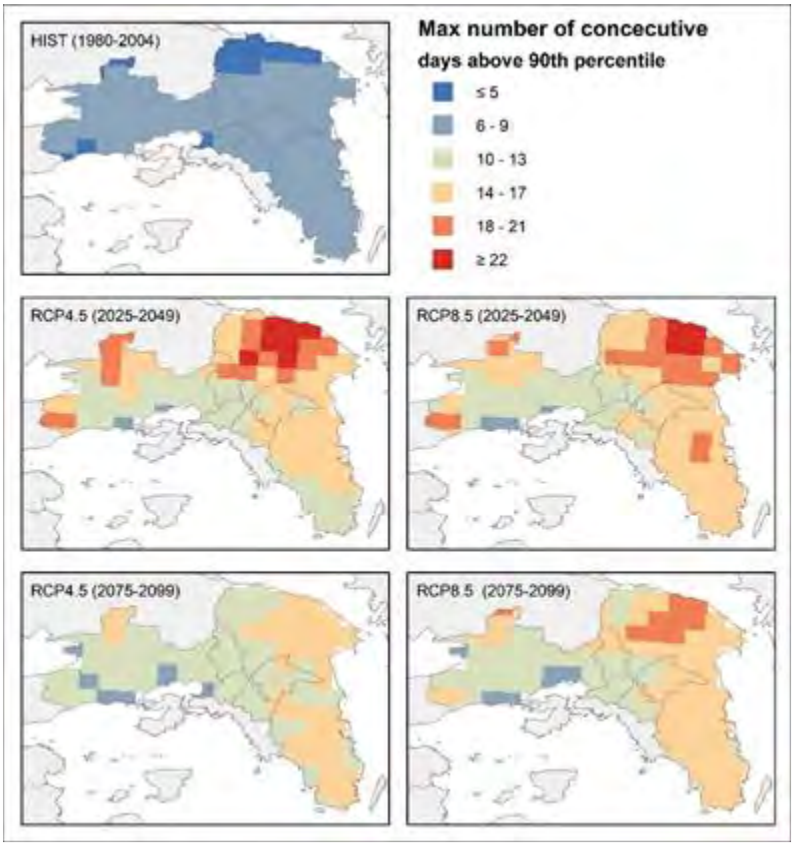


Figure 23: The maximum number with consecutive days above 90th percentile (threshold value is 90th percentile of the historical period for the specific cell) for historical period and RCP4.5 and RCP8.5 for the near and far future periods for PS5.

Copyright © FirEURisk Consortium. All rights reserved.

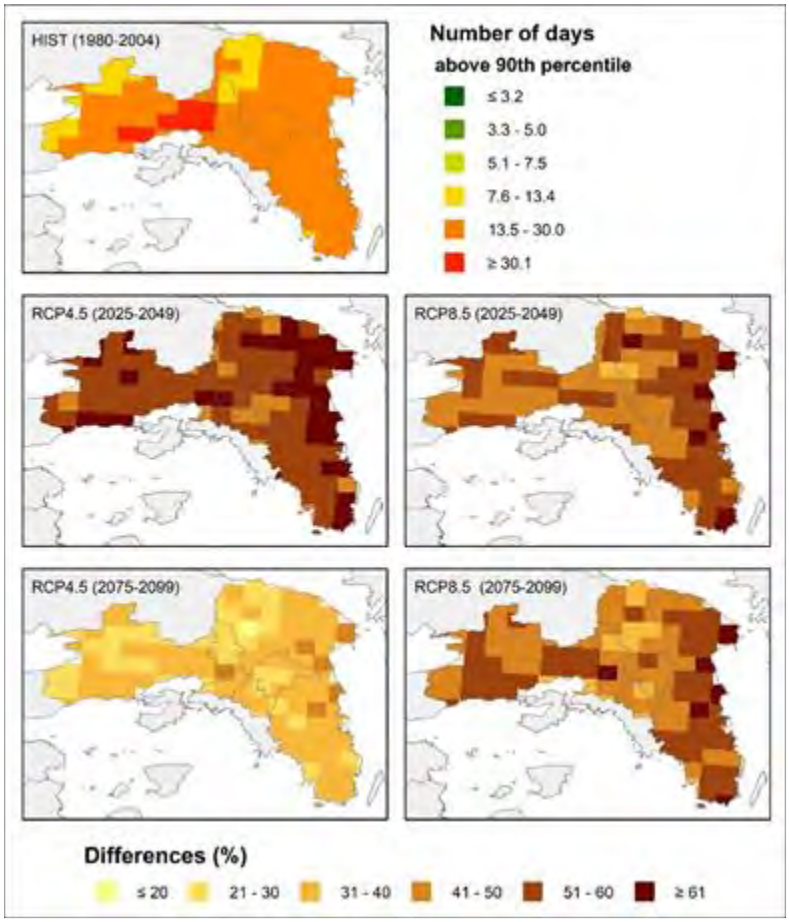


Figure 24: The mean value of Initial Spread Index for the historical period (top map) and future changes under RCP4.5 and RCP8.5 (in %) for the near and far future periods with respect to the historical period (middle and bottom maps) for PS5.

Main results are the following:

- During the historical period, values of the extreme percentile (FWI90) between 50 and 70 are observed in the north Attica region, while FWI90>75 are observed over the rest of the region, with the higher values in the part of the region.
- Overall large increases of FWI90 are observed in the study, during all periods and under both emission scenarios and mainly in the eastern part of the ps5.
- No more than 30 days were found above the threshold value (90th percentile of FWI) in the entire Attica region during the historical period.
- The increase in the number of days is more evident in the near future period in both scenarios and in the far future period under RCP8.5. It is estimated that the northern parts of ps5 will encounter more than 70 days of extreme fire weather during the fire seasons that correspond to a future change of an increase of more than 45 days compared to the historical period. The other part of the region will experience between 41 to 70 days of extreme fire weather with an exception during the far future and under RCP4.5 where less than 40 days are observed in the central western part of the region.
- The north-eastern part of ps5 will experience the higher future change in extreme consecutive fire weather days (with above 22 days), compared to the historical period in the near future. It is also observed that more than

Copyright © FirEURisk Consortium. All rights reserved.

14 consecutive days of extreme fire weather are expected during all periods and scenarios in the eastern Attica region.

- The majority of Attica region is characterized by high initial spread index to very high in the western part in the historical period. More than 50% change of ISI in almost the entire region (more than 60% in the east Attica region) in the near future under RCP4.5, while this change is restricted in the eastern Attica region under RCP8.5 in both periods. Finally, the lower changes are noticed in the far future and under RCP4.5.
- Overall, these results could be justified by the findings of Vlachogiannis et al 2022, where the same data had been used as in the current study, indicating that the probability of occurrence of extreme winds is higher almost all over the domain in the near future, under both scenarios compared to the far future period. In addition, the increased number of days with extreme fire weather can be related with the remarkable decrease of future precipitation, in the north-eastern part of Attica region under both periods and scenarios.

2.4.4 Product Description: Daily Fire Danger Index (DFDI) (ET)

Format: The Daily Fire Danger Index (DFDI) is a geospatial data in .tif format and it units are: percentage danger and categorical danger rating: very low danger, low danger, medium danger, high danger and extreme danger.
Resolution: 300 m.
Projection: ETRS89-extended / LAEA Europe
Access: https://fireurisk.satways.net/files/649069a8e4b0cdb64882013b
Description: The Daily Fire Danger Index is a new fire danger index based on weather data and satellite imagery. In particular, the product relies on the Sentinel-3 SYNERGY product to estimate the state of the vegetation in terms of the amount of available dead vegetation and in terms of the live fuel moisture content. The weather variables are used to calculate the dead fuel moisture content, the evapotranspiration and to obtain the wind speed at 2 meters height. These variables are normalized and weighted using the historical fire records of the area of interest. In addition, the weather forecast data is used to provide a fire danger forecast 1) at different times of the day and 2) for the following days.

Copyright © FirEUrisk Consortium. All rights reserved.

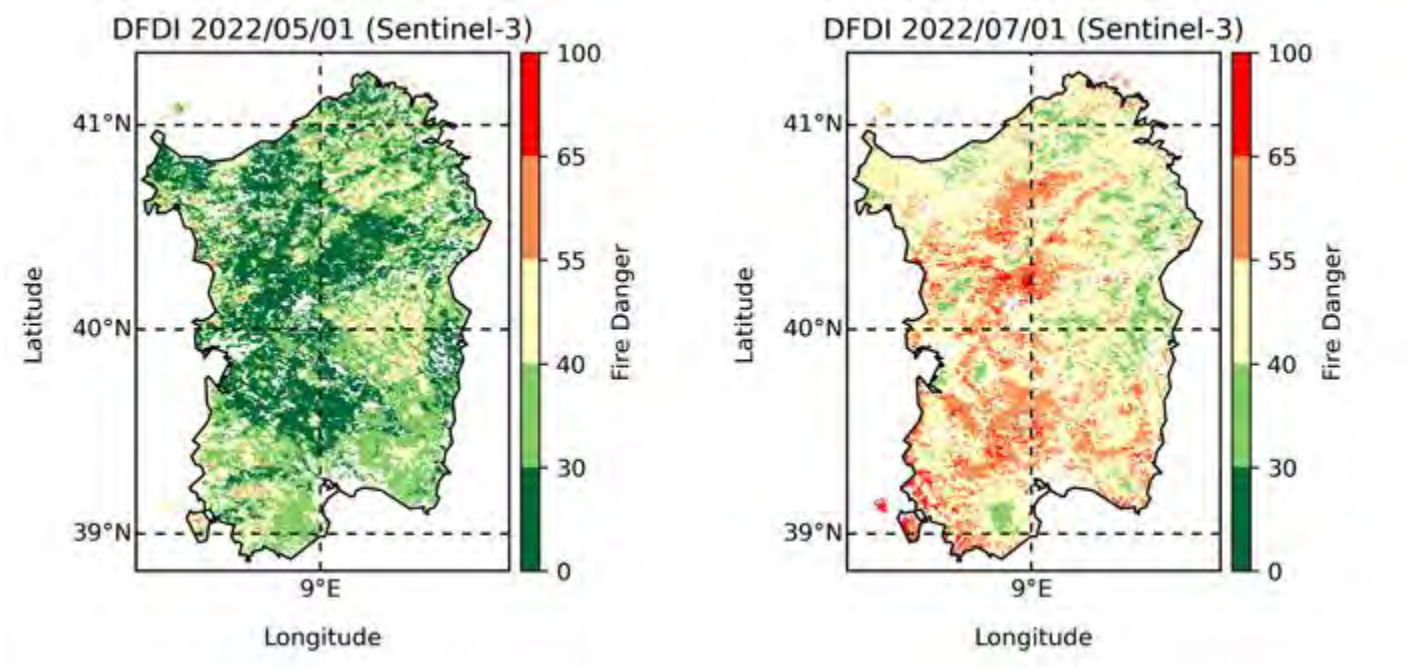


Figure 25: DFDI maps in DA5 (Sardinia) on May 1st (left) and July 1st (right) 2022

The DFDI derives from the tradition of satellite-based fire danger indices that starts from the Burgan's Fire Potential Index (FPI) and culminates with the Italian Daily Fire Hazard Index (DFHI). Differently than other fire danger indices based only on weather information (e.g. the Canadian Forest Fire Weather Index), these indices exploit satellite information to obtain estimates on the state of the vegetation. Originally, the FPI used historical NDVI measurements to calculate the Relative Greenness of a pixel, thus providing an estimate of the amount of dead vegetation present in the area. The DFHI built upon this foundation, and, among other improvements, used Ceccato's Global Vegetation Moisture Index to estimate the Equivalent Water Thickness (EWT) of the canopy, in order to provide a more direct assessment of the water content in the vegetation.
However, it is well-known that the EWT is only one of the two variables necessary to calculate the Live Fuel Moisture Content (LFMC) of the vegetation: in order to completely describe the moisture state of a live leaf, it is also necessary to have information about its weight per unit surface in terms of Dry Matter Content (DMC), whose value evolves according to the maturing and curing state of the leaf.
The DFDI improves upon the DFHI by using satellite measurements of canopy reflectance to estimate LFMC, and in addition, redefines the index calculation completely in order to incorporate directly the contributions of wind speed, evapotranspiration and of the LFMC itself.

Contact: In case of doubts and/or suggestions, forward an email to Giovanni Laneve (Giovanni.laneve@uniroma1.it) and Valerio Pampanoni (valerio.pampanoni@uniroma1.it).

2.4.5 Product Description: Fire Danger weather estimations at PS Greece (PS5)

Not applicable

Copyright © FirEUrisk Consortium. All rights reserved.

3 Natural fire ignitions: Lightning

3.1 Modelling lightning at ET scale

FMI has conducted a series of experiments with the lightning data obtained from several sources: national data from Spain and Sweden, lightning registries, and lightning models, in particular, evaluated the new lightning variable in the operational weather forecast of European Centre for Mid-range Weather Forecast, ECMWF. It has been shown that, albeit generally correlated in space, individual fires observed by MODIS practically never coincide with reported lighting. Therefore, a statistical lightning ignition sub-model has been targeted instead of deterministic one. With the lightning variables added to the Fire Forecasting Model FFM of IS4FIRES global fire information system, several regions with frequent lightning got noticeable changes in the fire predictions, better fitting to the observed fire patterns. This significance and absolute values corroborated with a consensus fraction of 10% of global fires ignited by lightning.

3.2 Modelling lightning at Pilot Site scale

Dependent variable: lightning strikes and fire ignitions

The core of our approach leverages a large and comprehensive dataset of cloud-to-ground lightning strikes recorded in the period 2009–2015. The dataset was compiled by the Spanish Meteorological Agency (AEMET) and provided by Meteogrid SL. AEMET's lightning detection system for the Spanish territory is composed of 14 detectors on the Spanish mainland, 1 in the Balearic Islands and 5 in the Canary Islands (the latter were not used in this work); Meteo-France provides data from 10 of its detectors and the Portuguese Meteorological Agency adds 4 extra sensors. All data from these 34 detectors are consolidated in the calculation and tracking system at the AEMET's climate service. The system is capable of detecting lightning strikes with a location accuracy of the order of 1 hm and a detection efficiency of 90% of total lightning strikes. The dataset used in this study consists of more than 17 million records in the period 2009–2020, reporting flash intensity, polarity and density. Lightning strikes were paired with actual lightning ignition data compiled by national agencies. Information about fire ignitions (location, date, cause and size) was retrieved from the Spanish (Estadística General de Incendios Forestales, EGIF; MAAyMA 2015) and Portuguese (Dispositivo Especial de Combate a Incêndios Florestais, DECIF; Pereira et al. 2011) databases. The Spanish dataset was used to identify those lightning strikes that started a fire while the Portuguese records were retained to evaluate the applicability of the model to the specific conditions of Portugal.

The response variable was constructed using historical ignitions in Spain. Approximately 2500 fires were matched to a lightning strike occurring within a radius of 1000 m and no more than 3 days after the ignition date (maximum holdover period according to Pineda et al. 2014). For each fire event, we retrieved all lightning strikes within a 3-day window. Then, we ranked lightning strikes by proximity to the fire's ignition point. The closest lightning was associated with that ignition and further considered as lightning that triggered a fire when building the response variable. Only those flashes within a 1000-m distance from an ignition source were considered owing to the uncertainty in flash detection. From this information, we built a binary response variable combining strikes that triggered a fire (1 or presence) or were not related to a fire (0 or absence). The response variable comprised both lightning strikes on days where a wildfire occurred (fire days henceforth) and a balanced set of strikes from days without observed lightning-caused fires (non-fire days). We implemented a stratified sampling procedure to

Copyright © FirEUrisk Consortium. All rights reserved.

prevent undesired effects from the largely unbalanced response (more 0 s than 1 s) and minimise spatial autocorrelation.

Independent variables

To predict the probability of ignition, we employed factors related to vegetation, topography and others directly linked to lightning features. Live fuel moisture content was characterised using the Drought Code (DC; Van Wagner 1987) as proxy, calculated following the standard procedure described in Wagner and Pickett (1985). DC was retrieved from the Copernicus Emergency System, which produces daily gridded (at 25 km resolution) historical data for a variety of meteorological fire danger indices, including the Canadian Fire Weather Index, to which DC belongs. We calculated the daily dead fuel moisture content (dFMC) as described in Nolan et al. (2016), previously used successfully on the Iberian Peninsula (Boer et al. 2017; Resco de Dios et al. 2022). The method is based on the exponential decline in dFMC with increasing vapour pressure deficit (VPD) and, in turn, it calculates VPD from MODIS Land Surface Temperature (MOD11A1 Collection 6). The dFMC measures 1–10 h fine fuels moisture while DC relates to seasonal drought conditions potentially affecting the moisture content of live vegetation (Viegas et al. 2001). The dFMC was calculated using surface temperature and relative humidity daily data from the ERA5-Land dataset at a 9 km spatial resolution (Muñoz Sabater 2019). Secondly, elevation and relief curvature (derived from elevation via topographic position index; Weiss 2001) were selected to depict the influence exerted by the terrain in the ignition of natural-cause fires. We retrieved elevation data from the NASADEM global digital elevation model at 30 m spatial resolution (NASA JPL 2020). The last landscape feature incorporated into the model was vegetation height, acting as a proxy for vegetation structure and cover. We used the global forest canopy height map using a novel dataset calibrated combining Global Ecosystem Dynamics Investigation (GEDI) footprints of canopy structure (Dubayah et al. 2020) and Landsat Operational Land Imager spectral imagery. All variables were regridded from their original resolution to 1 × 1 km. Topographic variables and vegetation height were aggregated by their median value into the 1 × 1 km destination cell while dFMC and DC were resampled using bilinear interpolation downscaling from 9 × 9 to 25 × 25 km. Our model also accounts for lightning-related features, such as strike intensity and polarity, and density of flashes, as provided by the lightning detection network.

Model calibration with Random Forest

The model was trained using Random Forest (Breiman 2001), a popular and effective algorithm for wildfire distribution modelling (Bar Massada et al. 2013; Rodrigues and de la Riva 2014; Vecín-Arias et al. 2016; Su et al. 2018). We trained a total of 100 models exploring different iterations of the response variable. In each realisation, we extracted a balanced sample of 1-presence (flashes igniting a fire; 1/3 of the final sample) and 0-absence (lightning strikes non-conducive to fire; 2/3 of the final sample distributed as 1/3 in fire days and another 1/3 in non-fire days). The process was stratified using a 100 × 100 km grid so that at each grid cell, we extracted a balanced sample of 1-presence and 0-absence to reduce the potential spatial autocorrelation (Wang et al. 2016). It must be noted that we only analysed the April-to-October period, coinciding with the brunt of the fire season.

Model calibration was conducted using the caret package (Kuhn 2008) in the R environment for statistical computing (R Core Team 2021). For each model realisation, we split data into a calibration (70% of data) and testing dataset (30% of data). During the calibration phase, we implemented a 5-fold repeated cross-validation (three repetitions), optimising model parameters: number of trees (ntree; from 100 to 2000 trees with steps of 100) and number of variables to use at each split (mtry; consecutive values from 1 to 6). The minimum node size (nodesize) parameter was kept constant at its default value for regression (5) because it had little influence on performance.

Copyright © FirEURisk Consortium. All rights reserved.

Once the model was calibrated, we evaluated the importance and explanatory sense of each covariate using partial dependence plots (Greenwell 2017), and the overall performance of each model via area under the receiver operating characteristic curve (AUC) (Bradley 1997), using the test sample in the latter and the out-of-bag sample in the first. Out of the set of 100 models, we selected the one attaining average prediction performance (AUC = 0.828; mtry = 2, ntree = 1000 and nodesize = 5) as the candidate model to forecast and map the daily evolution of lightning-related ignition probability. The model was subsequently evaluated calculating the AUC from the Portuguese fire data, which consisted in 105 lightning fires (>1 ha) in the period 2009–2015. Like the procedure followed in the calibration stage, we created multiple random samples of 0-absence to account for the non-occurrence of fires in Portugal. In this case, we created a balanced sample of 105 non-fire locations on fire days, placing as many absences as fires were reported. This procedure was repeated 100 times to check the potential effect of the random placement of 0-absence. Finally, to perform daily spatial predictions over the entire Iberian Peninsula, we used daily information about dFMC and DC. Vegetation height and topography were kept constant. We set constant values of intensity, polarity and density of strikes equal to their respective average value over the study area and period (i.e. −10 kA and five discharges, respectively).

4 Human ignition drivers & Public participation in fire prevention and preparedness

To generate human iginition probability map at European scale, a set of fire probability rasters were obtained by fitting a total of 100 Random Forest models using a binary response variable (fire presences vs fire absences), using a total of 10 human, environmental and land cover derived drivers. The models were fitted for the five pilot sites: PS1.- Northern Europe (Southeast of Sweden), PS2.- Central Europe, PS3.- Central Portugal, PS4.- Barcelona province (Spain) and PS5.- Attika region (Greece). The new version (v2) of human ignition probability maps have added the pilot site of Sewden (PS1) and also include some corrections needed. On the other hand, the variable of Population over 65 years old has been excluded in the models of Central-Eastern Europe. Moreover, we have updated the Portugal pilot site fire database with more number of fire records including several missed years (i.e. 2017). Finally, all the models have included a new version of no-fuel mask according to CLC 2018. In the case of the Barcelona pilot site, the fuel map employed is more detailed with a total of 11 categories and with a spatial resolution of 100 meters. The product estimates the probability that a human caused fire will be ignited. The product developed with active use of machine learning spatial-temporal empirical models of ignition probability based on socio-economic and territorial drivers of ignition from geospatial indicators and demographic databases. The predictive performance of the model was interpreted from the confusion matrix and the OOB error for the classification and the AUC for the probability analysis. The confusion matrices show balanced commission and omission errors below 20% in all models. The OOB for the global model is 11.8 %, for the global model only with the human components it is 11.94%, for the Mediterranean areas it is 16.35 %, non-Mediterranean areas it is 11.06 %, and for the season from May to September is 10.85 %.

Copyright © FirEURisk Consortium. All rights reserved.

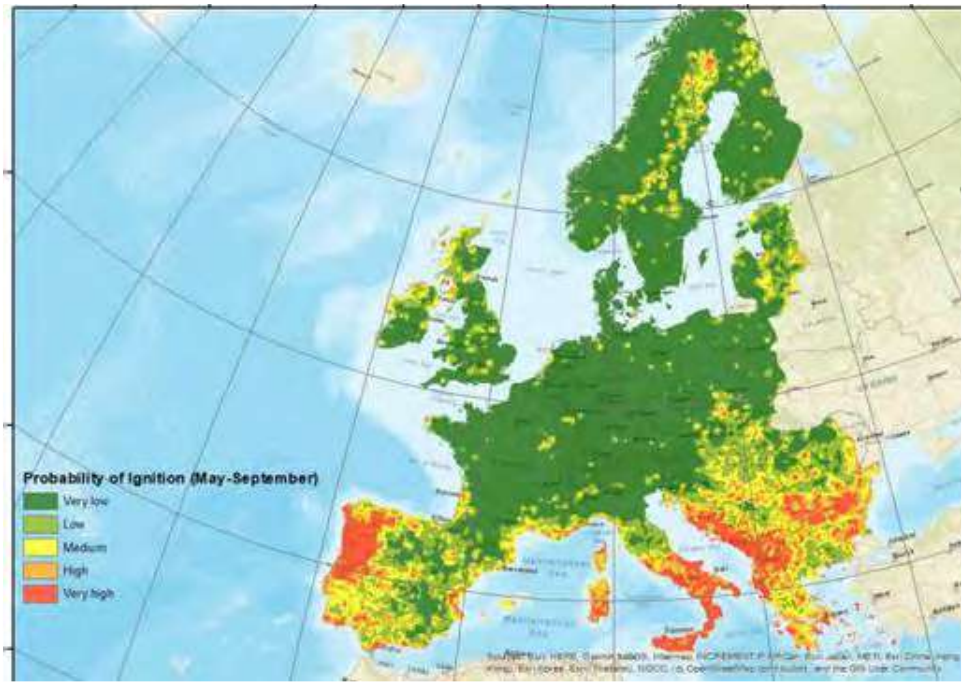


Figure 26: Human ignition probability map

To derivate human ignition probability maps at pilot site scale, were employed a total of eight fire records datasets (point shapefiles) delivered directly by FirEURisk members or national agencies, with diverse time periods, ranging from 1996 to 2022 (Table 19). The first four correspond to Central-Eastern Europe (north of Czech Republic, southwest of Poland, and the German regions of Saxony and Brandenburg). The remaining four datasets correspond to the Barcelona province (Spain), Attica region (Greece), the central region of Portugal and the south-east of Sweden. All the explanatory variables were resampled at 100 m and projected to ETRS89 LAEA Europe (EPSG: 3035).

- Percentage of population > 65 years old. We retrieved the data from EUROSTAT using year 2011 at municipality level. We calculated it using the formula: "Population over 65 / Total Population * 100".

- Distance to roads. We calculated the Euclidean distance using the original road network from the Global Roads Inventory Project (GRIP) by GLOBIO model (Available in the link: https://www.globio.info/download-grip-dataset).

- Fuel types. We reclassified the CLC 2018 into 4 classes: No fuel (for the continuous-discontinuous urban fabric, industrial or commercial units, road and rail networks, etc.), grassland (for pastures, natural grasslands and non-irrigated arable lands), shrubland (transitional woodland-shrub and sparsely vegetated areas) and forest (broad-leaved forest, coniferous and mixed forest). In the case of the Barcelona pilot site, the fuel map employed has a total of 11 categories and with a spatial resolution of 100 m.

- Distances to WAI, WUI and WGI. We employed the CLC 2018 to create 4 categories of coverage (urban, agricultural, wildland and grasslands) Then, we intersected agricultural vs wildland coverages, urban vs wildland, and grassland vs wildland. Finally, we computed the Euclidean distance to them.

Copyright © FirEURisk Consortium. All rights reserved.

- Percentage of urban, agricultural and wildland coverage. Using a regular square grid of 100 meters we calculated the area of each grid. After that, using CORINE urban, agricultural and wildland coverages, we calculated an Intersect between the regular grid and each of the land coverages. Then, we calculated the area of those three coverage that intersects the grid. Later, we dissolved them using the grid ID as a dissolving field and summed the intersected area. Then, we joined the result with the original regular grid, using the grid ID as the common field. Finally, we calculate the percentage of urban, agricultural and wildland coverage, using the formula: "Intersected area/Grid area * 100".

- Population density. The Population Density v4.11 was retrieved from the SEDAC website (available in the link: https://sedac.ciesin.columbia.edu/data/set/gpw-v4-population-density-rev11), which represents the number of persons per square kilometer, based on counts consistent with national censuses and population registers.

Before to fit the models, we created a raster stack with all the variables and extracted their values using each fire record point. Then, we created a binary dependent variable (fire presence: 1 vs fire absence: 0). We also used a randomly generating sample with the same number of absences per each fire record (i.e. same date). Then, we fitted 100 iterations of Random Forest, using the 70 % for training and 30% for testing. Finally, we created a set of rasters of predictions averaging the wildfire probability, as well as variables importance bar plots and partial dependence charts for the top four drivers more important.

The accuracy reached of the RF models for all PS was remarkable high (Table 20), obtaining values of AUC over 0,84 in four of the pilot sites, except for the case of Sweden (0,69). In relation to the most relevant variables that explaining the human fire ignition probability we found population density as the main driver (in four pilot sites). The rest of factors were found in three different pilot sites (fuel types, distance to roads, distance to WUI, and percentage of wildland coverage) and only once in the case of Percentage of agricultural coverage, percentage of urban coverage, distance to WAI and distance to WGI.

Regarding the spatial distribution of the human fire ignition probability, the pilot site with the greater extension of high likelihood values is Barcelona province, followed by Central-Eastern Europe, and ending with Portugal with the lowest values of ignition predictions. Note that in the case of Barcelona, the greater probability of human-caused fires is located along the road network together with the more densely populated areas. This behavior is also slightly observed in the case of Central-Eastern Europe, but maybe matched more noticeable with areas with the most density of population. In the rest of pilot sites, the highest likelihood values are restricted to the interfaces (WAI-WUI), specific fuel types of agricultural coverage.

Table 19: Names of pilot sites, country where is located or regions that contain, dates availability and total number of human-caused fires.

Pilot site	Country (Region)	Dates availability (from – to)	Number of human fires
Central Europe	Czech Republic	01/01/2016 – 31/12/2020	5,471
	Poland	11/01/2017 – 09/04/2022	17,036
	Germany (Saxony)	15/03/2008 – 05/04/2021	516
	Germany (Brandenburg)	21/03/2010 – 08/10/2020	942
Barcelona province	Spain	01/04/2008 – 06/10/2018	2,462

Copyright © FirEURisk Consortium. All rights reserved.

Pilot site	Country (Region)	Dates availability (from – to)	Number of human fires
Attica region	Greece	2017 - 2021	1,584
Central region Portugal	Portugal	21/02/2001 – 03/12/2015	24,625
Northern Europe	Southeast Sweden	01/01/1996 – 10/09/2020	11,067

Table 20: AUC values and the top four fire drivers more relevant in RF models for each pilot site.

Pilot site	AUC	Top four fire drivers
Central Europe	0.84	Population density, Fuel types, Distance to WUI, Distance to roads
Barcelona province	0.85	Population density, Distance to WUI, Distance to roads, Fuel types
Attica region	0.89	Population density, Percentage agricultural coverage, Percentage wildland coverage, Percentage urban coverage
Central region Portugal	0.87	Fuel types, Percentage wildland coverage, Population density, Distance to WGI
Northern Europe	0.69	Distance to WUI, Distance to WAI, Distance to roads, Percentage wildland coverage

4.1 Product description: Human ignition probability map (ET)

- **Format:** Human ignition probability map is a geospatial product in .tiff format (still to be decided) and in a probability scale from 0 to 100. In terms of temporal coverage is developed for 2020, although is a static layer.
- **Resolution:** 1 km.
- **Projection:** Lambert Conical Equal Area
- **Access:** https://fireurisk.satways.net/datasets/633d4250e4b0b33bb11dccf2
- **Contact:** In case of doubts and/or suggestions, forward an email to Emilio Chuvieco (emilio.chuvieco@uah.es) or Clara Ochoa: mclara.ochoa@edu.uah.es
- A paper describing the full methodologica process was submitted to a peer-reviewed journal and it is currently under review: Sueur-Ochoa, C., & Chuvieco, E. (2023). Mapping the likelihood of human-caused fire ignitions in the European territory Applied Geography.

4.2 Product description: Fire ignition data and driver variables (PS)

- **Format:** Human ignition probability is provided in .tif format in one single-band raster layer with 100 m pixel resolution for the five pilot sites. There are two different versions of the products. The most complete and corrected is the one called: New version of Human ignition probability.
- **Spatial resolution:** 100 m.
- **Spatial projection:** ETRS89 Lambert Azimuthal Equal Area (EPSG: 3035).
- **Access:** Data can be accessed by direct download from:
- https://fireurisk.satways.net/datasets/6343d705e4b0b33bef3a249f#folderId=637f9bffe4b0b33bef3c3dfb&page=0

Copyright © FirEUrisk Consortium. All rights reserved.

- **Description:** Human ignition probability is a set of fire probability rasters obtained by fitting a total of 100 Random Forest models using a binary response variable (fire presences vs fire absences), using a total of 10 human, environmental and land cover derived drivers. The models were fitted for the five pilot sites: PS1.- Northern Europe (Southeast of Sweden), PS2.- Central Europe, PS3.- Central Portugal, PS4.- Barcelona province (Spain) and PS5.- Attika region (Greece). The new version (v2) of human ignition probability maps have added the PS1.- Northern Europe (Southeast of Sweden) and also include some corrections needed. On the other hand, the variable of Population over 65 years old has been excluded in the models of Central Europe pilot site. Moreover, we have updated the Portugal pilot site fire database with more fire records including several missed years (i.e. 2017). Finally, all the models have included a new version of no-fuel mask according to CLC 2018. In the case of the PS4.- Barcelona province pilot site, the fuel map employed is more detailed with a total of 11 categories and with a spatial resolution of 100 meters.
- **Contact:** In case of doubts and/or suggestions, forward an email to Adrián Jiménez Ruano (jimenez@unizar.es) and Marcos Rodrigues (rmarcos@unizar.es).

5 Risk wise landscape and fuel models development

5.1 Fuel models development

For the ET area, the product includes the fuel type and parameters following the standard classification of fuels adopted for the FirEURisk project (Aragoneses et al., 2023). The final output – fuel classes and static fuel map with the spatial resolution of 1 km^2. Developer: UAH (Universidad de Alcalá). The product was developed within the Activity "A1.1.4 Risk-wise landscape and fuel models development". Methods to generate the ET fuel type map have been recently published: Aragoneses, E., García, M., Salis, M., Ribeiro, L.M., & Chuvieco, E. (2023). Classification and mapping of European fuels using a hierarchical-multipurpose fuel classification system. Earth System Science Data, 15, 1287–1315. The paper includes also validation data, with an overall agreement of 88.40 % (average commission errors of 37 %, average omission errors of 29 %) between the FirEURisk main fuel types and the LUCAS (Land Use and Coverage Area frame Survey), Google data, and the GlobeLand30 map databses. Further information can be found in the Product User Manual (PUM).

Copyright © FirEURisk Consortium. All rights reserved.

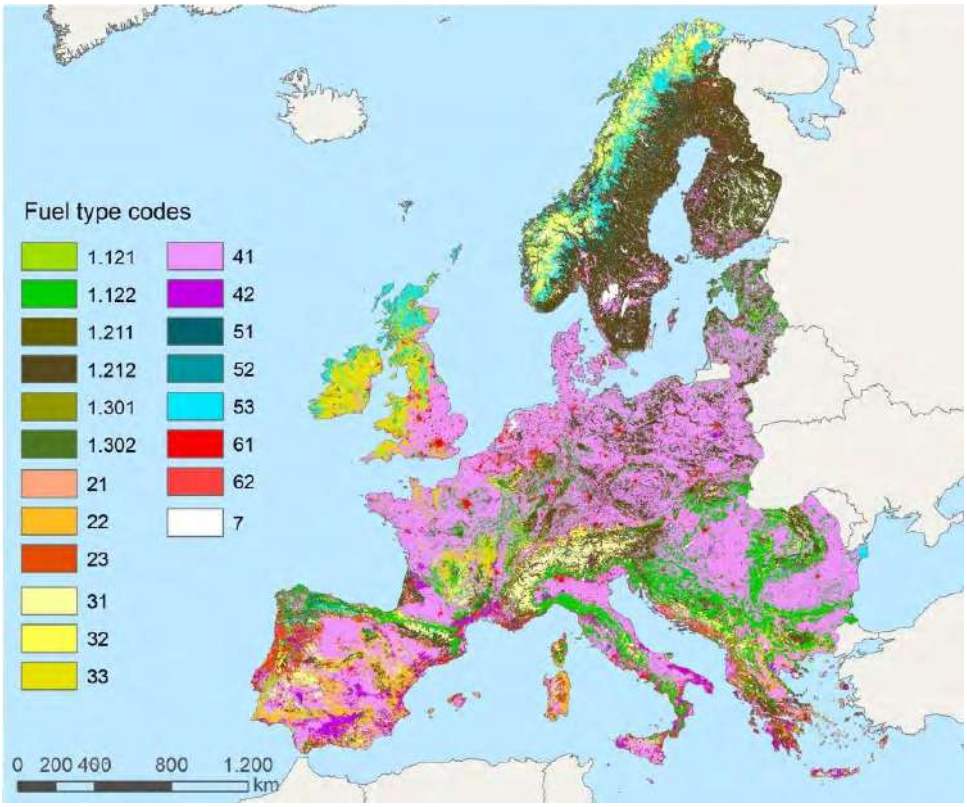


Figure 27: Fuel type map of the ET area. Classes codes correspond to the FirEURisk classification system (source: Aragoneses et al., 2023)

Format: Fuel type and model map is a geospatial product in .GeoTIFF format in one single-band categorical raster with 1 km x 1 km pixel resolution. In terms of the temporal coverage was developed for 2020 but is a static layer.
Projection: ETRS89 Lambert Azimuthal Equal Area (EPSG: 3035).
Data can be accessed by direct download from: (https://edatos.consorciomadrono.es/dataset.xhtml?persistentId=doi:10.21950/YABYCN, last access: 7 March 2023).

At PS scale, the landscape file was assembled at 100 m resolution, as required for fire simulation modeling, using the fuel model, canopy metrics, and topography data (aspect, elevation, and slope grids). The fuel model map was built from available land use land cover maps and global tree cover products considering the FirEURisk classification process and threshold values described in activity A114 (Aragoneses and Chuvieco 2021). We implemented a top-down approach based on canopy height and cover global products to differentiate between forest, shrubland, and grassland fuel classes (Sexton et al., 2013; Lang et al. 2022). The high-resolution Corine Land Cover plus Backbone product was used to differentiate between broadleaved deciduous, broadleaved evergreen, and conifer forests, as well as pastures and herbaceous crops (Probeck et al., 2021). In addition, the De Martone Aridity Index was used to differentiate between arid and humid areas within the pilot site to match the fuel types to standard fuel models (Scott and Burgan 2005). The non-burnable fuels, including urban development areas, irrigation farmlands, and water bodies, were finally masked on top of the map resulting from the classification.
We used the average values for various canopy cover interval classes (15 to 30, 30 to 45, 45 to 60, 60 to 75, 75 to 90, and > 90%) to generate the canopy base height (m), canopy height (m), canopy cover (%), and canopy bulk density (kg m-3) grids at 100 m resolution for the different forest fuel types (broadleaved evergreen, broadleaved

Copyright © FirEURisk Consortium. All rights reserved.

deciduous, and conifer forests) and climatic conditions (humid and dry). First, we extracted the canopy metric data for a randomly distributed large sample of points (n> 300,000 points) from a LiDAR-derived set of available grids from PREVINCAT (Krsnik et al. 2020). We then calculated the average values for every class, and these values were spatialized into a continuous cover set of grids using the former canopy cover, forest type, and aridity index maps. Therefore, we assumed average canopy metric values for different stand conditions rather than generating models so that these methods could be replicated in other FirEUrisk pilot sites where we lack LiDAR data.

Moreover, we conducted a fuel sampling campaign following the FirEUrisk protocol developed in activity A114 to characterize the prevalent custom fuel types in the pilot site of Barcelona. The fuel samples were processed in our laboratory (separated in different fractions, dried at 105°C for 48 hours, and weighted) at the University of Lleida to calculate the fuel load. Specifically, we calculated the dead (duff, litter, 1h, 10h, 100h, and 100h) and live (herbaceous and woody <6 mm) fuel load fractions for grassland (17 plots), shrubland (24 plots), and forest fuel types (21 plots of evergreen, 20 plots of deciduous, 24 plots for conifer, and 14 for mixed forests). Additionally, we calculated the percentage of organic carbon and nitrogen content with gas chromatography plus the percentage of ash content after muffle combustion in litter and duff samples of the primary forest types. These data can be used separately or in combination with standard fuel types to model fire spread and calculate smoke emissions in Mediterranean landscapes.

5.2 Landscape fuel map and custom fuels at PS scale

5.2.1 Product Description: Fuel types (ET)

- Description: Europe Forest fuel map
- Format: GeoTiff
- Resolution: 1 km.
- Projection: ETRS89 Lambert Azimuthal Equal Area (EPSG: 3035).
- Access: https://fireurisk.satways.net/datasets/62d662b9e4b0b33bb117b801
- Description: The European fuel map is a raster layer representing the first-level fuel types of the FirEUrisk fuel classification system for the continental scale. was generated through the integration of existing land cover datasets and bioclimatic modelling. Then, it was smoothed and resampled to the target spatial resolution (1 km). Finally, it was validated using LUCAS (Land Use and Coverage Area frame Survey), Google data, and the GlobeLand30 map. Further information can be found in the Product User Manual (PUM).
- Contact: Emilio Chuvieco (emilio.chuvieco@uah.es)

5.2.2 Product Description: Fuel types (PS)

- **Format**: GeoTiff
- **Resolution**: various resolutions 100 to 20 m.
- **Projection**: Pseudomercator EPSG 3857
- **Access:** https://fireurisk.satways.net/datasets/638270d4e4b0b33bef3c59af
- **Contact:** Marin Bugarić (marin.bugaric@fesb.hr)
- **Description: Section 5.1**

Copyright © FirEUrisk Consortium. All rights reserved.

6 Analysis of fire propagation, fuel consumption and smoke emission as risk factors

6.1 Propagation potential for European Territory (ET)

Propagation potential is important part of wildfire risk estimation having direct influence on Danger (hazard) and Exposure.

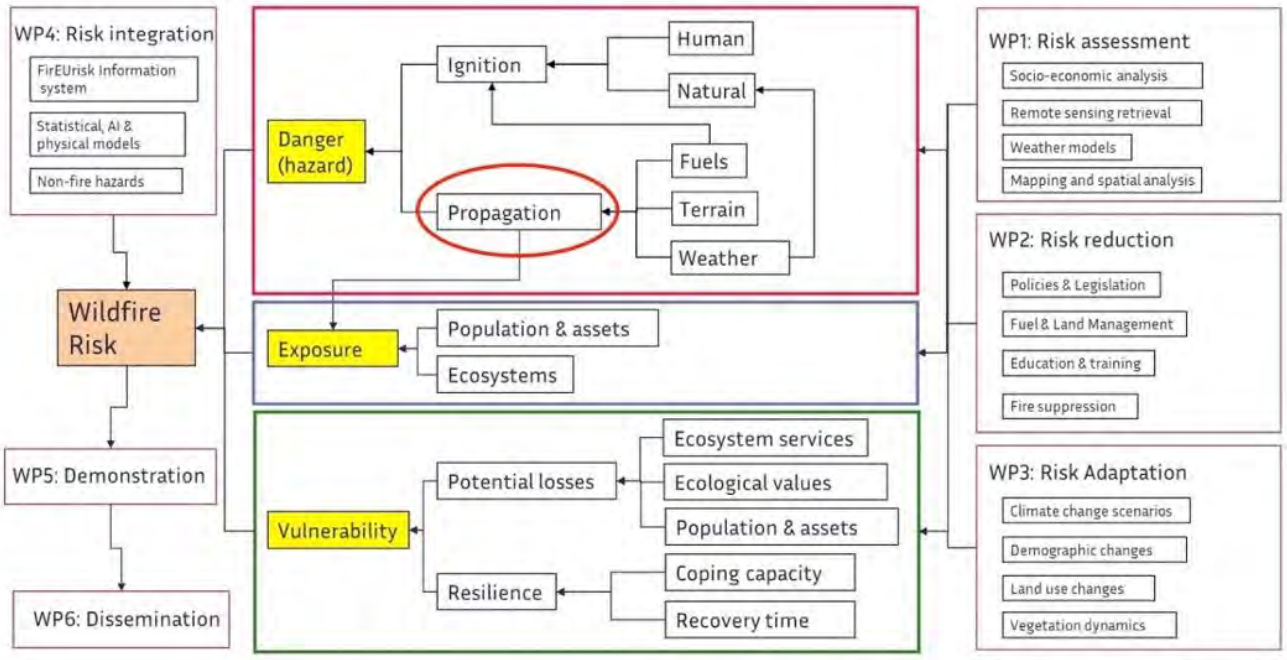


Figure 28: Conceptual integration of fire risk components within the FirEUrisk project (Chuvieco, Viegas, Eftychidis; 2022)

6.1.1 Methodology for propagation potential estimation at ET scale

In this section a detailed methodology for propagation potential calculation on the European Territory (ET) level is presented, as well as the analysis of all necessary input data and final results (GeoTiff maps at 1 km resolution for: Rate of Spread (R) [m/s], Reaction Intensity (RI) [kJ/(m2 s)], Fireline Intensity (FI) [kW/m] [kJ/(m s)] and Flame Length (FL) [m]). Resolution for propagation potential calculation on EU level is 1 km2, therefore pixel size will be 1 km x 1 km.

Methodology for calculation propagation potential at EU level is as follows:

1. From database of all past fires on EU territory from Jan 1,2001 to Dec 31, 2019 select dates of fires above 2000 ha.
2. For those dates of fires bigger than 2000 ha, select the weather data and EU weather maps from their current product resolution. Minimum number of weather maps for each fire dates are for: temperature, dew point and wind speed at 10m. From these maps fuel moisture at pixel level for all fuels (dead 1-h, 10-h, 100-h) will be calculated. For each weather parameter and selected date, a separate georeferenced

Copyright © FirEURisk Consortium. All rights reserved.

map of EU territory at resolution 1km have to be resampled from weather data current product resolution.

3. For propagation potential calculation two weather scenarios will be used:
    3.1. Average weather conditions (50th percentile of weather parameters) for selected fires, calculated for each pixel.
    3.2. Extreme weather conditions (5% percentile of fuel moisture content and 95th percentile of wind speed) for selected fires, calculated for each pixel looking for extreme values.
4. Propagation potential for the ET territory is calculated for all selected fires and their average and extreme conditions using pixel based calculation on EU raster maps for all inputs in 1 km resolution. Inputs are:
    4.1. New FirEURisk Fuel Map,
    4.2. Slope Map and Aspect map,
    4.3. Two maps for each weather variable (10m windspeed and 10h fuel moisture), one with average weather conditions and one with extreme weather conditions,
    4.4. Wind Direction Map,
    4.5. Crown Fuel Maps for Canopy Cover (CC), Canopy Height (CH), Canopy Base Height (CBH) and Canopy Bulk Density (CBD).

Note: Aspect must coincide with wind direction - If aspect is defined as upslope (0 deg means that aspect is facing south) then wind direction must be 'blowing to'(0 deg means wind is blowing from South to North). If aspect is defined as downslope (180 deg means that aspect is facing South) then wind direction must be 'blowing from'(180 deg means wind is blowing from South to Nord). In BehavePlus both wind direction and aspect are in degree starting from East, anti-clockwise (0 deg means wind is blowing from W to E, 450 means wind is blowing from SW to NE). If wind direction is not available, then the worst case is considered – wind always blowing upslope (angle between wind direction and aspect 0 deg.

The methodology used for propagation potential calculation is partly based on Fuel Class Classification System (FCCS), methodology that was used by Pettinari & Chuvieco (Pettinari & Chuvieco, 2017) for fire behavior simulation on global Earth level with few exceptions:

a) Instead of grouping all input environmental variables in classes, for two of them (wind and slope) exact values for each pixel are used. Fuel Moisture Content will remain grouped in 4 moisture content classes.
b) Instead of using FCCS software tool from Fuel and Fire Tools (FFT) the direct implementation of Rothermel equations for cell-based wildland landscape fire growth simulations is used.

Output of this procedure are GeoTiff raster maps of **surface fire behaviour:**

a) **Rate of Spread** (R) [m/s] – The linear rate of advance of a flaming front into unburned fuel in the direction perpendicular to the fire front. It is a significant factor affecting fireline intensity and flame size, which are important for determining fire effects.
b) **Heat per Area Unit** (HA) [kJ/m2] - heat release per unit area of the surface fire flaming front.
c) **Reaction Intensity** (RI) [kJ/(m2 s)] - heat release per unit area of the surface fire flaming front in one second.
d) **Fireline Intensity** (FI) [kW/m] [kJ/(m s)] - also called Byram's fire intensity is a fundamental fire characteristic. It express heat energy released per unit time from a one-meter-wide section of the fuel bed extending from the front to the rear of the flaming zone.

Copyright © FirEURisk Consortium. All rights reserved.

e) **Flame Length** (FL) [m] - measured in from midway in the active flaming combustion zone to the average tip of the flames. It is indicator of fireline intensity.

and **crown fire behaviour**:

a) **Crown Factor Burned** (CFB) [fraction]- A fraction between 0 and 1 indicating the severity of a crown fire. It is a proportion of tree crowns involved in the fire in a given area. Less than 10 percent is considered as surface fire, between 10 and 89 percent is intermittent crown fire, while over 90 percent is a continuous crown fire.
b) **Crown Fire Activity** (CFA) - Assignment of fire types. Transition to Crown Fire [yes/no] based on Surface Fireline Intensity (IB) [kW/m] and Critical Surface Fireline Intensity (I0). Active Crown Fire Conditions [yes/no] based on Active Crown Fire Rate of Spread (RC) and Critical Crown Fire Rate of Spread (R0). Four conditions are distinguished: Surface Fire, Conditional Crown Fire, Passive Crown Fire (Torching) and Active Crown Fire.
c) **Active or Passive Crown Fire Rate of Spread** [m/s] – the linear rate of advance of a active or passive crown fire flaming front into unburned fuel in the direction perpendicular to the fire front.
d) **Active or Passive Crown Fire Heat per Unit Area** [kJ/m2] - heat release per unit area of the crown and surface fire flaming front.
e) **Active or Passive Crown Fire Fireline Intensity** [kW/m] [kJ/(m s)] - heat energy released per unit time from a one-meter-wide section of the crown fuel bed extending from the front to the rear of the flaming zone.
f) **Active or Crown Fire Passive Flame Length** (FL) [m] - measured in from midway in the active flaming crown combustion zone to the average tip of the flames. It is indicator of fireline intensity.

Additional GeoTiff Maps of following parameters could be also created for crown fire behaviour:

a) The **transition ratio** TR is a Criterion for Crown Fire Initiation (CCFI) defined as the surface fireline intensity divided by the critical surface fireline intensity. If the active ratio is greater than or equal to 1, then the fire may be an active crown fire. The active ratio provides more information than the Yes or No answer provided by the active crown fire variable. It is instructive to know whether the active ratio is close to 1 or significantly different from 1. A value much higher than 1 may indicate that an active crown fire is more likely, while a value much less than 1 may indicate that the fire is more likely to remain a surface fire.
b) The **active ratio** AR is a Criterion for Active Crowning (CAC), crown fire rate of spread divided by the critical crown fire rate of spread. If the active ratio is greater than or equal to 1, then the fire may be an active crown fire. The active ratio provides more information than the Yes or No answer provided by the active crown fire variable. It is instructive to know whether the active ratio is close to 1 or significantly different from 1. A value much higher than 1 may indicate that an active crown fire is more likely, while a value much less than 1 may indicate that the fire is more likely to remain a surface fire.
c) **Active Crown Fire Spread Distance** (D) [m] - The active crown fire spread distance is the head fire (forward) spread distance of an active crown fire calculated from active crown fire rate of spread and elapsed time. Standard time could be 1 h.
d) **Crown Fire Length-to-Width Ratio** (D/W) is used to describe an elliptically shaped fire. For crown fire, it is based on midflame wind speed and is used to calculate crown fire perimeter and area.
e) **Active Crown Fire Area** (A)[m2] - Active crown fire area assumes an elliptically shaped fire. The crown fire is assumed to be active, and the area is calculated from the active crown fire spread distance, 20-ft wind speed, and crown fire length-to-width ratio.

Copyright © FirEUrisk Consortium. All rights reserved.

f) **Active Crown Fire Perimeter** (P) [m]- Active crown fire perimeter assumes an elliptically shaped fire. The crown fire is assumed to be active, and the perimeter is estimated as a shortest perimeter from the active crown fire spread distance D and 10-m wind speed

They will be used as surface and crown propagation potential indicator. For each output parameters two maps will be created, one for average weather conditions and one for extreme weather conditions.

6.1.2 Surface fire behaviour modelling at ET scale

The original Rothermel version of surface fire behaviour modelling for heterogeneous fuels (Rothermel, 1972; Andrews, 2018) shown in Table 16 (Andrews, 2018, p.19) and Table 17 (Andrews, 2018, p.27) is used.
Equations are used with the following assumptions:

- Steady state head fire.
- Flaming front (fine fuels).
- Uniform environmental variables (fuel moisture, wind and slope) in one cell (pixel).
- Heterogeneous mixtures of dead fuel particle sizes and different types of live fuels according to standard Scott-Burgan FBFM - Fire Behaviour Fuel Models, but in one cell (one pixel) only one fuel model could be present.
- The model predicts fire behavior at an equilibrium condition. The theory is that if all inputs remain the same, a fire will reach an equilibrium point where its behavior also remain constant.

Input variables are divided in three groups as Table 18 shows (Andrews, 2018, p.16):

a) fuel particles
b) fuel array and
c) environmental inputs

Copyright © FirEUrisk Consortium. All rights reserved.

Table 21: Equations for the basic fire spread model for heterogeneous fuel (Andrews, 2018, p.19)

Table 6c—Final fire spread model equations for heterogeneous fuel and source for the equations.

Element	Equation[a]
Heat source	
Maximum reaction velocity (min^{-1})	$\Gamma'_{max} = \sigma^{1.5}(495 + 0.0594\sigma^{1.5})^{-1}$
Optimum reaction velocity (min^{-1})	$\Gamma' = \Gamma'_{max}(\beta/\beta_{op})^{A} exp[A(1-\beta/\beta_{op})]$
	$A = 133\sigma^{-0.7913}$
Reaction intensity (Btu/ft^2-min)	$I_R = \Gamma' \sum_i (w_n)_i h_i (\eta_M)_i (\eta_s)_i$
Propagating flux ratio	$\xi = (192 + 0.2595\sigma)^{-1} exp[(0.792 + 0.681\sigma^{0.5})(\beta + 0.1)]$
No-wind, no-slope propagating flux (Btu/ft^2-min)	$I_R\xi$
Heat source	$I_R\xi\,(1 + \phi_w + \phi_s)$
Heat sink	
Heat of preignition for each size class, live and dead (Btu/lb)	$(Q_{ig})_{ij} = 250 + 1{,}116(M_f)_{ij}$
Heat sink (Btu/ft^3)	$\rho_b \epsilon Q_{ig} = \rho_b \sum_i f_i \sum_j f_{ij}[exp(-138/\sigma_{ij})](Q_{ig})_{ij}$
Rate of spread	
Zero-wind, zero-slope rate of spread (ft/min)	$R_0 = \frac{I_R\xi}{\rho_b \varepsilon Q_{ig}}$
Rate of spread (ft/min)	$R = R_0(1 + \phi_w + \phi_s)$

[a]Category is indicated by i = 1 for dead and i = 2 for live; size class is indicated by j.
[b]Source: [1] = Rothermel (1972), [2] = Albini (1976a).

Copyright © FirEURisk Consortium. All rights reserved.

Table 22: Equations of related models implemented in BehavePlus (Andrews, 2018, p.27)

Table 7— Related models as implemented in BehavePlus. These models are not technically part of the Rothermel surface fire spread model, but are often used with it. (Variables not defined here are found in tables 1 and 2.)

Element	Equation	Source
Effective midflame wind speed (ft/min)	$U_E = \left[\phi_E (\beta/\beta_{op})^E / C\right]^{-B}$ where $\phi_E = \phi_w + \phi_s$	Albini (1976b)
Residence time (min)	$t_r = 384/\sigma$	Anderson (1969)
Heat per unit area (Btu/ft²)	$H_A = I_R\, t_r$	Andrews and Rothermel (1982)
Fireline intensity (Btu/ft/s)	$I_B = H_A R/60$ $I_B = I_R t_r R/60$	Albini (1976a) Byram (1959)
Flame length (ft)	$F_B = 0.45\, I_B^{\,0.46}$	Byram (1959)
Dynamic fuel load transfer from live to dead herbaceous (fraction)	$T = -1.11\,M + 1.33,\ 0 \le T \le 1.0$ where M is herbaceous fuel moisture (fraction)	Burgan (1979)

Table 23: Input parameters for the basic fire spread model (Andrews, 2018, p.16)

Table 5—Input parameters for the final fire spread model.

Type	Symbol[a]	Parameter
Fuel particle	h_{ij}	Heat content (Btu/lb)
	$(S_T)_{ij}$	Total mineral content (fraction)
	$(S_e)_{ij}$	Effective mineral content (fraction)
	$(\rho_p)_{ij}$	Particle density (lb/ft³)
Fuel array	σ_{ij}	Surface-area-to-volume ratio (ft²/ft³)
	$(w_0)_{ij}$	Oven-dry fuel load (lb/ft²)
	δ	Fuel bed depth (ft)
	$(M_x)_1$	Dead fuel moisture of extinction (fraction)
Environmental	$(M_f)_{ij}$	Fuel moisture (fraction)
	U	Midflame wind speed (ft/min)
	tan ϕ	Slope steepness (fraction)

[a]Category is indicated by i = 1 for dead and i = 2 for live; size class is indicated by j.

Outputs of Rothermel equations and equations of related models after conversion to metric units are:
Rate of Spread – R [m/s]
Reaction intensity – RI [kW/m2]

Copyright © FirEURisk Consortium. All rights reserved.

Fireline Intensity – FI [kW/m]
Flame Length – FL [m]

It is important to emphasise that the Rothermel surface fire spread model was developed for upslope spread with the wind in the same direction, giving maximal possible rate of spread (ROS), fireline intensity (FI) and flame length (FL). Heat per unit area (HA) and Reaction Intensity (RI) is not affected by wind or slope.

Adaptations could be been made to find rate of spread, fireline intensity, and flame length when the wind is not blowing upslope and spread in directions other than maximum. Various methods and models have been developed. For example, one of these methods based on vector addition, applied in BehavePlus6 is described in (Andrews, 2018, pages 84 – 92). It takes into account also wind direction, usually relative to upslope, therefore aspect is also important. Influence of slope and wind are considered as vectors with their directions and magnitudes. For directions other than wind blowing upslope (both vectors have the same direction) ROS, FI and FL are lower.

Also, this methods result in small correction of final original Rothermel equation for Rate of Spred (final equation in Table 16):

$$R = R0 (1 + FW + FS)$$

where R0 is ROS for zero wind, zero slope, FW is wind correction factor and FS slope correction factor.

When wind and slope vectors are taking into account for calculating maximal ROS supposing the wind is blowing upslope, then vector addition gives corrected formula:

$$R = R0 (1 + FW) + R0 (1 + FS) = R0 (2 + FW + FS)$$

Differences are not very big. For example, for Fuel Model SH7, fuel moisture scenario D1L1, slope 100 and windspeed 10 m/s original Rothermel formula gives ROS = 0.691 m/s and corrected formula ROS = 0.705 m/s.
Both formulas are implemented in our Python code, but as differences are very small and every model is just a model, original Rothermel equation could be used. The same is for correction taking into account wind direction. For propagation potential indices estimation, the best is to consider the worst-case situation, therefore to apply basic Rothermel equation for wind blowing upslope. It gives maximal values for ROS, FI and FL. All models are approximative model and it is better to overestimate potential wildfire risk connected with propagation potential, then to underestimate it.

If wind direction correction must be included calculating procedure is based on vector summation. The biggest values of propagation potential indicators are when aspect and wind direction are the same. It is important to emphasise that aspect must coincide with wind direction - If aspect is defined as upslope (0deg means that aspect is facing south) then wind direction must be 'blowing to'(0 deg means wind is blowing from South to North). If aspect is defined as downslope (180 deg means that aspect is facing South) then wind direction must be 'blowing from'(180 deg means wind is blowing from South to Nord). In BehavePlus both wind direction and aspect are in degree starting from East, anti-clockwise (0 deg means wind is blowing from W to E, 45 deg means wind is blowing

Copyright © FirEUrisk Consortium. All rights reserved.

from SW to NE). If wind direction is not available, then the worst case is considered – wind always blowing upslope (angle between wind direction and aspect 0 deg.

In the methodology used by Pettinari & Chuvieco (Pettinari & Chuvieco, 2017) for fire behavior simulation on global Earth level all input environmental variables were grouped into a few classes:

- three Slope classes
- three midflame wind speed classes and
- four Fuel moisture content classes

therefore, a limited number (36 combinations) of environmental scenarios were defined and used together with global fuelbed parameters to calculate surface fire behaviour outputs.

In our approach exact pixel values for Slope and Midflame wind speed are used, but Fuel moisture content (FMC) is divided into four classes, according to 10-h Fuel Moisture Content (10-h FMC). Therefore, in one cell (pixel) only four possible moisture scenarios could be present:

1. D1L1: Very low dead FMC, fully cured herb
2. D2L2: Low dead FMC, 2/3 cured herb
3. D3L3: Moderate dead FMC, 1/3 cured herb
4. D4L4: High dead FMC, fully green herb

Details are explained in Section 6.1.2.3 Preparation of dynamic data – Fuel Moisture.

Procedure for propagation potential variables calculation includes:

1. Preparation of static data – Fuel Map and Slope Map
2. Preparation of dynamic data – Fuel Moisture Maps and Wind Speed Maps
3. Implementation of Rothermel equations for cell-based wildland landscape fire growth simulations with propagation potential variables as output: Rate of Spread (ROS), Flame Length (FL), Fireline Intensity (FI) and Reaction Intensity (RI). The model was implemented in Python, because it is very suitable for pixel-based calculations on georeferenced raster maps. This procedure is illustrated in Figure 29.

Copyright © FirEUrisk Consortium. All rights reserved.

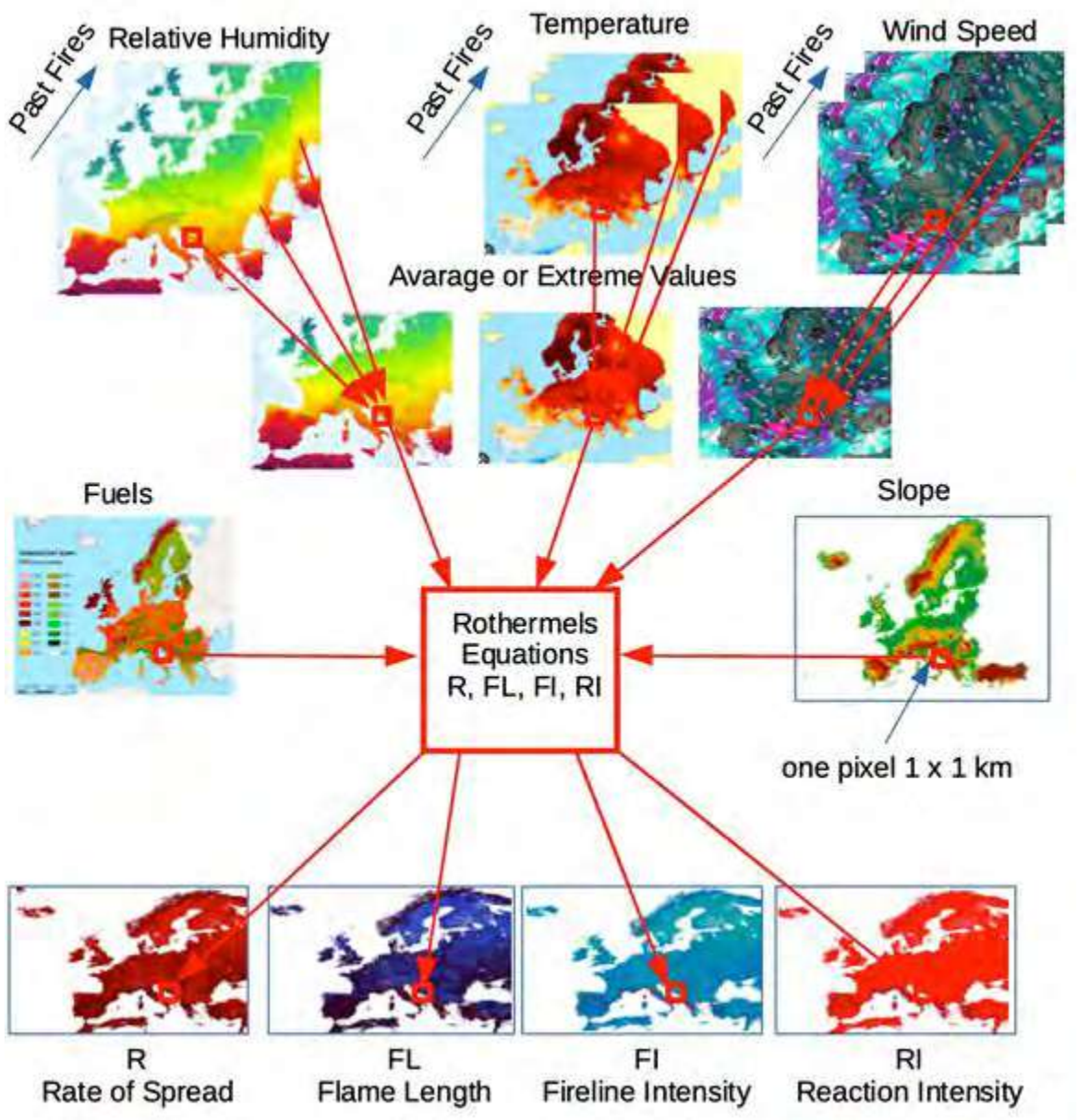


Figure 29: Procedure for cell based (pixel based) calculation of propagation potential variables on EU territory. Instead of temperature, relative and cloud cover (not shown in picture) weather input maps could be fuel moisture map for at least 10-h dead fuel and wind speed map at 10 m height.

All maps that have the same:
Coordinate Reference System (CRC): EPSG:3035 - ETRS89-extended / LAEA Europe
Extent: 2635914.0000000000000000,1384917.0000000000000000:
5955914.0000000000000000,5414917.0000000000000000
Dimensions: X: 3320 Y: 4030 Bands: 1
Pixel Size: 1000 m, -1000 m

6.1.2.1 Preparation of static data – Fuel Map

Fuel Map used for propagation potential calculation on EU territory level will be based on new FirEURiusk fuel models and fuel map developed in WP 1.1.4. New FirEURisk fuel models are based on new fuel classification system

Copyright © FirEURisk Consortium. All rights reserved.

that has 7 main (1st level) fuel classes (Forest, Shrubland, Grassland, Cropland, Peatlands, Urban and Nonfuel) and all together 74 categories after taking into account additional 5 levels for Forests (60 forest classes) and 1 additional level for others excluding Nonfuel (Aragoneses et al. 2022a).

FireEURisk WP A1.1.4 has produced FirEURisk EU Fuel data map at 1 km2 resolution (Aragoneses et al. 2023). This map has only 20 classes, reducing 60 possible Forest classes to only 6 classes (Table 19) taking into account only the 1st level (Figure 30).

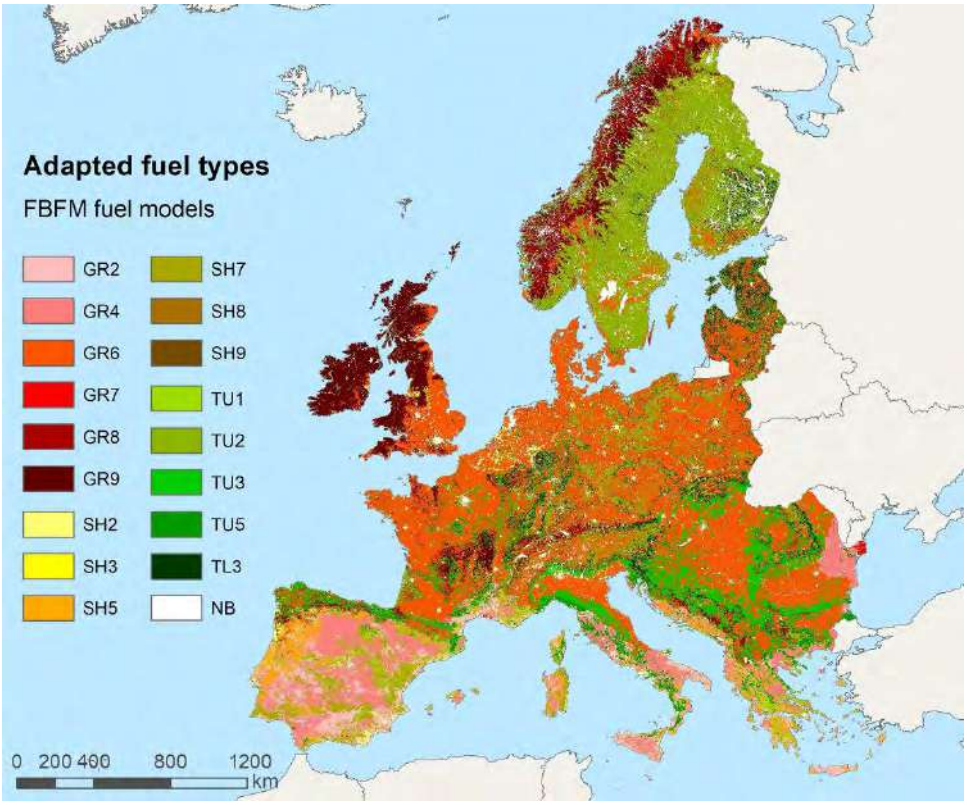


Figure 30: New FirEURisk EU fuel model map adapting the Fuel types to the Scott and Burgan fuel models (Aragoneses et al. 2023) - https://essd.copernicus.org/preprints/essd-2022-184/

Table 24: FirEURisk hierarchical fuel classification system present on EU territory – adapted from (Aragoneses et al. 2022a)

First level		
	Leaf type - Phenology	**Cover density (%)**
1. Forests	11. Broadleaf 112. Deciduous	1121. Open [15-70%)
		1122. Close [70-100%]
	12. Needleleaved 121. Evergreen	1211. Open [15-70%)
		1212. Close [70-100%]
	13. Mixed	1301. Open [15-70%)
		1302. Close [70-100%]
	Fuel depth	
2. Shrubland	21. Low [0-0.5m)	
	22. Medium [0.5-1.5m)	
	23. High (≥ 1.5m)	

Copyright © FirEURisk Consortium. All rights reserved.

3. Grassland	31. Low [0-0.3m)	
	32. Medium [0.3-0.7m)	
	33. High (≥ 0.7m)	
	Type	
4. Cropland	41. Herbaceous	
	42. Woody (shrub-tree)	
5. Wet and peat/ semi-peat land	51. Tree	
	52. Shrubland	
	53. Grassland	
6. Urban	61. Continuous fabric: urban fabric [80-100%]	
	62. Discontinuous fabric: vegetation and urban fabric [15-80%)	
7. Nonfuel		

Fuel parameters

For fuel model WP1.1.4 has prepared the final classification table connecting FirEURisk fuel classes and standard Scott-Burgan fuel models (FBFM - Fire Behaviour Fuel Models) (Scott and Burgam, 2005).

Conversion table is different for *A: arid/semi-arid regime, *H: sub-humid/humid regime (Figure 31). Main idea of this conversion is to use fuel parameters defined by Scott-Burgan fuel models adapted for EU territory.

Aragoneses et al. 2022
https://essd.copernicus.org/preprints/essd-2022-184/



Fuel Code	Fuel Description	Crosswalk A*	Crosswalk H*
1111	Open broadleaf ev. forest	SH7	SH8
1112	Closed broadleaf ev. forest	TU1	TU2
1121	Open broadleaf dec. forest	SH5	SH9
1122	Closed broadleaf dec. forest	TU5	TU3
1211	Open needleleaf ev. forest	SH7	SH8
1212	Closed needleleaf ev. forest	TU1	TU2
1221	Open needleleaf dec. forest	SH5	SH9
1222	Closed needleleaf dec. forest	TU5	TL3
1301	Open mixed forest	SH7	SH8
1302	Closed mixed forest	TU5	TL3
21	Low shrubland	SH2	SH3
22	Medium shrubland	SH7	SH8

Fuel Code	Fuel Description	Crosswalk A*	Crosswalk H*
23	High shrubland	SH5	SH9
31	Low grassland	GR2	GR6
32	Medium grassland	GR4	GR8
33	High grassland	GR7	GR9
41	Herbaceous cropland	GR4	GR6
42	Woody cropland	GR2	GR6
51	Tree wet & peatland	SH7	SH8
52	Shrubland wet & peatland	SH5	SH9
53	Grassland wet & peatland	GR7	GR9
61	Urban continuous fabric	NB	NB
62	Urban discontinuous fabric	SH2	SH3
7	Nonfuel	NB	NB

Standard Fuel Models of Scott and Burgan (2005)

Figure 31: Conversion table between new FirEURisk EU fuel categories and Scott-Burgan FBFM categories - Aragoneses et al. 2022c- https://essd.copernicus.org/preprints/essd-2022-184/

Copyright © FirEURisk Consortium. All rights reserved.

Figure 32 shows EU Fuel Map used for propagation potential calculation where negative values are used for arid zones and positive values for humid zones. Conversion into Scott-Burgan categories was performed inside Python code for Rothermel fire behaviour calculation.

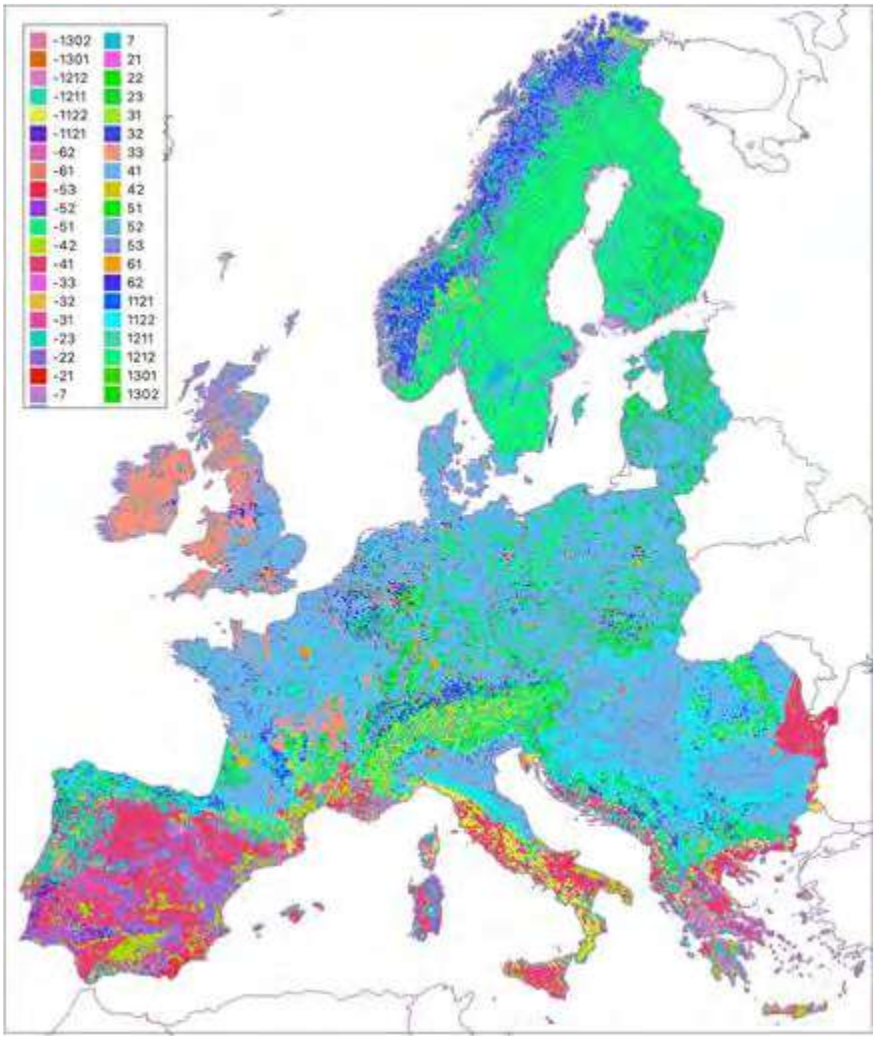


Figure 32: New FirEURisk EU fuel map used for propagation potential calculation (Map was part of material for 1st FirEUrisk workshop: Prof. Emilio Chuvieco and Elena Aragoneses, University of Alcalá (Spain), FirEUrisk training event online, focusing on "The FirEUrisk fuel classification system and the European fuel map", Feb 2nd, 2023, adapted for propagation potential calculation.)

Concerning fuel parameters, each Scott-Burgan fuel category is defined by 12 standard parameters describing surface fuels:

- SL – Fuel surface load (t/ha)
    - FL_D1h for dead 1-h
    - FL_D10h for dead 10-h
    - FL_D100h for dead 100-h
    - FL_LH for Live Herbaceous and
    - FL_LW for Live Woody

Copyright © FirEURisk Consortium. All rights reserved.

- SAV – Surface Ara/Volume Ratio (m2/m3 = 1/m)
    - SAV_D1h for Dead 1-h
    - SAV_LH for Live Herbaceous
    - SAV_LW for Live Woody
- ME – Dead Fuel Moisture of Extinction (%)
- FD – Fuel Bed Depth (m) – now named DEPTH
- HC – Heat Content of Fuel (kJ/kg) for:
    - HC_DEAD for Dead Fuel
    - HC_LIVE for Live Fuel

All parameters of Scott-Burgan standard fuels model of FBFM adapted for EU territory are shown in Table 20 adapted from (Aragoneses et al. 2022c).

Table 25: Scott-Burgan standard FBFM fuel model parameters for categories presented on EU territory (Aragoneses et al. 2022c) - https://essd.copernicus.org/preprints/essd-2022-184/ with corrections[1]

Table C1. Parameters of the standard fuel models of FBFM (Scott and Burgan, 2005) used for the crosswalk to the first-level FirEUrisk fuel types.

FBFM fuel model	Dead fuel load			Live fuel load		Surface Area to Volume ratio			Depth	Moisture of extinction	Heat content		Main fuel type	Description
	1h	10h	100 h	Herb	Woody	Dead 1h	Live herb	Live woody			Dead	Live		
	t ha^{-1}			t ha^{-1}		m^2 m^{-3}			m	%	kj kg^{-1}			
GR2	0.22	0.00	0.00	2.24	0.00	6562	5906	4921	0.30	15	18622	18622	Grasses	Low load. Dry climate grass
GR4	0.56	0.00	0.00	4.26	0.00	6562	5906	4921	0.61	15	18622	18622	Grasses	Moderate load. Dry climate grass
GR6	0.22	0.00	0.00	7.62	0.00	7218	6562	4921	0.46	40	18622	18622	Grasses	Moderate load. Humid climate grass
GR7	2.24	0.00	0.00	12.11	0.00	6562	5906	4921	0.91	15	18622	18622	Grasses	High load. Dry climate grass
GR8	1.12	2.24	0.00	16.36	0.00	4921	4265	4921	1.22	30	18622	18622	Grasses	High load. Very coarse. Humid climate grass
GR9	2.24	2.24	0.00	20.18	0.00	5906	5249	4921	1.52	40	18622	18622	Grasses	Very high load. Humid climate grass
SH2	3.03	5.38	1.68	0.00	8.63	6562	4921	5249	0.30	15	18622	18622	Shrubs	Moderate load. Dry climate shrub
SH3	1.01	6.73	0.00	0.00	13.90	5249	4921	4593	0.73	40	18622	18622	Shrubs	Moderate load. Humid climate shrub
SH5	8.07	4.71	0.00	0.00	6.50	2461	4921	5249	1.83	15	18622	18622	Shrubs	High load. Dry climate shrub
SH7	7.85	11.88	4.93	0.00	7.62	2461	4921	5249	1.83	15	18622	18622	Shrubs	Remarkably high load. Dry climate shrub
SH8	4.60	7.62	1.91	0.00	9.75	2461	4921	5249	0.91	40	18622	18622	Shrubs	High load. Humid climate shrub
SH9	10.09	5.49	0.00	3.47	15.69	2461	5906	4921	1.34	40	18622	18622	Shrubs	Remarkably high load. Humid climate shrub
TU1	0.45	2.02	3.36	0.45	2.02	6562	5906	5249	0.18	20	18622	18622	Litter & Understory	Low load. Dry climate timber-grass-shrub
TU2	2.13	4.04	2.80	0.00	0.45	6562	4921	5249	0.30	30	18622	18622	Litter & Understory	Moderate load. Humid climate timber-shrub
TU3	2.47	0.34	0.56	1.46	2.47	5906	5249	4593	0.40	30	18622	18622	Litter & Understory	Moderate load. Humid climate timber-grass-shrub
TU5	8.97	8.97	6.73	0.00	6.73	4921	4921	2461	0.30	25	18622	18622	Litter & Understory	Very high load. Dry climate timber-shrub
TL3	1.12	4.93	6.28	0.00	0.00	6562	4921	4921	0.09	20	18622	18622	Litter & Understory	Moderate load conifer litter

EU Map with Scott-Burgan standard FBFM categories, together with their fuel parameters from table 20 , will be used as **Fuel Map Inputs** to Rothermel equations for cell-based wildland landscape fire growth simulations.

[1] In original table published in https://essd.copernicus.org/preprints/essd-2022-184/ all values for Surface Area to Volume Ratio are defined, even for certain fuel models some categories are missing (for example for GR2 there is no Live Woody Fuel). In (Scott & Burgan, 2005, p.18) that was marked with 9999. In (Aragoneses et al. 2022c) the same values 4921 [m^{-1}] are assigned to all missing categories, but in BehavePlus , 9999 was replaced with 5906 [1/m] for SAV of Live Herb Fuels and with 4921 [1/m] for SAV of Live Woody Fuel.

Copyright © FirEURisk Consortium. All rights reserved.

The basic Rothermel fire spread model is based on one size class of dead and live fuel. When there are several size classes of dead (1-h, 10-h, 100-h) and live fuel (LH, LW), a **method of weighting** is used to define characteristic values to be used in the final calculations.

There are two weighting factors g_{ij} important for Fuel Surface Load and weighting factor f_{ij} important for Surface Area to Volume Ratio and Fuel Moisture. Indeks *i* correspond to dead or live fuels (*i=1* dead, *i=2* live).

For static fuels (SH2, SH3, SH5, SH7, SH8, TU2, TU5, TL3) both coefficients are equal $f_{ij} = g_{ij}$.

For dynamic fuels, that allow greater variability due to seasonal transitions in live fuels (GR2, GR4, GR6, GR7, GR8, GR9, Sh9, TU1, TU3) coefficients are different and depends of live fuel moisture content determinate by percentage of curing. In standard FBFM fuel models three categories are three categories: 100% cured (very dry), 50% cured (moderate dry), and 0% cured (not dry). As we are using 4 moisture scenarios explained in Section 6.1.2.4 D1L1 will correspond to 100% cured, D2L2 and D3L3 to 50% cured and D4L4 to 0% cured.

Inputs to Rothermel equations regarding fuel parameters, together with conversion factors from English to Metric units are:

H - HC - Heat Content - for all Scott - Burgan fuel models (Fig.9) this value is constant: 8000 [Btu/lb] = 18622 [kJ/kg]

S_T - Total Mineral Content (fraction) - constant value: 0.0555 (5.55%)

S_e - Effective Mineral Content (fraction) - constant value: 0.010 (1.0%)

ρ_P - Oven - Dry Particle Density - constant value: 32 [lb/ft^3] = 512.592 [kg/m^3]

w_0 - FL - Fuel Surface Load - 1 [lb/ft^2] = 48.8243 [t/ha]. In parameter table different values $(w_0)_{ij}$ for Dead 1-h, 10-h, 100-h, Live Herbaceous and Live Woody for each fuel model are defined.

Input parameter to Rothermel equation is **Net Fuel Load** of dead (*i=1*) and live fuels (*i=2*) defined as:

$$(w_n)_i = \sum_j g_{ij} \cdot (w_0)_{ij} \cdot (1 - S_T) \qquad (2)$$

where S_T is total mineral content (constant) and g_{ij} is weighting factor calculated using equations shown in Table 26 (Andrews, 2018, Table 6a, p.17):

Table 26: Calculation of weighting factors g_{ij} (Andrews, 2018, Table 6a, p.17).

Weighting factor for net fuel load

Fuel is partitioned by size into six subclasses: [2] (p. 15)

$\sigma \geq 1,200$
$1,200 > \sigma \geq 192$
$192 > \sigma \geq 96$
$96 > \sigma \geq 48$
$48 > \sigma \geq 16$
$16 > \sigma$

Members of each subclass are given the same weighting factor:

$$g_{ij} = \sum_{\substack{\text{subclass} \\ \text{to which} \\ i \text{ belongs}}} f_{ij}$$

For $\sigma < 16$, $g_{ij} = 0$

Andrews published tables with precalculated g_{ij} weighting factors (Andrews, 2018, Table 12, 13a, 13b, p.49-51). For certain dynamic fuel models weighting factor depends also on percentage of cured vegetation (fuel moisture scenarios – see Section 6.1.2.3). For propagation potential fire behaviour variables calculation we have applied both approaches:

- calculation of weighting factor g_{ij} according to Table 21 and

Copyright © FirEURisk Consortium. All rights reserved.

- using precalculated g_{ij} factors from (Andrews, 2018, Table 12, 13a, 13b, p.49-51).

For example, for shrub static fuel SH8 (Shrub) for all moisture scenarios there is only one set of g_{ij} parameters and for dynamic fuel SH9 there are three sets of fuel parameters for 0, 50 and 100% cured:

Table 27: Weighting factors according to table 21

Fuel	Cured (%)	Dead 1-h	Dead 10-h	Dead 100-h	Live Herb	Live Woody
		g_{11}	g_{12}	g_{13}	g_{21}	g_{22}
SH8	ANY	0.80	0.19	0.01	0	1
SH9	100	0.96	0.04	0	0	0
SH9	50	0.95	0.05	0	1	1
SH9	0	0.93	0.07	0	1	1

Therefore, for Net Fuel Load of static models SH8 is simple:

SH8 Dead - $(w_n)_1 = (0.8 \cdot 4.6 + 0.19 \cdot 7.62 + 0.01 \cdot 1.91) \cdot (1 - 0.0555) = 4.86\ [t/ha]$

SH8 Live - $(w_n)_2 = (0 \cdot 0 + 1 \cdot 9.75) \cdot (1 - 0.0555) = 9.21\ [t/ha]$

For dynamic SH9 fuel model it is important to know cured percentage and that is connected with fuel moisture scenarios (see Section 6.1.2.3). For example, for 50% cured (moisture scenarios D2L2 and D3L3):

SH9 Dead - $(w_n)_1 = (0.95 \cdot 10.09 + 0.05 \cdot 5.49 + 0 \cdot 0) \cdot (1 - 0.0555) = 9.31\ [t/ha]$

SH9 Live - $(w_n)_2 = (1 \cdot 3.47 + 1 \cdot 15.69) \cdot (1 - 0.0555) = 18.29\ [t/ha]$

σ - SAV - Surface Area to Volume Ratio (1 [ft^{-1}] = 3.2808 [m^{-1}]) - different values σ_{ij} for Dead 1-h, Live Herbaceous and Live Woody for each fuel model (Fig.9). For all fuel models values for 10-h and 100-h SAV are the same (Scott & Burgan, 2005, p.2):

- 10-h SAV: σ_{12} = 109 [ft^{-1}] = 357.6 [m^{-1}]
- 100-h SAV: σ_{13} = 30 [ft^{-1}] = 98 [m^{-1}]

Surface Area to Volume Ratio of dead fuels (i = 1) and live fuels (i=2) is equal to weighted sum of their surface area to volume ratios:

$$\sigma_i = \sum_j \sigma_{ij} \cdot f_{ij} \quad (3)$$

and total surface area to volume ratio of a certain fuel model is equal to:

$$\sigma = \sum_i \sigma_i \cdot f_i \quad (4)$$

where f_{ij} and f_i are weighting factors calculated with equations shown in Table 23 (Andrews, 2018, Table 6a, p.17):

Copyright © FirEURisk Consortium. All rights reserved.

Table 28: Calculation of weighting factors g_{ij} (Andrews, 2018, Table 6a, p.17)

Weighting factors		
Mean total surface area per unit fuel cell of each size class within each category	$A_{ij} = (\sigma)_{ij}(w_0)_{ij}/(\rho_p)_{ij}$	[1] (eq. 53)
Mean total surface area of the live and dead categories	$A_i = \sum_j A_{ij}$	[1] (eq. 54)
Mean total surface area of the fuel	$A_T = \sum_i A_i$	[1] (eq. 55)
Weighting factor for characteristic dead and live heat content, effective mineral content, moisture content, and surface-area-to-volume ratio	$f_{ij} = A_{ij}/A_i$	[1] (eq. 56)
Weighting factor for characteristic fuel bed surface-area-to-volume ratio	$f_i = A_i/A_T$	[1] (eq. 57)

Andrews published tables with precalculated f_{ij} weighting factors for static and dynamic standard FBFM fuel models (Andrews, 2018, Table 12, 13a, 13b, p.49-51). For certain dynamic fuel modesl weighting factor depends also on percentage of cured vegetation (fuel moisture scenarios – see Section 6.1.2.3). For propagation potential fire behaviour variables calculation, we have applied both approaches:

- calculation of weighting factor g_{ij} according to Table 21 and
- using precalculated g_{ij} factors from (Andrews, 2018, Table 12, 13a, 13b, p.49-51).

For example, for shrub static fuel SH8 (Shrub) there is only one set of and dynamic fuel SH9 for moisture scenario D2L2: Low dead FMC, 2/3 cured herb or D3L3: Moderate dead FMC, 1/3 cured herb coefficients are:

Table 29: weighting factors for static and dynamic standard FBFM fuel models

Fuel	Cured (%)	Dead 1-h	Dead 10-h	Dead 100-h	Live Herb	Live Woody	Dead	Live
		f_{11}	f_{12}	f_{13}	f_{21}	f_{22}	f_1	f_2
SH8	ANY	0.80	0.19	0.01	0	1	0.22	0.78
SH9	100	0.96	0.04	0	0	1	0.38	0.62
SH9	50	0.95	0.05	0	0.12	0.88	0.30	0.70
SH9	0	0.93	0.07	0	0.21	0.79	0.22	0.78

For dynamic SH9 fuel and 50 % cured (moisture scenarios D2L2 and D3L3) we have:

Dead $\sigma_1 = 2461 \cdot 0.95 + 357.8 \cdot 0.05 + 98 \cdot 0 = 2307\ [m^{-1}]$

Live $\sigma_2 = 5906 \cdot 0.12 + 4921 \cdot 0.88 = 5039\ [m^{-1}]$

Total $\sigma = 2307 \cdot 0.3 + 5039 \cdot 0.7 = 4219\ [m^{-1}]$

δ - FD - Fuel Depth - 1 [ft] = 0.3048 [m]) - unique value for each fuel model from Scott – Burgan table (Fig.9)

$(M_x)_1$ - ME - Moisture of Extinction od **dead fuels** [%] - unique value for each fuel model from Scott – Burgan table (Fig.9). $(M_x)_2$ - Moisture of Extinction of **live fuels** is calculated from dead fuel moistures, fuel loads and surface area to volume ratios (Andrews, 2018, p.16). More details in Section 6.1.2.3.

6.1.2.2 Preparation of static data – Slope Map

One of the inputs to Rothermel equations is slope ϕ.

Copyright © FirEURisk Consortium. All rights reserved.

Slope in degrees or radians is equal to the tangent of amount of elevation change (rise) divided by the amount of horizontal distance covered (run).
Elevation data are available for all EU territory in the form of EU DEM v1.1 - https://www.eea.europa.eu/data-and-maps/data/copernicus-land-monitoring-service-eu-dem
From elevation map slope map could be calculated. Figure 33 shows EU slope map in 1 km resolution.

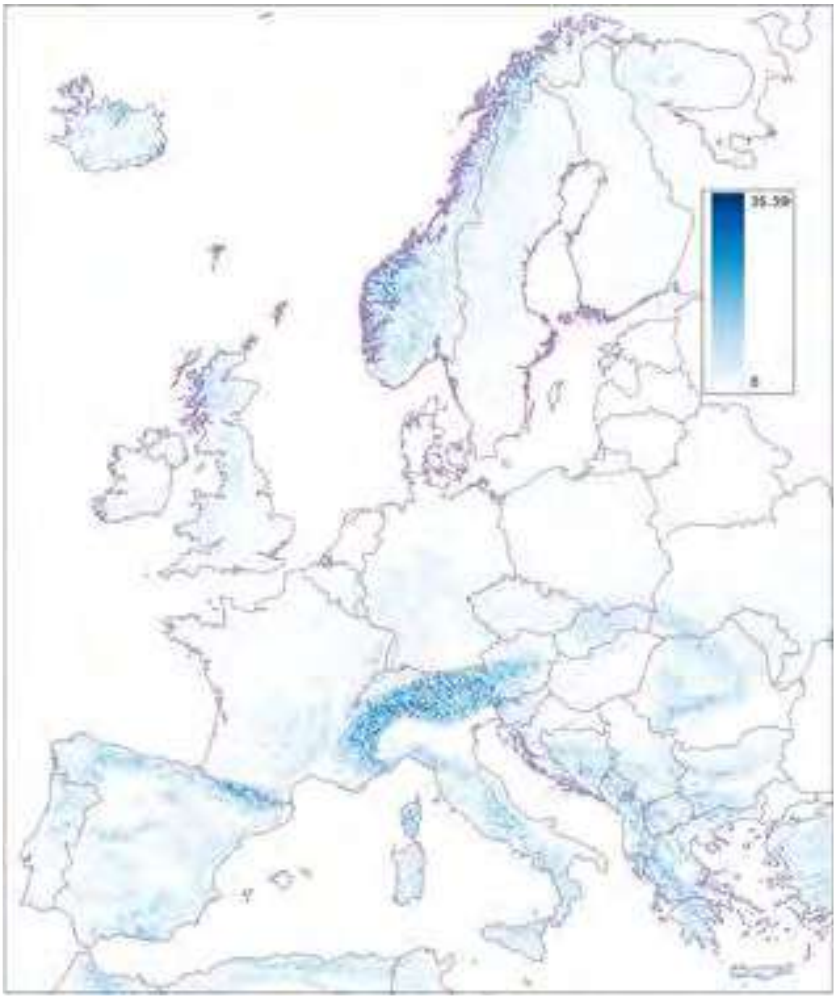


Figure 33: EU slope map

Statistical data concerning slope in 1km resolution on EU territory are:

- STATISTICS_MAXIMUM=35.39
- STATISTICS_MEAN=1.05
- STATISTICS_MINIMUM=0
- STATISTICS_STDDEV=2.50

Copyright © FirEURisk Consortium. All rights reserved.

6.1.2.3 Preparation of fire dynamic data

Dynamic data are related to weather conditions during past fires on the European territory from Jan, 1st 2001 to Dec, 31st 2019. The dataset has[2] 5,133 past fires. From this dataset, fires that have burned area larger than 2000 ha are selected. There are 403 such fires larger than 2000 ha.
Statistical properties of this dataset of large fires according to total burning area on EU territory for that particular date in [ha] are:

- STATISTICS_MAXIMUM= 304958 ha
- STATISTICS_MEAN= 2043 ha
- STATISTICS_MINIMUM= 8877 ha
- STATISTICS_STDDEV= 25198

The list of 403 past fires on EU territory is available. We focused on the 403 dates that included the fires larger than 2000 ha and later we used the 95 percentile for extreme and 50 percentile for average conditions, on EU raster maps for all inputs at 1 km resolution. Inputs are:

6.1.2.4 Preparation of dynamic data – Fuel Moisture

A single value of Moisture Content M_f expressed as a fraction (not %) is one of the required inputs.
Initial moisture content values are usually defined for three dead fuel classes (1-h, 10-h, 100-h) and two live classes (woody and herbaceous). Characteristic moisture content values of dead and live fuels are computed as a weighted average, where the weighting factors are the relative contribution of each class to the overall fuel particle surface area of the fuelbed (Scott, 2012 p.61). Calculation based on weighting factors gives more significance to certain moisture content values depending of relative contribution of each class to the overall fuel particle surface area of the fuelbed.
Considering fuel moisture content, a procedure proposed by Pettinari & Chuvieco (Pettinary & Chuvieco, 2017) used for fire behaviour simulation on global Earth level was adopted. **Fuel moisture content** (FMC) was divided into four **Fuel Moisture Scenarios**, according to **10-h Fuel Moisture Content** (m_{10h}):

D1L1: $m_{10h} < 5.5\%$
D2L2: $5.5\% \leq m_{10h} < 8.5\%$
D3L3: $8.5\% \leq m_{10h} < 10.5\%$
D4L4: $m_{10h} \geq 10.5\%$

In each FMC class, values of all fuel moisture contents (dead fuel, live fuel, live crown) are defined according to table shown on Table 30 (Pettinari & Chuvieco, 2017):

[2] Dataset of past fires on EU territory was prepared by Marcos Rodrigues Mimbrero, Universitat de Lleida, Lleida, Spain

Copyright © FirEURisk Consortium. All rights reserved.

Table 30: Fuel Moisture Scenarios (Pettinari & Chuvieco, 2017)

FMS Code	FMS Description	Fuel Moisture Content (%)					
		Herb	Shrub	Crown [1]	1 h	10 h	100 h
D1L1	Very low dead FMC, fully cured herb	30	60	60	3	4	5
D2L2	Low dead FMC, 2/3 cured herb	60	90	60	6	7	8
D3L3	Moderate dead FMC, 1/3 cured herb	90	120	120	9	10	11
D4L4	High dead FMC, fully green herb	120	150	150	12	13	14

[1] The Scott and Burgan original FMSs do not include FMCs for Crown. These data were extracted from the description of the variables inside the FCCS software.

In 6.1.2.3 we have mentioned that for dynamic fuel models weighting factors f_{ij} and g_{ij} depend of cured percentage. The sets of weighting factors were defined (Andrews, 2018, Table 12, 13a, 13b, p.49-51) for 100%, 50% and 0% cured. In moisture scenarios we have 100% cured (D1L1), 67% cured (D2L2, 33% cured (D3L3) and 0% cured (D4L4), therefore two moistures scenarios D2L2 and D3L3 were considered as 50% cured.
10-h FMC (m_{10h}) could be estimated (Bugarić at al., 2022):

- From standard **Fire Behaviour Analysis Tables** (**FBA Tables**) used in **78/88 National Fire Danger Rating System (NFDRS)** or from corrected **Basic Fuel Moisture Content (BFMC) tables** for southern Europe used by MeteoGrid for official Dead Fuel Moisture estimation in few southern Europe countries.
- From Equilibrium Moisture Content and Cohen & Deeming equations used in **1985 National Fire Danger Rating System (NFDRS).**
- From **Nelson model** used in in **2016 National Fire Danger Rating System (NFDRS)**.
- From Canadian **Fine Fuel Moisture Content (FFMC)** code.
- From **Vapour Pressure Deficit (D)**.

We have analysed all five methods in our Demonstration Area (Split – Dalmatia County) in order to find which one is the most suitable for propagation potential calculation (Stipaničev & Bugarić, 2023). Our conclusion was that two methods are best suited for this task:

- Corrected **Basic Fuel Moisture Content (BFMC) tables** for southern Europe used by MeteoGrid for official Dead Fuel Moisture estimation or
- The method based on Cohen & Deeming, equations used originally in **1985 National Fire Danger Rating System (NFDRS)**, but also for fire behaviour simulations from global fuel and climatic information (Pettinari & Chuvieco, 2017)

Both methods are described in detail in the report Propagation Potential - calculation methodology for Pilot Sites (PS) (Bugarić et al., 2022).
For propagation potential calculation on EU level MeteoGrid has calculated 10h Dead Fuel Moisture Content for average weather conditions (50th percentile) and extreme weather conditions (5th percentile) from weather data of past fires on EU territory using **Basic Fuel Moisture Content (BFMC) tables** for southern Europe with some limitations. The 10 hr humidity were obtained from Era5Land files interpolated to 1km. Input variables were Temperature, Dew Point, and Wind Speed, obtained from u and v components. Relative Humidity was calculated from Temperature and Dew Point. They have not taken into account corrections for cloudiness nor precipitation, partly for time reasons and partly for space reasons, the set of files occupies several TB.

Copyright © FirEURisk Consortium. All rights reserved.

Figure 34 shows GeoTiff map of average (FirEURisk_d10hr_12H_percentile_50_EU.tiff) and Figure 35 of extreme conditions (FirEURisk_d10hr_12H_percentile_5_EU.tiff).
Both fuel moisture contents are quite high. Mean value for average condition (50th percentile) is 16.6%, having minimal value of 6.6%. For extreme condition (5th percentile) mean value is 10.7% and minimal value 4.6%. Therefore, we expect quite low values of propagation potential variables.

6.1.2.5 Calculation of final Moisture Content Mf

From 10-h Dead Fuel Moisture Content (m_{10h}), an appropriate Fuel Moisture Scenario is defined, having specific values of all moisture content variables:

- Dead 1-h: $m_{1h} = (M_f)_{11}$
- Dead 10-h: $m_{10h} = (M_f)_{12}$
- Dead 100-h: $m_{100h} = (M_f)_{13}$
- Live Herb: $m_{LH} = (M_f)_{21}$
- Live Shrub $m_{LS} = (M_f)_{22}$

Final Moisture Content (M_f) depends of the fuel type and its weighting factor:

$$\left(\mathrm{M}_f\right)_{dead} = \sum_j \left(\mathrm{M}_f\right)_{1j} \cdot f_{1j} \quad (5)$$

$$\left(\mathrm{M}_f\right)_{live} = \sum_j \left(\mathrm{M}_f\right)_{2j} \cdot f_{2j} \quad (6)$$

where f_{ij} is weighting factor mentioned in 6.1.2.3 expressed as a fraction, not %.

Copyright © FirEURisk Consortium. All rights reserved.

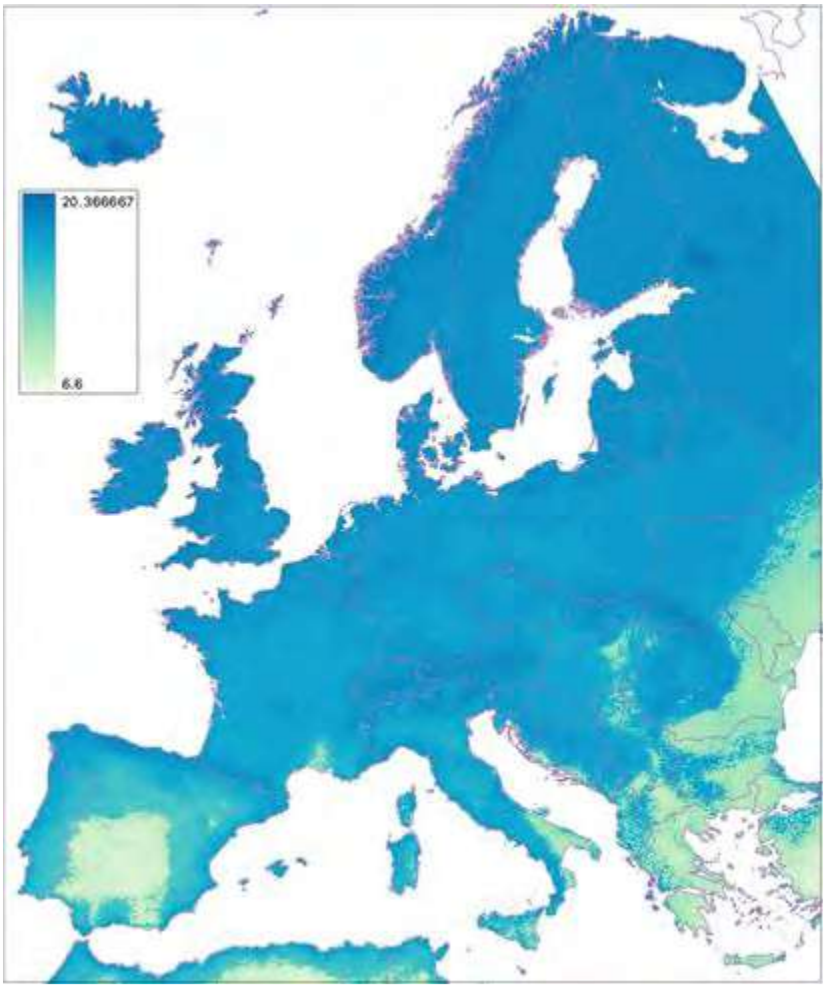


Figure 34: Map of average (50th percentile) 10h dead fuel moisture content in %, calculated by MeteoGRID from past fires on EU territory

Statistical data concerning average 10h dead fuel moisture conditions on EU territory are:

- STATISTICS_MAXIMUM=20.366666793823
- STATISTICS_MEAN=16.617126871063
- STATISTICS_MINIMUM=6.5999999046326
- STATISTICS_STDDEV=2.5739616220453

Copyright © FirEURisk Consortium. All rights reserved.

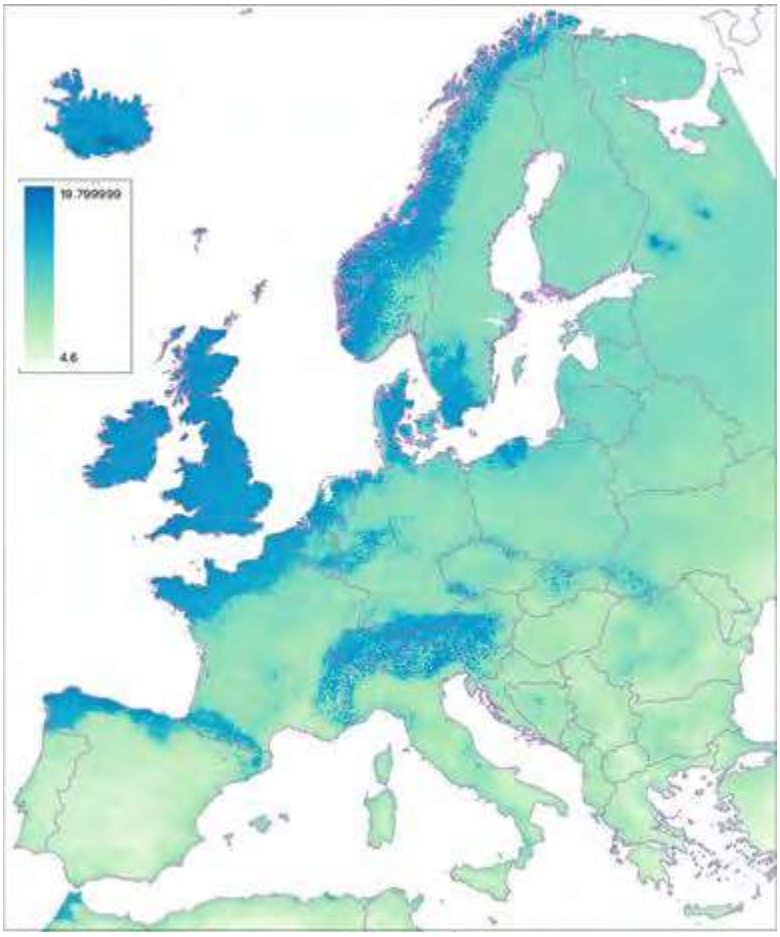


Figure 35: Map of extreme (5th percentile) 10h dead fuel moisture content in %, calculated by MeteoGRID from past fires on EU territory

Statistical data concerning extreme 10h dead fuel moisture conditions on EU territory are:

- STATISTICS_MAXIMUM=19.799999237061
- STATISTICS_MEAN=10.663044834113
- STATISTICS_MINIMUM=4.5999999046326
- STATISTICS_STDDEV=2.9797378121615

For example, let us suppose that moisture is D1L1 having:

- 1-h Dead $(M_f)_{11}$ = *3% = 0.03*
- 1-h Dead $(M_f)_{12}$ = *4% = 0.04*
- 1-h Dead $(M_f)_{13}$ = *5% = 0.05*
- Live Herb $(M_f)_{21}$ = *30% = 0.3*
- Live Shrub $(M_f)_{22}$ = *60% = 0.6*

and static fuel model SH8. Weighting factors are:

Copyright © FirEURisk Consortium. All rights reserved.

Table 31: Static fuel model SH8 weighting factors

Fuel	Dead 1-h	Dead 10-h	Dead 100-h	Live Herb	Live Woody
	f_{11}	f_{12}	f_{13}	f_{21}	f_{22}
SH8	0.80	0.19	0.01	0	1

$$(\mathrm{M}_f)_{dead} = 0.03 \cdot 0.8 + 0.04 \cdot 0.19 + 0.05 \cdot 0.01 = 0.031 \quad (7)$$

$$(\mathrm{M}_f)_{live} = 0.3 \cdot 0 + 0.6 \cdot 1 = 0.6 \quad (8)$$

$(M_x)_2$ - **Moisture of Extinction of Live Fuels** is calculated using equations from (Andrews, 2018, p.16) (Note: Equations are for moisture in %):

$$(\mathrm{M}_x)_2 = \max\left\{(\mathrm{M}_x)_1, 290\frac{W_{dead}}{W_{live}}\left(1 - \frac{(\mathrm{M}_f)_{fine_dead}}{(\mathrm{M}_x)_1}\right) - 22.6\right\} \quad (9)$$

$$W_{dead} = \sum_j (\mathrm{w}_0)_{1j} \cdot e^{-\frac{138}{\sigma_{1j}}} \quad (10)$$

$$W_{live} = \sum_j (\mathrm{w}_0)_{2j} \cdot e^{-\frac{500}{\sigma_{2j}}} \quad (11)$$

$$(\mathrm{M}_f)_{fine_dead} = \frac{\sum_j (\mathrm{M}_f)_{1j} \cdot (\mathrm{w}_0)_{1j} \cdot e^{-\frac{138}{\sigma_{1j}}}}{\sum_j (\mathrm{w}_0)_{1j} \cdot e^{-\frac{138}{\sigma_{1j}}}} \quad (12)$$

6.1.2.6 Preparation of dynamic data – Wind Speed

Meteorological wind speed is measured at 10 m altitude U_{10m} [m/s] in EU, or 20ft altitude in US, but in Rothermel calculations wind speed at midflame height U [ft/min] is used.

Various formulas have been proposed for this conversion. The simplest one is conversion formula used by (Pettinari & Chuvieco, 2017):

$$U = U_{10m} \cdot 0.348 \quad (13)$$

but better approach is based on **Wind Adjustment Factor** (WAF) proposed by Albini and Baughman (1979) and used by Scott (Scott, 2007) and implemented in BehavePlus, Firesite and FlamMap. WAF is defined for wind speed at 20ft altitude, therefore additional correction factor from 10m to 20ft has to be applied, for example 0.87 proposed by (Turner & Lawon, 1978, Appendix 6)

$$U = U_{10m} \cdot 0.87 \cdot WAF \quad [m/s] \quad (14)$$

WAF is different for each standard fuel model (Table 32).

Table 32: Wind Adjustment Factor (WAF) for standard fuel models (Scott, 2007)

Model	GR2	GR4	GR6	GR7	GR8	GR9	SH2	SH3	SH5	SH7	SH8	SH9	TU1	TU2	TU3	TU5	TL3
WAF	0.36	0.42	0.39	0.46	0.49	0.52	0.36	0.44	0.55	0.55	0.46	0.50	0.33	0.36	0.38	0.36	0.29

Input to Rothermel equations is wind speed in [ft/min] and and therefore additional correction from [m/s] to [ft/min] must be added:

$$U = U_{10m} \cdot 0.87 \cdot WAF \cdot 196.85 \quad [ft/min] \quad (15)$$

Copyright © FirEURisk Consortium. All rights reserved.

For propagation potential calculation on EU level MetoGrid has calculated average wind speed (50th percentile) and extreme wind speed (95th percentile) from weather data of past fires on EU territory from Era5Land u and v wind speed files interpolated to 1km. Figure 36 shows GeoTiff map of average wind speed (FirEUrisk_wind_speed_12H_percentile_50_EU.tiff) and Figure 37 of extreme wind speed (FirEUrisk_d10hr_12H_percentile_5_EU.tiff).

Wind speed maps are quite similar. Differences are in second decimals. Mean value is 5.4 m/s = 19.4 km/h, and maximal value 14.5 m/s = 52.2 km/h.

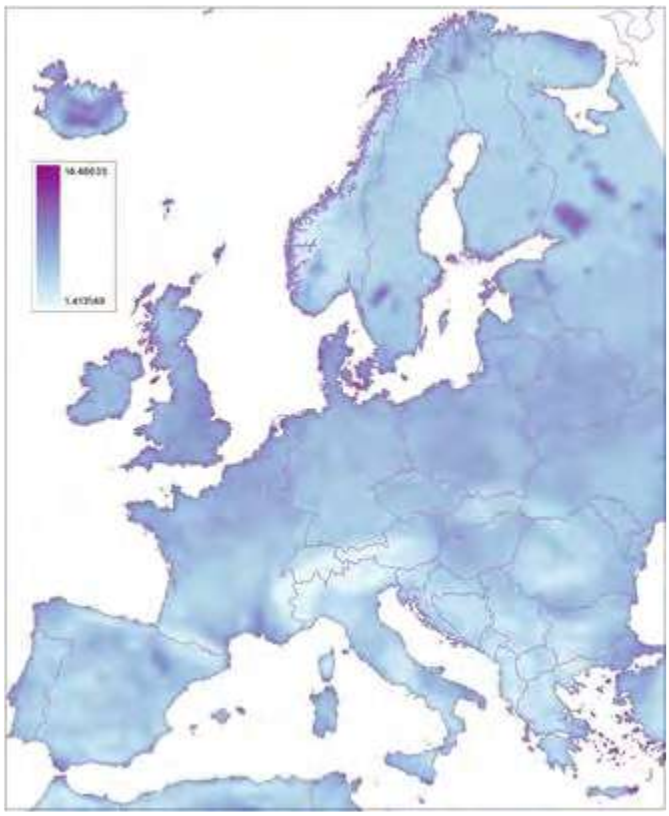


Figure 36: Map of average (50th percentile) wind speed in [m/s] calculated by MeteoGRID from past fires on EU territory

Statistical data concerning average wind speed on EU territory are:

- STATISTICS_MAXIMUM=14.466349601746
- STATISTICS_MEAN=5.3532013363071
- STATISTICS_MINIMUM=1.4131488800049
- STATISTICS_STDDEV=1.5106742908257

Copyright © FirEURisk Consortium. All rights reserved.

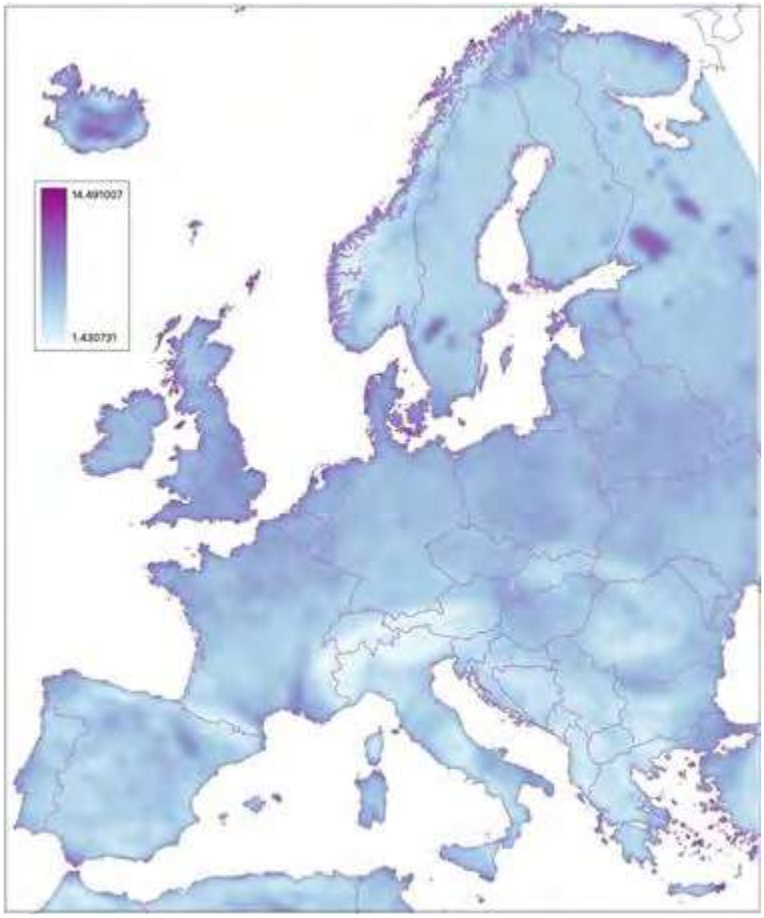


Figure 37: Map of extreme (95th percentile) wind speed in [m/s] calculated by MeteoGRID from past fires on EU territory

Statistical data concerning extreme wind speed on EU territory are:

- STATISTICS_MAXIMUM=14.491006851196
- STATISTICS_MEAN=5.3326972609518
- STATISTICS_MINIMUM=1.4307305812836
- STATISTICS_STDDEV=1.4990569061504

6.1.3 Verification of direct implementation of Rothermel equations for cell-based wildland landscape surface fire growth simulations

Rothermel equations for cell-based wildland landscape fire grown simulation in heterogeneous mixtures of dead fuel particle sizes and different types of live fuels were implemented in Python, quite suitable programming environment for cell based calculation on raster GeoTiff maps. Equations, fuel parameters and weighting factors are from (Andrews, 2018)

In order to verify implemented model as a referenced platform simulation program BehavePlus 6.0.0 was used, because it is also based on Rothermel fire behaviour model. We have used only Surface Fire Spread (SURFACE) module, standard Scott-Burgan fuel models, standard weather scenarios, midflame wind speed in [km/h] calculated for each fuel model from 10m wind speed using equation (15) and conversion from [ft/min] to [km/h] and slope steepness in degrees.

Copyright © FirEURisk Consortium. All rights reserved.

Comparation results of intermediate and final results are shown in tables below. Table 33 shows detail comparison of fuel model SH8 (High load, humid climate shrub) for cell-based simulation and BehavePlus simulations. There are some minor differences, but obtained results are quite satisfactory.

Table 33: Comparison of final and intermediate propagation potential variables calculated by direct implementation of Rothermel equations for cell-based wildland landscape fire growth simulations and BehavePlus 6.0.0 for fuel model SH8 (High load, humid climate shrub)

Propagation potential variables	Cell-based simulation	BehavePlus 6.0.0
Fuel Model	SH8 (148)	SH8 (148)
Windspeed at 10m [m/s]	14	10
Windspeed at Mid Flame [km/h]	20.17	20.17
Total Fuel Load Dead [t/ha]	14.129	14.12
Total Fuel Load Live [t/ha]	9.750	9.75
SAV [1/m]	4547.971	4549
Beta-Mean Packing Ratio	0.005119	0.0051
Beta Relative packing ratio	0.57186	0.569
Moisture Fuel Live [%]	60	60
Moisture Fuel Dead [%]	3	3
Moisture of Extinction Live [%]	201	200
RI - Reaction Intensity Dead [kW/m^2]	709.12	708
RI - Reaction Intensity Live [kW/m^2]	959.93	960
RI - Reaction Intensity [kW/m^2]	1669.05	1668
Slope (degrees)	30	30
Slope Coefficient	8.56	8.6
Wind Coefficient	50.77	51.7
Effective Wind Speed [km/h]	22.83	20.9
Heat Source [kW/m^2]	2848.52	2599
Heat Sink [kJ/m^3]	4291.04	4281
Rate of Spread [m/min]	40.49	36.4
Flame Residence Time [min]	0.277	0.28
Fire Heat per Unit Area [kJ/m^2]	27773.68	27725
Fireline intensity [kW/m]	18436.65	16828
Flame Length [m]	7.1	6.8

Similar situation is for other fuel models, too, as Table 34 shows. Moisture scenario was D1L1 (100% cured), slope 30^0 and wind speed at 10m height 14 m/s. There are some differences, particularly for dynamic fuel models. Cell-based model gives a little bit higher values, but all of them are within tolerance. For propagation potential calculation it is better to overestimate than to underestimate the risk of propagation potential.

Copyright © FirEURisk Consortium. All rights reserved.

Table 34: Comparison of propagation potential variables for all fuel models calculated by direct implementation of Rothermel equations for cell-based wildland landscape fire growth simulations (model) and BehavePlus 6.0.0 (BP)

Model	ROS -model [m/min]	ROS – BehavePlus [m/min]	RI -model [kW/m^2]	RI- BehavePlus [kW/m^2]	FI -model [kW/m]	FI – BehavePlus [kW/m]	FL-model [m]	FL- BehavePlus [m]x
GR2	74.66	67.8	245.8	234	3523.2	3342	3.32	3.2
GR4	185.5	164.8	477.2	455	16996.2	15761	6.84	6.6
GR6	177.4	176.1	1187.3	1305	36750.5	43962	9.75	10.6
GR7	300.9	296.5	1649.5	1599	95276.1	90228	15.12	14.7
GR8	289.1	251	2094.0	1964	159694.0	145403	19.17	18.4
GR9	564.3	414.4	3112.3	2996	378684.0	295720	28.52	25.4
SH2	10.8	9.6	1196.8	1201	2958.8	2650	3.06	2.9
SH3	6.9	6.3	387.9	390	749.7	683	1.63	1.6
SH5	120.6	112.8	1159.6	1164	43009.8	40291	10.49	10.2
SH7	78.3	72.7	1543.2	1548	37806.8	35061	9.88	9.5
SH8	39.8	36.4	1669.1	1668	18436.7	27725	7.1	6.8
SH9	98.9	74.6	3682.9	2680	116028.9	55707	16.55	11.8
TU1	4.3	3.7	363.3	364	361.3	322	1.16	1.1
TU2	17.0	15.3	410.8	411	1516.2	1368	2.25	2.1
TU3	47.11	40.5	836.4	825	9154.1	7959	5.15	4.8
TU5	11.8	10.2	1882.9	1815	6951.8	5783	4.53	4.2
TL3	1.7	1.5	173.3	178	74.79	66	0.56	0.5

6.1.4 Results – surface propagation potential maps for EU territory

EU GeoTiff raster maps for propagation potential indicators:

a) **Rate of Spread** (R) [m/s] – The linear rate of advance of a flaming front into unburned fuel in the direction perpendicular to the fire front. It is a significant factor affecting fireline intensity and flame size, which are important for determining fire effects.
b) **Heat per Area Unit** (HA) [kJ/m2] - heat release per unit area of the surface fire flaming front.
c) **Reaction Intensity** (RI) [kJ/(m^2 s)] - heat release per unit area of the surface fire flaming front in one second.
d) **Fireline Intensity** (FI) [kW/m] [kJ/(m s)] - also called Byram's fire intensity is a fundamental fire characteristic. It express heat energy released per unit time from a one-meter-wide section of the fuel bed extending from the front to the rear of the flaming zone.
e) **Flame Length** (FL) [m] - measured in from midway in the active flaming combustion zone to the average tip of the flames. It is indicator of fireline intensity.

were calculated for extreme (5th percentile fuel moisture and 95th percentile wind speed) and average weather conditions (50th percentile of fuel moisture and wind speed) of past fires larger than 2000 ha. In both cases, regarding wind direction and aspect maximal values are considered when wind direction and aspect coincides (both are in the same direction).

Calculated values are quite low, because fuel moisture content was quite large, but they are comparable with the same fire behaviour parameters calculated by Pettinary and Chuvieco on global world level (Pettinary & Chuvieco, 2017).

Two sets of output maps were produced:

- one for calculation of weighting factors f_{ij} and g_{ij} according to equations on Table 26 and Table 29 and

Copyright © FirEURisk Consortium. All rights reserved.

- another one based on precalculated values of factors f_{ij} and g_{ij}.

The difference is in treating dynamic fuels (GR2, GR4, GR6, GR7, GR8, GR9, SH9, TU1 and TU3). For dynamic fuels **weighting factors based on tables** have different values depending of percentage of cured (100%, 50% or 0%). In our case percentage of cured is directly connected with moisture scenarios. D1L1 is considered as 100% cured, D2L2 and D3L3 as 50% cured and D4L4 as 0% cured (see Table 30 and comment bellow Table 30), therefore for them different weighting factors were applied. Differences are small, but they exist. For example, for SH9 and 100% cured f_{11} is 0.96, for 50% cured 0.95 and for 0% cured 0.93. **Calculated weighting factors** are based on fuel parameters and they are independent of percentage of cured, they always have the same values. In both cases there is one exception. For 100% cured fuel (moisture scenario D1L1) all fuel was considered as dead fuel, therefore all fuel contributes to Rothermel equations factors connected with dead fuels. For both cases, results are similar. There are only minor differences in maximal values, but the frequency of that maximum values is negligible, therefore maps look almost the same.

In the rest of this Section, first output results will be presented, and after that a comparison of result will be given. Figure 35 & Figure 37 shows maps for extreme conditions, and Figure 34 & Figure 36 for average conditions, both of them generated for calculated weighting factors.

On the comparison of propagation potential variables for extreme and average values, there are no big differences, because both dynamic input variables (fuel moisture and wind speed) were similar. Table 35 compares their statistical properties (mean, maximal, minimal values and standard deviation).

Finally, a comparison was performed of maps generated using calculated weighting factors and weighting factors from tables.

Copyright © FirEURisk Consortium. All rights reserved.

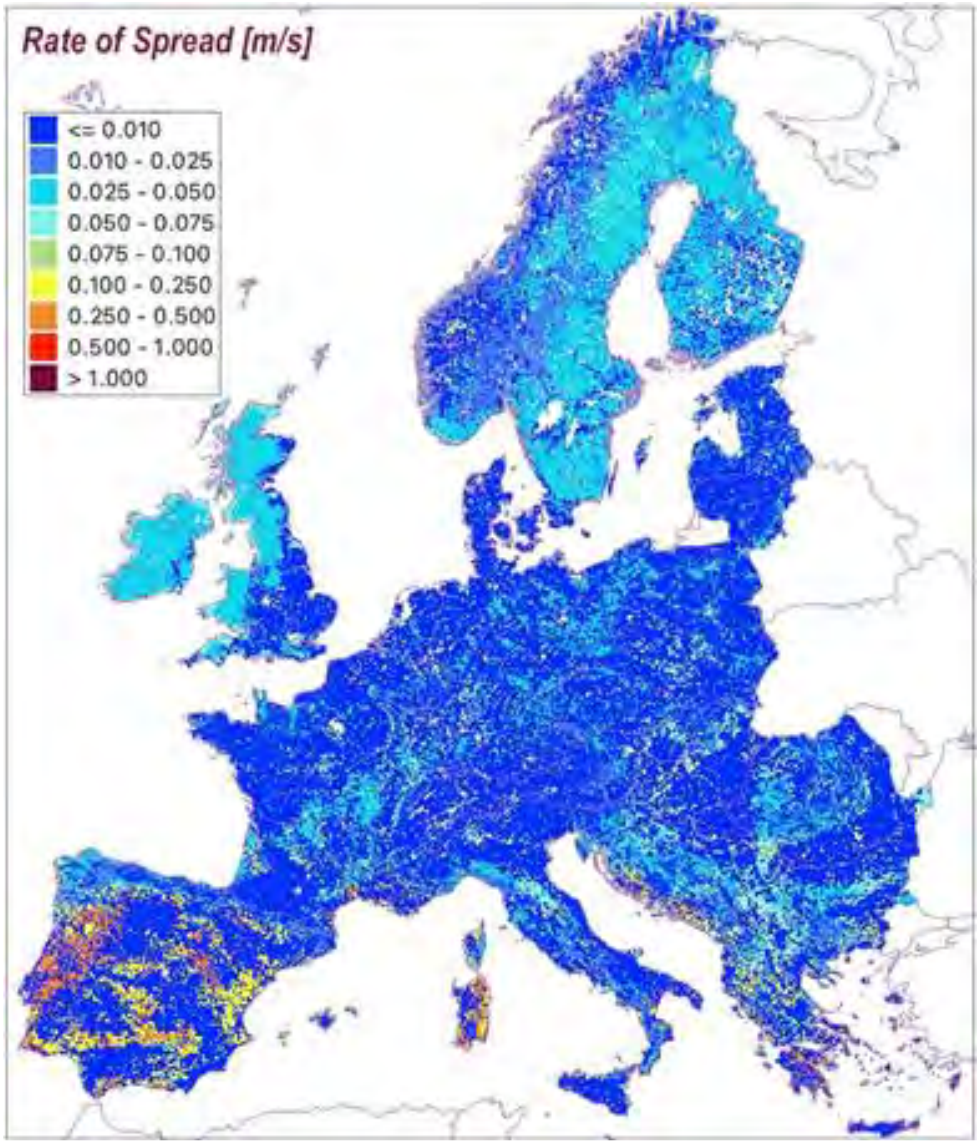


Figure 38: Map of Rate of Spread (ROS) [m/s] for extreme 95th percentile wind speed and 5th percentile fuel moisture

Statistical data concerning extreme Rate of Spread (ROS) on EU territory are:

- STATISTICS_MAXIMUM=3.3499999046326
- STATISTICS_MEAN=0.028880616198882
- STATISTICS_MINIMUM=0
- STATISTICS_STDDEV=0.071371356648745

Copyright © FirEURisk Consortium. All rights reserved.

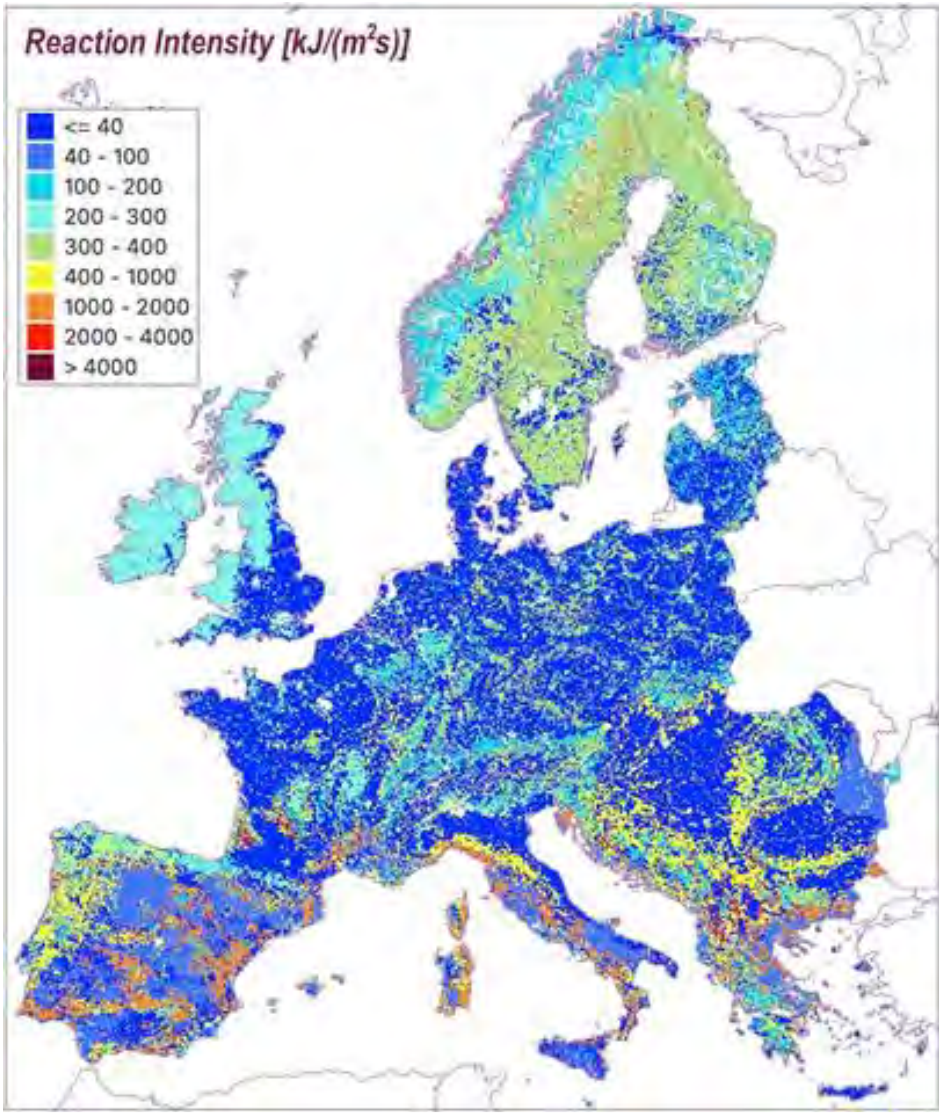


Figure 39: Map of Reaction Intensity (RI) [kJ/(m² s)] for extreme 95th percentile wind speed and 5th percentile fuel moisture

Statistical data concerning extreme Reaction Intensity (RI) on EU territory are:

- STATISTICS_MAXIMUM=3802.9399414062
- STATISTICS_MEAN=259.76844413511
- STATISTICS_MINIMUM=0
- STATISTICS_STDDEV=393.4853024171

Copyright © FirEURisk Consortium. All rights reserved.

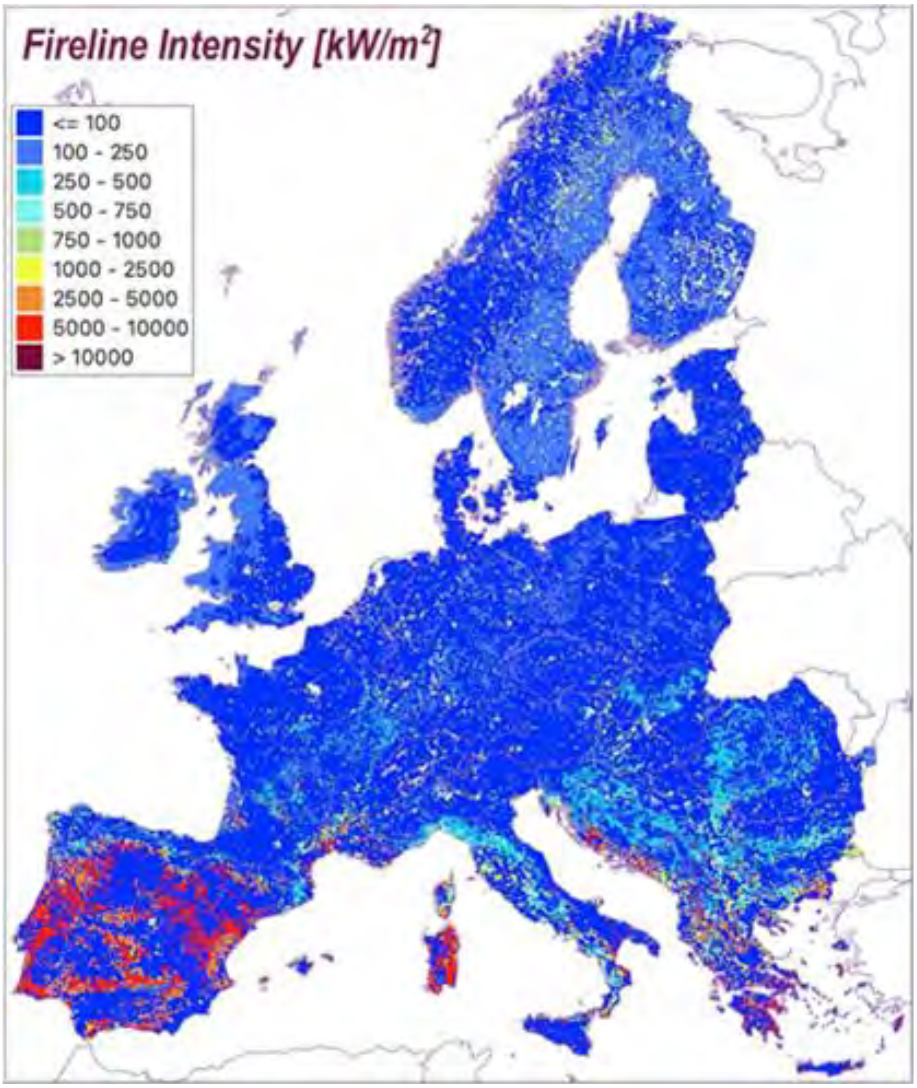


Figure 40: Map of Fireline Intensity (FI) [kW/m²] for extreme 95th percentile wind speed and 5th percentile fuel moisture

Statistical data concerning extreme Fireline Intensity (FI) on EU territory are:

- STATISTICS_MAXIMUM=320730.15625
- STATISTICS_MEAN=176.66434881861
- STATISTICS_MINIMUM=0
- STATISTICS_STDDEV=2316.5974351699

Copyright © FirEURisk Consortium. All rights reserved.

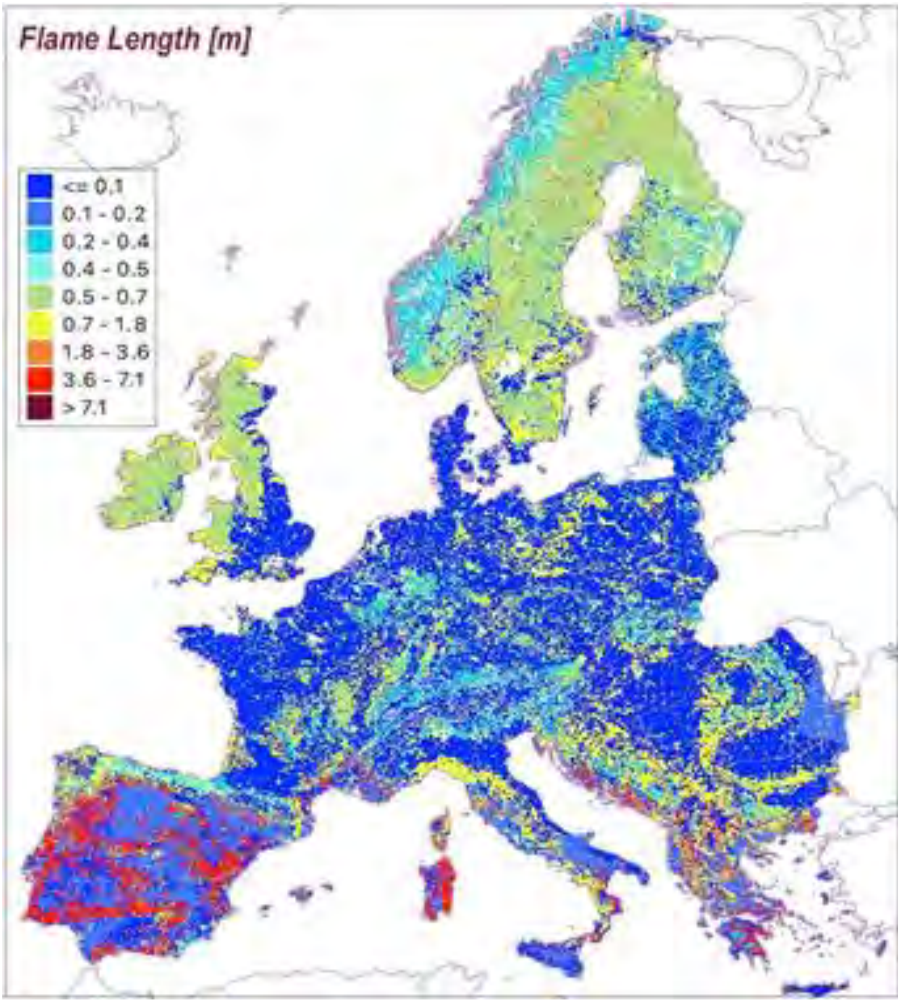


Figure 41: Map of Flame Length (FL) [m] for extreme 95th percentile wind speed and 5th percentile fuel moisture

Statistical data concerning extreme Flame Length (FL) on EU territory are:

- STATISTICS_MAXIMUM=17.829999923706
- STATISTICS_MEAN=0.60321730197917
- STATISTICS_MINIMUM=0
- STATISTICS_STDDEV=0.98539727565307

Copyright © FirEURisk Consortium. All rights reserved.

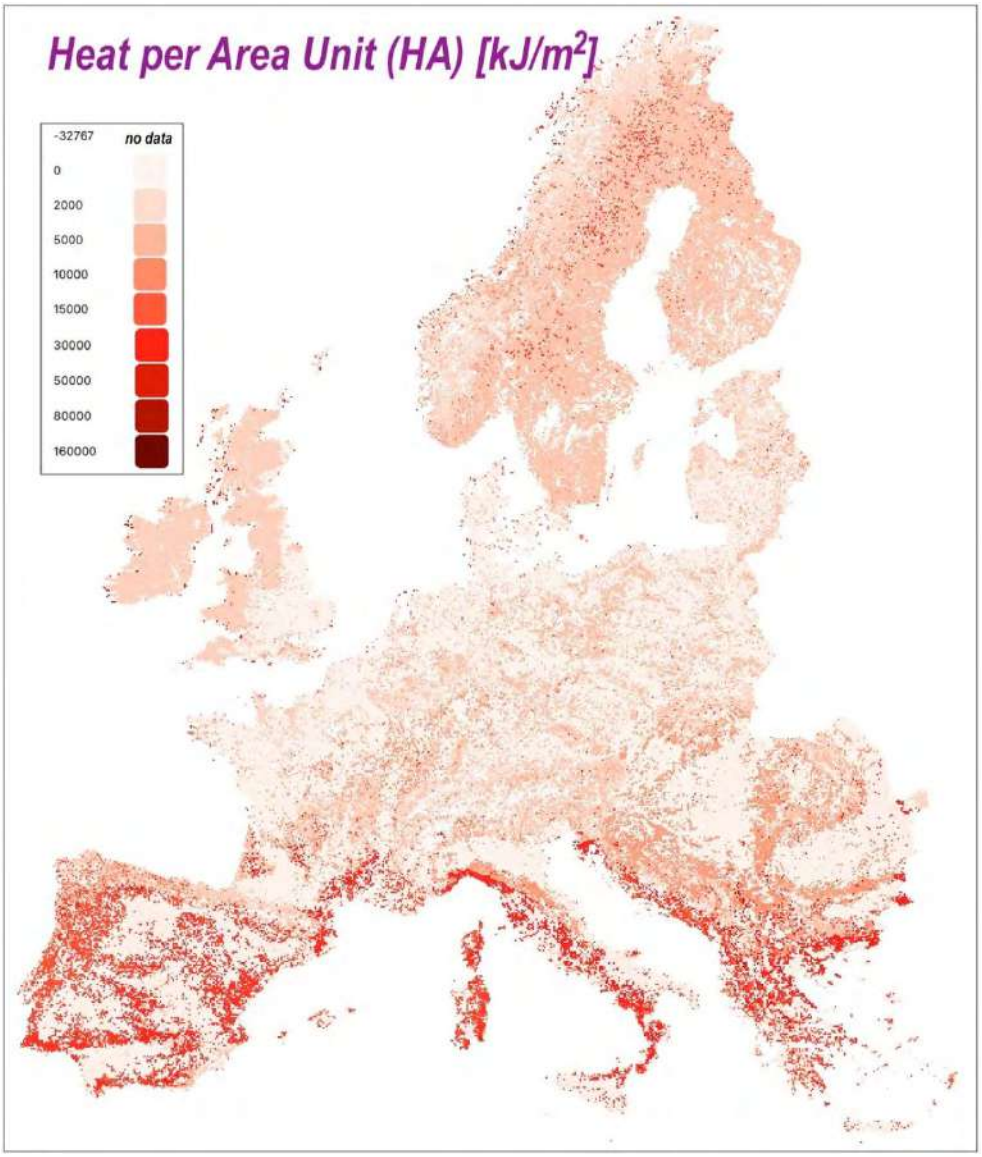


Figure 32a: Heat per Unit Area (HA) [kJ/m^2] for extreme 95th percentile wind speed and 5th percentile fuel moisture

Statistical data concerning extreme Flame Length (FL) on EU territory are:

- STATISTICS_MAXIMUM=70403.7265625
- STATISTICS_MEAN=4255.4936128618
- STATISTICS_MINIMUM=159.25
- STATISTICS_STDDEV=7059.9196620333

Copyright © FirEURisk Consortium. All rights reserved.

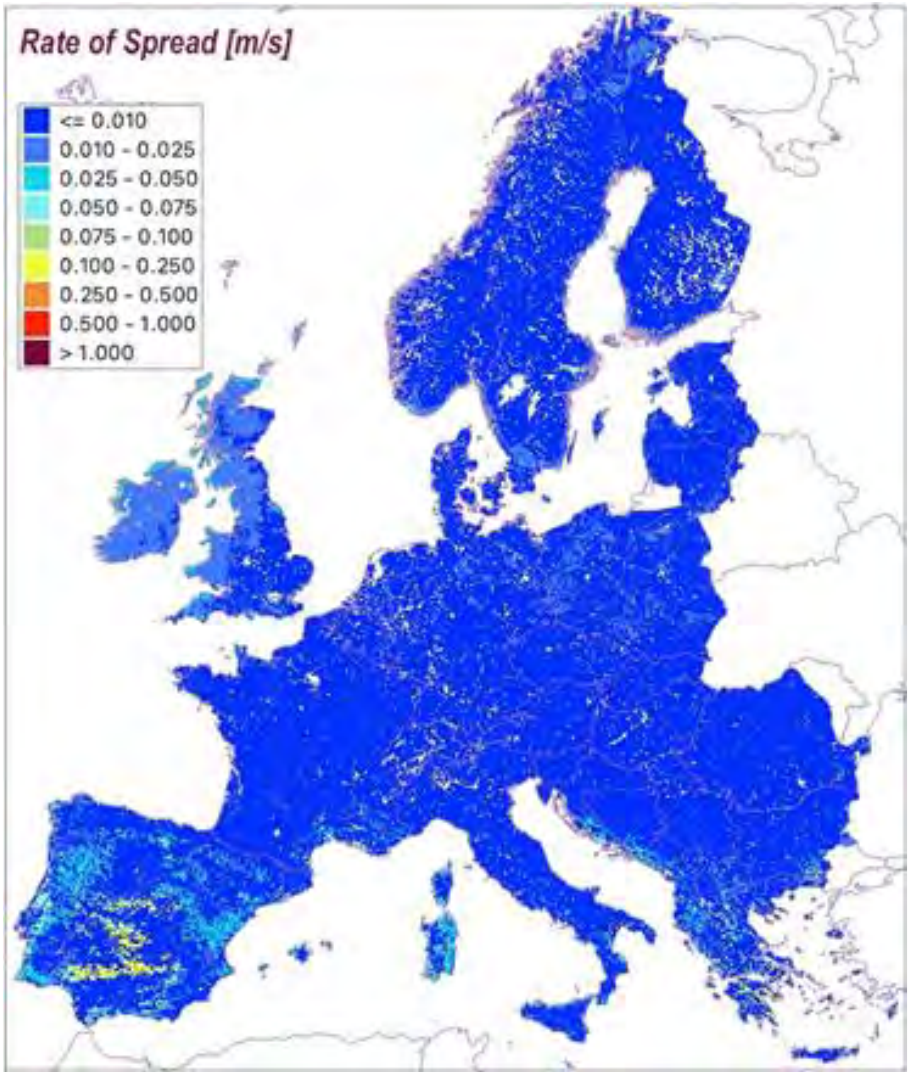


Figure 42: Map of Rate of Spread [m/s] for average 50th percentile wind speed and 50th percentile fuel moisture

Statistical data concerning average Rate of Spread (ROS) on EU territory are:

- STATISTICS_MAXIMUM=3.210000038147
- STATISTICS_MEAN=0.0094899926096364
- STATISTICS_MINIMUM=0
- STATISTICS_STDDEV=0.044515253766556

Copyright © FirEURisk Consortium. All rights reserved.

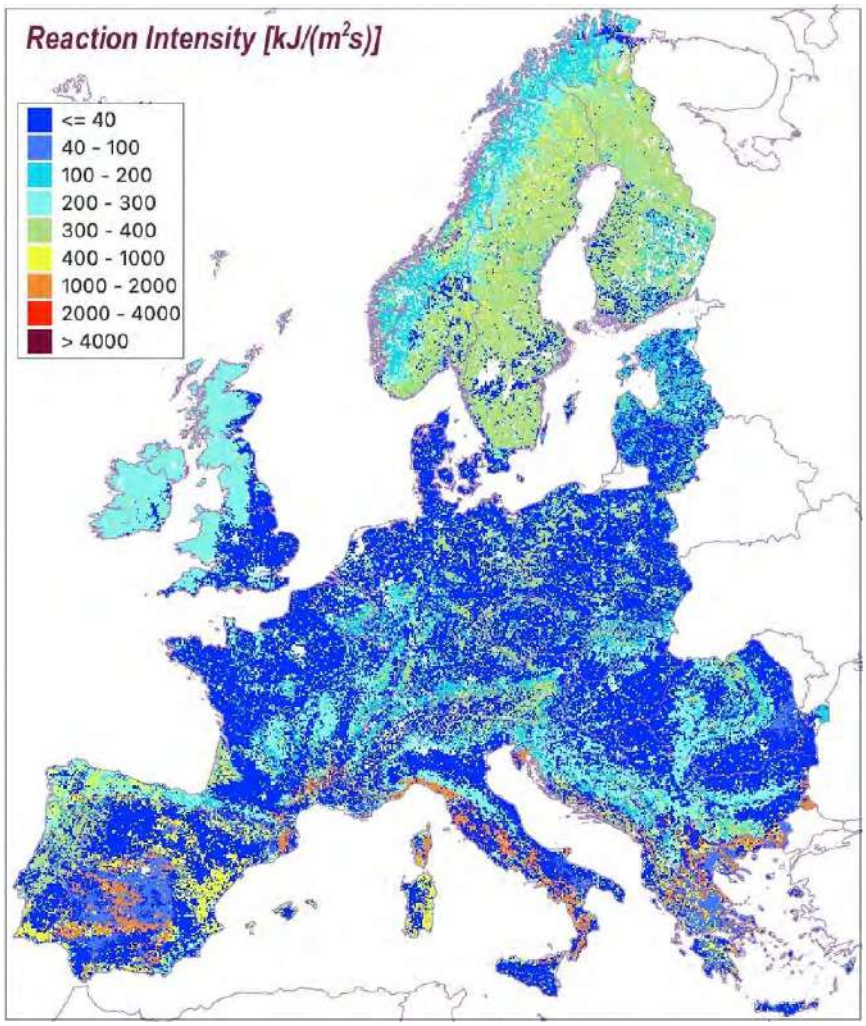


Figure 43: Map of Reaction Intensity [kJ/(m² s)] for average 50th percentile wind speed and 50th percentile fuel moisture

Statistical data concerning average Reaction Intensity (RI) on EU territory are:

- STATISTICS_MAXIMUM=3682.9499511719
- STATISTICS_MEAN=193.01674884334
- STATISTICS_MINIMUM=0
- STATISTICS_STDDEV=287.05764116323

Copyright © FirEURisk Consortium. All rights reserved.

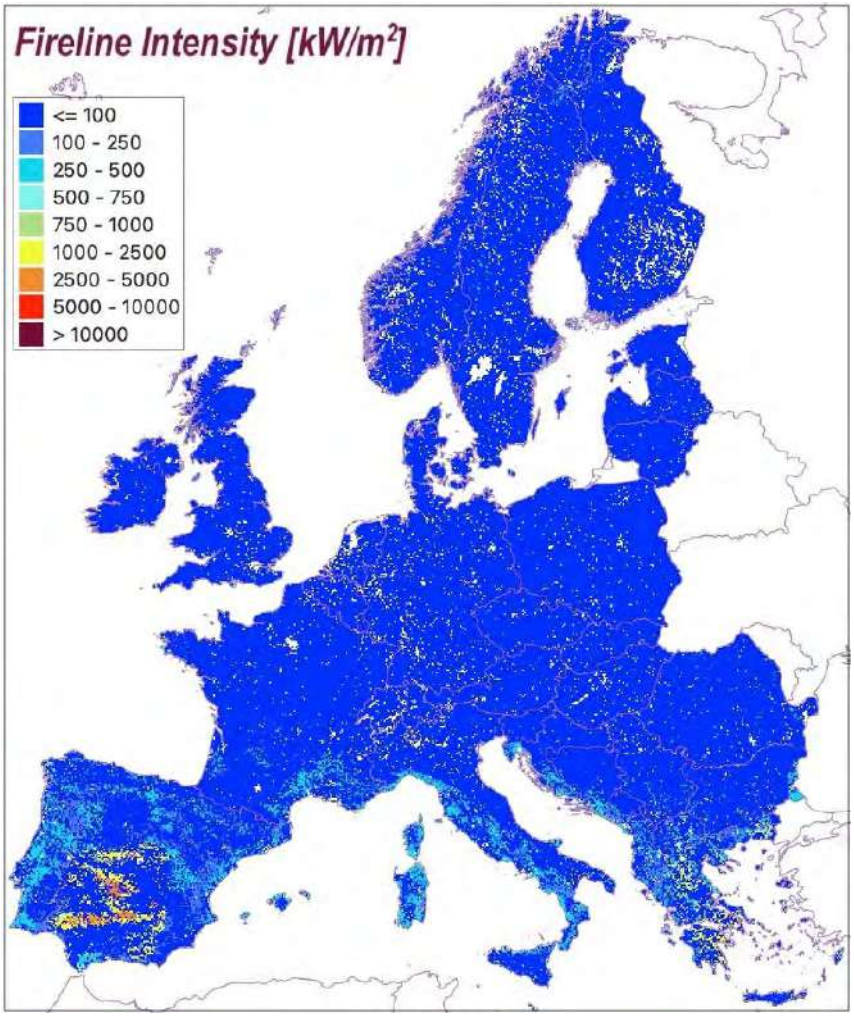


Figure 44: Map of Fireline Intensity [kW/m²] for average 50th percentile wind speed and 50th percentile fuel moisture

Statistical data concerning avarage Fireline Intensity (FI) on EU territory are:

- STATISTICS_MAXIMUM=x
- STATISTICS_MEAN=176.66434881861
- STATISTICS_MINIMUM=0
- STATISTICS_STDDEV=2316.5974351699

Copyright © FirEURisk Consortium. All rights reserved.

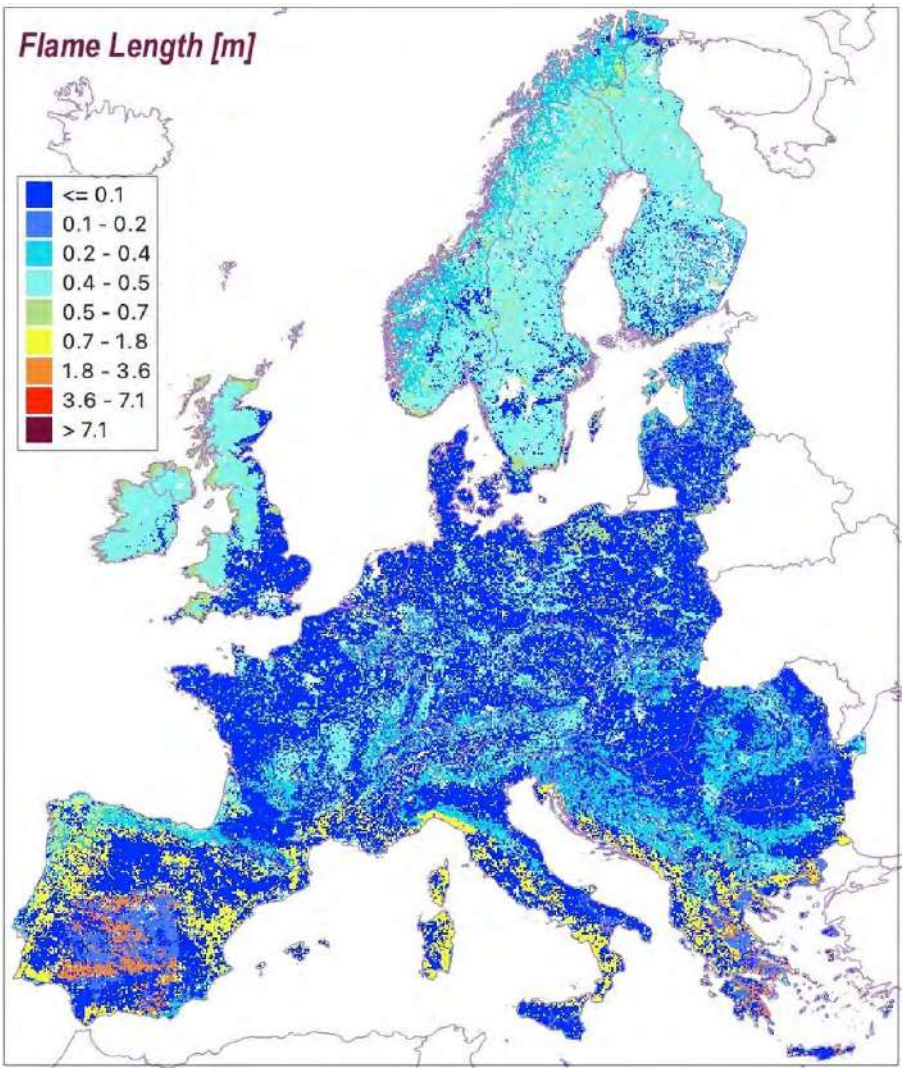


Figure 45: Map of Flame Length [m] for average 50th percentile wind speed and 50th percentile fuel moisture

Statistical data concerning average Flame Length (FL) on EU territory are:

- STATISTICS_MAXIMUM=x
- STATISTICS_MEAN=0.60321730197917
- STATISTICS_MINIMUM=0
- STATISTICS_STDDEV=0.98539727565307

Copyright © FirEURisk Consortium. All rights reserved.

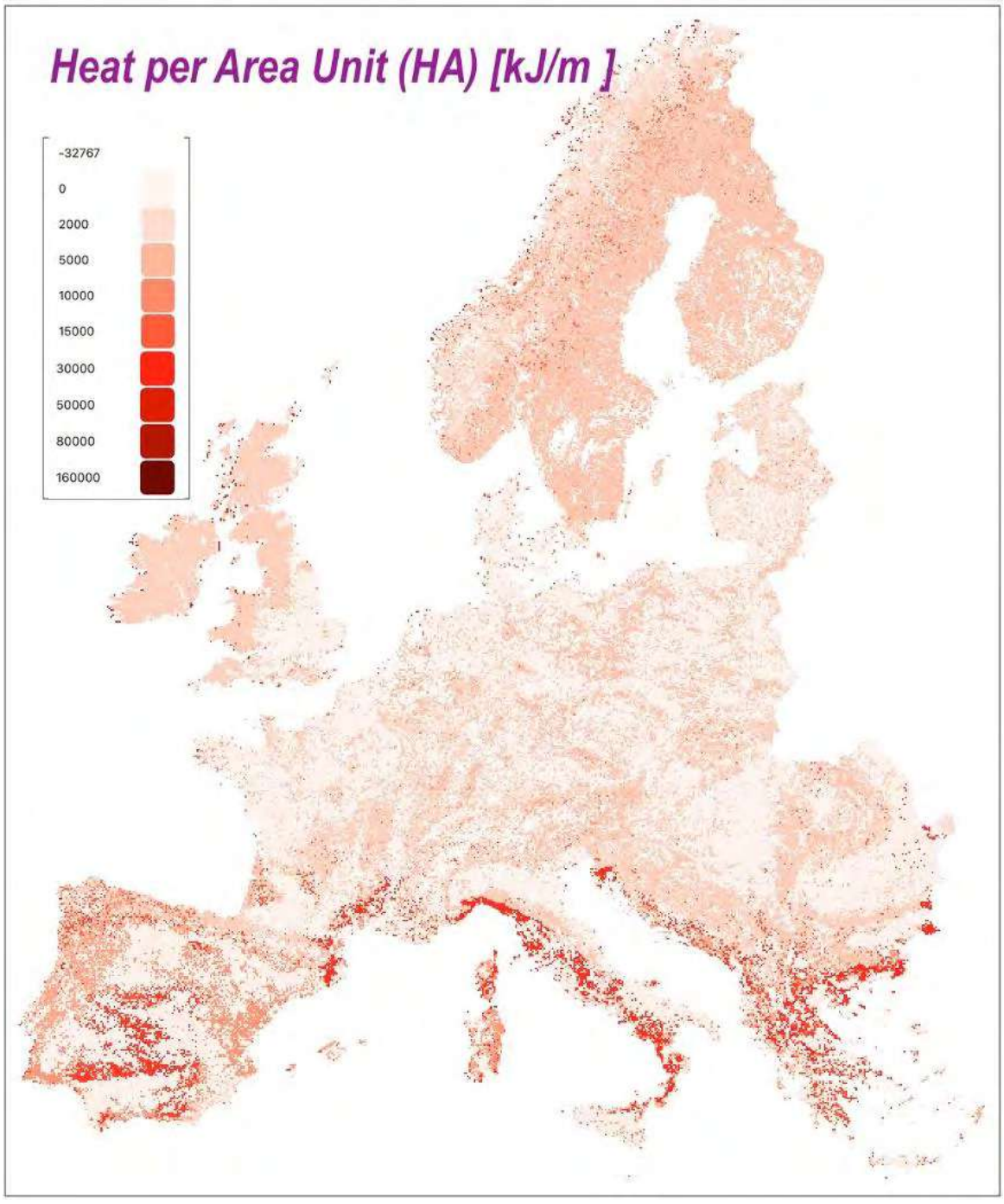


Figure 24a: Heat per Unit Area (HA) [kJ/m^2] for extreme 50th percentile wind speed and 50th percentile fuel moisture

Statistical data concerning extreme Flame Length (FL) on EU territory are:

- STATISTICS_MAXIMUM=70403.7265625
- STATISTICS_MEAN=3116.7661865566
- STATISTICS_MINIMUM=159.25
- STATISTICS_STDDEV=5004.5079818346

Copyright © FirEURisk Consortium. All rights reserved.

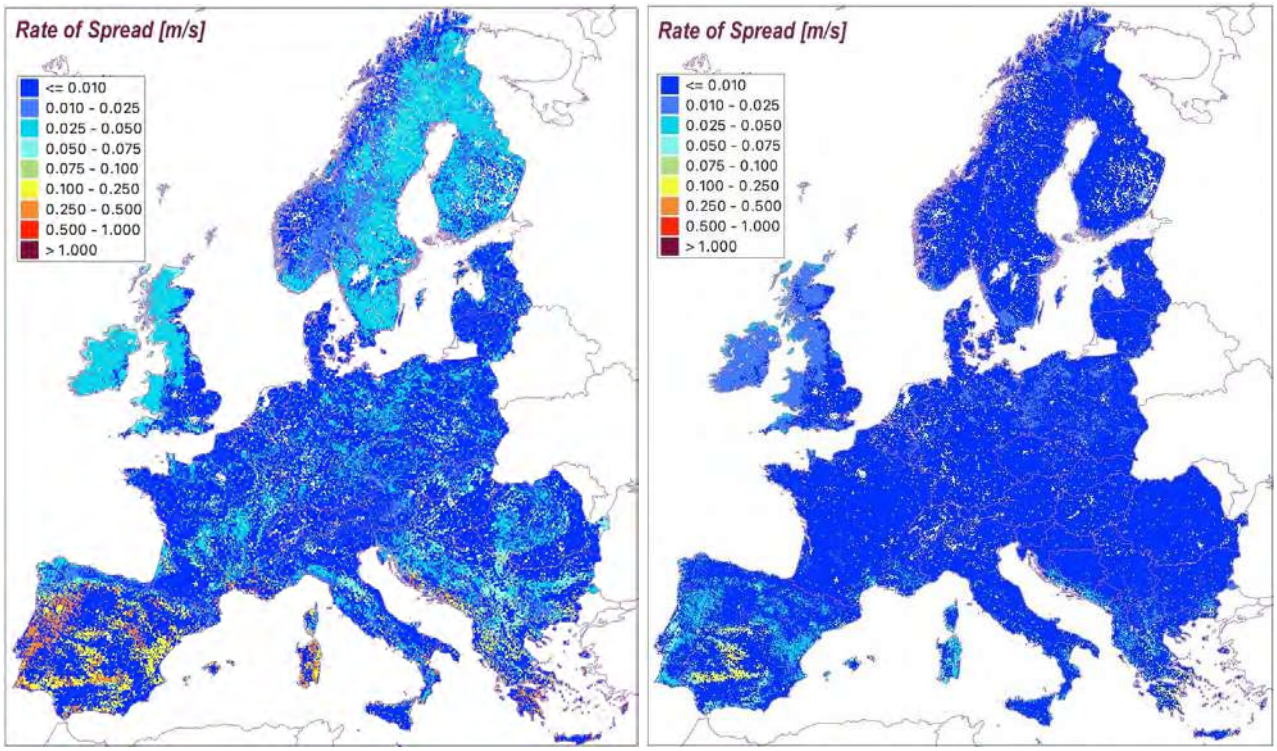


Figure 46: Comparison of Rate of Spread (ROS) [m/s] for extreme and average wind speed and fuel moisture (left – extreme, right – average)

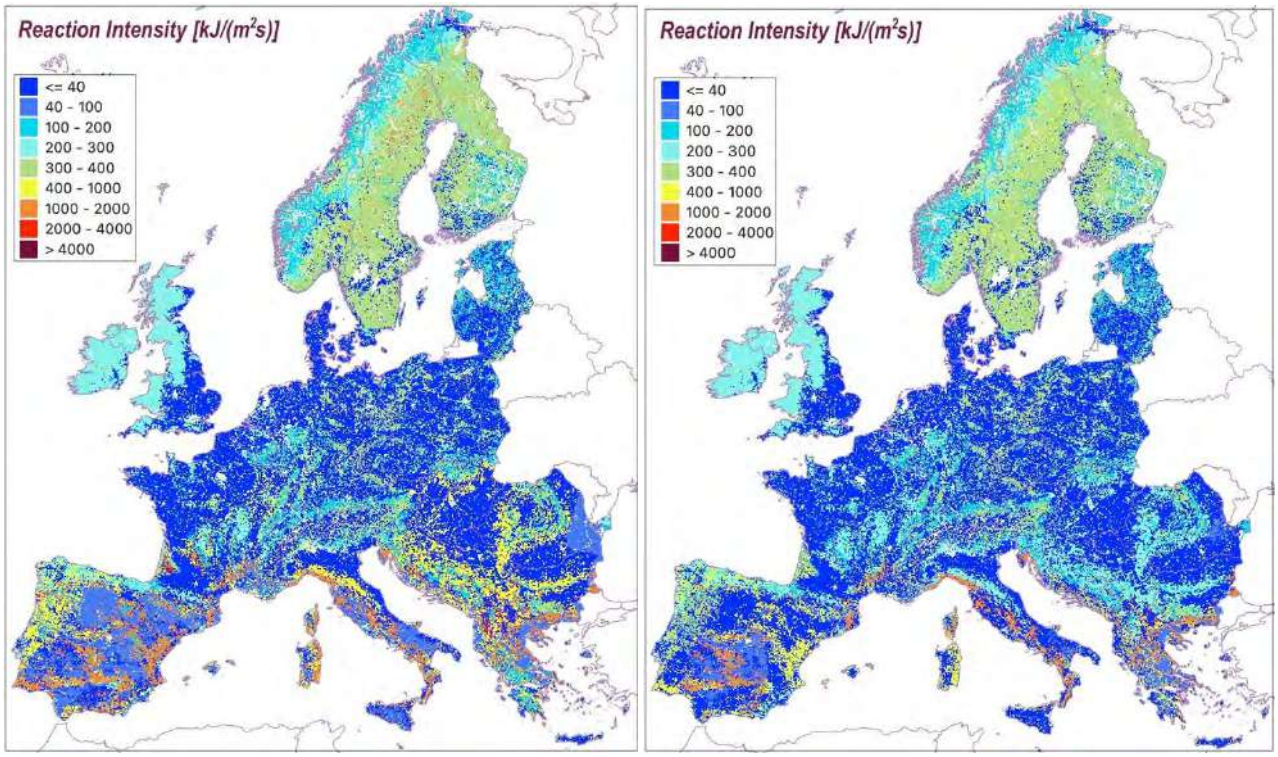


Figure 47: Comparison of Reaction Intensity (RI) [kJ/(m² s)] for extreme and average wind speed and fuel moisture (left – extreme, right – average)

Copyright © FirEURisk Consortium. All rights reserved.

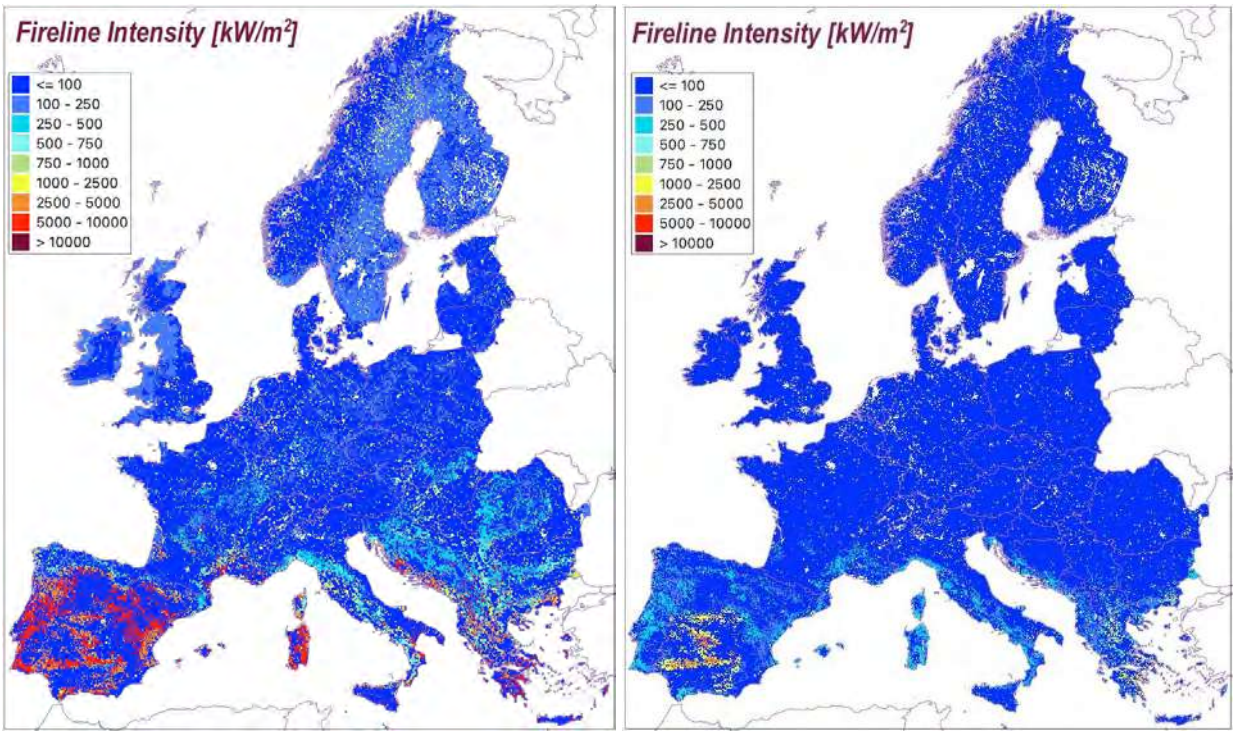


Figure 48: Comparison of Fireline Intensity (FI) [kW/m²)] for extreme and average wind speed and fuel moisture(left – extreme, right – average)

Table 35: Comparison of statistical property of propagation potential indicator variables (ROS – Rate of Spread, RI – Reaction Intensity, FI – Fireline Intensity, FL – Flame Length for average and extreme weather conditions

	ROS [m/s]		RI [kJ/(m² s)]		FI [kW/m²]		FL [m]	
	Extreme	*Average*	*Extreme*	*Average*	*Extreme*	*Average*	*Extreme*	*Average*
Maximal Value	*3.3499*	*3.2100*	*3803*	*3803*	*136310*	*57645*	*17.83*	*12.00*
Mean Value	*0.02888*	*0.0095*	*260*	*193*	*426*	*87*	*0.60*	*0.31*
Minimal Value	*0.0000*	*0.0000*	*0*	*0*	*0*	*0*	*0*	*0*
Standard Deviation	*0.07137*	*0.0445*	*393*	*282*	*2020*	*774*	*0.99*	*0.46*

Comparisons of Rate of Spread for extreme conditions and weighting factors f_{ij} and g_{ij} calculated or derived from tables are given on Figure 49 for Rate of Spread and Figure 50 for Fireline Intensity. Table 36 compares their statistical properties (mean, maximal, minimal values and standard deviation). Differences could be hardly noticed on maps, although statistical properties, particular for Fireline Intensity are different. Differences are particularly in maximal values, but their frequency is very low, therefore it is hard to notice them on maps. Similar situation is with other propagation potential indicators.

Copyright © FirEURisk Consortium. All rights reserved.

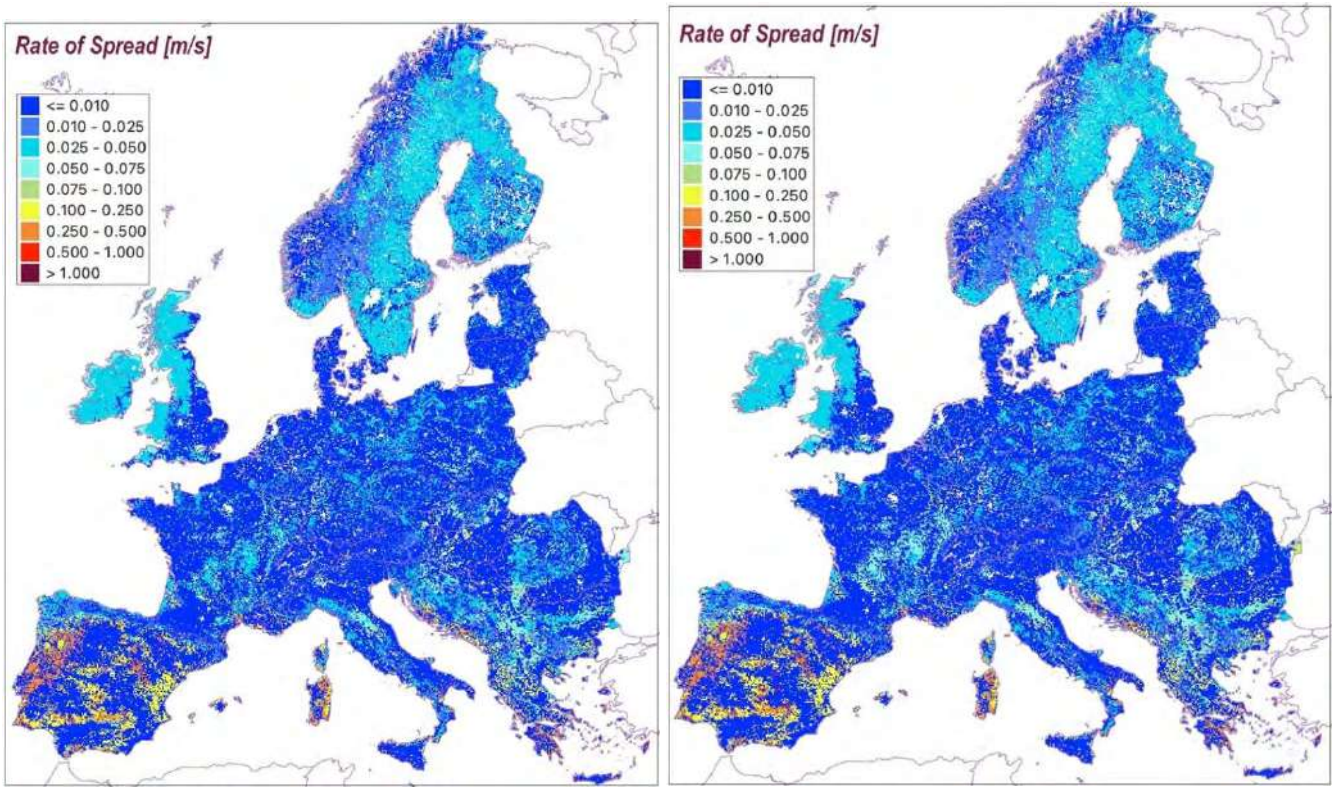
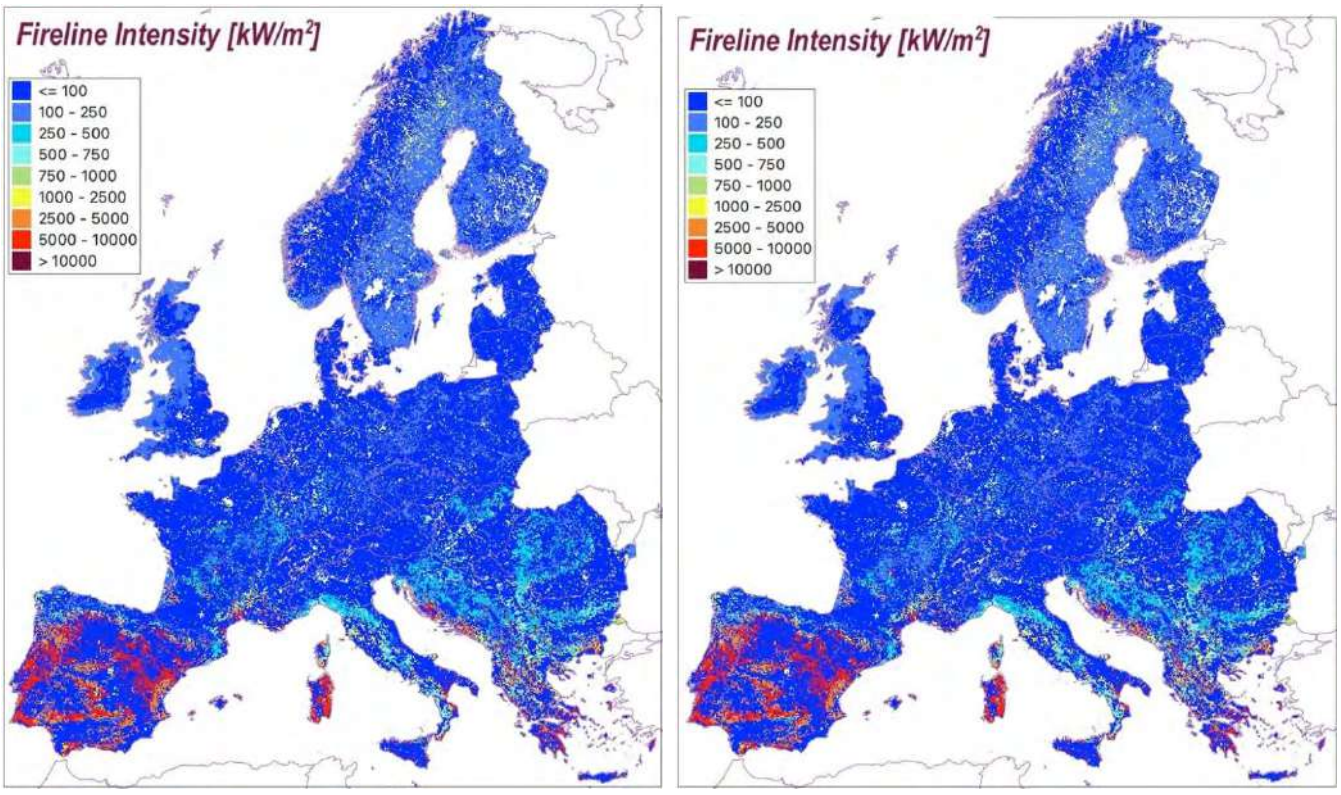


Figure 49: Comparison of Rate of Spread (ROS) [m/s] for extreme weather conditions and weighting factors f_{ij} and g_{ij} calculated (left) or derived from tables (right)



Copyright © FirEURisk Consortium. All rights reserved.

Figure 50: Comparison of Fireline Intensity (FI) [kW/m²)] for weighting factors f_{ij} and g_{ij} calculated (left) or derived from tables (right)

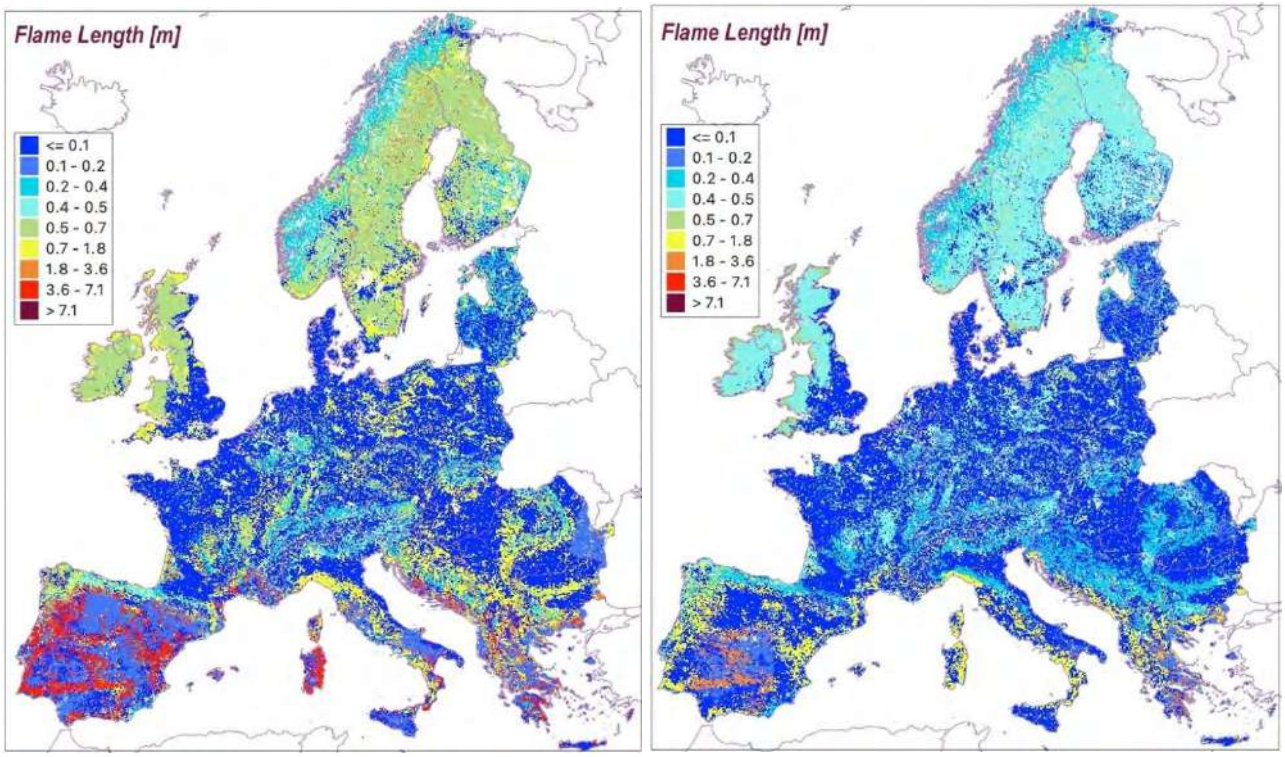


Figure 51: Comparison of Flame Length (FL) [m] for extreme and average wind speed and fuel moisture (left – extreme, right – average)

Table 36: Comparison of statistical property of propagation potential indicator variables (ROS – Rate of Spread, RI – Reaction Intensity, FI – Fireline Intensity, FL – Flame Length for calculated weighting factors f_{ij} and g_{ij} (Calculated) and weighting factors derived from tables

	ROS [m/s]		RI [kJ/(m² s)]		FI [kW/m²]		FL [m]	
	Calculated	Tables	Calculated	Tables	Calculated	Tables	Calculated	Tables
Maximal Value	3.3499	7.9699	3803	3683	136310	320730	17.83	26.42
Mean Value	0.02888	0.01138	260	259	426	508	0.60	0.65
Minimal Value	0.0000	0.0000	0	0	0	0	0	0
Standard Deviation	0.07137	0.0688	393	394	2020	3843	0.99	1.06

In conclusion, propagation potential for EU territory was calculated at 1 km² resolution, based on pixel calculation. From the list of past fires from Jan, 1st 2001 and Dec, 31st 2019 on EU territory, fires larger than 2000 ha were selected. There were 403 such fires. For their dates maps of meteorological parameters were extracted and resampled to 1 km resolution. 10h Fuel Moisture Content and wind speed were calculated for each data. For each pixel on weather maps, two weather scenarios were calculated:

a) average weather conditions (50th percentile) and

b) extreme weather conditions (5th percentile for fuel moisture and 95th percentile for wind speed).

Copyright © FirEURisk Consortium. All rights reserved.

Propagation potential for the ET territory for each pixel was calculated using standard Rothermel equations having propagation potential variables as output:

a) **Rate of Spread** (R) [m/s] – The linear rate of advance of a flaming front into unburned fuel in the direction perpendicular to the fire front. It is a significant factor affecting fireline intensity and flame size, which are important for determining fire effects.

b) **Flame Length** (FL) [m] - measured in from midway in the active flaming combustion zone to the average tip of the flames. It is indicator of fireline intensity.

c) **Fireline Intensity** (FI) [kW/m] [kJ/(m s)] - also called Byram's fire intensity is a fundamental fire characteristic. It express heat energy released per unit time from a one-meter-wide section of the fuel bed extending from the front to the rear of the flaming zone.

d) **Heat per Area Unit** (HA) [kJ/m2] - heat release per unit area of the surface fire flaming front.

e) **Reaction Intensity** (RI) [kJ/(m^2 s)] - heat release per unit area of the surfface fire flaming front in one second.

For each output parameters two map sets were created, one for extreme weather condition and one for average weather conditions. They will be used as **surface fire propagation potential indicators**.

6.1.5 Crown fire behaviour modelling at ET scale

Definitions of **Crown Fire**:

- (Van Wagner, 1977) - Crown fire is the interaction between separate fuel layers in forested areas.
- (CIFFC Canadian Wildland Fire Glossary, 2023) - Crown fire is a fire that advances through the crown fuel layer, usually in conjunction with the surface fire. Crowning can be classified according to the degree of dependence on the surface fire phase.
- (European Glossary for Wildfires and Forest Fires, 2012) - Crown fire is when a fire burns freely in the upper foliage of trees and shrubs.

Considering **fire behaviour of crown fires** both Glossaries differs:

- **Running Fire** - A fire rapidly spreading and with a well-defined head. A fire with high rate of spread.
- **Torch or Torching** - A fire that burns from the ground through the surface and aerial fuels and into the crown of a single tree or small parcel of trees. A single tree or a small clump of trees is said to "torch" when its foliage ignites and flares up, usually from bottom to top. Synonym - Candle or Candling.
- **Spotting** - Fire behaviour where sparks and hot burning members are transported by the wind or convection column to land beyond the fire perimeter resulting in spot fires. A fire producing firebrands carried by the surface wind, a fire whirl, and/or convection column that fall beyond the main fire perimeter and result in spot fires. Note Solid Mass or Ember Transport under Heat Transfer.
- **Crowning** - When a fire burns freely in the upper foliage of trees and shrubs. A fire ascending into the crowns of trees and spreading from crown to crown.

Van Wagner (Van Wagner, 1977) describes two processes and models connected with crown fires:

Copyright © FirEUrisk Consortium. All rights reserved.

- **Crown Fire Initiation** as an indicator of the potential for surface fire to ignite tree crown and produce either passive or active crown fire.
- **Crown Fire Propagation** (Crown Spread) as an indicator of the potential for continuous spread through the tree crowns.

Considering **Crown Fire Propagation** there are four **types of crown fires**:

- **Passive Crown Fire** - A fire in the crowns of trees in which trees or groups of trees torch, ignited by the passing front of the fire. A fire in which trees discontinuously torch, but rate of spread is controlled by the surface fire phase. Synonym is **Intermittent Crown Fire**. The torching trees reinforce the spread rate, but these fires are not basically different from surface fires.
- **Active Crown Fire** - A fire that advances with a well-defined wall of flame extending from the ground surface to above the crown fuel layer. It is a fire in which a solid flame develops in the crowns of trees, but the surface and crown phases advance as a linked unit dependent on each other. Probably most crown fires are of this class. Development of an active crown fire requires a substantial surface fire, and thereafter the surface and crown phases spread as a linked unit. Synonym is **Dependent Crown Fire**.
- **Independent Crown Fire** - A fire that advances through aerial fuels only. The fire no longer depends in any way on the surface phase and can run ahead on its own. Synonym is **Running Crown Fire**.
- **Conditional Crown Fire** - A fire cannot transition into a crown fire in this area, but active crown fire is possible if the fire transitions to the overstory outside the area and burns into the canopy.

All of them depend on various input variables connected with fuels, terrain, weather and specific parameters connected with forest crown characteristics.

Output variables of crown fire models are **crown fire indicators**. They are usually:

- **Crown Fraction Burned** (CFB) [fraction]- A fraction between 0 and 1 indicating the severity of a crown fire. It is a proportion of tree crowns involved in the fire in a given area. Less than 10 percent is considered as surface fire, between 10 and 89 percent is can intermittent crown fire, while over 90 percent is a continuous crown fire.
- **Crown Fire Activity** (CFA) [indicator] - An indication what kind of fire behaviour concerning crown fires could be expected defined by four classes (non-burnable, surface fire, passive fire, active fire and conditional crown fire). Independent crown fire is usually not considered in CFA.
- **Passive Crown Fire Rate of Spread** [m/s] - It is the head fire (forward) spread rate of a passive crown fire. It is the estimated rate of spread as a fire transitions from a surface fire to a crown fire.
- **Passive crown fire heat per unit area** [kJ/m^2] – It is the sum of surface fire heat per unit area and canopy heat per unit area. It is used to calculate passive crown fireline intensity.
- **Passive Crown Fireline Intensity** [kW/m] - It express heat energy released per unit time from a one-meter-wide section of the fuel bed extending from the front to the rear of the flaming zone in passive crown fires. Passive crown fireline intensity is used to calculate passive crown fire flame length.
- **Passive crown fire flame length** [m] - Passive crown fire flame length, based on 20-foot wind speed, is calculated from passive crown fireline intensity. Flame Length measured from midway in the active flaming combustion zone to the average tip of the flames.

Copyright © FirEURisk Consortium. All rights reserved.

- **Active Crown Fire Rate of Spread** [m/s] - Active crown fire rate of spread is the head fire (forward) spread rate of an active crown fire.
- **Active crown fire heat per unit area** [kJ/m^2] – It is the sum of surface fire heat per unit area and canopy heat per unit area. It is used to calculate active crown fireline intensity..
- **Active Crown Fireline Intensity** [kW/m] - Active crown fireline intensity assumes the crown fire is fully active. It is calculated from surface fire heat per unit area, crown fire heat per unit area, and active crown fire rate of spread. Active crown fireline intensity is used to calculate active crown fire flame length.
- **Active crown fire flame length** [m] - Active crown fire flame length, based on 20-foot wind speed, is calculated from active crown fireline intensity. Active crown fire flame length is also used to find spotting distance from active crown fire. Flame Length measured from midway in the active flaming combustion zone to the average tip of the flames.

6.1.5.1 Inputs for calculation crown fire indicators

Wildfire crown fire indicators depends on standard weather, terrain and fuel parameters:

- **Wind speed and direction** - Strong winds can cause fires to spread rapidly and can carry flames up into the tree canopy.
- **Terrain** - Steep slopes, canyons, or areas with complex topography can create wind tunnels and other conditions that increase the risk of crown fires. Terrain parameters are elevation, slope and aspect.
- **Fuel moisture** - Dry fuels such as dead leaves, branches, and needles can increase the likelihood of fire ignition and spread. For crown fires particularly is important **foliar moisture content**.
- **Weather conditions** - High temperatures, low relative humidity, and drought conditions can increase the risk of fire ignition and spread. Weather conditions are usually included in fuel moisture calculation.
- **Fuel maps and fuel models** – Crown fires are connected only with forest fuel models, therefore it is important to have fuel maps with appropriate fuel models categorisation. In FirEUrisk forest fuelmodels are fuel categories starting with 1 as Table 1 shows:

Table 32: FirEUrisk hierarchical fuel classification system for forests fuels present on EU territory – adapted from (Aragoneses et al., 2023)

First level		
	Leaf type - Phenology	**Cover density (%)**
1. Forests	11. Broadleaf 112. Deciduous	1121. Open [15-70%)
		1122. Close [70-100%]
	12. Needleleaved 121. Evergreen	1211. Open [15-70%)
		1212. Close [70-100%]
	13. Mixed	1301. Open [15-70%)
		1302. Close [70-100%]

Copyright © FirEUrisk Consortium. All rights reserved.

Specific parameters connected with forest crown characteristics are Canopy Cover (CC), Canopy Height (CH), Canopy Base Height (CBH) and Canopy Bulk Density (CBD). All these maps will be produced by FirEUrisk project member Elena Aragoneses, University of Alcalá, Alcalá de Henares, Spain, for ET in 1 km resolution by some, not so recent maps exist on ET level:

- **Canopy Cover** (CC) [fraction or %] - Canopy cover is a measure of canopy density. Trees with denser canopies are more likely to allow fire to spread from one tree crown to another, creating a continuous path for the fire to follow. It refers to the amount of area in a particular location that is covered by the vegetation when viewed from above. Canopy cover is typically expressed as a percentage of the total area, and it can vary widely depending on the type and density of the vegetation present. Canopy Cover (CC), could be calculated from 2018 Tree Cover Density Maps[1] in 10m resolution for 2018. In FlamMap unit for CC is %.

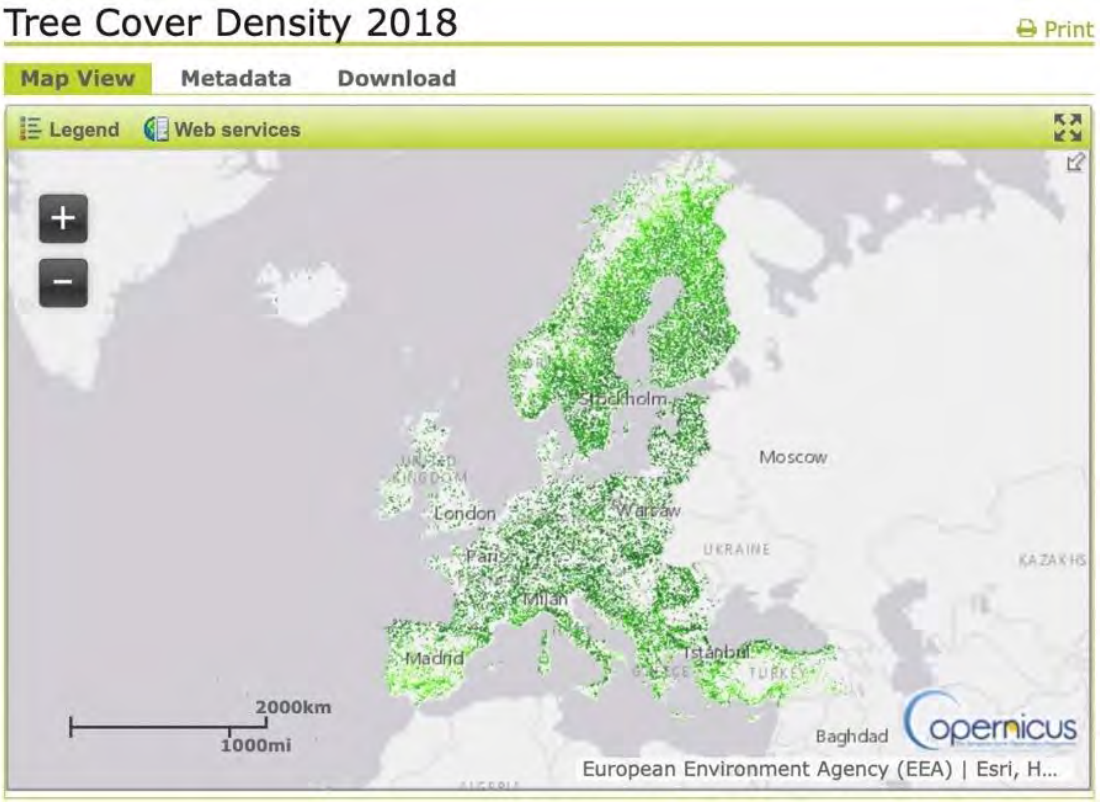


Figure 43: Canopy Cover for EU countries in 10 m resolution

- **Canopy Height** (CH) [m] is a measure of the vertical distance between the ground surface and the top of the vegetation canopy. Canopy height describes the average tree height in a stand. In surface wildfire spread models, canopy height affects calculation of the wind adjustment factor (WAF). If canopy height is less than 6 feet (1.8 meters), then the unsheltered WAF calculation is used. In crown wildfire spread models, canopy height is multiplied by canopy bulk density to get crown load, which is used to calculate crown flame length. In spot wildfire models, canopy height

Copyright © FirEUrisk Consortium. All rights reserved.

is used to calculate spotting distance from active crown fire. Canopy height at the site of the fire may be different from downwind canopy height in the direction firebrands are carried. Downwind canopy height is used to calculate maximum spotting distance in SPOT and is the mean cover height in the downwind direction as it affects the distance a firebrand is carried. It is typically calculated using remote sensing techniques, such as lidar (light detection and ranging) or radar, which can provide highly accurate measurements of vegetation structure and height. Canopy height can vary widely depending on the type and density of vegetation. It could be calculated by resample from the **Global Forest Canopy Height**[2] for 2019 or from **high-resolution canopy height model of the Earth**[3] (Lang et al. 2022) for 2020 in 10 m resolution. In FlamMap Canopy Height class is obtained by multiplying real height with 10, so unit is m*10.

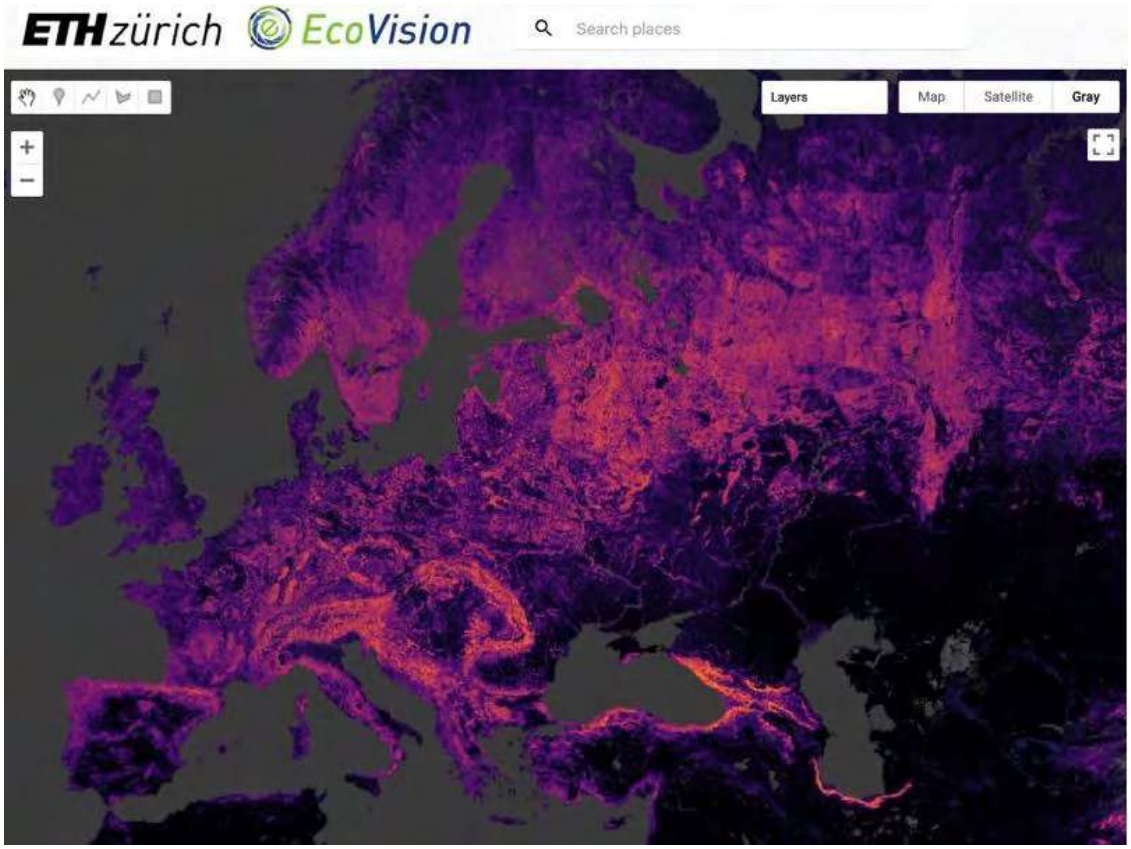


Figure 44: Canopy Height for EU countries in 10 m resolution for 2020 (Lang et al. 2022)

[1] https://land.copernicus.eu/pan-european/high-resolution-layers/forests/tree-cover-density/status-maps
[2] https://glad.umd.edu/dataset/gedi
[3] https://langnico.github.io/globalcanopyheight/

- **Crown Base Hight** (CBH) [m] is the vertical distance from the ground to the lowest branches of a tree's canopy. The canopy base height for an individual tree is the height at which there is sufficient fuel density to sustain canopy ignition. For a stand of trees, canopy base height considers both the main canopy layer and ladder fuels in the understory. It is an important parameter for forest management and planning, as it

Copyright © FirEURisk Consortium. All rights reserved.

can affect the amount of light and resources available to the understory vegetation, as well as the risk of crown fires. Canopy base height and foliar moisture content are used to calculate critical fireline intensity for transition to crown fire. Trees with lower crown base heights have a greater likelihood of allowing ground fires to climb up into the canopy, potentially igniting the crowns and leading to a crown fire. Crown base height can vary widely depending on the species, age, and site conditions of the tree, and it can also be affected by management practices such as thinning or pruning. Crown base height is typically measured using ground-based or remote sensing techniques, and it is often used in conjunction with other parameters such as tree height and canopy cover to estimate forest structure and biomass. Figure 5 illustrate difference between canopy height and canopy base hight.

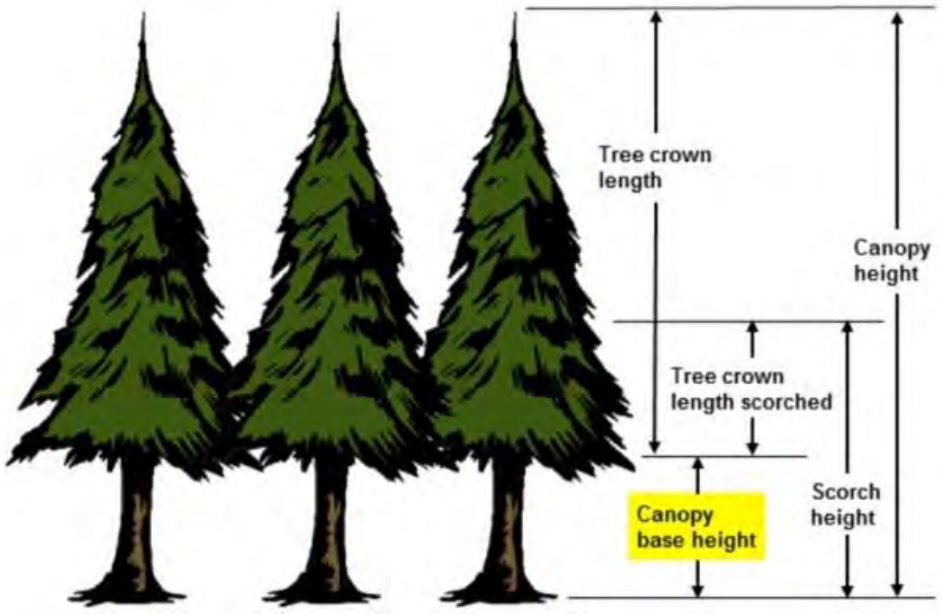


Figure 45: Illustration of canopy height and canopy base height

- **Crown Bulk Density** (CBD) [kg/m^3] is a measure of the mass of a tree's canopy per unit of canopy volume. It is a stand description of weight of canopy fuels per unit of canopy volume. It is used to calculate the crown fuel load input to canopy heat per unit area for active crown fire. Canopy bulk density is also used to calculate critical crown fire rate of spread, which in turn determines the threshold necessary to transition to active crown fire (Van Wagner, 1977). It is calculated by dividing the dry mass of the canopy by its volume. Crown bulk density can provide information about the structure and condition of a tree's canopy, as well as its potential for fire risk. Higher crown bulk density can indicate more compact and potentially flammable foliage, while lower crown bulk density can indicate more open and less flammable foliage.

Canopy Base Height (CBH) and **Canopy Bulk Density** (CBD) maps are not available at global scale. The easiest way is to **use conversation tables** made by **Universitat de Lleida, Lleida, Catalunya, Espagna**(**Fermin Alcasena**) and tested for Barcelona region. Estimation is based on three inputs:

Copyright © FirEURisk Consortium. All rights reserved.

- FirEURisk fuel category - only for forests canopy types:

FuelType	Description
1111	Open broadleaf evergreen forest
1112	Closed broadleaf evergreen forest
1121	Open broadleaf deciduous forest
1122	Closed broadleaf deciduous forest
1211	Open needleleaf forest
1212	Closed needleleaf forest

- Climate type – Arid or Humid – values are different for arid and humid climate.
- Canopy Cover (CC) (%)

Conversion table is below on Figure 46.

	Canopy cover class					
CBH (m)	15 - 30	30 - 45	45 - 60	60 - 75	75 - 90	90 - 100
1111_A	3,33	3,77	4,01	4,23	4,63	5,23
1112_A	2,84	3,55	4,16	4,51	4,73	4,98
1121_A	3,87	4,02	4,53	4,90	5,11	5,30
1122_A	4,12	3,99	4,94	5,13	5,62	5,62
1211_A	2,80	3,29	3,60	4,18	4,66	4,88
1212_A	2,46	3,18	3,34	3,57	3,91	3,90
1111_H	3,55	3,99	4,24	4,41	4,60	4,79
1112_H	3,30	4,14	4,66	4,81	4,89	5,00
1121_H	3,75	4,05	4,20	4,36	4,52	4,80
1122_H	3,87	4,36	4,62	4,75	4,85	5,17
1211_H	2,92	3,05	3,27	3,34	3,44	3,54
1212_H	2,73	3,05	3,24	3,42	3,49	3,53
	Canopy cover class					
CBD (kg m^{-3})	15 - 30	30 - 45	45 - 60	60 - 75	75 - 90	90 - 100
1111_A	0,05	0,08	0,11	0,14	0,16	0,16
1112_A	0,05	0,09	0,12	0,15	0,17	0,17
1121_A	0,04	0,08	0,10	0,12	0,15	0,16
1122_A	0,04	0,07	0,09	0,11	0,14	0,15
1211_A	0,06	0,10	0,13	0,15	0,17	0,17
1212_A	0,05	0,09	0,14	0,16	0,19	0,21
1111_H	0,05	0,09	0,12	0,15	0,17	0,17
1112_H	0,05	0,09	0,13	0,16	0,18	0,18
1121_H	0,04	0,07	0,09	0,11	0,13	0,13
1122_H	0,04	0,07	0,08	0,10	0,11	0,10
1211_H	0,06	0,09	0,12	0,16	0,18	0,19
1212_H	0,06	0,09	0,12	0,14	0,18	0,20

*Figure 46: Conversion table for estimation of Canopy base height (CBH) and Canopy bulk density (CBD) from FirEURisk Fuel Models (first colon – only for forest canopy cover together with climate type (arid A or humid H). The third input is Canopy cover class (**Fermin Alcasena** - **Universitat de Lleida**)*

For detection of Arid/Semi-arid – Sub-humid/Humid zones a map shown in Figure 7 could be used.

Copyright © FirEURisk Consortium. All rights reserved.

Humid/Arid zones could be also detected using De Martonne index introduced in 1926. (De Martonne, 1926.), but still used for detection of Humid/Arid zones (Pellicone et al, 2019). De Martonne aridity index (I_{DM}) is quite simple defined as:

$$I = P/(T_a + 10) \quad (16)$$

where P is annual amount of rainfall in mm and T_a is mean annual air temperature in ^{0}C. According to De Martonne Arid/Humid type of climate is defined by table:

Type	Value
Semi-arid	15≤I<24
Moderately-arid (Mediterranean)	24≤I<30
Slightly-arid	30≤I<35
Moderately-humid	35≤I<40
Humid	40≤I≤<50
Very-humid	50≤I<60
Excessively-humid	60≤I<187

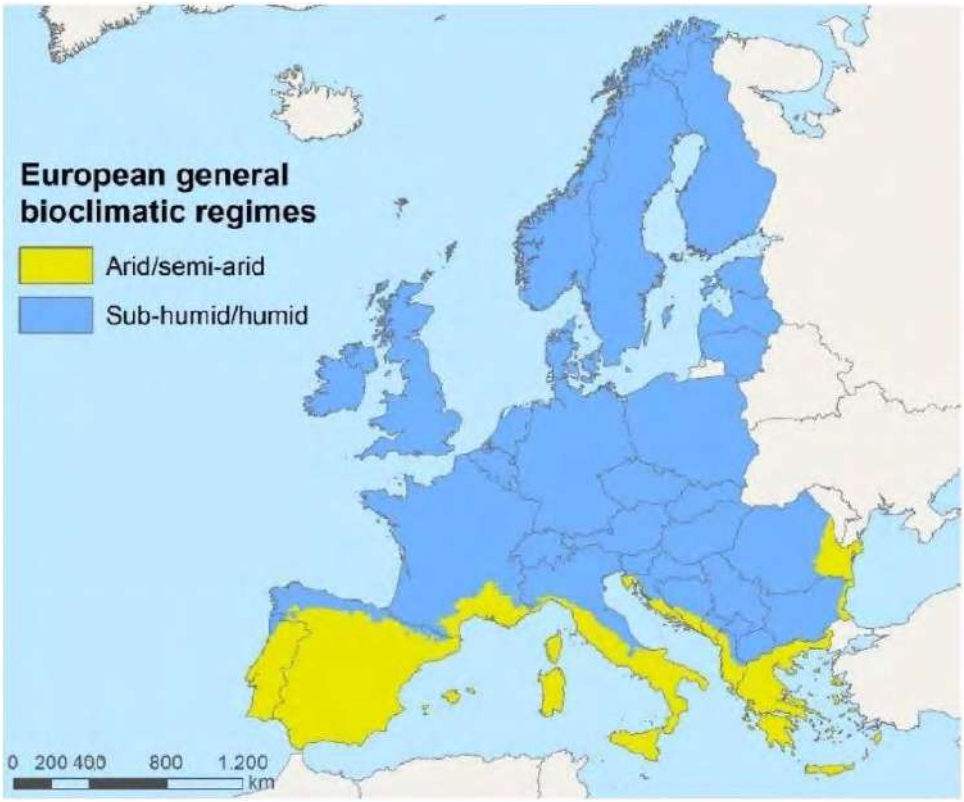


Figure 47: Location of Arid/Semi-arid – Sub-humid/Humid zones in EU – (Aragoneses et al. 2023) - https://essd.copernicus.org/articles/15/1287/2023/essd-15-1287-2023.html

Copyright © FirEURisk Consortium. All rights reserved.

We only need two zones:

- Arid/Semi-arid if I < 35
- Sub-humid/Humid if I ≥ 35

Variables P - annual amount of rainfall in mm and T_a - mean annual air temperature in ^{0}C could be found on WorldClim website[4] where GeoTIFF file of average bioclimatic variables for the years 1970-2000 could be find (Fick & Hijmans, 2017). For De Martonne index variables BIO1 = Annual Mean Temperature and BIO12 = Annual Precipitationare required.
In FlamMap Canopy Base Height (CBH) class is obtained by multiplying real height with 10, so unit is m*10, and Canopy Bulk Density (CBD) class by multiplying real density with 100, so unit is (kg/m3)*100.
For example for Open broadleaf evergreen forest in arid climate (1111_A) CBH is 3,33*10=33,3 and CBD 0,05*100=5.

Figure 48 shows non-verified CBD map produced for ET in 1 km resolution by Marin Bugarić:

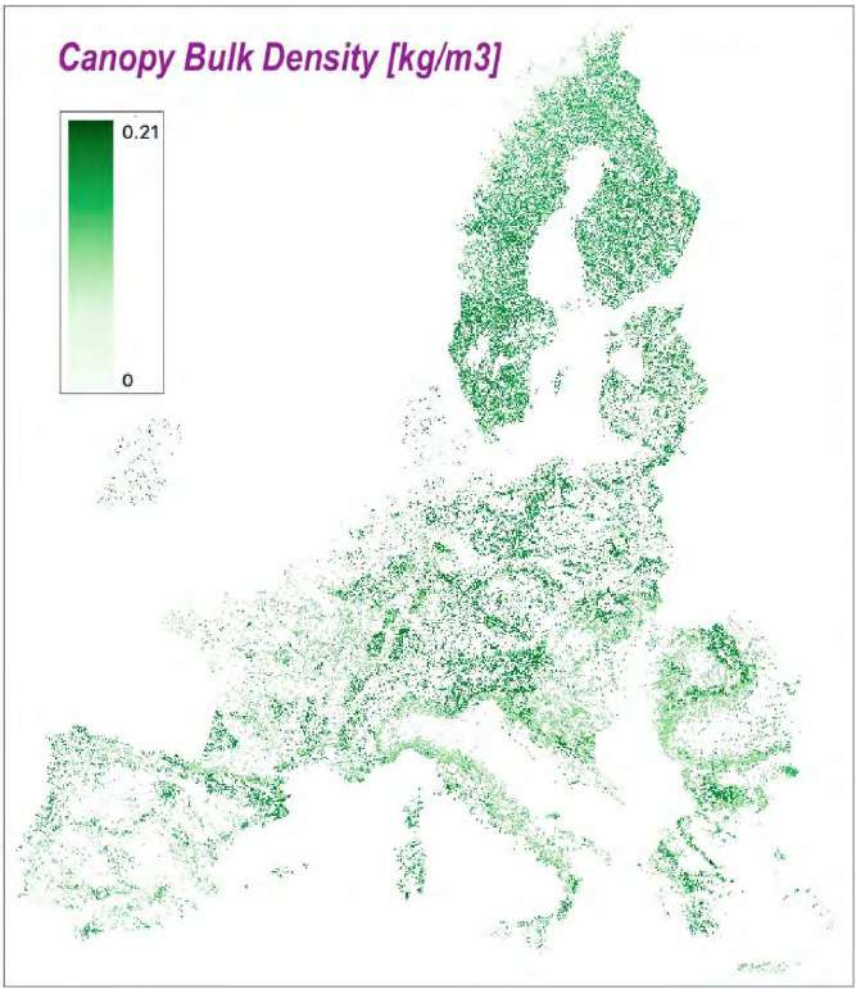


Figure 48: ET CBD map – (Bugarić, FirEUrisk project2, 023)

[4] https://www.worldclim.org/data/worldclim21.html

Copyright © FirEUrisk Consortium. All rights reserved.

6.1.5.2 Calculation of crown fire indicators

Two processes and models for estimating crown fire potential defined by (Van Wagner, 1977) are:

- **Crown Fire Initiation** as an indicator of the potential for surface fire to ignite tree crown and produce either passive or active crown fire. Inputs include the gap between the surface fuels and the tree crowns (Canopy Base Height – CBH), the foliar moisture content (FMC) of the tree crowns. The result is a threshold surface fire intensity required to produce some crown fire.
- **Active Crown Fire Propagation** (Crown Spread) is an indicator of the potential for continuous spread through the tree crowns. Inputs include only a characterization of the canopy fuel density in a single number. The result is a threshold rate of spread required to sustain a "solid crown flame…with associated horizontal spread."

Concerning crown fires initiation and propagation **Crown Fire Activity** (CFA) is important as an indication what kind of fire behaviour concerning crown fires could be expected. Five situations could be encountered:

- **Non-burnable** – Portions of the landscape fuels that will not support combustion. Generally associated with bodies of water or non-vegetated areas of the landscape (for example rocks and water).
- **Surface Fire** – Fire spreads through the surface fuels that may include litter, grass, shrubs, and dead twigs. Surface fuels are generally defined to be less than about 6 feet (1.8 meters) deep.
- **Passive Crown Fire** - A fire in the crowns of trees in which trees or groups of trees torch, ignited by the passing front of the fire. A synonym is **Intermittent Crown Fire. T**he torching trees reinforce the spread rate, but these fires are not basically different from surface fires. This type of crown fire happened in case of either low windspeed and low fuel moisture or low Crown Bulk Density (CBD), low Canopy Cover (CC) and high Crown Base Hight (CBH).
- **Active Crown Fire** - A fire in which a solid flame develops in the crowns of trees, but the surface and crown phases advance as a linked unit dependent on each other. Synonym is **Dependent Crown Fire**. This type of crown fire happened in case of either higher windspeed and low foliar moisture or high Crown Bulk Density (CBD), low Canopy Cover (CC) and low Crown Base Hight (CBH).
- **Conditional Surface Fire** - A fire cannot transition into a crown fire in this area, but active crown fire is possible if the fire transitions to the overstory outside the area and burns into the canopy.

Independent Crown Fire is usually not considered because they are short-lived phenomena. Van Wagner (Van Wagner, 1993) doubt about this type of wildfire behaviour

Copyright © FirEUrisk Consortium. All rights reserved.

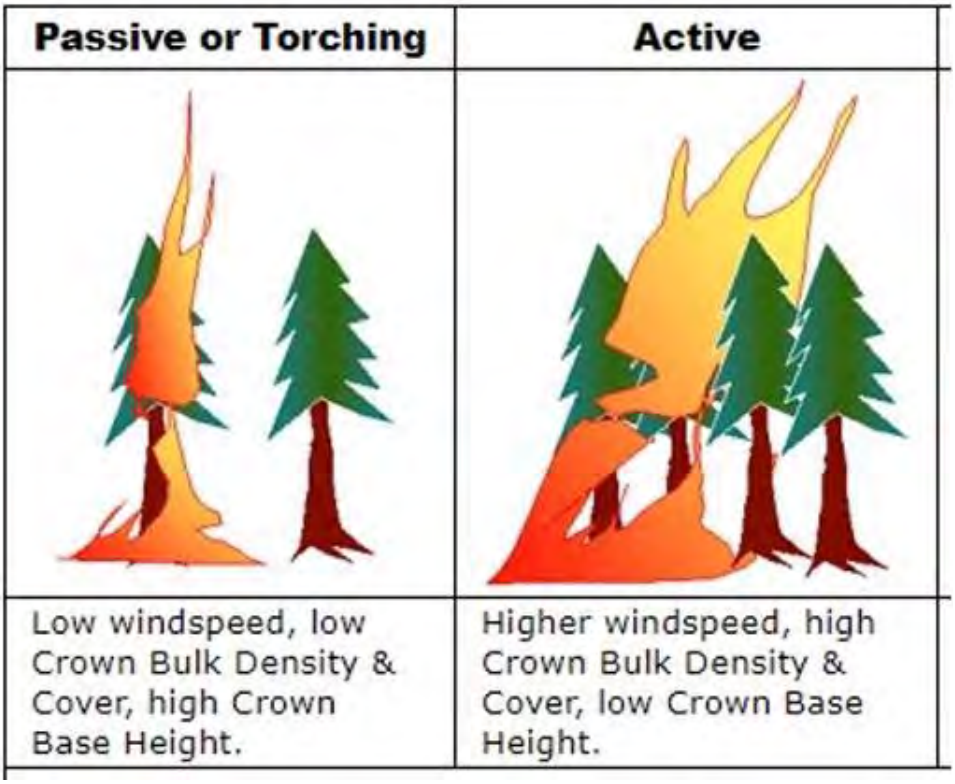


Figure 49: Illustration of passive and active crown fire

The Crown Fire Initiation and Active Crown Fire Propagation models work together to estimate when fires will remain as surface, when they will produce torching, or passive crown fire, behaviour in the canopy, and when they will progress to active crown fires.
Well known programs for wildfire propagation modelling and simulation include various models for crown fire initiation and propagation. Our models of crown fire indicators calculation are based on two of them: BehavePlus and FlamMap.

6.1.5.3 Crown fire models in BehavePlus and FlamMap

Crown fire models in BehavePlus and FlamMap are based on:

1. Rothermel's (Rothermel, 1972) surface fire spread model,
2. Van Wagner's (Van Wagner, 1977) crown fire initiation model,
3. Rothermel's (Rothermel, 1991) crown fire spread model,
4. Finney's (Finney, 1998) crown fire behaviour model,
5. Scott and Reinhardt's (Scott & Reinhart, 2001) crown fire behaviour model.

Rothermel's surface fire spread model (1971)

Rothermel's surface fire spread model (1971) calculates surface wildfire behaviour. Its application in propagation potential calculation for European Territory (ET) is described in details in (Stipaničev et al., 2023). Variables important for crown fire are:

Copyright © FirEUrisk Consortium. All rights reserved.

- **Surface Heat per Unit Area** (H_A) [kJ/m^2] - the amount of heat released per unit area during the short period of continuous flaming. Heat per Unit Area is not affected by wind speed, slope, or direction of spread. It is calculated as a product of Reaction Intensity [kJ/(m^2 s)] and Flame Residence Time [s] or Heat of Combustion [kJ/kg] and Fuel Consumed [kg/m^2].
- **Surface Fireline Intensity** (I_B) [kW/m] - also called Byram's fire intensity that express heat energy released per unit time from a one-meter-wide section of the fuel bed extending from the front to the rear of the flaming zone. It is calculated as a product of Heat per Unit Area [kJ/m^2] and Fire Rate of Spread [m/s].
- **Surface Flame Length** (FL) [m] - measured in from midway in the active flaming combustion zone to the average tip of the flames. It is directly proportional to Surface Fire Intensity.
- **Rate of Spread of Surface Fire** (R) [m/s] - The linear rate of advance of a flaming front into unburned fuel in the direction perpendicular to the fire front. It is a significant factor affecting fireline intensity and flame size.

Van Wagner's crown fire initiation model (1977)

Van Wagner's crown initiation model (Van Wagner, 1977) is a semi-empirical model derived from physical theory and empirical observation. It defined quantitative criteria to predict the possibility of crown fire initiation based on surface fireline intensity. **Critical Fireline Intensity** (I_0)[kW/m] is calculated from **Foliar Moisture Content** (*FMC*)[%] and **Canopy Base Height** (*CBH*)[m]:

$$I_0 = \left(C \cdot CBH \cdot (460 + 25.9 \cdot FMC)\right)^{1.5} \qquad (17)$$

C is a constant, a criterion for initial crown combustion estimated by Van Wagner to be 0.01 based on a single experimental fire conducted in a red pine (*Pinus resinosa*) plantation stand (CBH = 6 m, FMC = 100%, I_0 = 2500 kW/m). Foliar Moisture Content (FMC) is the moisture content of conifer needles in three crowns.

Van Wagner Crown Fire Initial Model is based on three conditions:

1. If $I_B < I_0$ we have Surface Fire only.
2. If $I_B \sim I_0$ we have transition from Surface Fire to Crown Fire.
3. If $I_B > I_0$ we have Crown Fire.

Instead of surface fireline intensity, **surface flame length** FL [m] could be used, because it depends only on fireline intensity. Critical flame length could be calculated using equation:

$$FL_0 = 0.13716 \cdot (I_0)^{0.46} = 0.13716 \cdot (C \cdot CBH \cdot (460 + 25.9 \cdot FMC))^{0.69} \qquad (18)$$

Figure 50 shows plot of equation (17) and (18) (NVCG, 2021).

We will introduce the **Criterion for Crown Fire Initiation** (CCFI):

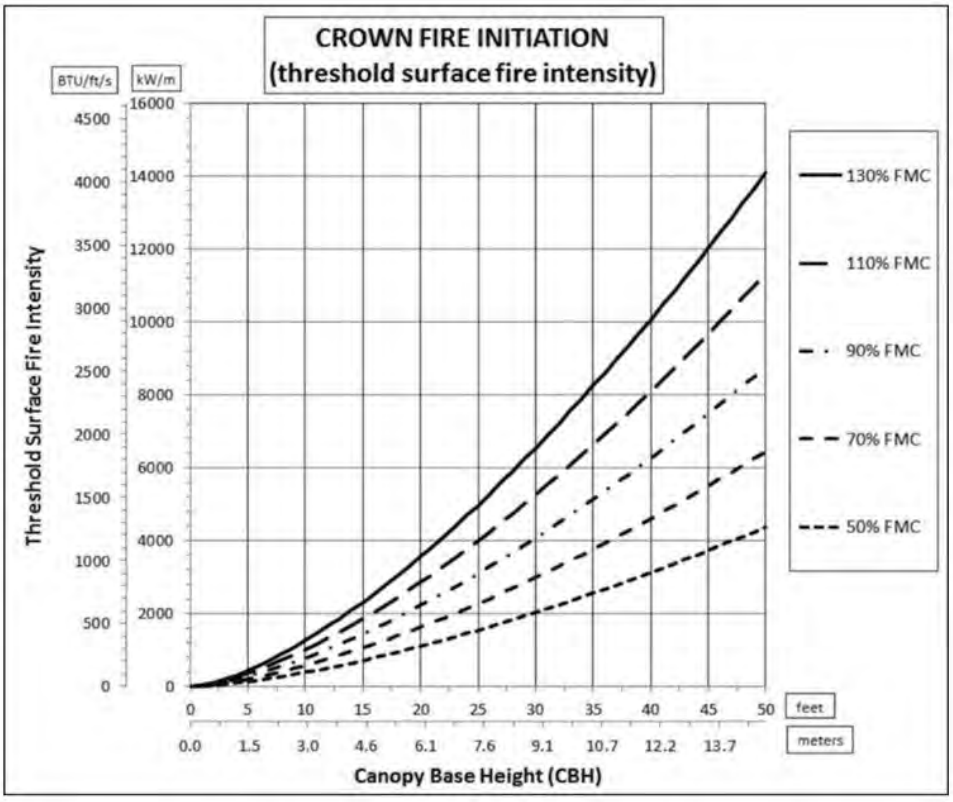
$$CCFI = I_B / I_0 = FL / FL_0 \qquad (19)$$

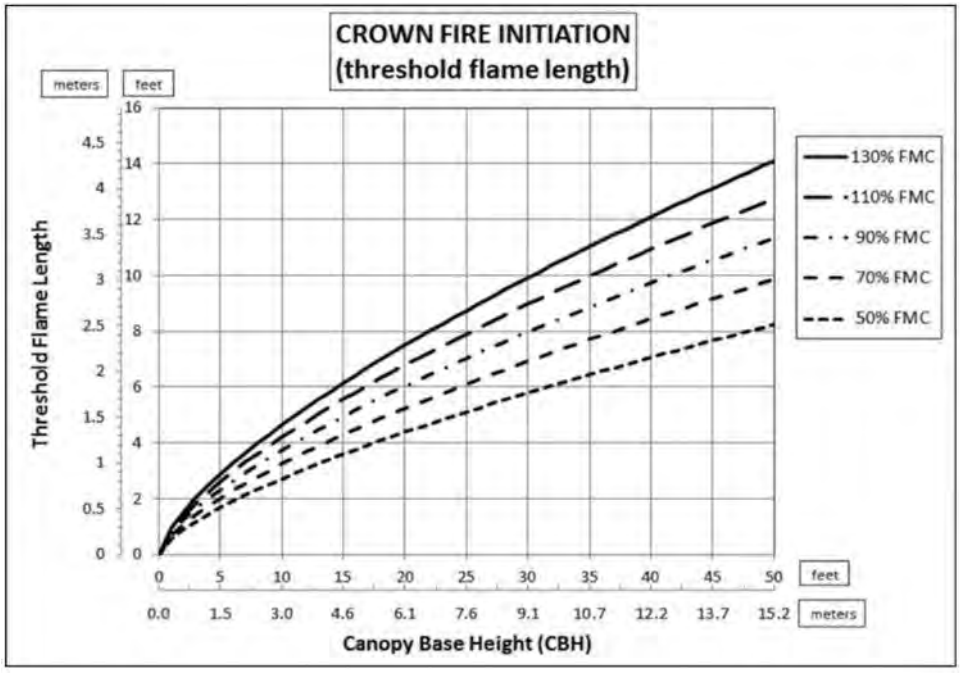
Copyright © FirEURisk Consortium. All rights reserved.

Van Wagner (Van Wagner, 1993) has latter converted Critical Fireline intensity I_0 to **Critical Rate of Spread for Critical Fireline Intensity** [m/s]:

$$R_{I_0} = I_0 / H_A \quad (20)$$

where H_A is **Surface Heat per Unit Area** [kJ/m^2] and I_0 is **Critical Fireline Intensity** [kJ/(m s)]. This variable was used by Scott and Reinhard to determine **Crown Fraction Burned** (CFB) (see latter).





Copyright © FirEURisk Consortium. All rights reserved.

Figure 50: Van Wagner threshold surface fire intensity I_0 and Threshold Surface Flame Length FL (NVCG, 2021)

Inputs for calculation of Critical Fireline Intensity I_0 (equation (2)) are: Canopy Base Height (CBH) and Foliar Moisture Content (FMC). Rothermel later (Rothermel, 1991) published a very good table for Foliar Moisture Content estimation according to season. Table shows Figure 51.

	Seasonal moisture condition				
Class	Early spring before greenup	Late spring after greenup	Normal summer	Drought summer	Late summer severe drought
1-h	8	9	6	4	3
10-h	14	11	8	5	4
100-h	18	15	10	7	6
live	65	195	117	78	70

Figure 51: Fuel moisture content values (percent) by size class for five seasonal moisture conditions (Rothermel, 1991)

Foliar Moisture Content (FMC) is the moisture content of conifer needles in three crowns, therefore 'live' moisture content from this table could be used.

Another, even better approach could be a procedure proposed by Pettinary & Chuvieco (Pettinary & Chuvieco, 2017) used for fire behaviour simulation on global Earth level. **Fuel moisture content** (FMC) was divided into four **Fuel Moisture Scenarios Classes**. In each FMC class, values of all fuel moisture contents (dead fuel, live fuel, live crown) are defined according to table shown on Figure 52 (Pettinary & Chuvieco, 2017):

FMS Code	FMS Description	Fuel Moisture Content (%)					
		Herb	Shrub	Crown [1]	1 h	10 h	100 h
D1L1	Very low dead FMC, fully cured herb	30	60	60	3	4	5
D2L2	Low dead FMC, 2/3 cured herb	60	90	60	6	7	8
D3L3	Moderate dead FMC, 1/3 cured herb	90	120	120	9	10	11
D4L4	High dead FMC, fully green herb	120	150	150	12	13	14

[1] The Scott and Burgan original FMSs do not include FMCs for Crown. These data were extracted from the description of the variables inside the FCCS software.

Figure 52: Fuel Moisture Content Scenarios (Pettinary & Chuvieco, 2017)

Foliar Fuel Moisture is now live crown fuel moisture.

Van Wagner's crown fire initiation model is quite simple and easy to implement, but it has a lot of disadvantages like (Cruz & Alexander, 2010):

- Separate *C* values are required for distinctly different fuel complexes – furthermore, currently used value (0.010) is essentially based on a single observation in red pine stand.

Copyright © FirEURisk Consortium. All rights reserved.

- Doesn't allow for variable duration of heating (presently the flame front residence time is a constant 50 sec) – thus, quite possible for two surface fires to have the same intensity but significantly different residence times (e.g., grass vs. conifer needle forest floor).
- Surface burning conditions (i.e., temp, RH, plus in-stand wind and thus fire plume angle) a constant rather than a variable.

Anyway, beside all these disadvantages and although another crown fire initiation models were proposed in meantime (Cruz & Alexander, 2010) like:

- Xanthopoulos (1990) Crown Fire Initiation Model (Xanthopoulos, 1990)
- Alexander (1998) Crown Fire Initiation Model (Alexander, 1998)
- Cruz, Alexander and Wakimoto (2004) Crown
- Crown Fire Occurrence Probability Model (Cruz et al., 2004)
- Cruz, Butler, Alexander and Viegas (2006) semi-physical crown fire initiation model (Cruz et al., 2006)

Van Wagner crown fire initiation model is still used today in almost all North American fire behaviour prediction systems (Canadian FBA and Prometheus, BehavePlus, Firesite and FlamMap), but always with some initial limitations on input variables:

- **Minimum Crown Bulk Density** (CBD) to Define the Canopy Base Height (CBH). Various values ware proposed and the lowest is for Scot and Reinhard model (Scott & Reinhard, 2001): 0.011 kg/m^3.
- **Threshold for critical surface fire intensity for initial crown combustion** (Alexander, 2006) proposed by Rothermel (Rothermel, 1983): 3460 kW/m.

Rothermel Crown Fire Propagation Model (1991)

Rothermel's crown fire propagation model (Rothermel, 1991) calculates rate of spread (ROS) for active crown fires. Passive crown fire rate of spread is assumed to be the same as surface fire rate of spread. Active crown fire rate of spread is the head fire (forward) spread rate of a crown fire. It is the overall spread for a sustained run over several hours and implicitly includes the effects of spotting. It does not consider a description of the overstory. The active crown fire rate of spread is calculated from wind speed and surface fuel moisture values.

The Rothermel active crown fire spread model is not physically-based, but is rather a simple correlation between the spread rates of several crown fires and calculations of the Rothermel surface fire model (Rothermel, 1972). The model does not include a description of either the surface or crown fuel. It is a function of only the 20-foot (or 10-m) wind speed and surface fuel moisture values, using Albini-Anderson fuel model 10 - Timber (litter and understory) (Anderson, 1982) to represent surface fuel characteristics. Windspeed at midflame of fuel model 10 is assumed to be 40% or wind speed at 6.1 m (20 ft) height.

Rothermel termed this value the "average rate of spread." He suggests that a "near maximum" rate of spread can be 1.7 times this average value.

Figure 53 shows corelation between surface fire ROS of fuel model 10 and crown fire ROS.

Copyright © FirEUrisk Consortium. All rights reserved.

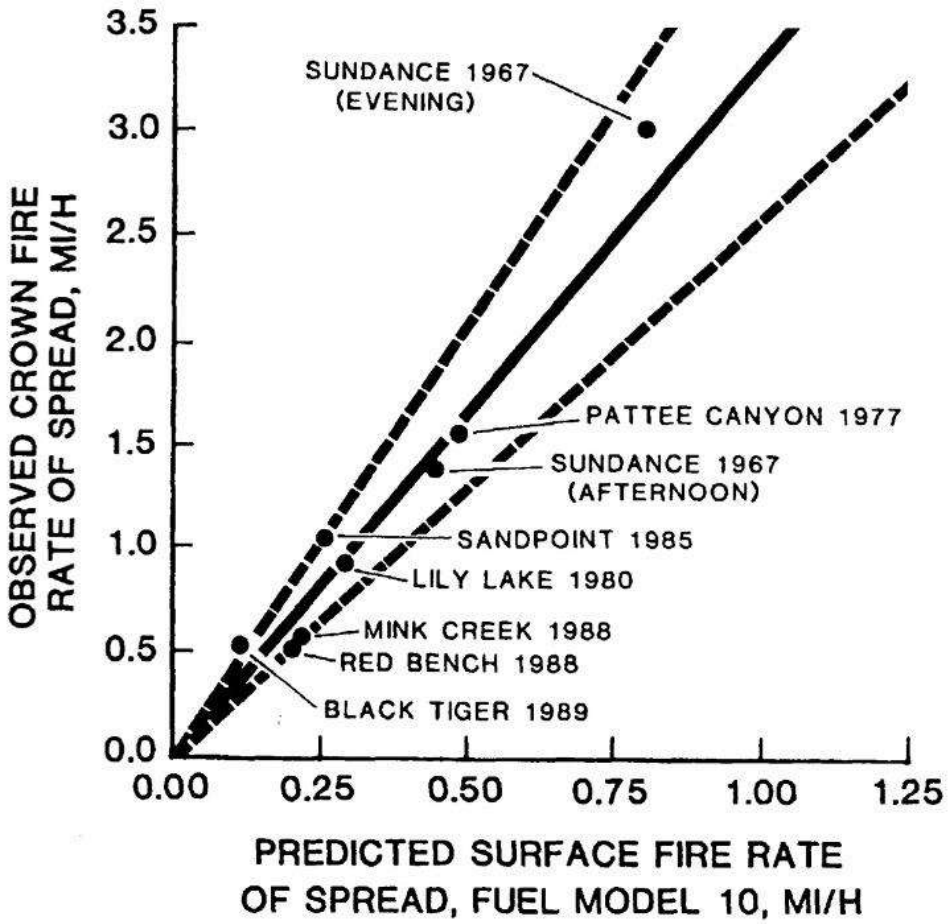


Figure 53: Rothermel correlation between surface fire Rate of Spread (ROS) of Fuel Model 10 and crown fire ROS for observed 7 fires between 1967 and 1989 (Rothermel, 1991)

Rothermel has suggest following correlations:

Ave. Crown Fire ROS (R_C) = 3.34 · Surface Fire ROS of Fuel Model 10 (R_{10}) (21)

Max. Crown Fire ROS (R_{Cmax}) = 1.7 · Ave. Crown Fire ROS (R_C) (22)

It is important to emphasise **that windspeed at midflame of fuel model 10 is assumed to be 40% or wind speed at 6.1 m (20 ft) height**.

Rothermel model for Surface ROS calculation (R) (Rothermel, 1972):

$$R = \frac{I_R \cdot \xi \cdot (1+\phi_w+\phi_s)}{\rho_b \cdot \epsilon \cdot Q_{ig}} \quad (23)$$

where:

I_R - Reaction Intensity [kW/m^2]

ξ - Propagation Flux Ratio

ρ_b - Mean Bulk Density [kg/m^3]

ϵ – Effective Heating Number

Copyright © FirEURisk Consortium. All rights reserved.

Q_{ig} – Heat of Preignition [kJ/kg]

ϕ_w – Wind Correction Factor

ϕ_s – Slope Correction Factor

Rate of Spread of Fuel Model 10 (R_{10}) has fixed fuel parameters of Fuel Model 10, but wind speed and fuel moisture content are variable. Wind speed has influence only on Wind Correction Factor (windspeed at midflame of fuel model 10 is assumed to be 40% or wind speed at 6.1 m (20 ft) height), but fuel moisture content has influence on Reaction Intensity and Heat of Preignition . Fuel parameters of Albini-Anderson fuel model 10 - Timber (litter and understory) (Anderson, 1982) are given in Table 33.

Table 33: Table with parameters for Albini-Anderson fuel model 10 (Anderson, 1982)

Dead Fuel Load [t/ha]			Live Fuel Load [t/ha]		Surface Area to Volume Ratio (SAV) - Dead [1/m]			SAV – Live [1/m]		Depth [m]	Moisture of Extinction [%]	Heat Content [kJ/kg]	Bulk Density [kg/m^3]	Relative Packing Ratio
1h	10h	100h	Herb	Woody	1h	10h	100h	Herb	Woody					
7.41	4.94	12.36	0	4.94	6562	357.6	98	4821	4921	0.3048	25	18622	8.81	2.35
Dead Fuel Load [t/acre]			Live Fuel Load [t/acre]		Surface Area to Volume Ratio (SAV) - Dead [1/ft]			SAV – Live [1/ft]		Depth [ft]	Moisture of Extinction [%]	Heat Content [Btu/lb]	Bulk Density [lb/ft^3]	Relative Packing Ratio
1h	10h	100h	Herb	Woody	1h	10h	100h	Herb	Woody					
3	2	5	0	2	2000	109	30		1500	1	25	8000	0.55	2.35

The basic Rothermel fire spread model is based on one size class of dead and live fuel, but when there are several size classes of dead (1-h, 10-h, 100-h) and live fuel (LH, LW), a **method of weighting** is used to define characteristic values to be used in the final calculations.

There are two weighting factors g_{ij} important for Fuel Surface Load and weighting factor f_{ij} important for Surface Area to Volume Ratio and Fuel Moisture. Indeks *i* correspond to dead or live fuels (*i=1* dead, *i=2* live).

Fuel Model 10 is static fuel therefore both coefficients are equal $f_{ij} = g_{ij}$ and shown in Table 34:

Table 34: Weighting factors for Albini-Anderson fuel model 10 (Anderson, 1982)

Fuel	Dead 1-h	Dead 10-h	Dead 100-h	Live Herb	Live Woody	Dead	Live
	$f_{11} = g_{11}$	$f_{12} = g_{12}$	$f_{13} = g_{13}$	$f_{21} = g_{21}$	$f_{22} = g_{22}$	f_1	f_2
AA 10	0.94	0.03	0.02	1	1	0.68	0.32

For Fuel Model 10 fixed parameters are Fuel Surface Load, Surface Area to Volume Ratio (SAV), Propagation Flux Ratio ( ) that depend on SAV and Mean Packing Ratio, Mean Bulk Density ( ) that depends on Net Fuel Load and Fuel Bed Depth and Effective Heating Number ( ) that depends on SAV.

Copyright © FirEURisk Consortium. All rights reserved.

This calculated active crown fire rate of spread R_C is compared to a critical crown fire rate of spread R_0 (Van Wagner 1977) to determine whether an active crown fire is possible. **Critical crown fire rate of spread** is:

$$R_0 = S_0/(CBD \cdot 60) \quad (24)$$

where R0 is the critical minimum spread [m/s]. In original equation rate of spread is in [m/min], therefore there is no factor 60 in denominator. This factor is introduced when rate of spread is in [m/s]. In order to sustain a continuous flame front within the crown fuel layer, S0 is the critical mass flow rate for solid crown flame [kg/(m2 min)], and CBD is the canopy bulk density [kg/m3]. S0 is regarded as an empirical constant to be derived from field observations. Best available estimate was S0 =3.0 based on single experiment in red pine plantation where CBD = 0.23 kg/m3:

$$R_0 = 0.05/CBD \quad (25)$$

Figure 54 shows plot of this equation (Van Wagner 1977).

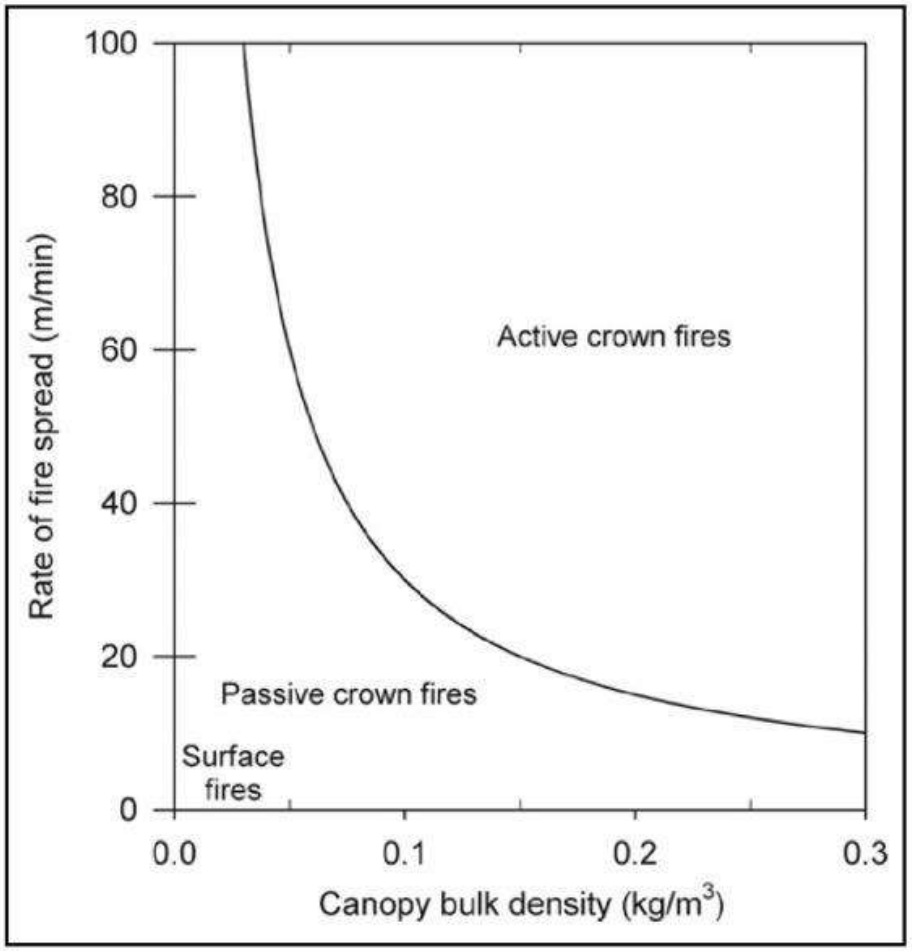


Figure 54: Critical minimum surface fire spread rate for active crowning in a conifer forest stand as a function of canopy bulk density according to (Van Wagner 1977). On plot Rate of Spread is in [m/min], therefore it is a plot of equation $R_0 = 3/CBD$.

Later (Cruz et al., 2005) prove the robustness of this value, as well as threshold values of CBD:

Copyright © FirEURisk Consortium. All rights reserved.

- No passive crown fires with CBD < 0.05 kg/m^3
- No active crown fires with CBD < 0.11 kg/m^3

Rules for determination of active crown fires based on Rothermel crown fire model are:

1. If $R_C < R_0$ Than a Surface Fire is expected to prevail or Passive Crown Fire (Torching).
2. If $R_C \geq R_0$ Than an Active Crown Fire is presumed to be possible or

Quotient of R_C and R_0 is sometimes called the **Criterion for Active Crowning** (CAC):

$$CAC = R_C / R_0 \quad (26)$$

Figure 14 (NVCG, 2021) combines both criteria for crown fire initiation and active crown fire propagation according to (Scott & Reinhardt, 2001) showing linking between surface and crown fires testing two criteria:

a. Relation between Surface Fireline Intensity or Flame Length and Critical Surface Fireline Intensity or Flame Length (CCFI).
b. Relation between Crown Rate of Spread and Critical Crown Rate of Spread (CAC).

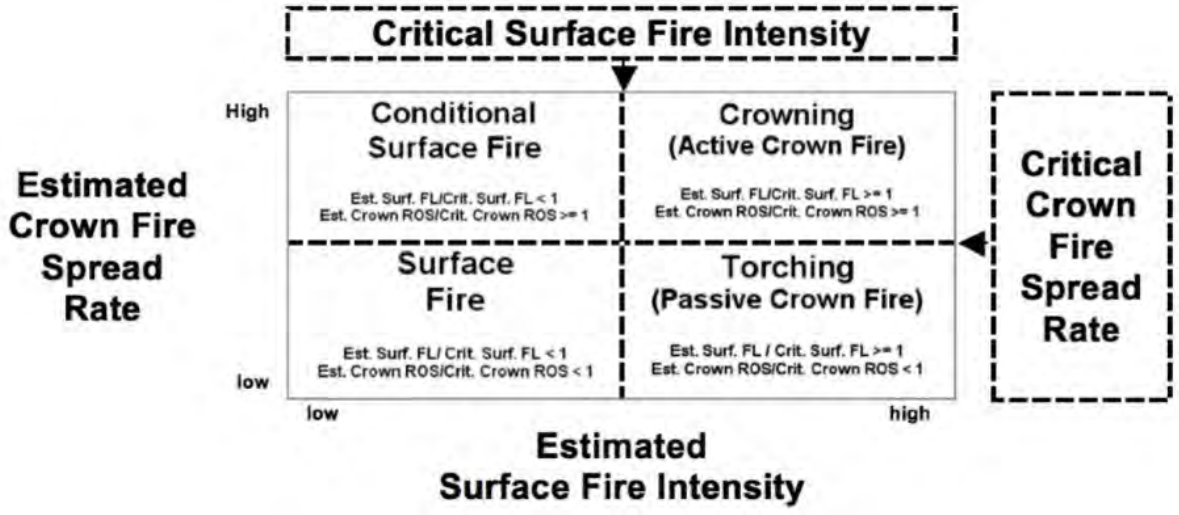


Figure 55: Linking between surface and crown fires (NVCG, 2021)

Four situations are possible:

1. CCFI < 1 & CAC < 1 → Surface Fire
2. CCFI < 1 & CAC ≥ 1 → Conditional Surface Fire
3. CCFI ≥ 1 & CAC < 1 → Passive Crown Fire
4. CCFI ≥ 1 & CAC ≥ 1 → Active Crown Fire

Scott & Reinhardt (Scott & Reinhardt, 2001) also draw an interesting Crown Fire Assessment Chart (Figure 15) that connect all important factors. Correlation with our notations are:

$R_{surface}$ – R (Surface Fire Rate of Spread – ROS)

R_{active} – R_C (Active Crown Fire Rate of Spread)

$R'_{initiation}$ – (Critical Rate of Spread for Critical Fireline Intensity)

Copyright © FirEURisk Consortium. All rights reserved.

R'_{active} – (Critical Crown Fire Rate of Spread)

R'_{SA} – (Predicted surface fire spread rate that correspond to the environmental conditions (wind) for which active crown fire is equal to critical crown fire $R_C = R_0$)

$O'_{initiation}$ – *TI - Torching Index* (Wind Spread when Surface Fire reach Critical Fireline Intensity)

$O'_{iactive}$ – *CI - Crowning Index* (Wind Spread when Active Fire reach Critical Crown Fire Rate of Spread)

A surface fire is expected at windspeeds below Torching Index TI. Windspeeds greater than TI but less than Crowning Index CI lead to passive crowning. Active crown fire is expected at windspeeds above CI.

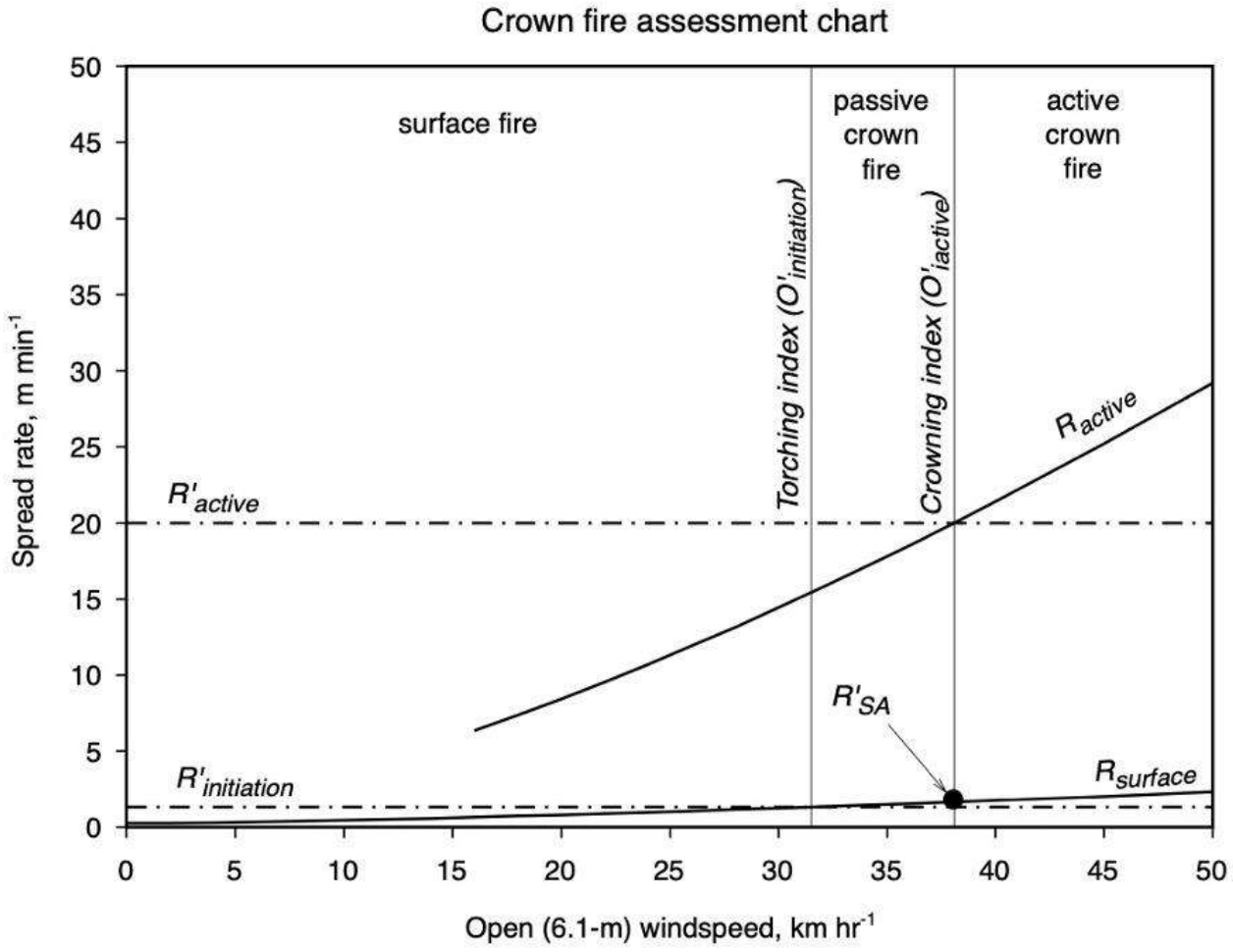


Figure 56: Critical Rates of Spreads and Torching and Crowning Indexes as a function of Wind Speed for fuel model 10 - timber litter and understory (Anderson 1982), canopy base height = 1.5 m, canopy bulk density = 0.15 kg m-3, foliar moisture content = 100 %, normal summer surface fuel moisture condition (Rothermel 1991, table 4), and wind reduction factor = 0.15 (Scott & Reinhardt, 2001, Fig.8)

Scott and Reinhardt Crown Fire Propagation Model (2001)

Copyright © FirEURisk Consortium. All rights reserved.

Scott and Reinhardt's method (Scott & Reinhard, 2001) calculates fire behaviour for both active and passive crown fires. Active crown fire behaviour is the same as for Rothermel (1991) (Equations (5) and (6). Passive crown fire rate of spread is assumed to be greater than the surface fire rate of spread and less than the active crown fire rate of spread. Passive crown fire behaviour is based on the canopy fraction burned.

First let us introduce variable:

Crown Fraction Burned (CFB) [fraction] - A fraction between 0 and 1 indicating the severity of a crown fire. It is a proportion of tree crowns involved in the fire in a given area. Less than 10 percent is considered as surface fire (CFB < 0.1) , between 10 and 90 percent is can intermittent crown fire ($0.1 \leq CFB < 0.9$), while over 90 percent is a continuous crown fire ($CFB \geq 0.9$). More precise division is:

$0 < CFB \leq 0.001$ Surface fire
$0.001 < CFB \leq 0.25$ Low-grade passive crown fire
$0.25 < CFB \leq 0.6$ Mid-grade passive crown fire
$0.6 < CFB \leq 0.9$ High-grade passive crown fire
$CFB > 0.9$ Active crown fire

Van Wagner (Van Wagner, 1989) proposed a method to calculate the Crown Fraction Burned (CFB) that takes into account Canopy Bulk Density (CBD) through Critical crown fire rate of spread (R_0):

$$CFB = 1 - e^{-\left(a\cdot(R-R_{I_0})\right)} = 1 - e^{-\left(0.23\cdot 60\cdot(R-R_{I_0})\right)} \quad (24)$$

Where R is a surface fire rate of spread [m/s] and is a Critical Rate of Spread for Critical Fireline Intensity [m/s] (. Factor 60 is because rate of spreads are in [m/s] and not in [m/min] like in original formula.
Van Wagner (Van Wagner, 1993) modified equation in 1993 to permit dynamic calculation of the coefficient a

$$CFB = 1 - e^{(-a\cdot(R-R_{I_0}))} = 1 - e^{\left(-2.558\cdot\frac{R-R_{I_0}}{R_0-R_{I_0}}\right)} \quad (25)$$

Canadian Canadian FFBP System defines CFB on another way, therefore Scott and Reinhart (Scott & Reinhard, 2021) propose new formula that is consistent with Van Wagner and Canadian FFBP:

$$CFB = (R - R_0)/(R_{SA} - R_0) \quad (26)$$

where R_{SA} is the predicted surface fire spread rate that correspond to the environmental conditions (wind) for which $R_C = R_0$ (see Figure 56). From Figure 56 it could be also noticed that wind speed that will give R_{SA}correspond to Crowning Index.
Crowning Index (*CI* or O'_{active} from Figure 15) [m/s] is the 10-m windspeed at which active crowning is possible, based on Rothermel's (1991) crown fire spread rate model and Van Wagner's (1977) criterion

Copyright © FirEURisk Consortium. All rights reserved.

for active crown fire spread. According to Scott and Reinhard Crowning Index is calculated using simplified equation for Fuel Model 10:

$$CI = O'_{active} = ((0.0457 \cdot 1.149)/3.6) \cdot \left(\frac{\frac{R_0 \cdot \rho_{B10} \cdot \varepsilon 10 \cdot Q_{ig10}}{3.34 \cdot I_{R10} \cdot \xi 10} - \phi_{S10} - 1}{0.001612} \right)^{0.7} \quad (27)$$

where constants are from Rothermel surface model (Equation (8), all for Fuel Model 10:

ρ_{B10} is Mean Bulk Density

$\varepsilon 10$ is Effective Heating Number

Q_{ig10} is Heat of Preignition

$\rho_{B10} \cdot \varepsilon 10 \cdot Q_{ig10}$ is Heat Sink (denominator of Rothermel Rate of Spread equation)

I_{R10} is surface Reaction Intensity

$\xi 10$ is Propagating Flux Ratio

ϕ_{S10} is Slope Factor and

R_0 is Critical Crown Fire Rate of Spread.

For Fuel Model 10 constant factors for Fuel Model 10 are ρ_B and ξ (ρ_B = 9.7278 [kg/m^3], ξ = 0.0654685). Correction factor from 20-ft to 10-m wind speed is 1.149 ($U_{10m} = U_{6.1m} \cdot 1.149$) and correction factor from [km/h] to [m/s] is (1/3.6).

Torching Index (*TI* or $O'_{initiation}$ from Figure 15) [m/s] is the 10-m windspeed at which surface fire rate of spread *R* is equal to Critical Rate of Spread for Critical Fireline Intensity . It is calculated for any fuel load (not only for Fuel Model 10 as Crowning Index):

$$TI = O'_{active} = ((0.0457 \cdot 1.149)/(3.6 \cdot WAF)) \cdot \left(\frac{\frac{I_0 \cdot \rho_B \cdot \varepsilon \cdot Q_{ig}}{HA \cdot I_R \cdot \xi} - \phi_S - 1}{C \cdot \left(\frac{\beta}{\beta_{opt}}\right)^{-E}} \right)^{\left(\frac{1}{B}\right)} \quad (28)$$

where

WAF is wind reduction factor (from tables for different fuel models)

I_0 is Critical Fireline Intensity [kW/m]

HA is Heat per Area Unit [kJ/m^2]

I_R is Reaction Intensity [kW/ m^2]

and other parameters are standard parameters from Rothermel model, but for real Fuel Model (not for Fuel Model 10).

Overall Fire Spread Rate (R_{final}) whether surface or crown, is computed as

$$R_{final} = R + CFB\,(R_C - R) \quad (29)$$

where:

R is a surface fire rate of spread (ROS)

R_C is an active crown rate of spread (Equation (5))

CFB is Crown Factor Burned mentioned previously.

Copyright © FirEURisk Consortium. All rights reserved.

For *CFB* = 0 (a surface fire) eq. (14) reduces to $R_{final} = R$; for *CFB* = 1 (active crown fire), $R_{final} = R_C$. At intermediate values of *CFB*, R_{final} is scaled proportionally between *R* and R_C.

Canopy Heat per Unit Area (H_C) [kJ/m^2] is defined as:

$$H_C = CFB \cdot CFL \cdot h_{canopy} \quad (30)$$

CFB is Crown Factor Burned mentioned previously

CFL is available **Canopy Fuel Load** [kg/m^2]. It could be calculated from Canopy Bulk Density (CBD) [kg/m3] and Canopy Depth (CD) [m]:

$$CFL = CBD \cdot CD \quad (31)$$

Canopy Depth (CD) could be estimated from Canopy Height (CH) and Canopy Base height (CBD):

$$CD = CH - CBH \quad (32)$$

It is important to emphasise that Canopy Depth is sometimes defined differently, but this could be a satisfactory estimation.

Also in Fuel Models Parameters Tables for different fuel model categories (Scott & Burgan, 2005) there is a parameter named Live Fuel Load, separately defined for Live Herbaceous and Live Woody. Live Woody could be used for CFL estimation. It is 0 for all non-woody fuel models. For example for Albini-Anderson fuel model 10 - Timber (litter and understory) (Anderson, 1982) used by Rothermel to define active crown propagation Live Woody load is 4.4834 [t/ha] = 0.44834 [kg/m^2].

h_{canopy} is the heat yield of canopy fuels - for all fuels it is 18622 kJ/kg or 8000 Btu/lb.

Canopy Fireline Intensity (I_{BC}) [kW/m] is defined as:

$$I_{BC} = H_C \cdot R_C \quad (33)$$

where H_C is Canopy Heat per Unit Area [kJ/m^2] and R_C is Crown Fire Rate of Spread [m/s].

Overall Fireline Intensity (I_{final}) [kW/m] is computed from surface fireline intensity and canopy fireline intensity

$$I_{final} = (I_B + I_{BC}) \cdot R_{final} \quad (34)$$

where:

I_B is surface fireline intensity

I_{BC} is canopy fireline intensity

R_{final} is overall fire spread rate (equation (15))

To conclude for Scott and Reinhardt Crown Fire Propagation Model Figure 15 is crucial with following conclusions:

Copyright © FirEURisk Consortium. All rights reserved.

1. Wildfire is **Surface Fire** when its Rate of Spread *R* calculated using standard Rothermel equations is lower than Critical Rate of Spread for Critical Fireline Intensity (equation (5)).
2. Wildfire is **Active Crown Fire** when Surface Fire Rate of Spread *R* is equal or higher than Critical Rate of Spread for Critical Fireline Intensity , but also Active Fire Rate of Spread R_C calculated by equation (6) is equal or higher than Critical Crown Fire Rate of Spread R_0.
3. Wildfire is **Passive Crown Fire** when Surface Fire Rate of Spread *R* is equal or higher than Critical Rate of Spread for Critical Fireline Intensity , but also Active Fire Rate of Spread R_C is lower than Critical Crown Fire Rate of Spread R_0. Passive Crown Fire Rate of Spread is the same as Active (equation (6)), but values are lower.

Few years later in 2005 Cruz, Alexander and Wakamoto have proposed propagation model where passive crown fire rate of spread is lower than active crown fire rate of spread.

Cruz, Alexander and Wakamoto Crown Fire Propagation Model (2005)

More recently Cruz, Alexander and Wakamoto (Cruz et al., 2005) proposed models for predicting crown fire rate of spread in conifer forest stands. They have used CAC (Equation (11)) to detect Active Crown Fire:

Active Crown Fires: CAC $\geq$ 1.0

$$CROS_A = 11.02 \cdot (U_{10})^{0.9} \cdot CBD^{0.19} \cdot e^{-0.17 \times EFFM} \quad (35)$$

Passive Crown Fires: CAC < 1.0

$$CROS_P = CROS_A \cdot e^{-CAC} \quad (36)$$

where CROSA is the active crown fire rate of spread [m/s], and CROSP is the passive crown fire rate of spread [m/min], CAC is the criterion for active crowning [dimensionless], CBD is the canopy bulk density [kg/m3], U10is the 10-m open wind speed [km/h], EFFM is the estimated fine fuel moisture [%].

This model gives much higher values than Rothermel model. In 2006 Scott made a interesting comparison of all three models (Rothermel Average, Rothermel Maximal and Cruz et al.) (Scott, 2006) for different stands. Figure 16 shows his results for a ponderosa pine/Douglas-fir where stand as basal area (BA) is removed to simulate low thinning. For details see (Scott, 2006)

Copyright © FirEURisk Consortium. All rights reserved.

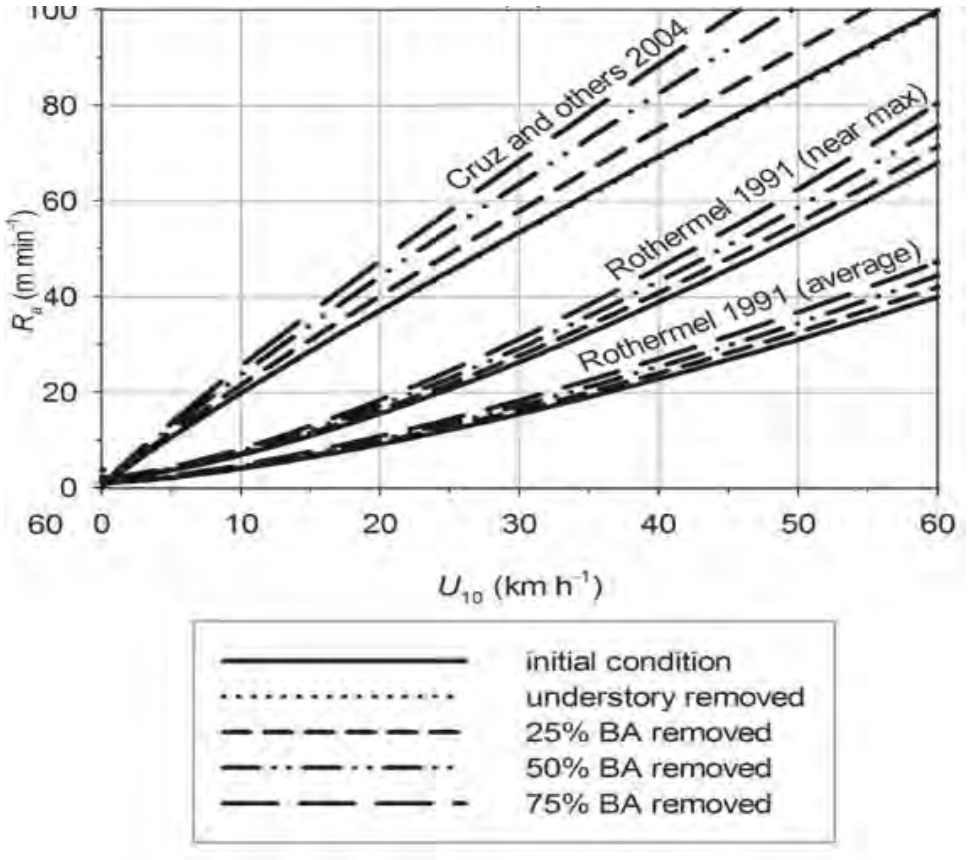


Figure 57: Potential active crown fire rate of spread (Ra) as predicted by three different models for a range of open wind speeds (U10) in a ponderosa pine/Douglas-fir stand as basal area (BA) is removed to simulate low thinning

Difference is obvious. This model is implemented in software package CFIS – Simulation of Crown Fire Initiation and Spread - https://www.frames.gov/partner-sites/applied-fire-behavior/cfis/ .

6.1.6 Results – crown propagation potential maps for EU territory

The procedure for crown fire initiation and propagation models is based mostly Scott and Reinhardt's method (Scott & Reinhard, 2021) also implemented in BehavePlus and FlamMap. In both of them Scott and Reinhardt's method (Scott & Reinhard, 2001) is used based on Rothermel crown fire rate of spread estimation (Rothermel, 1991).

Output Crown Fire Variables GeoTiffs for:

a) **Crown Factor Burned** (CFB) [fraction]- A fraction between 0 and 1 indicating the severity of a crown fire. It is a proportion of tree crowns involved in the fire in a given area. Less than 10 percent is considered as surface fire, between 10 and 89 percent is intermittent crown fire, while over 90 percent is a continuous crown fire.

b) **Crown Fire Activity** (CFA) - Assignment of fire types. Transition to Crown Fire [yes/no] based on Surface Fireline Intensity (IB) [kW/m] and Critical Surface Fireline Intensity (I0). Active Crown Fire Conditions [yes/no] based on Active Crown Fire Rate of Spread (RC) and Critical Crown Fire Rate of Spread (R0). Four conditions are distinguished: Surface Fire, Conditional Crown Fire, Passive Crown Fire (Torching) and Active Crown Fire.

Copyright © FirEURisk Consortium. All rights reserved.

c) **Active or Passive Crown Fire Rate of Spread** [m/s] – the linear rate of advance of a active or passive crown fire flaming front into unburned fuel in the direction perpendicular to the fire front.
d) **Active or Passive Crown Fire Heat per Unit Area** [kJ/m2] - heat release per unit area of the crown and surface fire flaming front.
e) **Active or Passive Crown Fire Fireline Intensity** [kW/m] [kJ/(m s)] - heat energy released per unit time from a one-meter-wide section of the crown fuel bed extending from the front to the rear of the flaming zone.
f) **Active or Crown Fire Passive Flame Length** (FL) [m] - measured in from midway in the active flaming crown combustion zone to the average tip of the flames. It is indicator of fireline intensity.

were calculated for extreme (5th percentile fuel moisture and 95th percentile wind speed) and average weather conditions (50th percentile of fuel moisture and wind speed) of past fires larger than 2000 ha. In both cases, regarding wind direction and aspect maximal values are considered when wind direction and aspect coincides (both are in the same direction).

Copyright © FirEUrisk Consortium. All rights reserved.

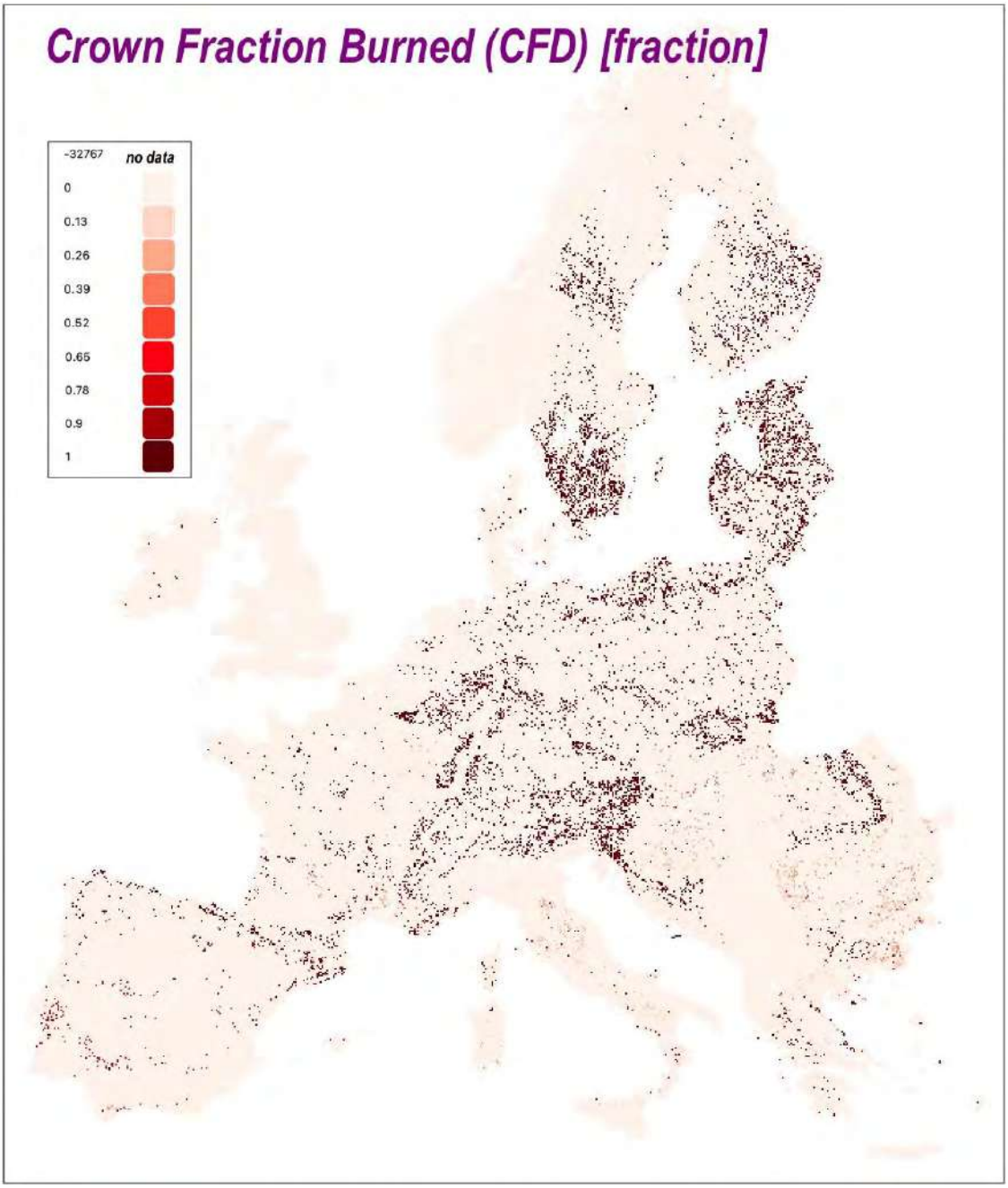


Figure 58: Map of Crown Fraction Burned (CFB) [fraction] for extreme 95th percentile wind speed and 5th percentile fuel moisture for 1993 Van Wagner formula (equation (25))

Statistical data concerning extreme Crown Fraction Burned (CFB) on EU territory are:

- STATISTICS_MAXIMUM=1
- STATISTICS_MEAN=0.052276838159082
- STATISTICS_MINIMUM=0
- STATISTICS_STDDEV=0.21684505185937

Copyright © FirEURisk Consortium. All rights reserved.

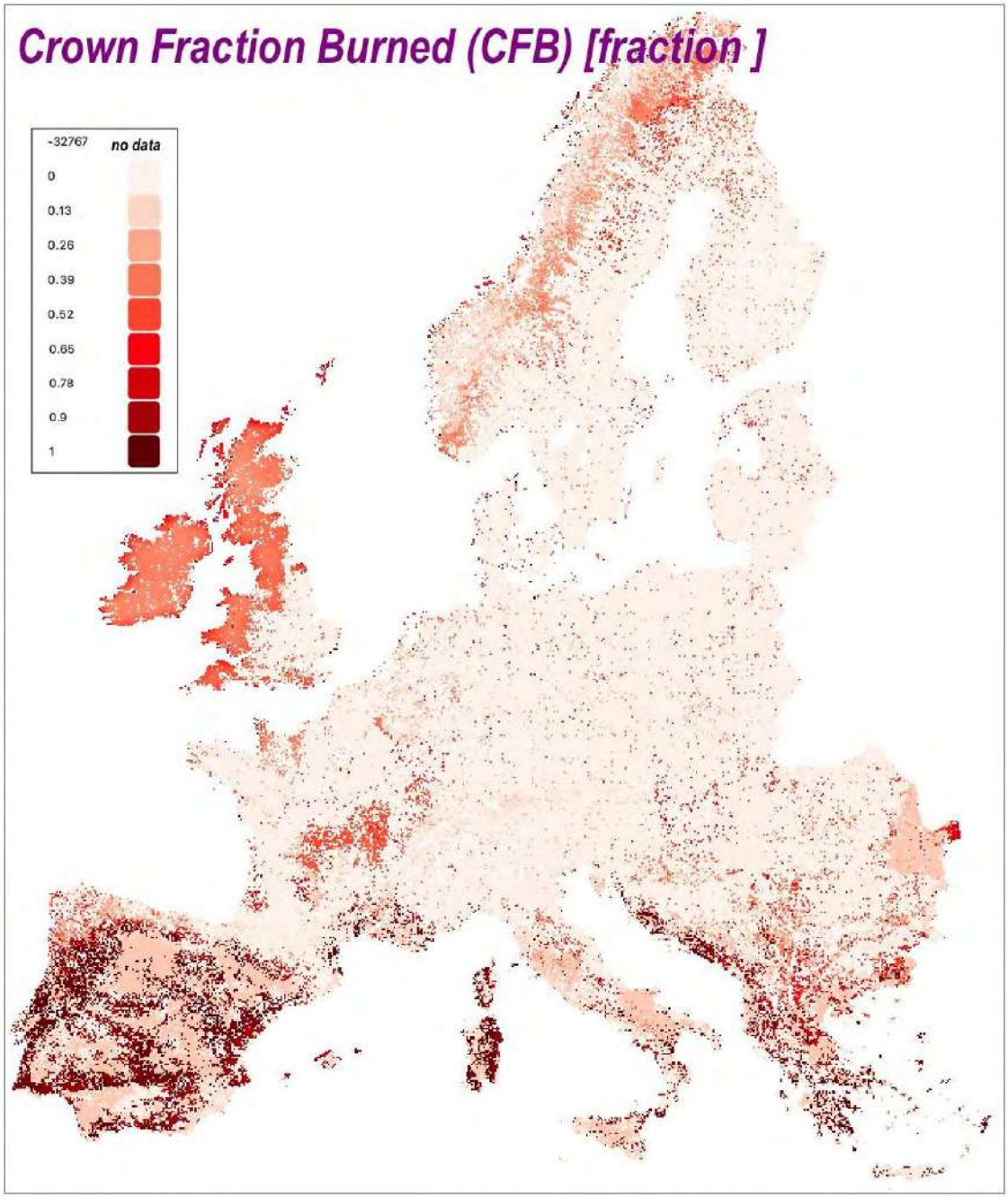


Figure 59: Map of Crown Fraction Burned (CFB) [fraction] for extreme 95th percentile wind speed and 5th percentile fuel moisture for 1989 Van Wagner formula (equation (24))

Statistical data concerning extreme Crown Fraction Burned (CFB) on EU territory are:

- STATISTICS_MAXIMUM=1
- STATISTICS_MEAN= 0.13530096924995
- STATISTICS_MINIMUM=0
- STATISTICS_STDDEV= 0.2510653970977

Copyright © FirEURisk Consortium. All rights reserved.

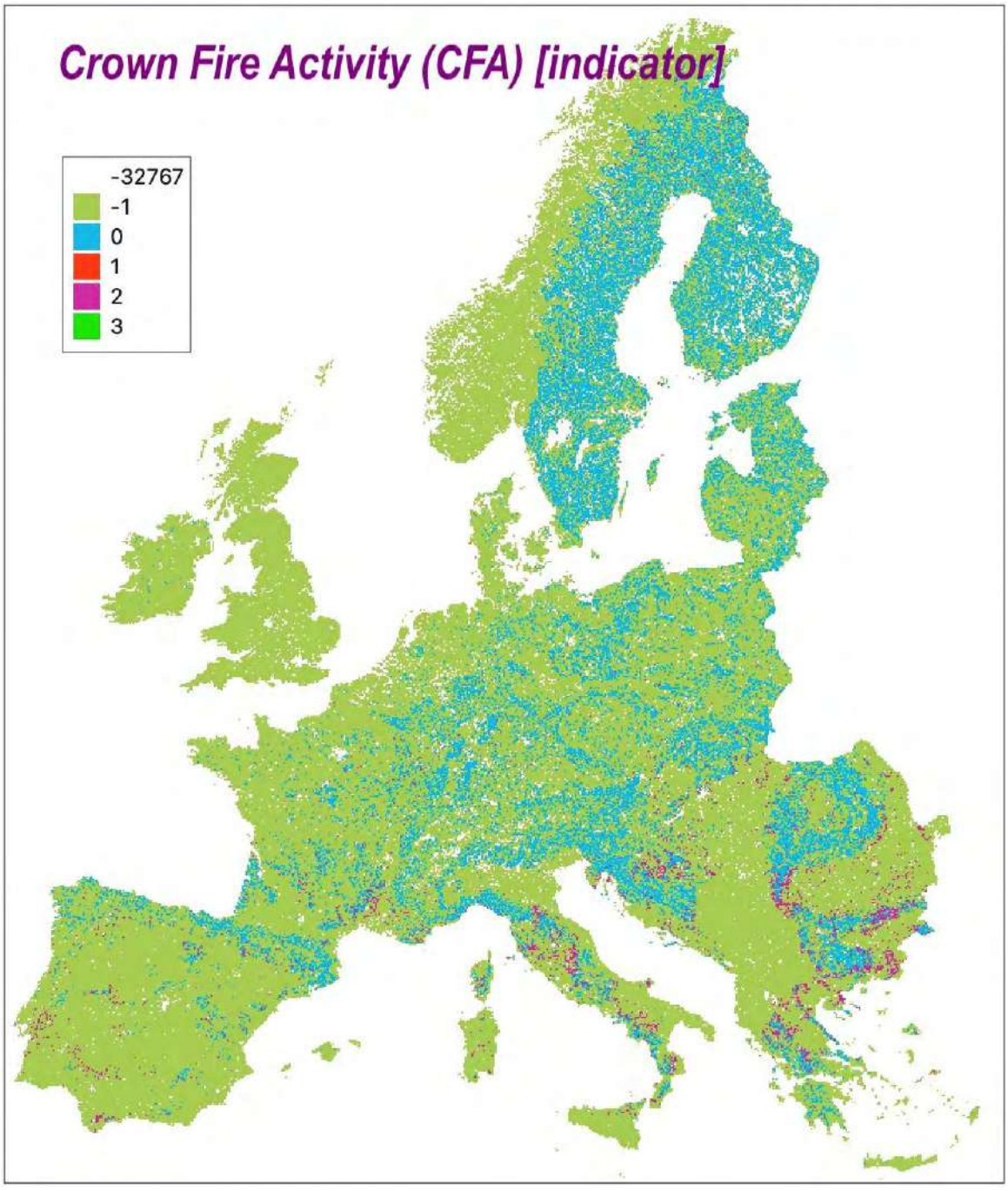


Figure 60: Map of Crown Fire Activity (CFA) [indicator] for extreme 95th percentile wind speed and 5th percentile fuel moisture

Copyright © FirEURisk Consortium. All rights reserved.

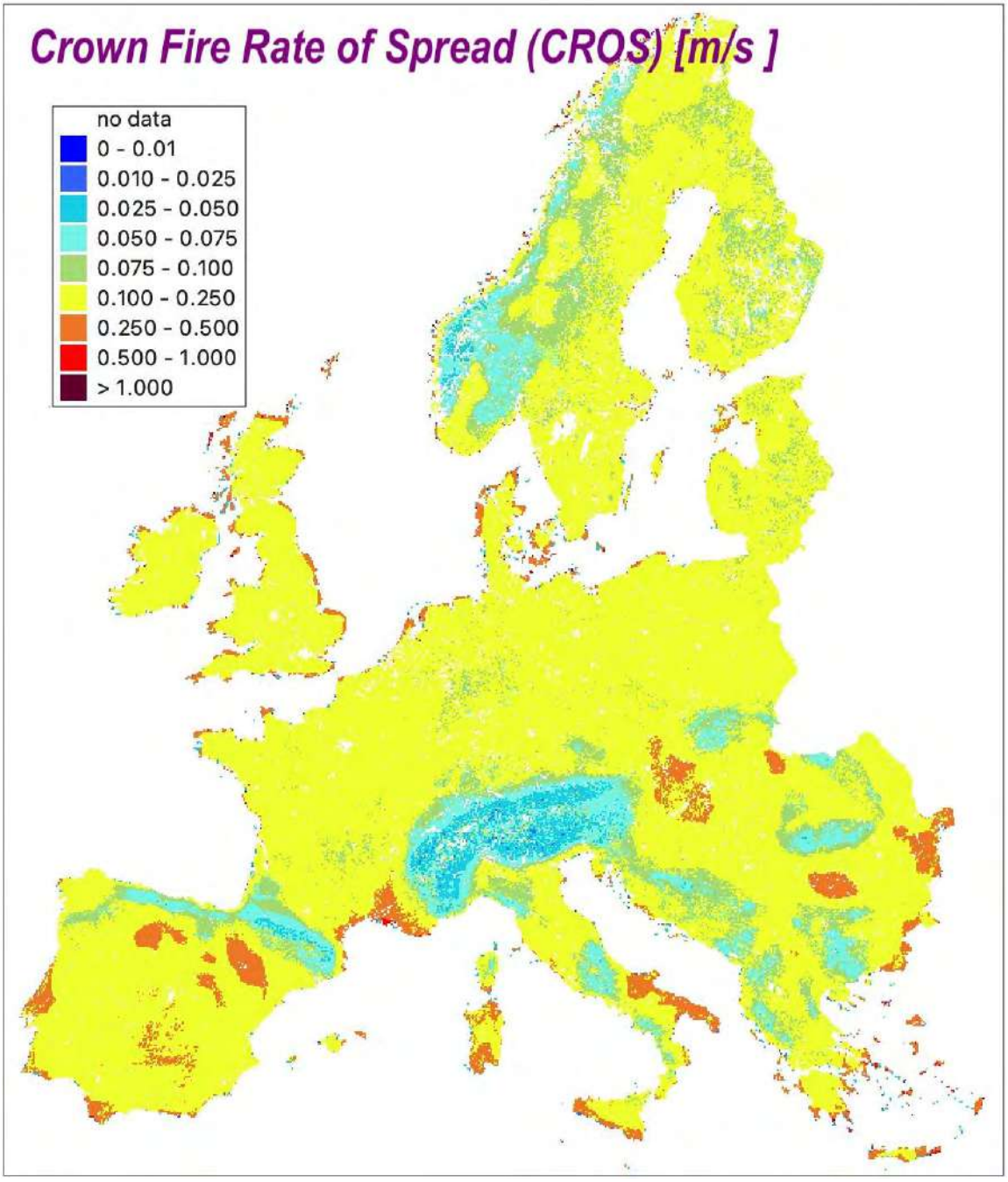


Figure 61: Map of Crown Fire Rate of Spread (CROS) [m/s] for extreme 95th percentile wind speed and 5th percentile fuel moisture

Statistical data concerning extreme Crown Fire Rate of Spread (CROS) on EU territory are:

- STATISTICS_MAXIMUM= 7.9699997901917
- STATISTICS_MEAN= 0.031430965733704
- STATISTICS_MINIMUM=0
- STATISTICS_STDDEV= 0.11160778078908

Copyright © FirEURisk Consortium. All rights reserved.

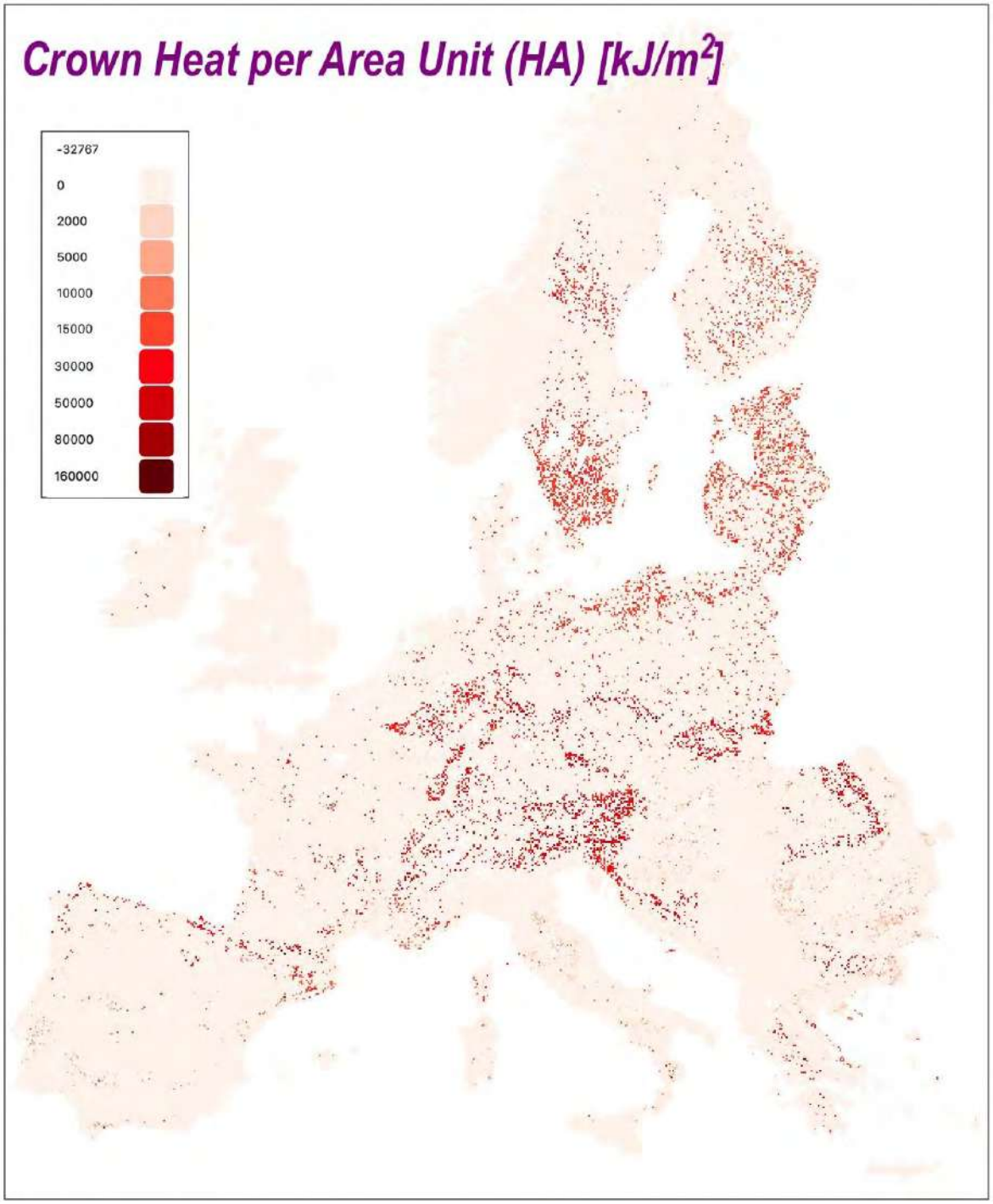


Figure 62: Map of Crown Fire Heat per Unit Area (CHA) [kJ/m²] for extreme 95th percentile wind speed and 5th percentile fuel moisture

Statistical data concerning extreme Crown Fire Heat per Unit Area (CHA) on EU territory are:

Copyright © FirEURisk Consortium. All rights reserved.

- STATISTICS_MAXIMUM=70403.7265625
- STATISTICS_MEAN=4255.4936128618
- STATISTICS_MINIMUM=159.25
- STATISTICS_STDDEV=7059.9196620333

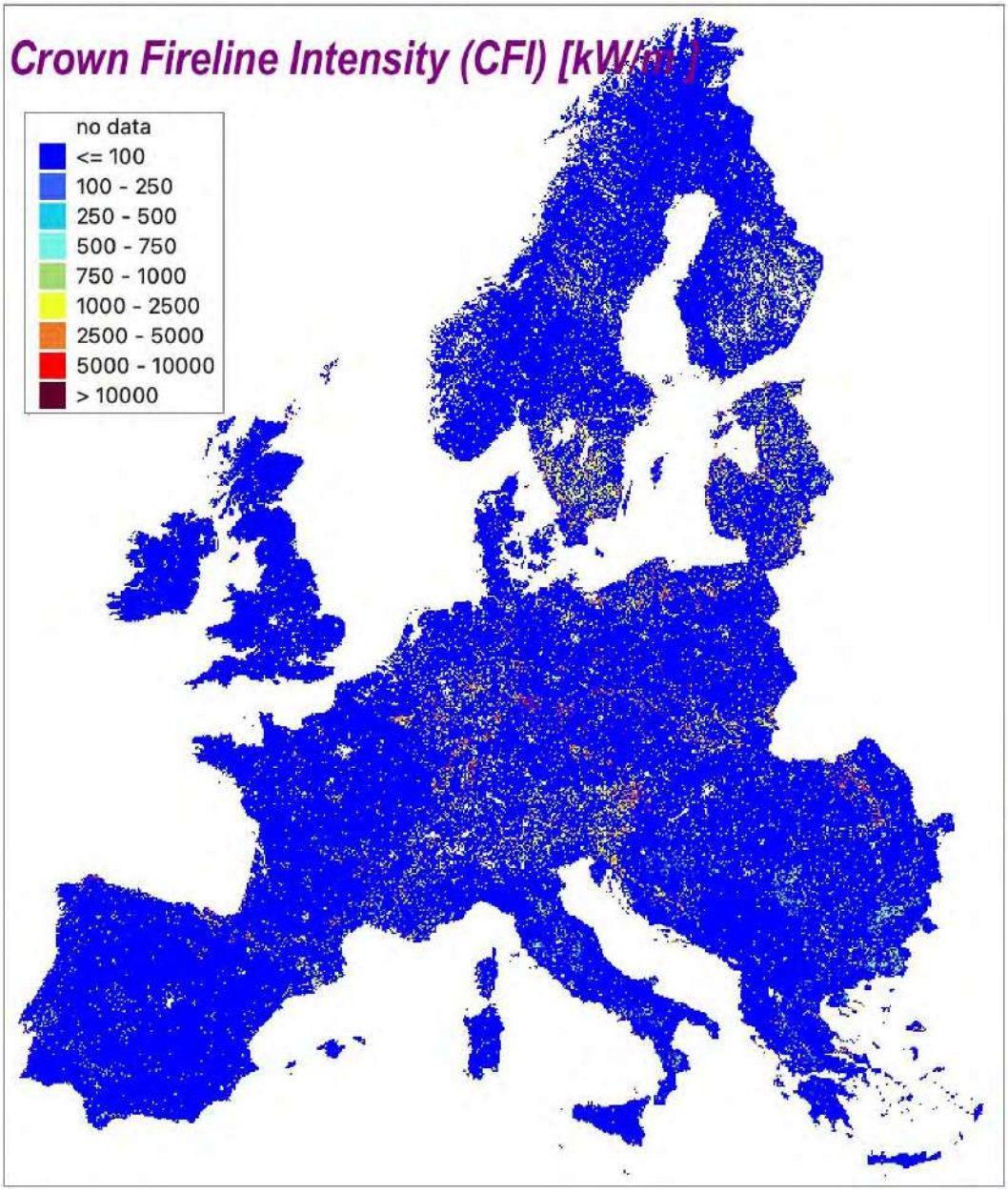


Figure 63: Map of Crown Fireline Intensity (CFI) [kW/m] for extreme 95th percentile wind speed and 5th percentile fuel moisture

Statistical data concerning extreme Crown Fireline Intensity (CFI) on EU territory are:

Copyright © FirEURisk Consortium. All rights reserved.

- STATISTICS_MAXIMUM=10049.8203125
- STATISTICS_MEAN=117.24114981407
- STATISTICS_MINIMUM=0
- STATISTICS_STDDEV=565.19524502083

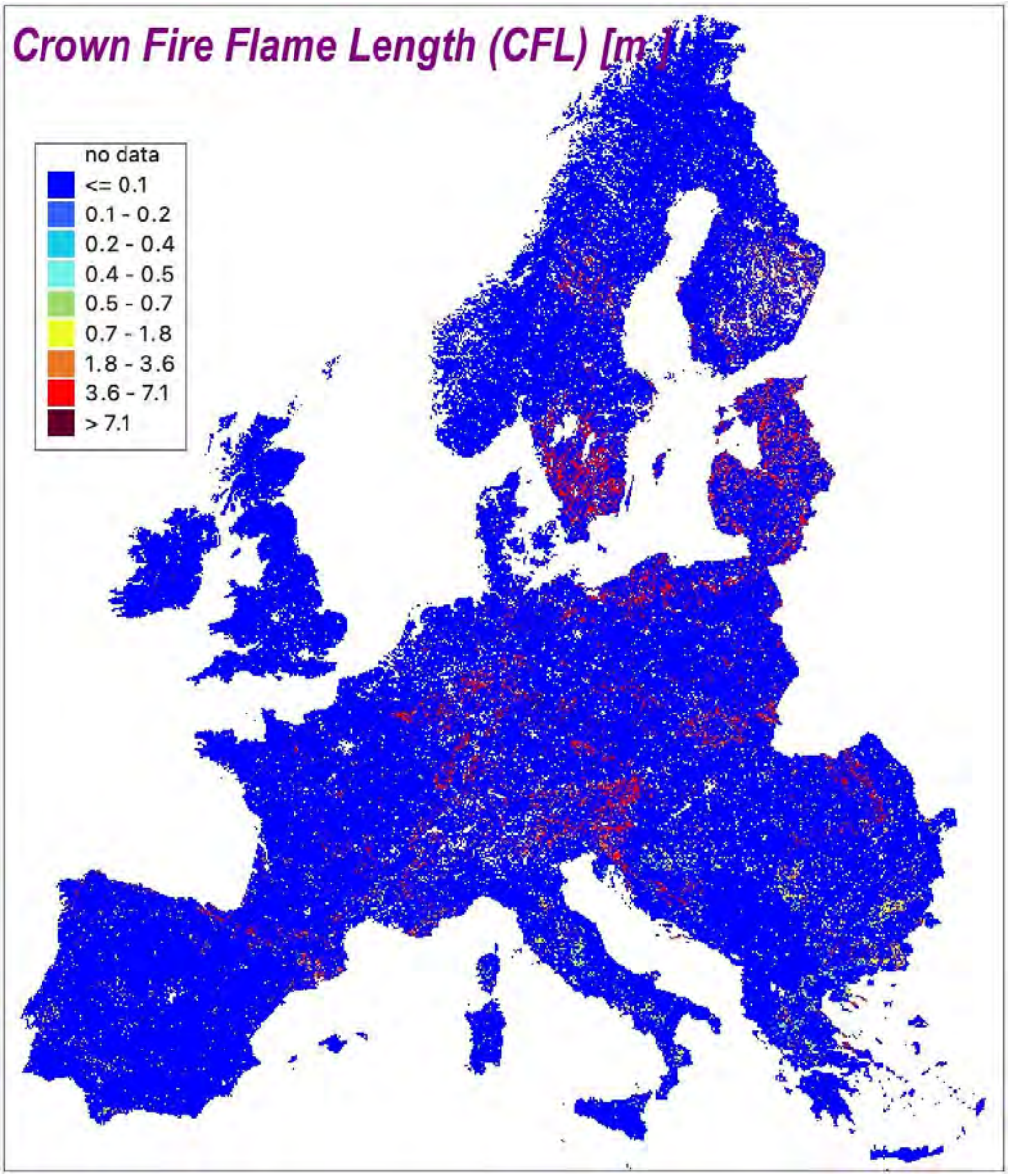


Figure 64: Map of Crown Flame Length (CFL) [m] for extreme 95th percentile wind speed and 5th percentile fuel moisture

Statistical data concerning extreme Crown Flame Length (CFL) on EU territory are:

- STATISTICS_MAXIMUM=12.449999809265
- STATISTICS_MEAN=0.2397377928761
- STATISTICS_MINIMUM=0
- STATISTICS_STDDEV=1.0423308541748

Copyright © FirEURisk Consortium. All rights reserved.

6.1.7 Product Description: Fire propagation (ET)

This product will include GeoTIFF raster maps of propagation potential indicators for European Territory, as well as report with detail description of methodology and obtained results. Propagation potential for EU territory will be calculated in 1 km2 resolution, based past fires on EU territory from Jan, 1st 2001 to Dec, 31st 2019, fires larger than 2000 ha were selected. Outputs will be typical propagation potential indicators: Rate of Spread – R [m/s], Reaction intensity – RI [kW/m2], Fireline Intensity – FI [kW/m] and Flame Length – FL [m]. Developer FESB SPLIT. The product developed within the Activity "A1.1.5 *Analysis of fire propagation, fuel consumption and smoke emission as risk factors*".

Propagation potential for EU territory will be calculated in 1 km2 resolution, based on custom implementation of Rothermels model (in Python) for cell-based wildland landscape fire growth simulations. From the list of past fires on EU territory from Jan, 1st 2001 to Dec, 31st 2019, fires larger than 2000 ha were selected. There were 403 of such fires. For their dates, maps of meteorological parameters were extracted from ERA5 and resampled to 1 km resolution. 10h Fuel Moisture Content and wind speed were calculated for each date, based on two weather scenarios: average weather conditions (50th percentile) and extreme weather conditions (5th percentile for fuel moisture and 95th percentile for wind speed). Propagation potential for the ET territory are calculated for each pixel using standard Rothermel equations for surface wildfire spread modelling. Input maps were wind speed, 10h dead fuel moisture, slope and fuel models. Outputs will be typical propagation potential indicators: Rate of Spread – R [m/s], Reaction intensity – RI [kW/m2], Fireline Intensity – FI [kW/m] and Flame Length – FL [m] and Heat per Area Unit (HA) [kJ/m2] for surface fire and Crown Factor Burned (CFB) [fraction], Crown Fire Activity (CFA), Active or Passive Crown Fire Rate of Spread [m/s], Active or Passive Crown Fire Heat per Unit Area [kJ/m2], Active or Passive Crown Fire Fireline Intensity [kW/m] [kJ/(m s)] and Active or Crown Fire Passive Flame Length (FL) [m] for crown fire..

- **Format:** Propagation potential indicators for European Territory (ET) is a geospatial product in .tiff format and a static layer.
- **Resolution:** 1 km
- **Extent:** 2636414.0000000000000000,1385417.0000000000000000 : 5955414.0000000000000000,5414417.0000000000000000
- **Width:** 3320
- **Height:** 4030
- **Projection:** EPSG:3035 - ETRS89-extended / LAEA Europe
- **Access:** https://fireurisk.satways.net/collection/6419e316e4b054e2ce4278d9
- **Description:** European territory (ET) propagation potential products: Rate of Spread (R) [m/s], Reaction Intensity (RI) [kJ/(m2 s)], Fireline Intensity (FI) [kW/m] [kJ/(m s)] and Flame Length (FL) [m] for surface fire and Crown Factor Burned (CFB) [fraction], Crown Fire Activity (CFA), Active or Passive Crown Fire Rate of Spread [m/s], Active or Passive Crown Fire Heat per Unit Area [kJ/m2], Active or Passive Crown Fire Fireline Intensity [kW/m] [kJ/(m s)] and Active or Crown Fire Passive Flame Length (FL) [m] for crown fire, as well as input data: Fuel Map, Slope Map, 10h Fuel Moisture Content (5th and 50th percentile) and and Wind Speed (95th and 50th percentile) for past European fires.

Copyright © FirEURisk Consortium. All rights reserved.

Contact: Darko Stipaničev (darko.stipanicev@fesb.hr).

6.2 Fire propagation modelling at PS scale

Well known software for wildfire behaviour simulation FlamMap has few tools that can be used for propagation potential:

a. Basic Fire Behaviour (BFB) or Landscape Fire Behaviour (Basic)
b. Minimum Travel Time Fire Spread (MTT) and
c. Landscape Burn Probability (LBP).

Each of these has different outputs that can be used for propagation potential estimation. We used **FlamMap Basic Fire Behaviour** to create 'static' propagation potential maps based on historical past fires in analysed area (Pilot Sites) for the last 20 years having as outputs:

- Rate of Spread (m/s)
- Heat per Unit Area (kJ/m^2)
- Flame Length (m)
- Fireline Intensity (kW/m)
- Crown Fraction Burned (%) and
- Crown Fire Activity

We also used **FlamMap Landscape Burn Probability** to create 'dynamic' propagation potential maps having as output

- Landscape Burn Probability

A detailed methodology for propagation potential calculation described **on Pilot Sites (PS) scale** (100 m^2 resolution) using FlamMap simulations is given next. Last version of FlamMap is 6.2.7 from November 2022. Help file could be found on: https://owfflammaphelp62.firenet.gov.

The following are the inputs that had to be prepared for FlamMap simulations (and how they can be prepared). In the next section (Section 4), a detailed analysis of availability of input data is described.
The most time-consuming part of propagation potential calculation using FlamMap (apart the calculation of burn probability), is to prepare input data in FlamMap format. For each PS, several datasets had to be collected.

Minimal inputs for FlamMap simulations are:

Copyright © FirEUrisk Consortium. All rights reserved.

File name	File ext.	File type	Required	Optional
Landscape	.LCP	Raster	Fuel Model, Slope, Aspect, Elevation, and Canopy Cover	Canopy Bulk Density, Canopy Base Height, and Stand Height
Weather	.WTR	Text	none	FlamMap requires a .WTR file to utilize the optional dead fuel moisture model. Same files as used in FARSITE.
Wind	.WND	Text	none	FlamMap requires a .WND file to utilize the optional dead fuel moisture model. Same files as used in FARSITE.
Initial Fuel Moisture	.FMS	Text	FlamMap needs beginning live and dead fuel moisture values.	none
Custom Fuel Models	.FMD	Text	none	For fuel models other than the 13 or 40 standard models

Table 1 – FlamMap input data files (required and optional).

Figure 52: Input data for FlamMap simulations - source: FlamMap 3 instruction manual - https://wfdss.usgs.gov/wfdss/pdfs/intro_flammap3_(desktop).pdf.

Additionally, in FlamMap 6:

- Instead of Lanscape raster file in .LCP format with separate Projection file .PRJ a multi-bend GeoTIFF file in .TIFF format could be used (and even created from FireMap) where the projection information is stored with the feature information in one file.
- If dead fuel moisture is conditioned, instead of Weather file (.WDR) and Wind file (.WND), Weather Stream file (.WXS) is used. It could be created from .WDR and .WND file by special tool.

Landscape file (.LCP) or multi-bend GeoTIFF file (.TIFF) and Custom Fuel Models (.FMD) are static files defined once for all simulations. Other files are dynamic files that has to be changed for every FlamMap simulation. The most important of them are Initial Fuel Moisture file (.FMS) and essential wind dana (wind speed and direction) inserted directly or through Wind file (.WDR). Simulations could not be started without them.
Weather file (.WTR) together with data about Cloud Cover from Wind file (.WDR) and needed only **if Dead Fuel Moisture has to be conditioned taking into account topography, shading, weather and conditioning period length**. In FlamMap 6 instead of these two files Weather Stream file (.WXS) could to be used.

6.2.1 Procedure for propagation potential calculation using FlamMap

There are few steps in propagation potential calculation for each Pilot Site:

1. Collecting essential weather data and fuel moisture data of past fires on PS territory in the last 20 years.
2. Preparation of input data in FlamMap form including estimate of other necessary fuel moisture input data that is calculated from initial data set.
3. Divide input weather and moisture data according to wind directions.
4. Filter the data and take only wind direction scenarios that are responsible for *>10%* historical fires.
5. Calculate annually burned area on average per wind direction scenarios.
6. Calculate 95-percentile and 50-percentile values for: live woody fuel moisture content, wind speed (gust) and 1h dead fuel moisture for selected wind direction scenarios.
7. Run FlamMap simulations for each combination of wind direction, wind speed and fuel moisture content.

Copyright © FirEUrisk Consortium. All rights reserved.

8. The last step is to combine all the results. For the **basic FlamMap run**, burned area is used as a factor to combine the overall result. The procedure is to calculate the percentage of burned area (from overall burned area) that is happening for a certain combination of input data. It is important to know whether to assign the burned area to extreme or average scenario (the 50-percentile and the 95-percentile) for that wind direction scenario.
9. For the **dynamic FlamMap run**, all perimeters are put together. For dynamic mode, it is important to decide about duration of fires (we need to test different durations – 4h, 6h, 8h, 10h …), and results need to correlate to real historic data. To keep it simple, we will just take a look at larger fires. Additional step of calibration is necessary to decide this.

Detail procedure for input data preparation is as described in the next section.

6.2.2 Procedure for propagation potential calculation using FlamMap

In this section we describe what was our intention and an example of what our final results for each step were in the end.

We required historical data for past fires (last 20 years) in this format (for some PS these were obtained as Excel file, and for others as ESRI shapefile):

Fire No.	Date	Coordinates of the ignition[1]	Source[2]	Burned area (m^2)	Wind direction (deg)	Wind speed (average) at noon that day (m/s)	Wind speed (gust) at noon that day (m/s)	Live woody fuel moisture (%)	Dead 1h fuel moisture[3] (%)
1	2001-01-01 12:00:00	43.564321 N 17.34567 E	RE	10000	300	5	15	80	3
2	…			…	…	…	…	…	…

[1] Not necessary to be very precise – approximation is ok.

[2] Sources could be: remote sensing (RS), fire-fighters data (FD) and field research (FR).

[3] If it is not possible to calculate Dead 1h fuel moisture then following weather data has to collected for each past fire: at least temperature (^{0}C), relative humidity (%), but if Dead 1h fuel moisture will be calculated from Fire Behavior Analysis Tables (FBA Tables) using corrections then also elevation (m), slope (%), aspect (deg) and fuel shading (%) is necessary.

This was obtained for 4 Pilot Sites, in various format, ranging from ESRI shapefiles, Excel tables and simple tables:

- PS2: Central-Eastern Europe
- PS3: Mediterranean - Portugal
- PS4: Mediterranean – Spain
- PS5: Mediterranean – Greece

The data was not available for PS:

- PS1: North Europe - Sweden

Copyright © FirEURisk Consortium. All rights reserved.

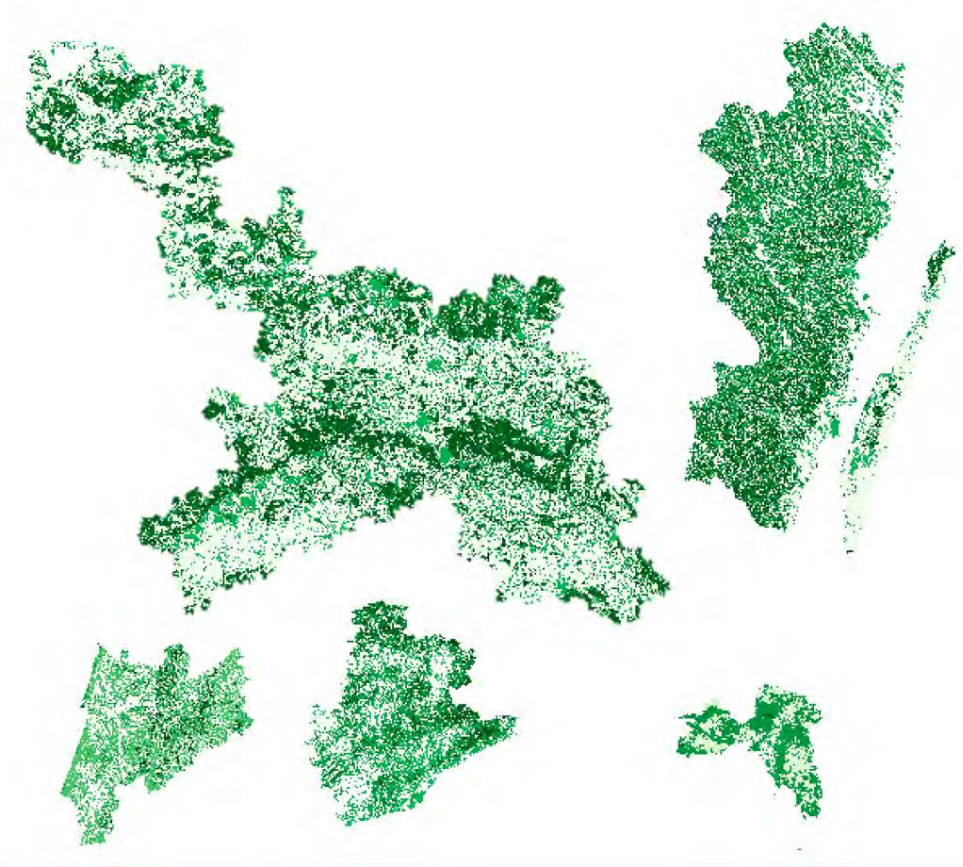


Figure 3: Comparison of all PSs in FirEURisk project

Copyright © FirEURisk Consortium. All rights reserved.

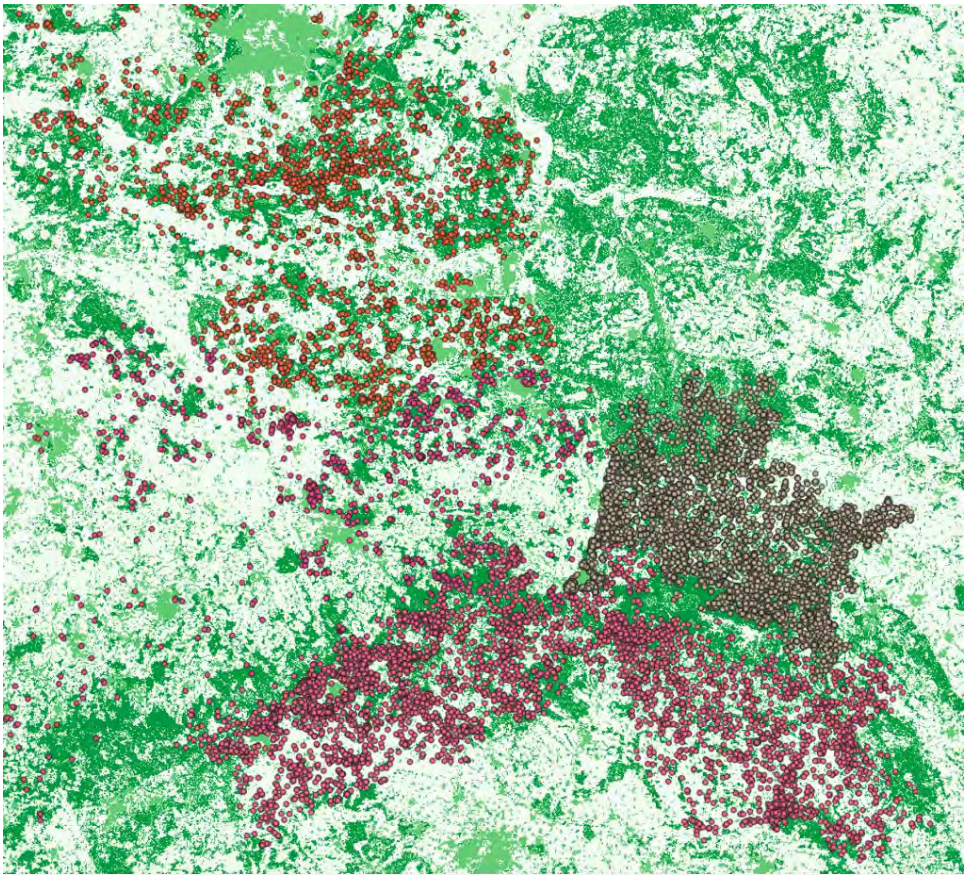


Figure 4: An example of historical fire records stored in ESRI shapefile for PS2: Central-Eastern Europe

6.2.3 Preparation of input data for FlamMap simulations

Our next step was to estimate *Live herbaceous fuel moisture*, *Dead 10h fuel moisture* and *Dead 100h fuel moisture* from *Live woody fuel moisture* and *Dead 1h fuel moisture* because they are also inputs for FlamMap simulations.

Fire No.	Date	Coordinates of the ignition	Burned area (m^2)	Wind direction (deg)	Wind speed (m/s)	Wind speed (gust) (m/s)	Live woody fuel moisture (%)	Live herbaceous fuel moisture (%)	Dead 1h fuel moisture (%)	Dead 10h fuel moisture (%)	Dead 100h fuel moisture (%)
1	2001-01-01 12:00:00	43.564321 N 17.34567 E	10000	300	5	15	80	80	3	4	5
2	…		…	…	…	…	…	…	…	…	…

After that input data are divided according to 8 wind direction categories (deg):

1. North (337.5-22.5)

Copyright © FirEURisk Consortium. All rights reserved.

2. Northeast (22.5-67.5)
3. East (67.5-112.5)
4. Southeast (112.5-157.5)
5. South (157.5-202.5)
6. Southwest (202.5-247.5)
7. West (247.5-292.5)
8. Northwest (292.5-337.5)

Based on these 8 wind direction categories, all fire records had to be categorised.

scenario	percentile	wind speed (gust)	live woo	1h dea	10h dea	100h d	burned area (sum)	burned a	number	average fire size	fire size stdev
north	95 percentile	15.447567605972285	62.024	6	7	8	11056.830300000001	3.31	96	115.18	375.67
north	50 percentile	9.262443542480469	78.92	11	12	13	5104.239199999996	1.53	208	24.54	145.31
northeast	95 percentile	12.836349487304686	63.43400	6	7	8	28235.443000000003	8.46	39	723.99	3660.46
northeast	50 percentile	7.689583778381348	77.71000	8	9	10	39146.80439999997	11.73	208	188.21	755.02
east	95 percentile	13.234856271743775	62.674	6	7	8	15559.240100000005	4.66	86	180.92	548.3
east	50 percentile	7.608935356140137	87.01	8	9	10	9457.228599999999	2.83	266	35.55	141.43
southeast	95 percentile	14.260925674438479	63.544	6	7	8	18105.499999999996	5.42	47	385.22	1745.4
southeast	50 percentile	8.144530296325684	88.74	8	9	10	99059.59017099308	29.68	126	786.19	5830.9
south	95 percentile	17.29566125869753	61.162	6	7	8	4603.310000000001	1.38	32	143.85	421.83
south	50 percentile	7.708327293395996	78.16	8	9	10	24588.02999999999	7.37	111	221.51	1809.32
southwest	95 percentile	14.214701080322257	62.10599	6	7	8	1730.8200000000004	0.52	32	54.09	118.9
southwest	50 percentile	7.132607460021973	77.24	9	10	11	3346.372	1.0	73	45.84	212.43
west	95 percentile	8.7667649269104	61.78200	6	7	8	3644.003999999999	1.09	50	72.88	163.82
west	50 percentile	6.739497184753418	75.72999	9	10	11	7986.529999999999	2.39	154	51.86	361.54
northwest	95 percentile	12.296253395080566	62.846	7	8	9	54915.53600000001	16.45	124	442.87	3134.38
northwest	50 percentile	8.702553749084473	79.52	12	13	14	7272.522400000004	2.18	353	20.6	103.71

Figure 5: Stage 1 summary table for PS3 Mediterranean – Portugal

scenario	percentile	wind speed (gust)	live woo	1h dead fuel moisture	1h dfmc (72.5p)	burned are	burned ar	numb	average f	fire size stdev
north	95 percentile	18.47157287597656	51.58	6.16804738536729	6.668374890955569	3428.89999	5.5	61	56.21	181.83
north	50 percentile	13.797237396240234	71.8	7.185881688005548	6.668374890955569	36354.95	58.36	280	129.84	1195.12
northeast	95 percentile	16.22541046142578	53.405	6.0322490921625675	6.267838192200549	9339.45	14.99	55	169.81	1129.17
northeast	50 percentile	9.876169204711914	73.66	6.687534603808452	6.267838192200549	306.1	0.49	76	4.03	5.48
east	95 percentile	9.017182111740112	49.949	6.420146306157526	7.514772544758362	21.8	0.03	6	3.63	2.91
east	50 percentile	6.522336006164551	79.555	9.503457005673734	7.514772544758362	111.25	0.18	16	6.95	12.74
southeast	95 percentile	10.094186019897458	66.32000	6.037946473982612	6.797061755698586	153.1	0.25	6	25.52	56.11
southeast	50 percentile	7.810154914855957	86.61	9.26323841310161	6.797061755698586	908.800000	1.46	19	47.83	182.48
south	95 percentile	14.457603645324706	58.368	6.1862651343106805	6.846088920041264	518.5	0.83	6	86.42	202.62
south	50 percentile	8.582232475280762	81.04	7.4800806259593635	6.846088920041264	319.45	0.51	39	8.19	31.69
southwest	95 percentile	13.115006065368648	65.524	6.215600490546066	6.60589266697622	75.0	0.12	10	7.5	15.31
southwest	50 percentile	8.724564552307129	78.67	7.614055320371794	6.60589266697622	1238.5	1.99	39	31.76	96.64
west	95 percentile	15.759596776962276	57.1295	5.992763030461462	6.242505761129193	1672.1	2.68	24	69.67	254.02
west	50 percentile	9.991112232208252	78.38	6.905480047466471	6.242505761129193	5559.5	8.92	40	138.99	799.12
northwest	95 percentile	12.27118992805481	66.3125	5.978327410773624	6.925366273615219	2145.2	3.44	9	238.36	679.73
northwest	50 percentile	7.8366827964782715	87.45	8.21701691168557	6.925366273615219	140.2	0.23	27	5.19	10.6

Figure 6: Stage 1 summary table for PS5 Mediterranean – Greece

Copyright © FirEURisk Consortium. All rights reserved.

scenario	percentile	wind speed (gust)	1h dead fuel moisture	1h dfmc (72.5p)	burned area (sum)	burned a	number of fires	average fire size	fire size stdev
north	95 percentile	11.12280392646789	7.4308510568726405	13.618563500109339	211.11999999999998	1.44	59	3.58	4.41
north	50 percentile	6.224161148071289	17.39268589479297	13.618563500109339	281.8	1.93	159	1.77	1.55
northeast	95 percentile	11.586869239807127	6.985442484271598	11.626357505338246	588.489	4.03	60	9.81	34.78
northeast	50 percentile	6.747329711914063	15.87661454171587	11.626357505338246	482.95499999999999	3.31	161	3.0	7.95
east	95 percentile	13.00866699218750	7.126091371611988	11.781585026065862	971.4200000000001	6.65	140	6.94	22.88
east	50 percentile	8.581618309020996	15.101324192703864	11.781585026065862	1024.9100000000003	7.01	401	2.56	4.65
southeast	95 percentile	13.148336505889892	6.486067482933433	10.26912280973192	454.7	3.11	121	3.76	6.84
southeast	50 percentile	8.193625450134277	14.05491254059475	10.26912280973192	667.0613999999999	4.57	294	2.27	2.25
south	95 percentile	13.469901561737060	7.389128028826764	12.592961236267858	2263.9130999999998	15.49	198	11.43	63.51
south	50 percentile	8.360235691070557	15.703340744910511	12.592961236267858	1569.8799999999999	10.74	558	2.81	10.84
southwest	95 percentile	13.695022010803225	7.978876244001514	11.98503687889402	1195.83	8.18	158	7.57	34.47
southwest	50 percentile	8.569026947021484	16.029643500424772	11.98503687889402	1031.0049999999999	7.06	451	2.29	2.19
west	95 percentile	16.648635864257812	8.201917719412414	13.070544630538151	1483.3154999999997	10.15	170	8.73	30.21
west	50 percentile	9.592805862426758	17.52028045039452	13.070544630538151	928.268	6.35	403	2.3	4.05
northwest	95 percentile	14.833181858062744	8.258991063094895	14.217311946533181	687.63	4.71	115	5.98	12.63
northwest	50 percentile	8.946209907531738	17.837377703424856	14.217311946533181	769.97	5.27	292	2.64	6.39

Figure 7: Stage 1 summary table for PS2 Central-Eastern Europe

The next step was to filter the data and take only wind direction scenarios that are responsible for *>10%* historical fires. Annually burned area on average per all wind direction scenarios was calculated in order to analyse burn probability):

Wind direction scenario	no# fires	Percentage	Total burned area (m²)
North (337.5-22.5)	100	60%	1000000000
…	…		…

For each wind direction scenario, we calculated 95-percentile and 50-percentile values:

- live woody fuel moisture content
- wind speed (gust) and
- 1h dead fuel moisture.

	Wind direction scenario	Wind speed (gust) (m/s)	Live woody fuel moisture (%)	Dead 1h fuel moisture (%)
95-percentile:	North (337.5-22.5)	15	100	3
50-percentile:		7	110	4
95-percentile:	Northeast (22.5-67.5)	10	105	2
50-percentile:		4	106	3
	…	…	…	…

6.2.4. FlamMap simulations and preparation of final outputs

Finally, one FlamMap simulation had to be started for each combination of wind speed, wind direction and fuel moisture content, in other words – one FlamMap run per row of last table.
The final step is to combine all the results in one final propagation potential map.

Copyright © FirEURisk Consortium. All rights reserved.

For the **basic FlamMap run**, burned area was used as a factor to combine the overall result. The procedure is to calculate the percentage of burned area (from overall burned area) that is happening for a certain combination of input data. It is important to know whether to assign the burned area to extreme or average scenario (the 50-percentile and the 95-percentile) for that wind direction scenario. To do so it is necessary to:

- take all the ignitions (we have 1h dead fuel moisture and other parameters for every ignition)
- rank ignitions from the lowest 1h dead fuel moisture to the highest
- identify 72.5 percentile value of 1h dead fuel moisture
- everything equal or below the breakpoint goes to the 50-percentile scenario
- everything above the breakpoint goes to the 95-percentile scenario

The result was a table like this:

	Wind direction scenario	Wind speed (gust)	Live woody fm	Dead 1h fm	Burned area (% and km^2)	No ignitions (historic) (% and no.)	Average (plus stand. Dev)
95-percentile:	North (337.5-22.5)	15	100	3	**30% (3000km^2)**	**10% (100)**	**x**
50-percentile:		7	110	4	**10% (1000km^2)**	**30% (300)**	**y**
95-percentile:	Northeast (22.5-67.5)	15	100	3	**15% (1500km^2)**		
50-percentile:		7	110	4	**5% (500km^2)**		
	…	…	…	…	**…**		

Along with burned area (% + km^2), it was necessary to calculate the number of historic ignitions happening for that scenario. Base on this analysis we knew if big fires were responsible for large-burned area. Also, we calculated the average fire size (and possibly standard deviation) for that scenario – this was used for dynamic FlamMap mode and is even more important for larger fires.

- 95-percentile will probably mean bigger fires, smaller in number, but that burn larger areas.
- 50-percentile will mean many smaller fires.

In the sample case above, 30% of the burned area is happening for the first combination, 10% for the second, etc. However, there were more fires for the second combination.

Once the overall number of ignitions was defined, we ran simulations. After that, we were able to define the number of simulations happening under one combination. Chosen number of ignitions should respect the number of real historical ignitions. (this step needed calibration for each row of the table).

Copyright © FirEURisk Consortium. All rights reserved.

	Wind direction scenario	Wind speed (gust)	Live woody fm	Dead 1h fm	Burned area (%)	#no. ignition points
95-percentile:	North (337.5-22.5)	15	100	3	30%	**30 fires – 10h**
50-percentile:		7	110	4	10%	**30 fires – 1h**
95-percentile:	Northeast (22.5-67.5)	15	100	3	15%	**150**
50-percentile:		7	110	4	5%	**50**
	…	…	…	…	…	**…**

In this above sample case, 30 ignitions will burn under first combination conditions, 150 under the second, etc. All these ignition points are separate points, each generated using ignition probability grid.

For the **dynamic FlamMap run**, all perimeters were put together. For dynamic mode, it is important to decide about duration of fires (we need to test different durations – 4h, 6h, 8h, 10h …), and results need to correlate to real historic data. To keep it simple, we will just take a look at larger fires.

scenario	percentile	wind speed (gust)	live wo	1h d	10h d	100h	burned area (sum)	burned a	numbe	average f	fire size std
northeast	95 percentile	12.836349487304686	63.4340	6	7	8	28235.443000000003	11.44	39	723.99	3660.46
northeast	50 percentile	7.689583778381348	77.7100	8	9	10	39146.80439999997	15.87	208	188.21	755.02
southeast	95 percentile	14.260925674438479	63.544	6	7	8	18105.499999999996	7.34	47	385.22	1745.4
southeast	50 percentile	8.144530296325684	88.74	8	9	10	99059.59017099308	40.15	126	786.19	5830.9
northwest	95 percentile	12.296253395080566	62.846	7	8	9	54915.53600000001	22.26	124	442.87	3134.38
northwest	50 percentile	8.702553749084473	79.52	12	13	14	7272.522400000004	2.95	353	20.6	103.71

Figure 8: Stage 2 summary table for PS3 Mediterranean – Portugal

scenario	percentile	wind speed (gust)	live woo	1h dead fuel moisture	1h dfmc (72.5p)	burned ar	burned	numbe	average fire size	fire size stdev
north	95 percentile	18.47157287597656	51.58	6.16804738536729	6.668374890955569	3428.8999	6.05	61	56.21	181.83
north	50 percentile	13.797237396240234	71.8	7.185881688005548	6.668374890955569	36354.95	64.16	280	129.84	1195.12
northeast	95 percentile	16.22541046142578	53.405	6.0322490921625675	6.267838192200549	9339.45	16.48	55	169.81	1129.17
northeast	50 percentile	9.876169204711914	73.66	6.687534603808452	6.267838192200549	306.1	0.54	76	4.03	5.48
west	95 percentile	15.759596776962276	57.1295	5.992763030461462	6.242505761129193	1672.1	2.95	24	69.67	254.02
west	50 percentile	9.991112232208252	78.38	6.905480047466471	6.242505761129193	5559.5	9.81	40	138.99	799.12

Figure 9: Stage 2 summary table for PS5 Mediterranean – Greece

For 'dynamic' runs (burn probability), the main idea was to saturate the PS area with enough fires. The initial idea was to simulate what would represent 1000 years of fire activity for each PS. In our case, that would mean:

Portugal - 358800 points / 98694500 ha / saturated 145 times

Central Europe - 991600 points / 4187652 ha / saturated 1.27 times

Greece - 214400 points / 22664608 ha / saturated 78 times

Copyright © FirEURisk Consortium. All rights reserved.

Another possible approach was to find the number of points where we burn N times the size of PS, for example, 25 times.
For that we would need:
Portugal - 61000 points
Central Europe - 19500000 points
Greece - 68000 points

Also, for a relatively high-end laptop, simulating 1000 years would mean:
Portugal - 609 hours to run simulations
Central Europe - 1685 hours to run simulations - approx 2.5 months to run the simulation
Greece - 364 hours to run simulations

Simulating 25 times burned PS years would mean for us:
Portugal - 103 hours to run simulations
Central Europe - 33150 hours to run simulations - approx 4 years to run simulations
Greece - 115 hours to run simulations

In the end, to make the research feasible, we decided to choose a constant (large) number of ignitions, multiply it by number of rows in summary 2 table and then multiply if by percentage that scenario takes in overall burned area value.

6.2.4 Availability of input data for propagation potential calculation for Pilot Site using FlamMap

Minimal inputs for FlamMap simulations are:

- GeoTIFF file (.TIFF) or Landscape file (.LCP)
- Initial Fuel Moisture file (.FMS)
- Essential wind data (wind speed and direction) directly inserted through Input form.

Optional files were:

- Weather Stream File (.WXS) file where all meteorological data are defined. It is needed **only if Dead Fuel Moisture has to be conditioned taking into account topography, shading, weather and conditioning period length**. Weather Stream File could be created from Weather File (.WTR) and Wind file (.WDR) using special FlamMap tool.
- Custom Fuel Models (.FMD) if new FirEURisk fuel models parameters will be available.

In FlamMap five **raster data themes** are required in GeoTIFF (.TIFF) file. This file could be created from raster Landscape file (.LCP) used in FARSITE and FlamMap 3. Landscape raster file in .LCP format needs separate Projection file .PRJ and in multi-bend GeoTIFF file in .TIFF format ,the projection information is stored with the feature information in one file.

At minimum, five **raster data themes** are required:

Copyright © FirEURisk Consortium. All rights reserved.

- Elevation
- Slope
- Aspect
- Fuel model [FM] and
- Canopy Cover [CC].

Other GIS layers are described as "optional":

- Canopy Height [CH]
- Canopy Base Height [CBH]
- Canopy bulk density [CBD]

“Optional” means only that they are not required to run a surface fire simulation. However, these themes are required to calculate some aspects of fire behaviour (such as crown fire) that could be very important to your analysis.

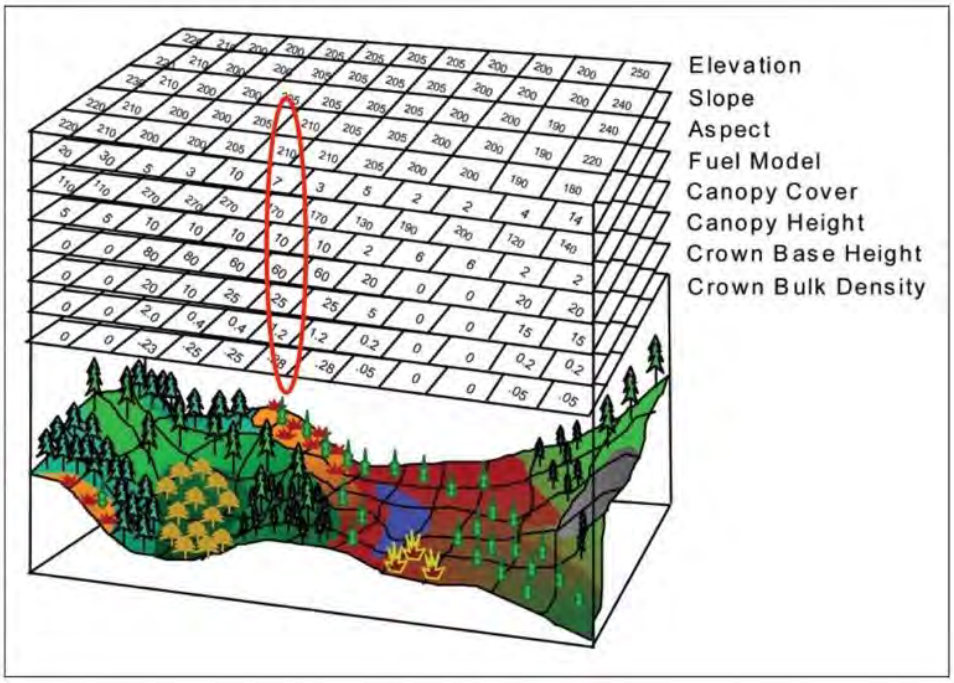


Figure 10: Input raster data themes required to run FlamMap

Each cell of the raster file comprises all the themes “sandwiched” together.
For PS Barcelona everything was available at PREVINCAT - http://previncat.ctfc.cat/en/index.html but for other PS still a lot of layers were missing.

Below is a detailed procedure where and how certain layers were collected and calculated.
Elevation data are available for all EU territory in the form of EU DEM v1.1 - https://www.eea.europa.eu/data-and-maps/data/copernicus-land-monitoring-service-eu-dem
From elevation, map aspect map and slope map had to be calculated.

Copyright © FirEURisk Consortium. All rights reserved.

Slope in degrees is equal to the tangent of amount of elevation change (rise) divided by the amount of horizontal distance covered (run).

Aspect is the orientation of slope, measured clockwise in degrees from 0 to 360, where 0 is north-facing.
Tutorial for calculation of aspect and slope in Python –
https://www.earthdatascience.org/tutorials/get-slope-aspect-from-digital-elevation-model/

New FirEUrisk fuel model (WP1.1.4.) based on new fuel classification system has 7 main (1st level) fuel classes (Forest, Shrubland, Grassland, Cropland, Peatlands, Urban and Nonfuel) all together 74 categories taking into account additional 5 levels for Forests and 1 additional level for others excluding Nonfuel.

FirEUrisk WP A1.1.4. has produced FirEUrisk EU Fuel data map at 1 km^2 resolution (Aragoneses et al. 2022b; 2022c; 2022d), having only 20 classes, reducing 60 possible Forest classes to only 6 classes (Table 1) considering only First level.

There are various methods for producing them. EU fuel map at 1 km resolution shown in Figure 12 was produced using various input map data by procedure shown in Figure 13. Detail procedure description including more details about input data are described in (*Aragoneses et al. 2022*b and 2022c).
Both official and "*unofficial*" version of fuel maps at 100 m resolution for all PS are calculated and uploaded to FirEURisk data repository:

- PS1: North Europe
- PS2: Central-Eastern Europe – TUD
- PS3: Mediterranean -Portugal
- PS4: Mediterranean – Spain
- PS5: Mediterranean – Greece

Unofficial maps (not validated and created by FESB) were used to prepare methodology and run initial simulations.

For fuel model WP114 has prepared the final classification table connecting FirEUrisk fuel classes and standard Scott-Burgan fuel models (**FBFM** - **Fire Behaviour Fuel Models**) (Scott and Burgan, 2005). Conversion table has even more new fuel classes than FirEUrisk EU map.

Conversion table is different for * A: arid/semi-arid regime, *H: sub-humid/humid regime.
Main idea of this conversion is to use fuel parameters defined by Scott-Burgan fuel models, although some adaptation will be needed.

In FlamMap Landscape File (.LCP) or GeoTIFF file (see Figure 10) we need also 4 additional parameters describing **canopy fuels**:

- CC – Canopy Cover (%)
- CH – Canopy Height or SH – Stand Height (m)
- CBH – Canopy Base Height (m)

Copyright © FirEURisk Consortium. All rights reserved.

- CBD – Canopy Bulk Density (kg/m^3)

These parameters could be calculated as follows:

- Canopy Cover (CC), could be calculated from 2018 Tree Cover Density - https://land.copernicus.eu/pan-european/high-resolution-layers/forests/tree-cover-density/status-maps in 10m resolution for 2018. In FlamMap unit for CC is %).

Canopy Base Height (CBH) and Canopy Bulk Density (CBD) data are not available at global scale. For certain PS they exist, for example for Barcelona PS - PREVINCAT - http://previncat.ctfc.cat/en/index.html but for most PS they have to be calculated. The easiest way is to **use conversation tables** made by **Universitat de Lleida, Lleida, Catalunya, Espagna** (**Fermin Alcasena**) and tested for Barcelona region. Estimation is based on three inputs:

- FirEURisk fuel category - only for forests canopy types:

FuelType	Description
1111	Open broadleaf evergreen forest
1112	Closed broadleaf evergreen forest
1121	Open broadleaf deciduous forest
1122	Closed broadleaf deciduous forest
1211	Open needleleaf forest
1212	Closed needleleaf forest

- Climate type – Arid or Humid – values are different for arid and humid climate.
- Canopy Cover (CC) (%)

Conversion table is below:

Copyright © FirEURisk Consortium. All rights reserved.

	Canopy cover class					
CBH (m)	15 - 30	30 - 45	45 - 60	60 - 75	75 - 90	90 - 100
1111_A	3,33	3,77	4,01	4,23	4,63	5,23
1112_A	2,84	3,55	4,16	4,51	4,73	4,98
1121_A	3,87	4,02	4,53	4,90	5,11	5,30
1122_A	4,12	3,99	4,94	5,13	5,62	5,62
1211_A	2,80	3,29	3,60	4,18	4,66	4,88
1212_A	2,46	3,18	3,34	3,57	3,91	3,90
1111_H	3,55	3,99	4,24	4,41	4,60	4,79
1112_H	3,30	4,14	4,66	4,81	4,89	5,00
1121_H	3,75	4,05	4,20	4,36	4,52	4,80
1122_H	3,87	4,36	4,62	4,75	4,85	5,17
1211_H	2,92	3,05	3,27	3,34	3,44	3,54
1212_H	2,73	3,05	3,24	3,42	3,49	3,53

	Canopy cover class					
CBD (kg m^{-3})	15 - 30	30 - 45	45 - 60	60 - 75	75 - 90	90 - 100
1111_A	0,05	0,08	0,11	0,14	0,16	0,16
1112_A	0,05	0,09	0,12	0,15	0,17	0,17
1121_A	0,04	0,08	0,10	0,12	0,15	0,16
1122_A	0,04	0,07	0,09	0,11	0,14	0,15
1211_A	0,06	0,10	0,13	0,15	0,17	0,17
1212_A	0,05	0,09	0,14	0,16	0,19	0,21
1111_H	0,05	0,09	0,12	0,15	0,17	0,17
1112_H	0,05	0,09	0,13	0,16	0,18	0,18
1121_H	0,04	0,07	0,09	0,11	0,13	0,13
1122_H	0,04	0,07	0,08	0,10	0,11	0,10
1211_H	0,06	0,09	0,12	0,16	0,18	0,19
1212_H	0,06	0,09	0,12	0,14	0,18	0,20

*Figure 22: Conversion table for estimation of Canopy base height (CBH) and Canopy bulk density (CBD) from FirEURisk Fuel Models (first colon – only for forest canopy cover together with climate type (arid A or humid H). The third input is Canopy cover class (**Fermin Alcasena** - **Universitat de Lleida**)*

In FlamMap Canopy Base Height (CBH) class is obtained by multiplying real height with 10, so unit is m*10, and Canopy Bulk Density (CBD) class by multiplying real density with 100, so unit is (kg/m3)*100.
For example for Open broadleaf evergreen forest in arid climate (1111_A) CBH is 3,33*10=33,3 and CBD 0,05*100=5.
Concerning Fuel Maps and Fuel parameters for PS we could conclude:

- Fuel Maps for all PS using new FirEURisk fuel models are calculated in 100 m resolution.
- In this moment the new Fuel Parameters particularly tuned for new FirEURisk Fuel Model do not exist, therefore standard Scott-Burgan fuel parameters could be applied using conversion table from Figure 15.

It was necessary to adapt certain Scott-Burgan fuel parameters to better match specific vegetation characteristics of certain PS. For example, one important fuel parameter is ME –Dead Fuel Moisture of Extinction. Its values in Scott-Burgan fuel parameter was quite low and unreal for grass vegetation:

1. Scott-Burgan model GR1 – 15%
2. Scott-Burgan model GR2 – 15%
3. Scott-Burgan model GR4 – 15%

Copyright © FirEURisk Consortium. All rights reserved.

particularly for Mediterranean region, and therefore it must be increased. This problem was mentioned by (Chuvieco et al. 2004), (Yebra et al 2007) and in analysis of Kornati Fire Accident in Croatia (Stipaničev and Viegas, 2008) it was increased to 40%.

Dynamic files had to be defined for before each FlamMap simulation. The most important are:

- Initial Fuel Moisture file (.FMS) and essential wind data (speed and direction), but if Dead Fuel Moisture has to be conditioned taking into account topography, shading, weather and conditioning period length then

Before staring FlamMap simulation following input data had to be defined through Input Data dialog box (Figure 23).
There are 4 groups of Inputs:

- Fuel Moisture Files
- Winds Data
- Canopy Characteristics and
- Fuel Moisture Settings

6.2.5 Outputs of wildfire propagation potential calculation

FlamMap has few tools that could be used for propagation potential:

a. Basic Fire Behaviour (BFB) or Landscape Fire Behaviour (Basic)
b. Minimum Travel Time Fire Spread (MTT) and
c. Landscape Burn Probability (LBP).

Each of them has different outputs that was used for propagation potential estimation. Our intention was to use primarily **FlamMap Basic Fire Behaviour** to create 'static' propagation potential maps based on historical past fires in analysed area (Pilot Sites) for the last 20 years having as outputs:

- Rate of Spread (m/s)
- Heat per Unit Area (kJ/m^2)
- Flame Length (m)
- Fireline Intensity (kW/m)
- Crown Fraction Burned (%) and
- Crown Fire Activity

Also, we used **FlamMap Landscape Burn Probability** to create 'dynamic' propagation potential maps having as output

- Landscape Burn Probability.

Copyright © FirEUrisk Consortium. All rights reserved.

6.2.5.1 Rate of Spread

The linear rate of advance of a flaming front into unburned fuel in the direction perpendicular to the fire front. Rate of Spread (ROS):

1. contributes to how large the wildfire can become during a specified period of time,
2. is a significant factor affecting fireline intensity and flame size, which are important for determining fire effects.

PS1: North Europe – Sweden
Results not available

PS2: Central-Eastern Europe:

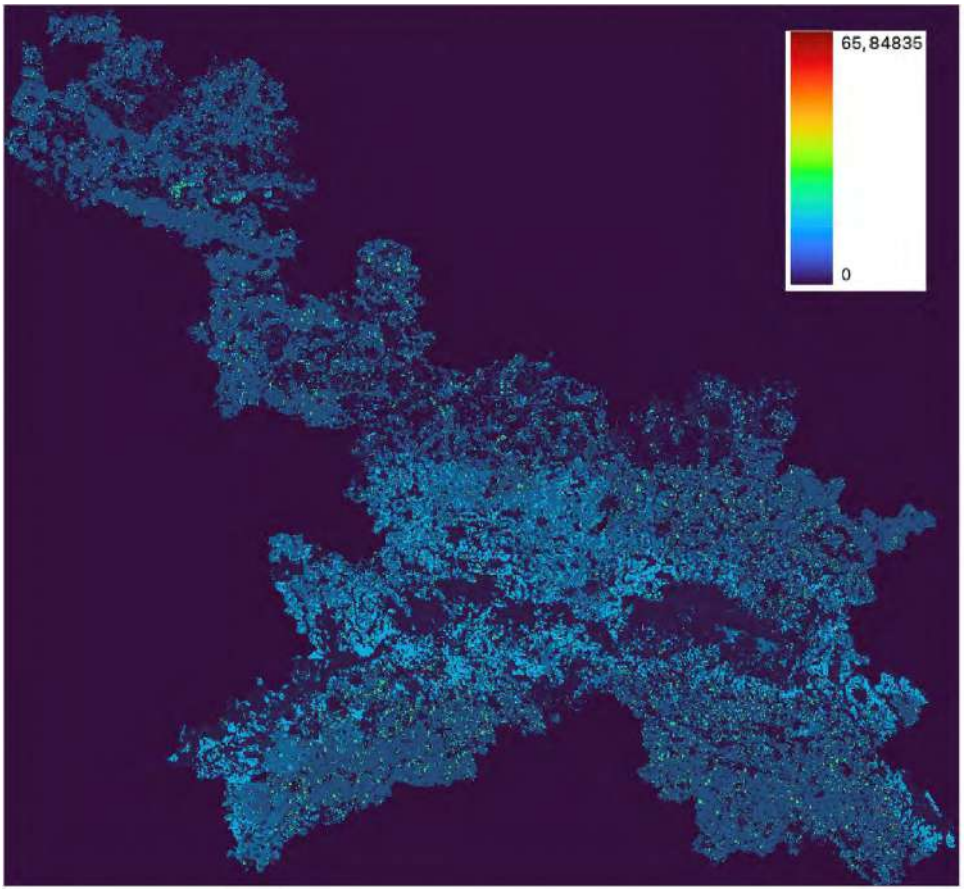


Figure 35: Rate of Spread for PS2 Central-Eastern Europe

PS3: Mediterranean – Portugal:

Copyright © FirEURisk Consortium. All rights reserved.

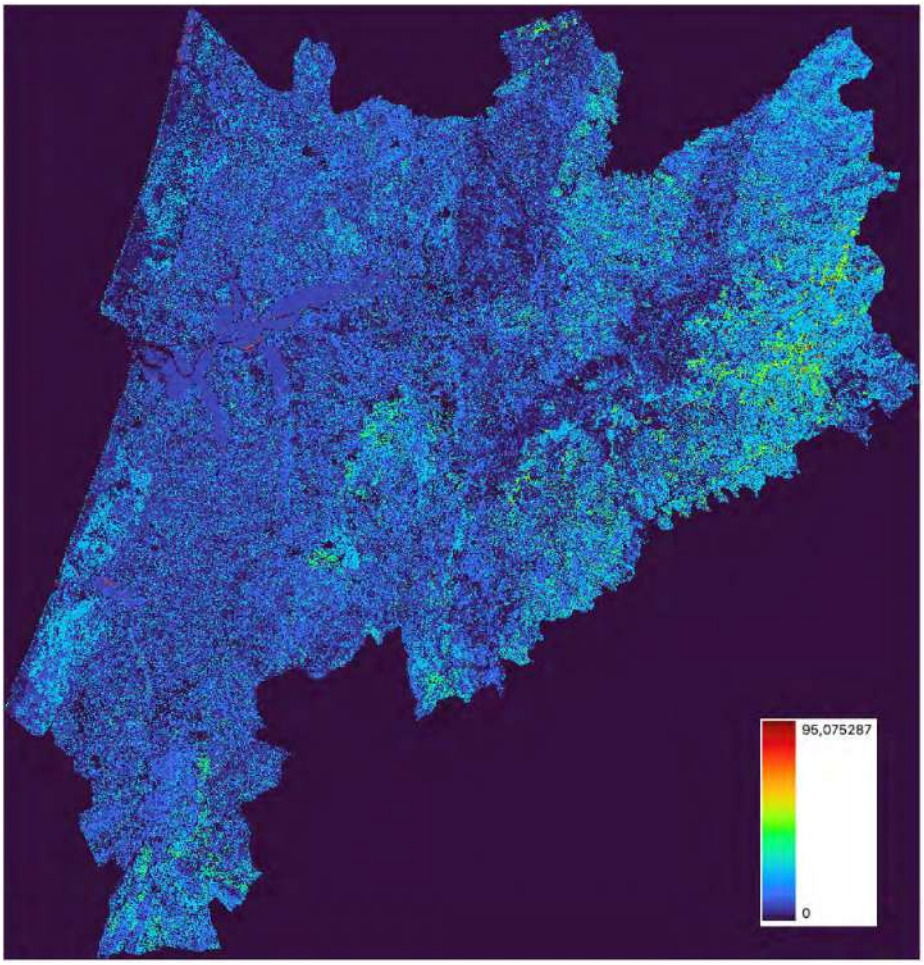


Figure 36: Rate of Spread for PS3: Mediterranean – Portugal

PS4: Mediterranean – Spain:

Copyright © FirEURisk Consortium. All rights reserved.

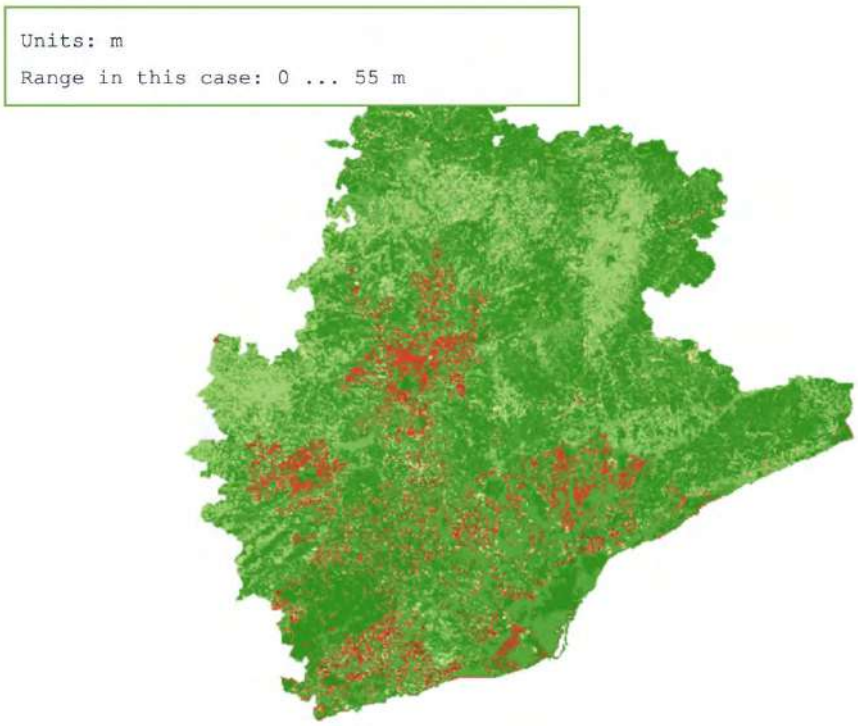


Figure 37: Rate of Spread for PS4: Mediterranean – Spain

PS5: Mediterranean – Greece:

Copyright © FirEURisk Consortium. All rights reserved.

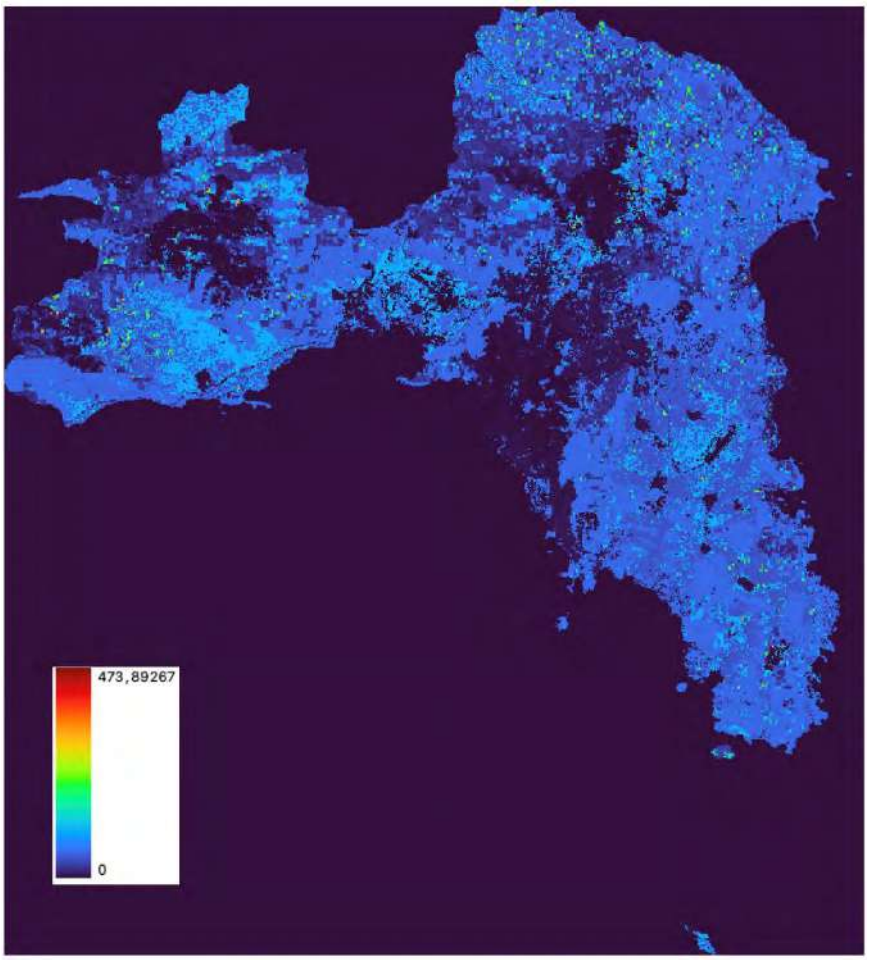


Figure 38: Rate of Spread for PS5: Mediterranean – Greece

6.2.5.2 Heat per Unit Area

Heat per Unit Area is the amount of heat released per unit area during the short period of continuous flaming. Heat per Unit Area is not affected by wind speed, slope, or direction of spread.

PS1: North Europe – Sweden
Results not availablež

PS2: Central-Eastern Europe:

Copyright © FirEURisk Consortium. All rights reserved.

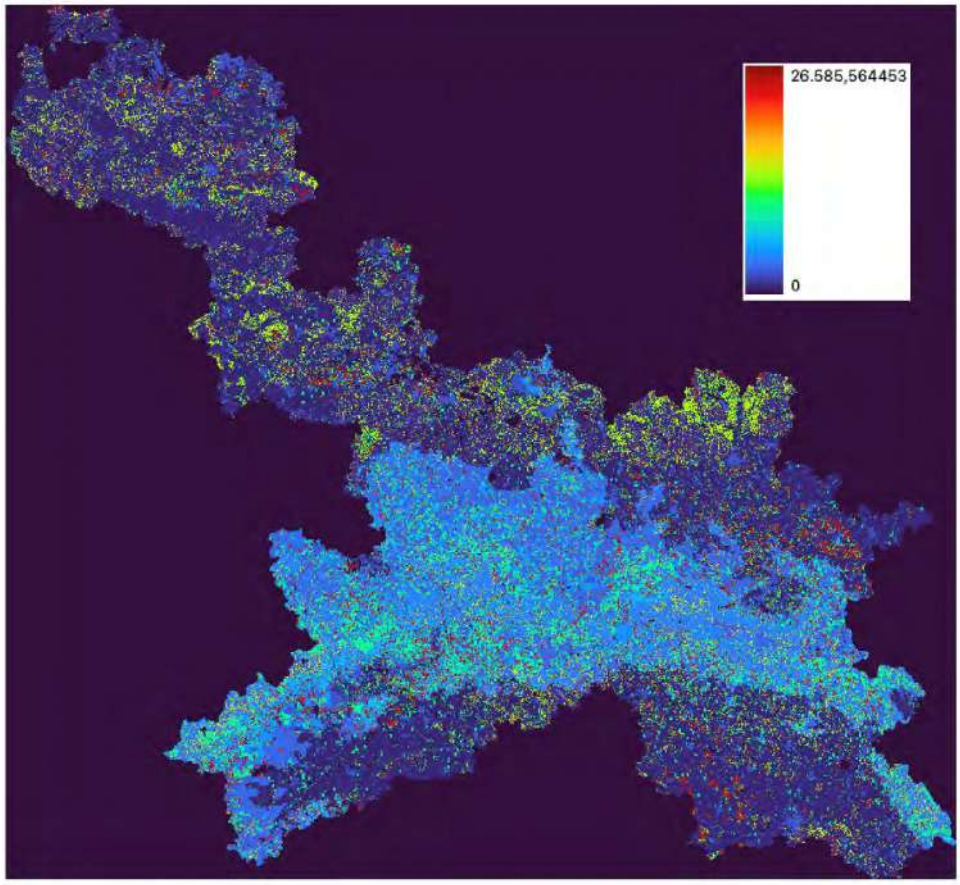


Figure 39: Heat per Unit Area for PS2 Central-Eastern Europe

PS3: Mediterranean – Portugal:

Copyright © FirEURisk Consortium. All rights reserved.

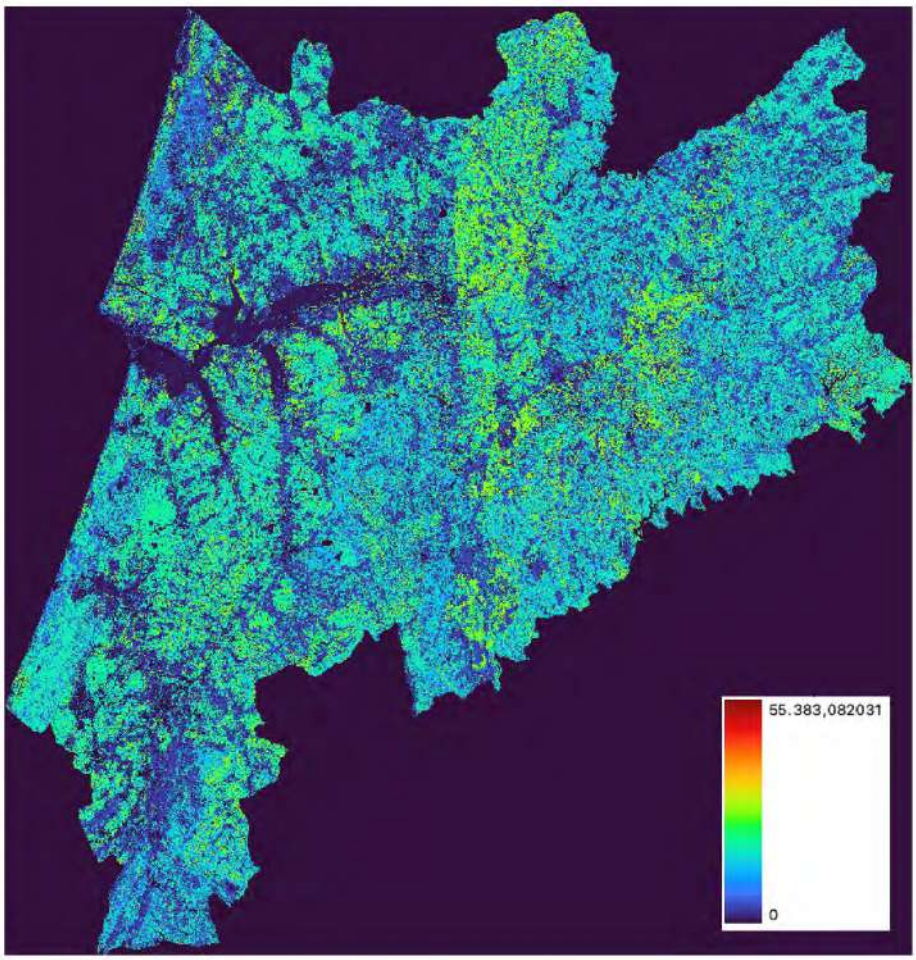


Figure 40: Heat per Unit Area for PS3: Mediterranean – Portugal

PS4: Mediterranean – Spain:

Copyright © FirEURisk Consortium. All rights reserved.

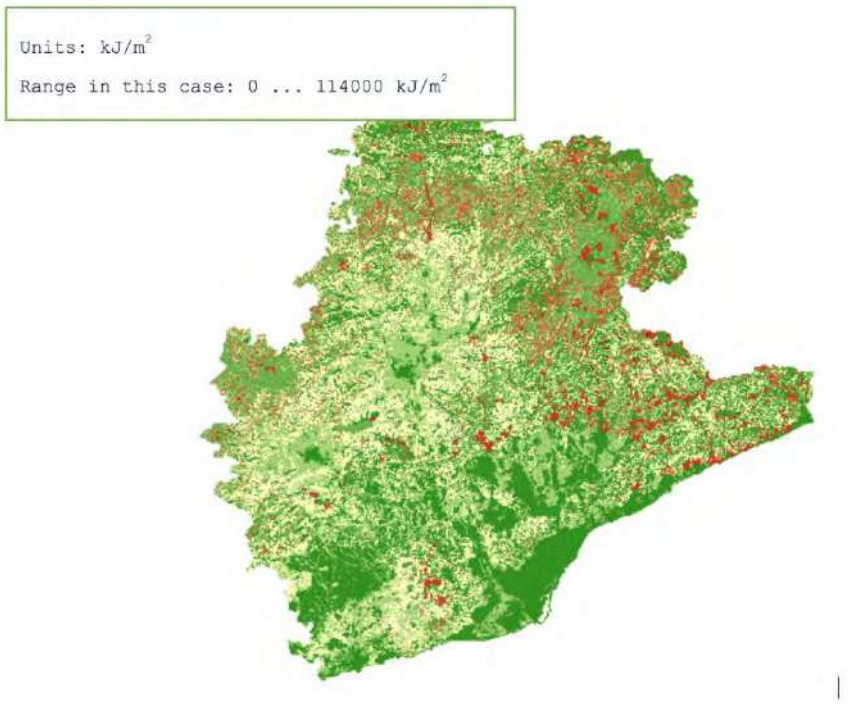


Figure 41: Heat per Unit Area for PS4: Mediterranean – Spain

PS5: Mediterranean – Greece:

Copyright © FirEURisk Consortium. All rights reserved.

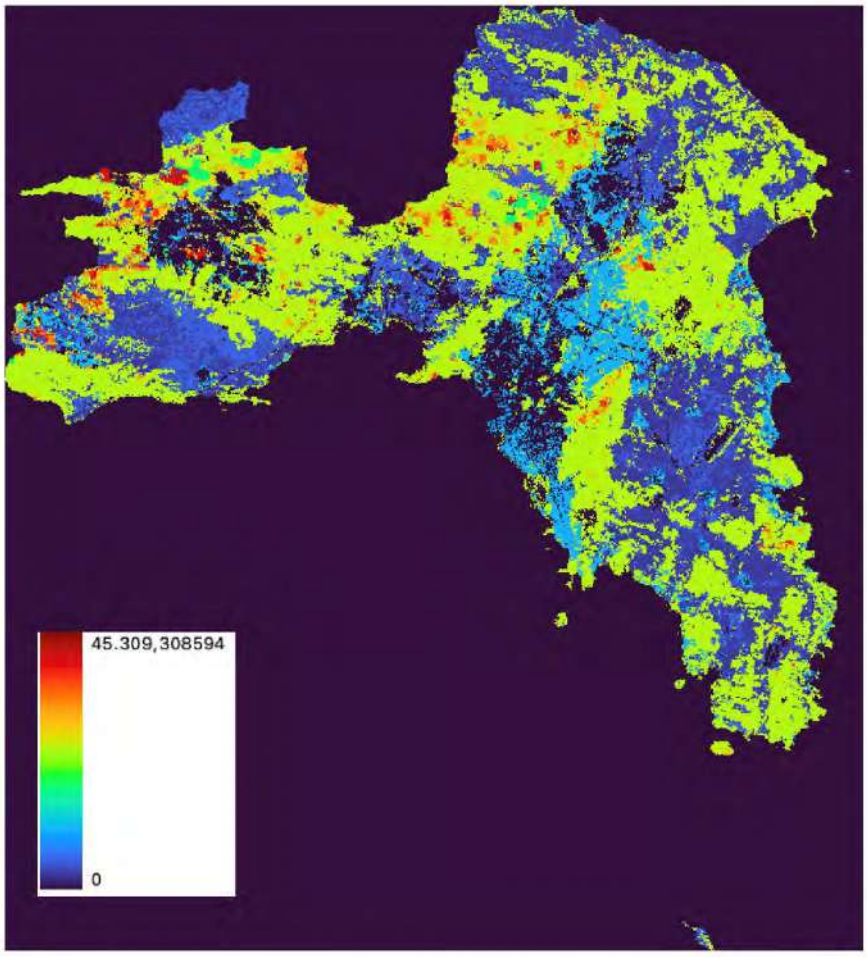


Figure 42: Heat per Unit Area for PS5: Mediterranean – Greece

6.2.5.3 Flame Length

Flame Length measured from midway in the active flaming combustion zone to the average tip of the flames. It is indicator of fireline intensity.

PS1: North Europe – Sweden
Results not available

PS2: Central-Eastern Europe:

Copyright © FirEUrisk Consortium. All rights reserved.

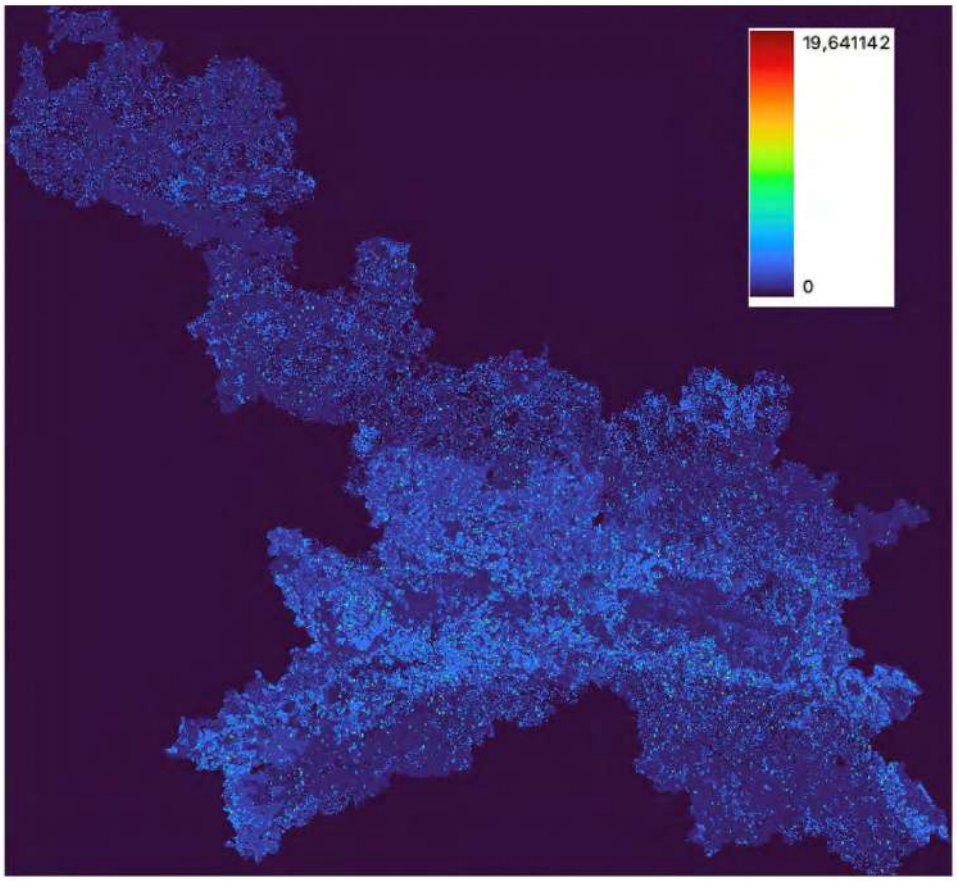


Figure 43: Flame Length for PS2 Central-Eastern Europe

PS3: Mediterranean – Portugal:

Copyright © FirEURisk Consortium. All rights reserved.

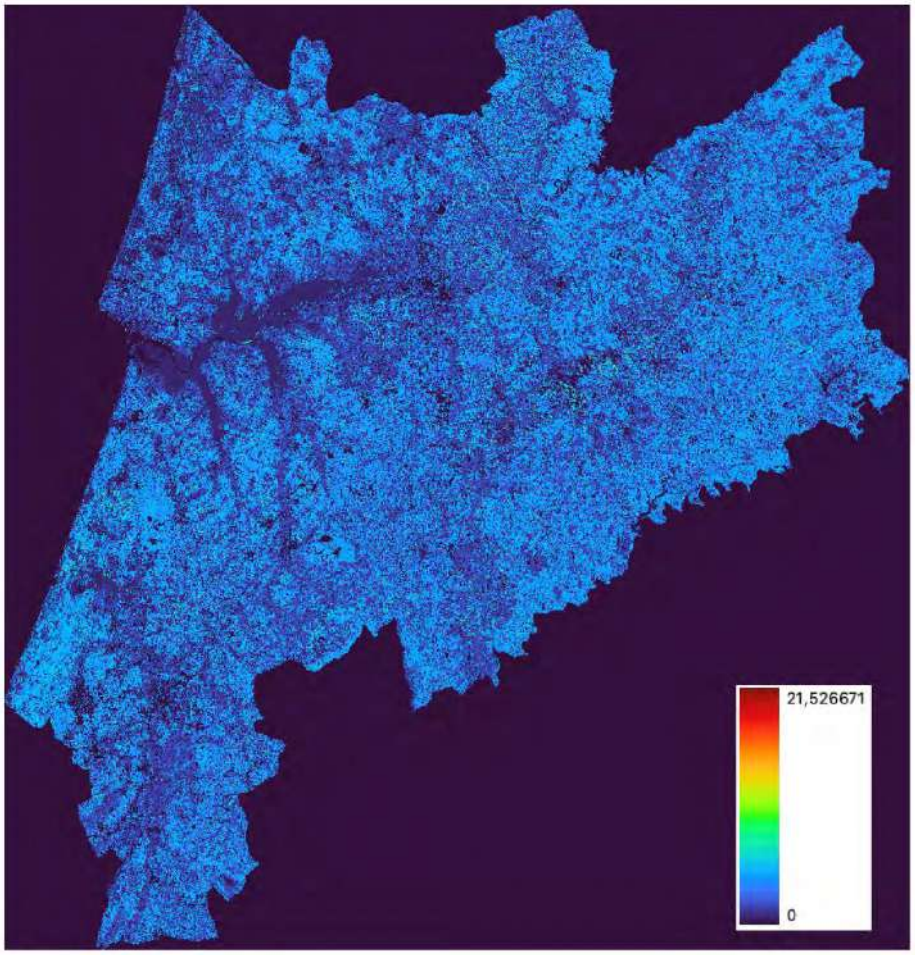


Figure 44: Flame Length for PS3: Mediterranean – Portugal

PS4: Mediterranean – Spain:

Copyright © FirEURisk Consortium. All rights reserved.

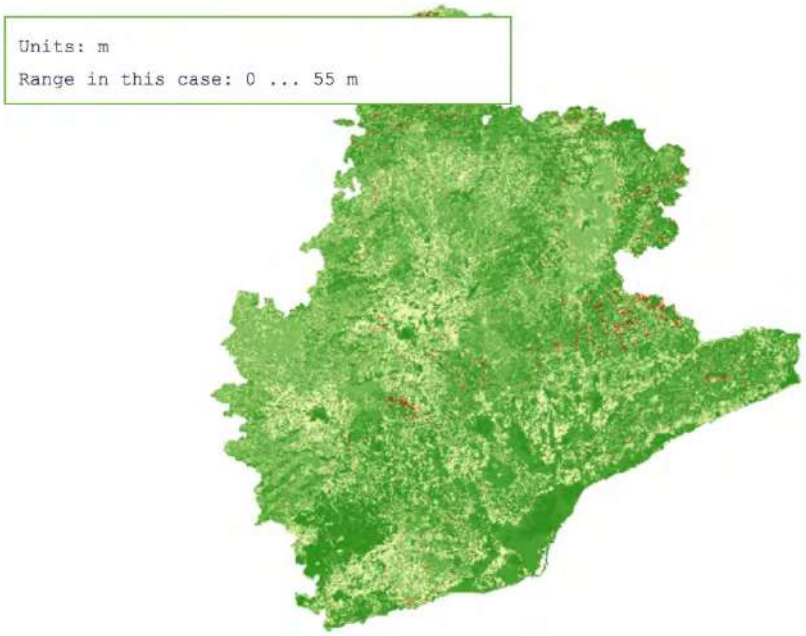


Figure 45: Flame Length for PS4: Mediterranean – Spain

PS5: Mediterranean – Greece:

Copyright © FirEURisk Consortium. All rights reserved.

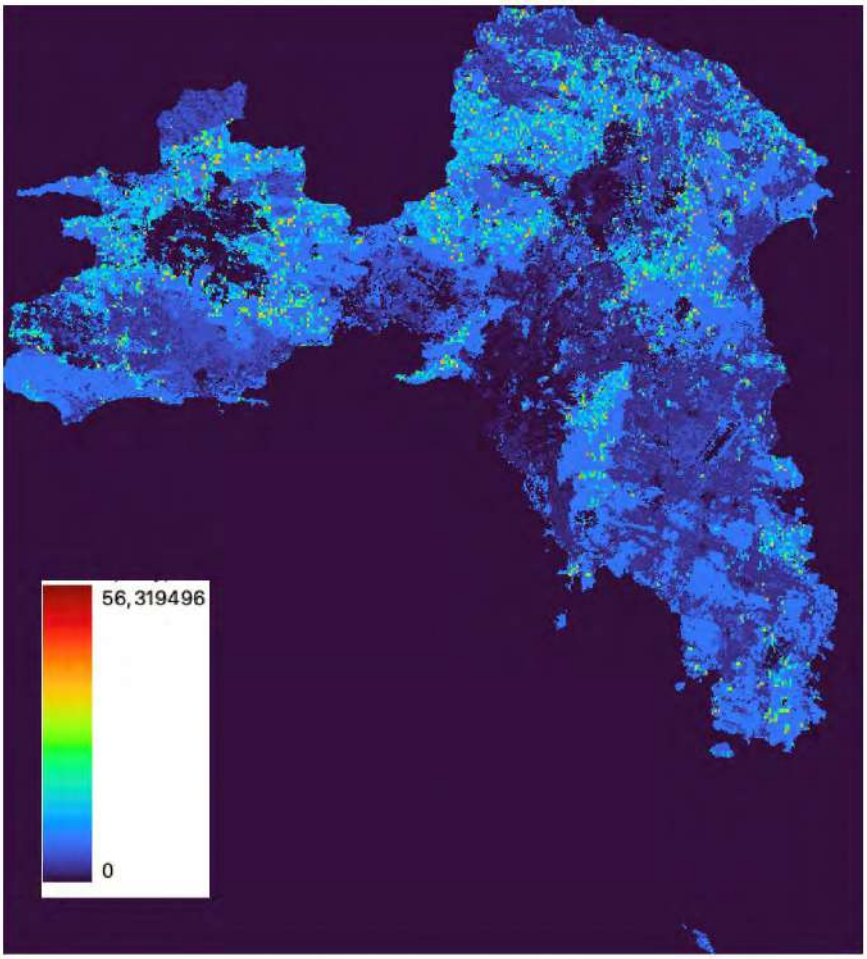


Figure 46: Flame Length for PS5: Mediterranean – Greece

6.2.5.4 Fireline Intensity

Fireline Intensity also called Byram's fire intensity is a fundamental fire characteristic.
It express heat energy released per unit time from a one-meter-wide section of the fuel bed extending from the front to the rear of the flaming zone.
Fireline intensity is a function of rate of spread and heat per unit area, and is directly related to flame length. Sometime it is explained as *"Fireline Intensity is about as much information about a fire's behaviour as can be crammed into one number"*

PS1: North Europe – Sweden
Results not available

PS2: Central-Eastern Europe:

Copyright © FirEUrisk Consortium. All rights reserved.

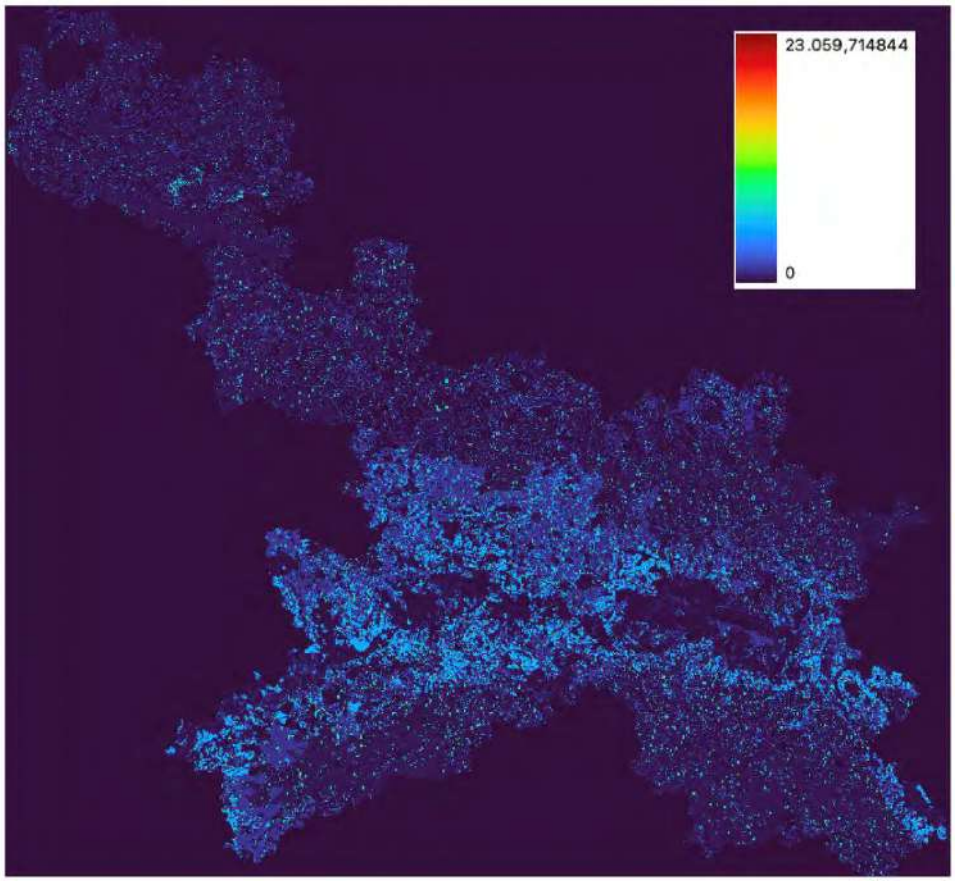


Figure 47: Fireline Intensity for PS2 Central-Eastern Europe

PS3: Mediterranean – Portugal:

Copyright © FirEUrisk Consortium. All rights reserved.

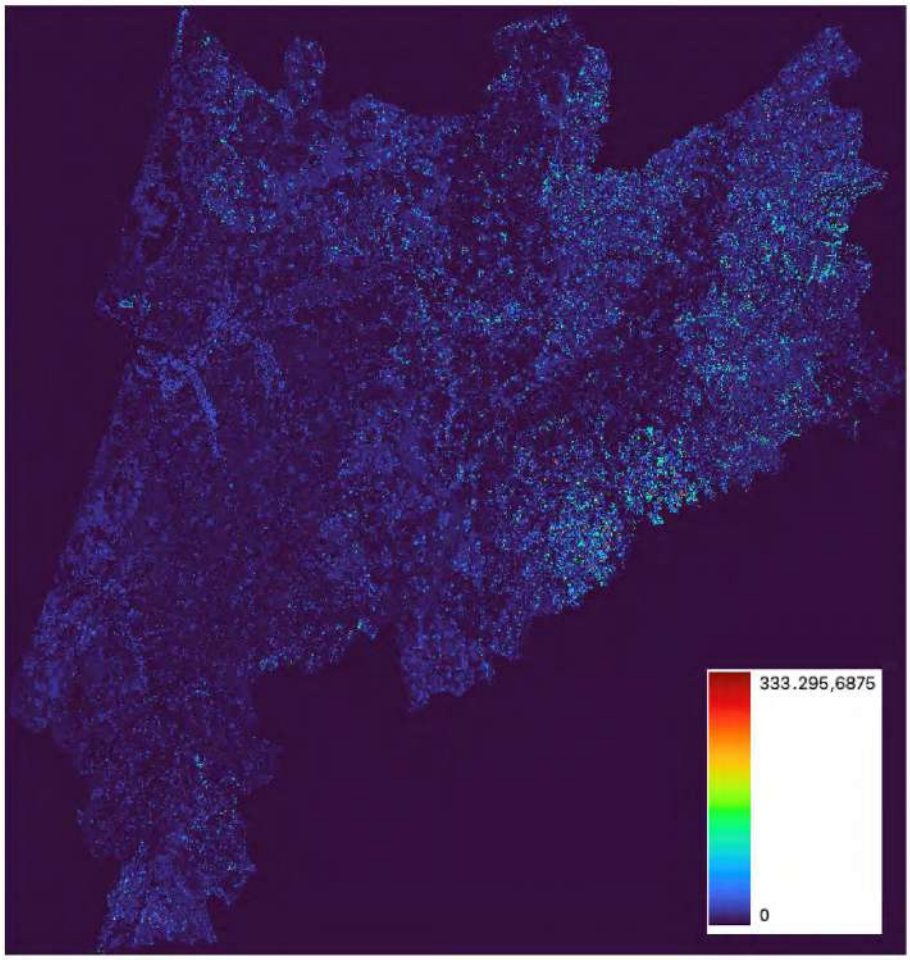


Figure 48: Fireline Intensity for PS3: Mediterranean – Portugal

PS4: Mediterranean – Spain:

Copyright © FirEURisk Consortium. All rights reserved.

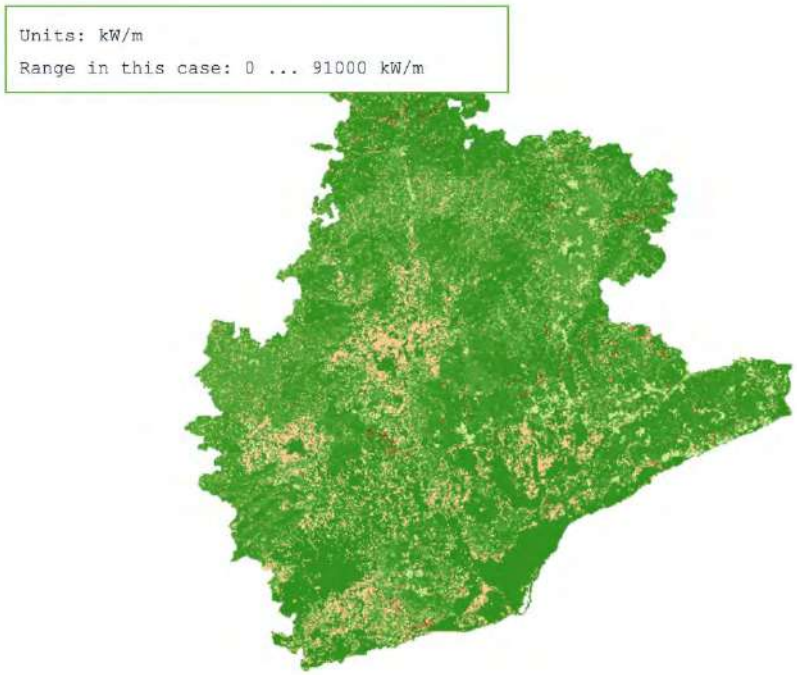


Figure 49: Fireline Intensity for PS4: Mediterranean – Spain

PS5: Mediterranean – Greece:

Copyright © FirEURisk Consortium. All rights reserved.

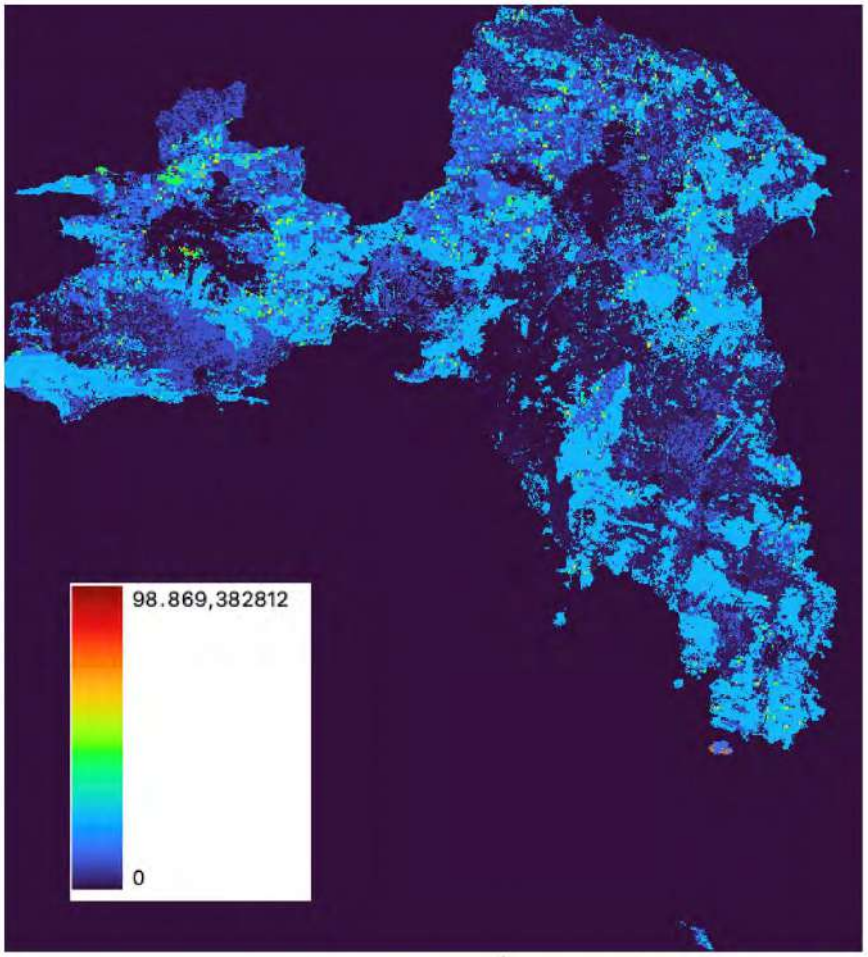


Figure 50: Fireline Intensity for PS5: Mediterranean – Greece

6.2.5.5 Crown Fraction Burned

A fraction between 0 and 1 indicating the severity of a crown fire. 0.0 indicates a surface fire while 1.0 represents an active crown fire. Intermediate values represent a scaled value of passive crown fire severity.

PS1: North Europe – Sweden
Results not available

PS2: Central-Eastern Europe:

Copyright © FirEURisk Consortium. All rights reserved.

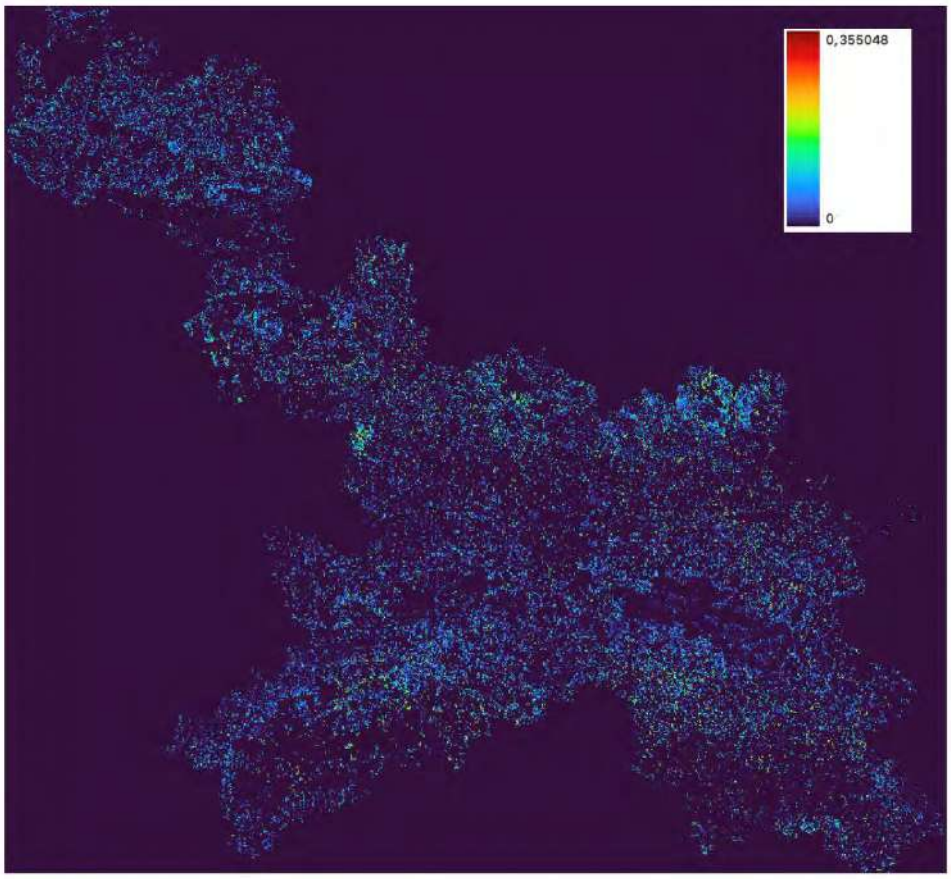


Figure 51: Fireline Intensity for PS2 Central-Eastern Europe

PS3: Mediterranean – Portugal:

Copyright © FirEURisk Consortium. All rights reserved.

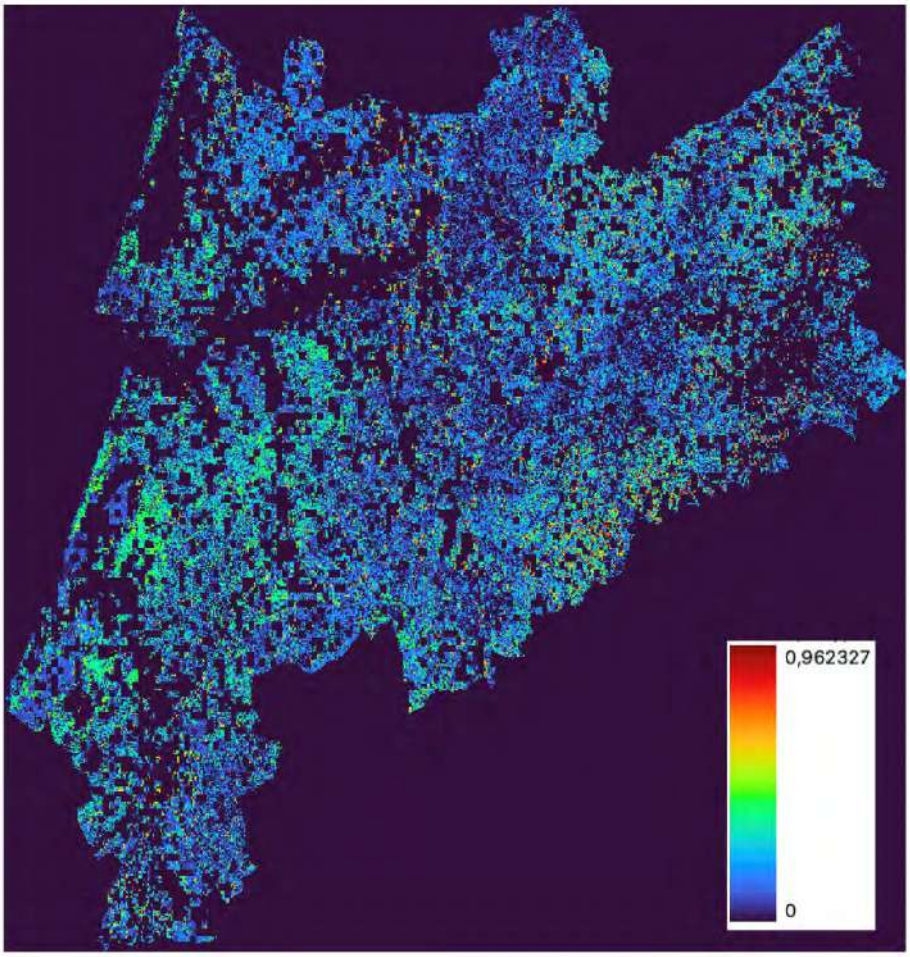


Figure 52: Fireline Intensity for PS3: Mediterranean – Portugal

PS4: Mediterranean – Spain:

Copyright © FirEUrisk Consortium. All rights reserved.



Figure 53: Crown Fraction Burned for PS4: Mediterranean – Spain

PS5: Mediterranean – Greece:

Copyright © FirEURisk Consortium. All rights reserved.

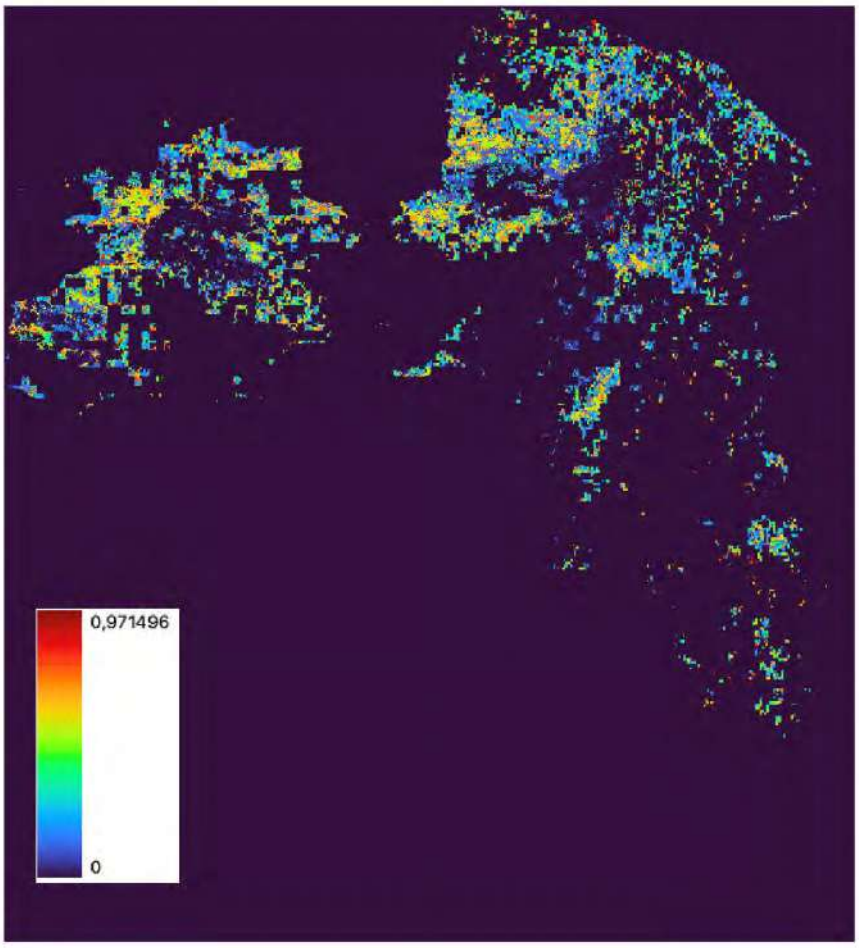


Figure 54: Fireline Intensity for PS5: Mediterranean – Greece

6.2.5.6 Crown Fire Activity

The Crown fire activity describes fire activity in the forest or shrub canopy. Characterized as surface fire, passive crown fire (torching), active crown fire or non-burnable.

- **Surface Fire**: Fire that burns loose debris on the surface, which includes dead branches, leaves, and low vegetation.
- **Passive Crown Fire**: A fire in the crowns of trees in which trees or groups of trees torch, ignited by the passing front of the fire. The torching trees reinforce the spread rate, but these fires are not basically different from surface fires.
- **Active Crown Fire**: A fire in which a solid flame develops in the crowns of trees, but the surface and crown phases advance as a linked unit dependent on each other.
- **Non-burnable**: Portions of the landscape fuels that will not support combustion. Generally associated with bodies of water or non-vegetated areas of the landscape.

PS1: North Europe – Sweden

Results not available

Copyright © FirEURisk Consortium. All rights reserved.

PS2: Central-Eastern Europe:

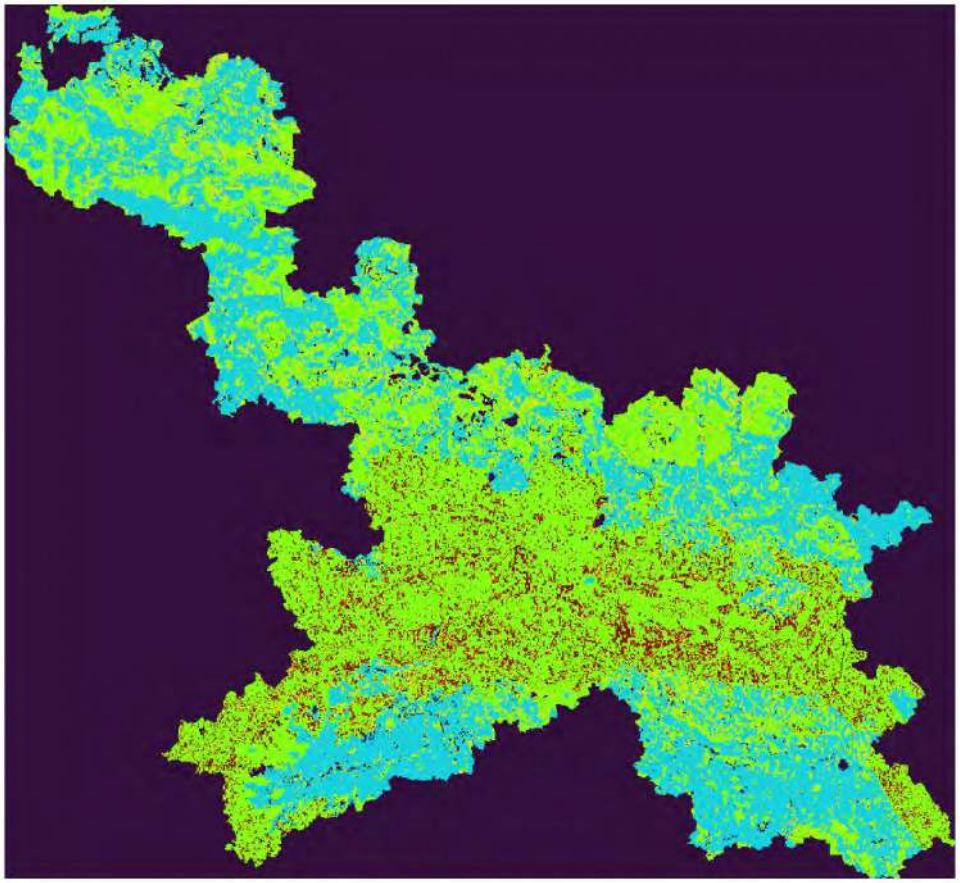


Figure 55: Crown Fire Activity for PS2 Central-Eastern Europe

PS3: Mediterranean – Portugal:

Copyright © FirEURisk Consortium. All rights reserved.

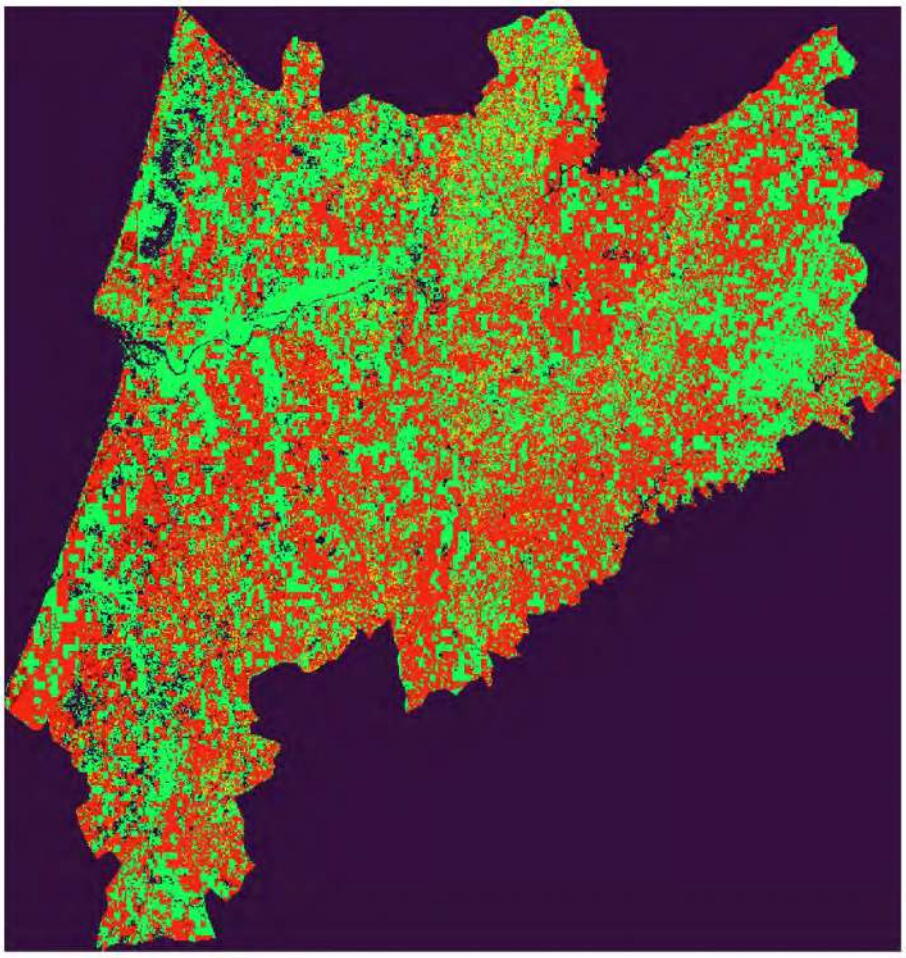


Figure 56: Crown Fire Activity for PS3: Mediterranean – Portugal

PS4: Mediterranean – Spain:

Copyright © FirEURisk Consortium. All rights reserved.

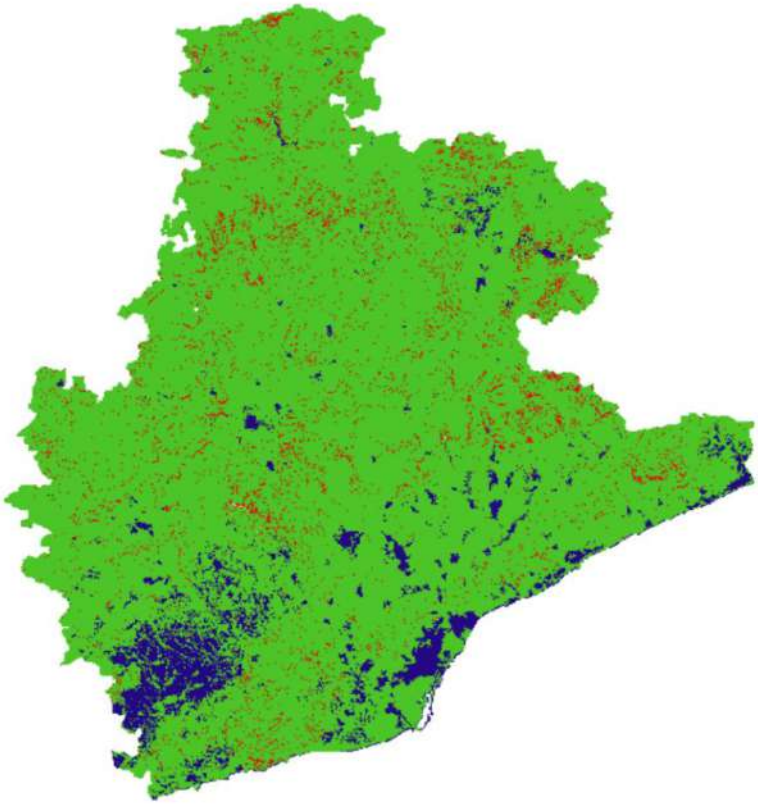


Figure 57: Crown Fire Activity for PS4: Mediterranean – Spain

PS5: Mediterranean – Greece:

Copyright © FirEURisk Consortium. All rights reserved.

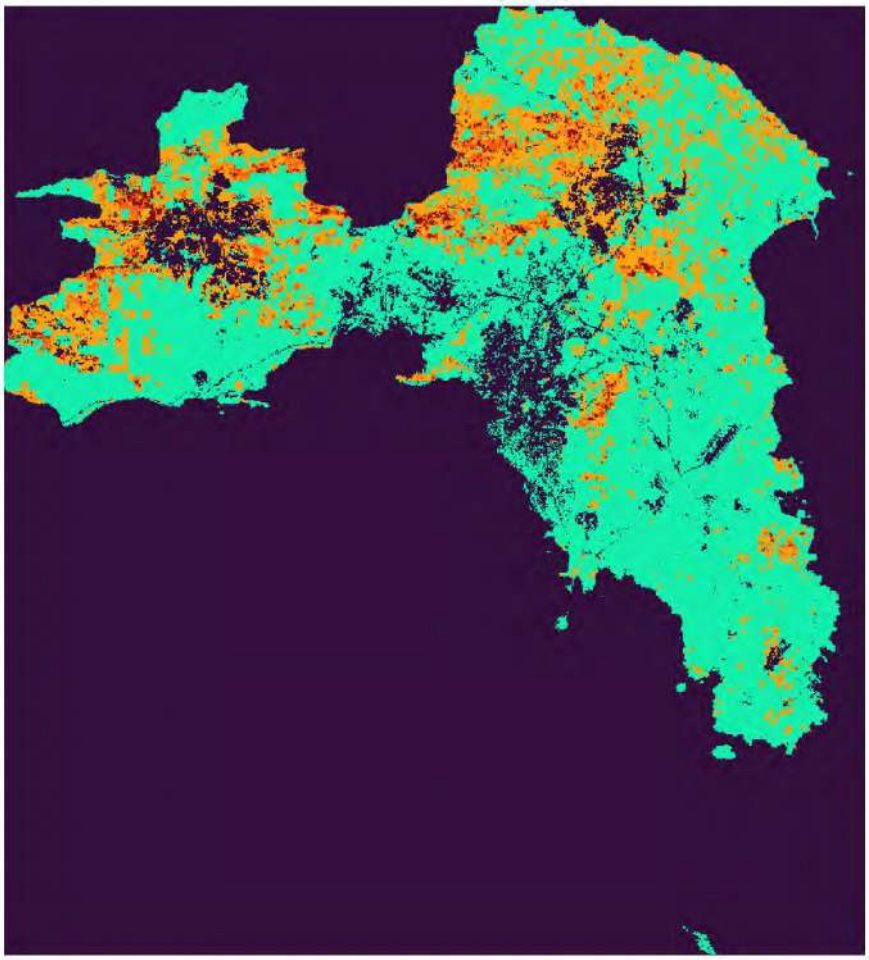


Figure 58: Crown Fire Activity for PS5: Mediterranean – Greece

6.2.6 Burn probability (dynamic run)

PS1: North Europe – Sweden

Results not available

PS2: Central-Eastern Europe:

Copyright © FirEURisk Consortium. All rights reserved.

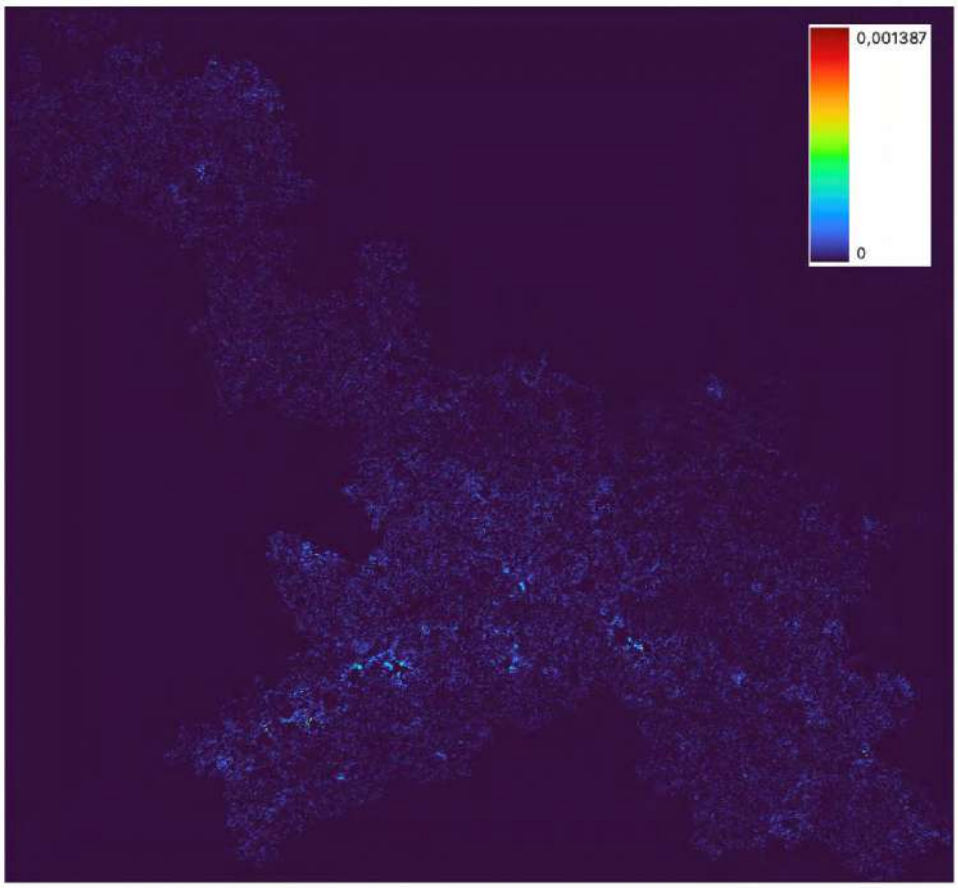


Figure 59: Burn probability for PS2 Central-Eastern Europe

PS3: Mediterranean – Portugal:

Copyright © FirEURisk Consortium. All rights reserved.

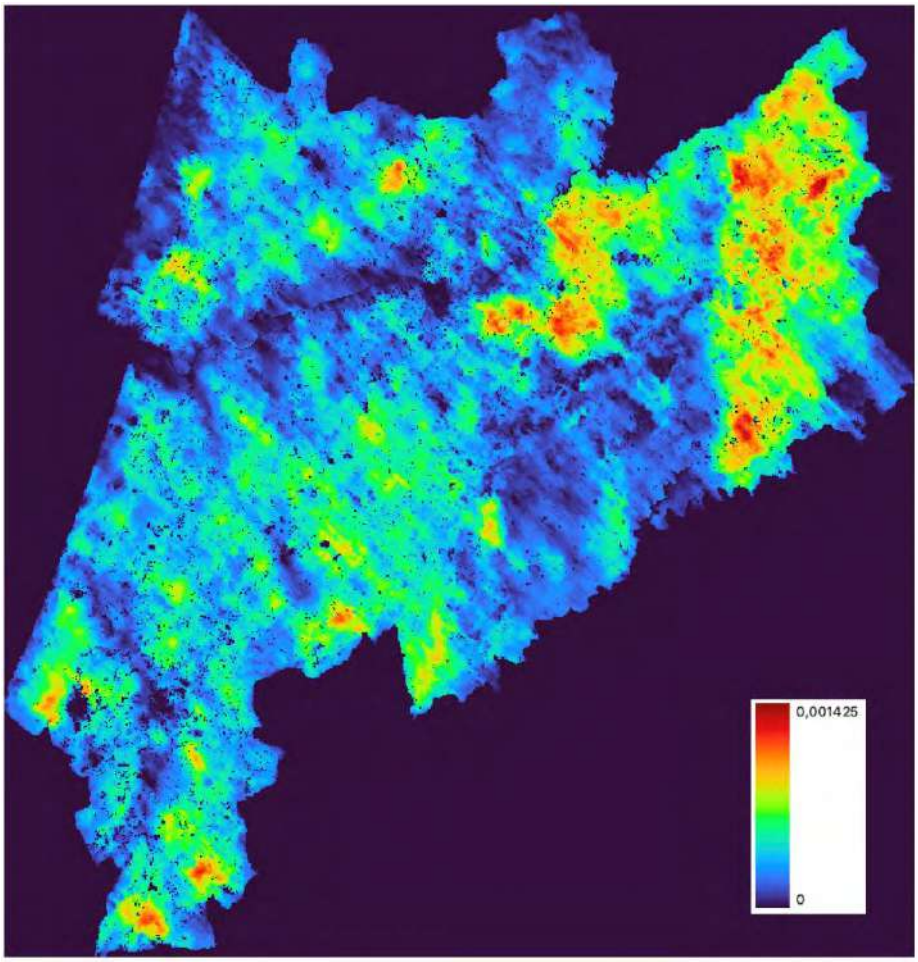


Figure 60: Burn probability for PS3: Mediterranean – Portugal

PS4: Mediterranean – Spain:

Copyright © FirEURisk Consortium. All rights reserved.

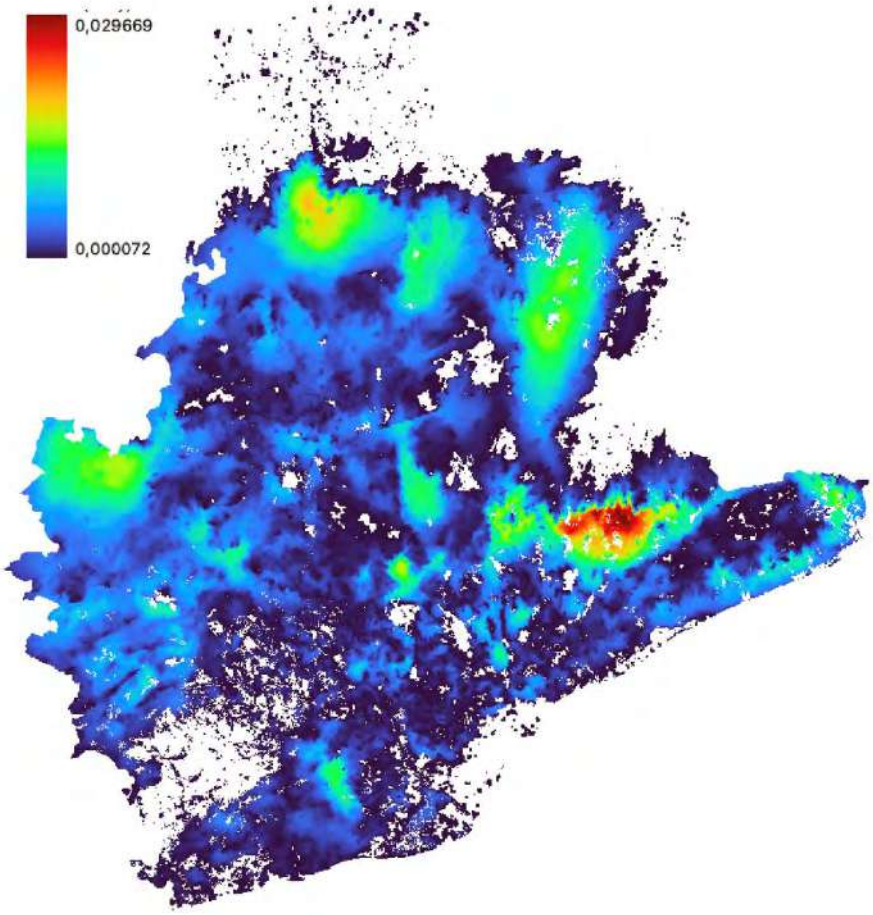


Figure 61: Burn probability for PS2: Mediterranean – Spain

PS5: Mediterranean – Greece:
Results not available

6.2.7 Product description: Fire propagation (PS)

- **Description:** This product will include GeoTIFF raster maps of propagation potential indicators for Pilot Sites, as well as report with detail description of methodology and obtained results. Our intention is to use primarily FlamMap Basic Fire Behaviour to create something like 'static' propagation potential maps based on historical past fires in analysed area (Pilot Sites) for the last 20 years having as outputs: Rate of Spread (m/s), Heat per Unit Area (kJ/m2), Flame Length (m), Fireline Intensity (kW/m), Crown Fraction Burned (%) and Crown Fire Activity. Developer FESB SPLIT. The product developed within the Activity "*1.3.1. Risk assessment integration*". Propagation potential is important part of Wildfire risk estimation having direct influence on Danger (hazard) and Exposure. In this document a detail methodology for propagation potential calculation on Pilot Sites (PS) level is presented, as well as analysis of all necessary input data and how they could be collected for FirEURisk Pilot Sites (PS). Well known software for wildfire behaviour simulation FlamMap has few tools that could be used for propagation potential: a) Basic Fire Behaviour

Copyright © FirEURisk Consortium. All rights reserved.

(BFB) or Landscape Fire Behaviour (Basic), b) Minimum Travel Time Fire Spread (MTT) and c) Landscape Burn Probability (LBP).

- **Format:** Propagation potential indicators for Pilot Sites (PS) is a geospatial product in .tiff format and is a static layer. The temporal coverage ranges from 2001 to 2020.
- **Resolution:** 100 m.
- **Projection:** Pseudomercator EPSG: 3857
- **Access:** The datasets are available in different links for each pilot site: for PS1. North Europe: https://fireurisk.satways.net/datasets/6419dff4e4b054e2ce42787d; for PS2: Central-Eastern Europe Propagation Potential: https://fireurisk.satways.net/datasets/63ff40fbe4b054e2ce418930; PS3. Mediterranean – Portugal Propagation Potential: https://fireurisk.satways.net/collection/6422f678e4b054e2ce42c988; for PS5. Mediterranean - Greece Propagation Potential: https://fireurisk.satways.net/datasets/63ff3fdbe4b054e2ce41866b.
- **Contact:** Marin Bugarić (marin.bugaric@fesb.hr).

7 Smoke potential emissions

Wildland fires can be responsible for substantial emissions of nitrogen oxides (NOx), carbon monoxide (CO), ammonia (NH_3), carbon dioxide (CO_2), methane (CH_4), and particulate matter (PM10 and PM2.5) to the atmosphere. These atmospheric emissions affect the global atmospheric chemistry , impact the radiative transfer in the atmosphere and reduce visibility. Moreover, they strongly impair the air quality , with important effects on human health.

The particles (PM10, and PM2.5) and gaseous (NOx, CO, NH_3, CO_2, CH_4) pollutants emitted during wildland fires were estimated by combustion phase (i.e., flaming and smouldering) and fuel type (e.g., open evergreen broadleaf, and cropland herbaceous) using a bottom-up approach based on the following equation (Fernandes et al., 2022):

$$E_{i,j,k} = EF_{i,j,k} \times \beta \times B \times A$$

where, $E_{i,j,k}$ is the emission of compound i (g) by combustion phase j and fuel type k, $EF_{i,j,k}$ is the quantity of the pollutant i, emitted by fuel k burnt during the combustion phase j ($g.kg^{-1}$ fuel burned, dry basis), β the burning efficiency (in percentage), B the fuel load ($kg.m^{-2}$), and A the burned area (m^2).

The fuel type and fuel load were obtained from the FirEUrisk products (see Section 5). A literature review was performed to obtain the most suitable emission factors by fuel type and combustion phase for the European Region. A large set of modelled fire perimeters corresponding to more than 12,000 years or iterations using the FlamMap algorithm were used to generate fireline intensity and wildfire rate of spread for each grid cell. Fire intensity was estimated from fireline intensity (kW/m) and flame length (m) per grid cell provided by the FlamMap simulations (see Section 6). This fire parameter was used to provide separate estimates of flaming and smoldering for each fuel type by assuming that flaming combustion cannot be sustained below an intensity of about 15 kW m^{-2}. The burned area per grid cell was also estimated using the fire progression provided by the output results from FlamMap while the fuel consumption was estimated using an empirical model developed by Prichard et al. (2017).

Copyright © FirEURisk Consortium. All rights reserved.

8 Appendix I: Fire danger index classification for Chornobyl Exclusion Zone

Determining the numerical indicator of the fire hazard of the territory contaminated because of the accident at the Chernobyl nuclear power plant is of great importance in the mobilization and deployment of fire extinguishing equipment. Studies of recent decades have established the dependence of the level of fire danger both on meteorological indicators and on the state of ground vegetation, which can be determined from remote sensing data. In this study, an approach based on the use of Earth remote sensing data and historical meteorological data was tested and adapted to determine the daily fire hazard index in Chernobyl Exclusion Zone.

Combination of remote sensing and meteorological data in estimating fire hazard was introduced by Burgan et al., 1998. He developed so called Fire Potential Index (FPI) that was calculated using fuel type maps, satellite sensor images and meteorological data. Integration of satellite sensor data, fuel type maps and meteorological observations for evaluation of forest fire risk at the pan-European scale was considered by López et al., 2002. For the territory of China Qin et al., 2008 proposed Fuel State Index (FSI) that was estimated using Moderate Resolution Imaging Spectroradiometer (MODIS) data, meteorological data and data the distribution of fuel types on national territory.

8.1 Data used

Remote sensing data used in our research were taken for the period since 2006 up to 2020 years from March to November.

MODIS-based products MOD09GA (4125 images) and MOD13Q1 (270 images) were downloaded using LP DAAC2Disk Download Manager that is available by reference https://lpdaac.usgs.gov/tools/daac2diskscripts/ in hdf format.

The MOD09GA images with 500 m resolution were used for obtaining pixel values from channels sur_refl_b02_1 (Near Infrared or NIR) and sur_refl_b06_1 (Short-wave Infrared or SWIR). For excluding pixels with clouds and snow the quality channel state_1km_1 was used.

The MOD13Q1 images were used for picking values of Normalized Difference Vegetation Index (NDVI) from the channel ”250m 16 days NDVI”.

Hourly historical meteorological data (relative humidity, temperature, wind speed) were uploaded to a table in Postgresql database with the use of NASA API using the following parameterized reference:
https://power.larc.nasa.gov/api/temporal/hourly/point?start={0}&end={1}&latitude={2}&longitude={3}&community=ag&parameters={4}&format=csv&user=Vadym&header=true&time-standard=lst.

For obtaining values of meteorological indicators 477 locations were distributed in grid nodes with
16.5 km resolution (fig. 1). From 2010 to 2020 there are 96430 hourly records at each location 45997110 in total.

Copyright © FirEUrisk Consortium. All rights reserved.

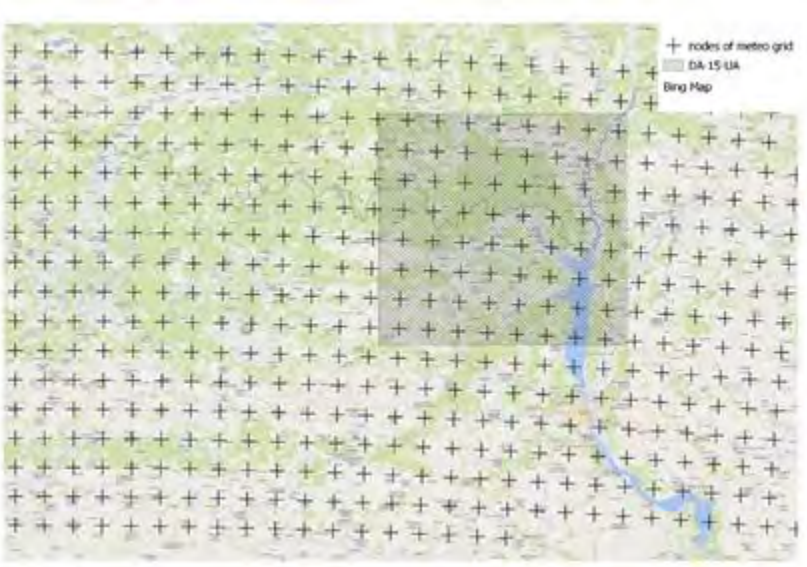


Figure 53: Nodes of meteorological data

Extinction moisture content is taken for the exact fuel type taken from Fuel Type Map that was described in REEFMC contribution to A1.1.4 (Risk-wise landscape and fuel models development).

For assessing the effectiveness of the resulting fire hazard index 1331 fire polygons for the period from 2010 to 2020 years were downloaded in shape format from the repository of MCD64A1 product that accessed using host fuoco.geog.umd.edu (fig. 2). Then these data were uploaded to a special table in Posgresql database. It was evaluated that burned areas cover area of 113200 hectares that constitutes 6.3 % from the total value of demonstration area. As shown in table 1 total burned area that was registered by MCD64A1 product is 119032,8 hectares. Comparing these two values of burned area (113200 and 119033) it can be concluded that area of 5833 hectares were burned at least twice.

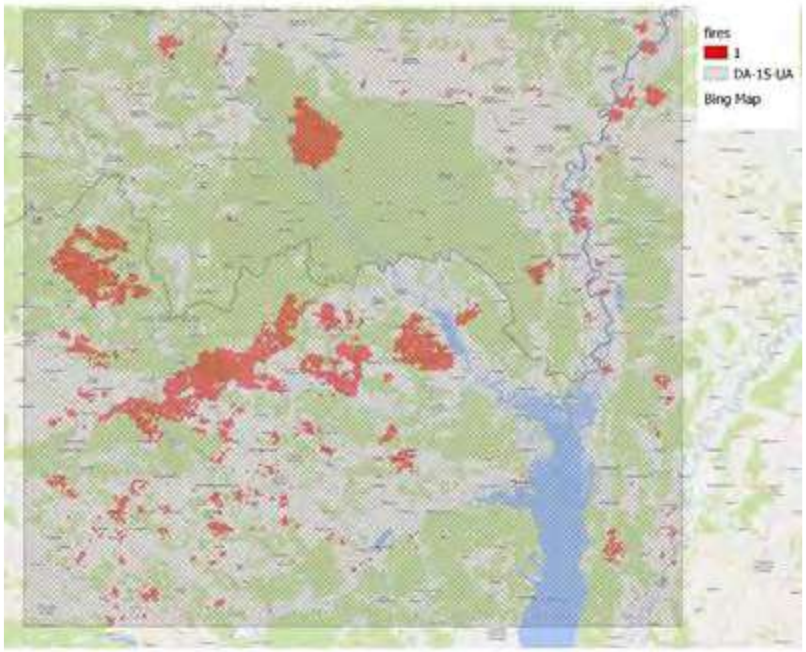


Figure 54: Fires inside demonstration area for the period since 2010 to 2020 years

Copyright © FirEURisk Consortium. All rights reserved.

For the convenience of further processing all the source images were reprojected to EPSG:3857.

8.2 Methodology

In this study a modified version of Daily Fire Hazard Index (DFHI) provided in Laneve et al., 2020 was estimated on the territory of demonstration area that includes Chenobyl exclusion zone. The change in the index calculation algorithm consists in adjusting the moisture content in dead fuel and such modified index will be called UDFHI (Ukrainian Daily Fire Hazard Index). Below math apparatus for calculation the index is provided.

$$UDFHI = \frac{Dead_{content} * Dryness_{10hr}}{100} \quad (1)$$

where:

$Dead_{content}$ – the content of dead vegetation, %;

$Dryness_{10hr}$ – dryness of fuel

$$Dead_{content} = (1 - L_{fc}) * 100 \quad (2)$$

where: L_{fc} – corrected fraction of live vegetation

$$Dryness_{10hr} = (1 - TN_f) * 100$$

TN_f - fraction of ten-hours timelag fuel moisture

Calculation of corrected live vegetation fraction starts with obtaining value of Relative Greenness:

$$RG = \frac{NDVI - NDVI_{min5y}}{NDVI_{max5y} - NDVI_{min5y}} * 100 \quad (3)$$

where: $NDVI$ – normalized difference vegetation index, obtained from the MODIS product MOD13Q1;

$NDVI_{max5y}$ and $NDVI_{min5y}$ – the maximum and minimum NDVI values registered in each pixel in the last five years.

$$L_f = \frac{RG_f * (35 + 40 * \frac{NDVI_{mx} - 100}{100})}{100} \quad (4)$$

where: RG_f –fractional value of RG that can be obtained by omitting 100 in formula 3

$$NDVI_{mx} = 100 * NDVI_{max5y} + 100 \quad (5)$$

$$L_{fc} = L_f * (1 + 0.2 * (\overline{EWT} - 1)) \quad (6)$$

$$\overline{EWT} = \frac{EWT}{\langle EWT \rangle + 2 * \sigma(EWT)} \quad (7)$$

where:

$\overline{EWT}$ - normalized version of the Equivalent Water Thickness (EWT) on the DA;

$\langle EWT \rangle$ - mean EWT on the DA;

$\sigma(EWT)$ - standard deviation computed on the DAж

$$EWT = \frac{-(a*d+c-d*GVMI) + \sqrt{(a*d+c-d*GVMI)^2 - 4*c*d*(a+b-GVMI)}}{2*c*d} \quad (8)$$

where:

EWT - Equivalent Water Thickness;

$GVMI$ - Global Vegetation Moisture Index;

(a = 0.4743, b = −0.3967, c = 5.853e − 5, d = 0.006577);

$$GVMI = \frac{(NIR+0.1) - (SWIR+0.02)}{(NIR+0.1) + (SWIR+0.02)} \quad (9)$$

Where NIR is channels 2 and SWIR is channel 6 of the 500 m resolution MOD09GA product

$$TN_f = \frac{Fm_{10h} - 2}{MX_d - 2} \quad (10)$$

Copyright © FirEURisk Consortium. All rights reserved.

where: Fm_{10h} - ten-Hours timelag fuel moisture expressed as a percent moisture content;
MX_d - the extinction moisture of the dead fuel, which is the moisture content that a certain type of dead fuel must have to prevent the fire from spreading.
The values of extinction moisture content in dead fuel depends on the fuel type and provided in Burgan et al., 1998.
According to Fosberg, 1977

$$Fm_{10h} = K_{CHEZ} * \ 1.28 * emc \quad (11)$$

$$emc = 0.03229 + 0.262573 * rh - 0.001 * rh * T_{eq} \quad if\ rh < 10\%$$

$$emc = 1.7544 + 0.160107 * rh - 0.2661 * T_{eq} \quad if\ 10 \le rh \le 50$$

$$emc = 21.0606 + 0.005565 * rh^2 - 0.00063 * rh * T_{eq} - 0.494399 * rh \quad if\ rh > 50\%$$

K_{CHEZ}-coefficient taken from measurements of fuel moisture content and equal 0.6
T_{eq} - equivalent temperature
Estimation of T_{eq} is based on the reference evapotranspiration determined using the Penman–Monteith equation (12) and described in details in the Food and Agriculture Organization (FAO) guidelines (Allen et al., 1998).

$$ET_0 = \frac{0.408*\Delta*(R_n-G)+\gamma*\frac{900}{T+273}*u_2*(e_s-e_a)}{\Delta+\gamma*(1+0.34*u_2)} \quad (12)$$

where:
ET_0 - reference evapotranspiration, mm day−1;
R_n - net radiation at the crop surface, MJ m−2 day−1;
G - soil heat flux density, MJ m−2 day−1;
T - mean daily air temperature at 2 m height, ◦C;
u_2 - wind speed at 2 m height, m s−1;
e_s - saturation vapour pressure, kPa;
e_a - actual vapour pressure, kPa;
$e_s - e_a$ - saturation vapour pressure deficit, kPa;
Δ - slope vapour pressure curve, kPa/◦C;
γ - psychrometric constant, kPa/◦C.

For estimating equivalent temperature an array of values for temperatures from 0 to 86 with step 2 are calculated for the wind speed 2 m/s with averaging input parameters over the whole demonstration area. Then evapotranspiration of each pixel compared with the values contained in the array and the equivalent temperature is taken for the value that corresponds to the minimum difference of evapotranspiration.

8.3 Software implementation

Calculation of UDFHI values was implemented using Python 3.10 in IDE PyCharm (Community Edition) with the use of different packages: Psycopg2, Rasterio, GDAL, Numpy, Rioxarray, Geopandas, Fiona, Multiprocessing and others. The processing of the initial data presented in the Data chapter was carried out in several stages:

1. Formation of images bounded by a rectangle of the demonstration area taken from source images in hdf-format MOD09GA and MOD13Q1 with extracting only needed channels and transforming to EPSG:3857.
2. Generating images corresponding to minimum and maximum NDVI for the last 5 years for each year.
3. Generating images corresponding to Equivalent Water Thickness.
4. Transforming meteorological data from Postgresql database to multichannel images for every day.
5. Generating daily images corresponding to equivalent temperature.

Copyright © FirEURisk Consortium. All rights reserved.

6. Generating daily images with UDFHI values.

To speed up the execution, most of the image-generating functions were called using parallelism and executed simultaneously on 13 processor cores.

8.4 Results

UDFHI images were generated for the period from 76 (March 16) to 329 (November 24) day for 11 years (2010-2020). This is 2794 images in total. One of such images is shown on fig. 3. The image was produced for 13.06.2015 which was one of the most fire-dangerous days. The map painted according to the ranges of UDFHI values according to the table 2.

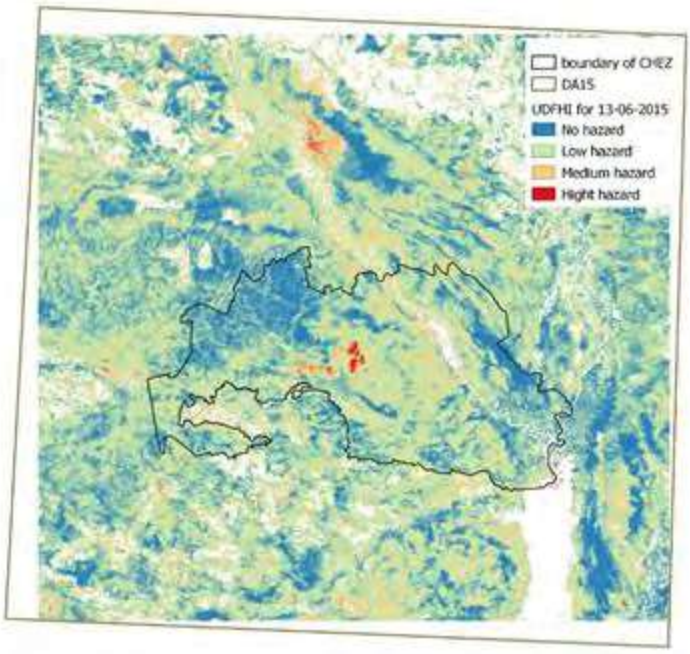


Figure 55: Map of UDFHI in DA-15 for June 13th, 2015

To estimate the effectiveness of the index its values on the whole territory were compared to the ones inside burned areas. The fires with areas less than or equal to 25 hectares were excluded because of the resolution of the product MCD64A1 that is equal to 500 m (https://lpdaac.usgs.gov/products/mcd64a1v006/). Each pixel of this product covers 25 hectares and smaller areas may be considered as artifacts or actual burned area in such pixel is much smaller than its area.

Average values of UDFHI on the total area and inside the burned areas on the days when fires took place represented in the Table 37.

Copyright © FirEURisk Consortium. All rights reserved.

Table 37: Statistics of UDFHI on days with fires

Number	Date	Fires		Average UDFHI per day, %	
		Area, hectare	Count	Total area	On burned areas
1	17.03.2010	30,0	1	45	43
2	20.03.2010	270,9	3	38	40
3	21.03.2010	465,9	3	37	37
4	22.03.2010	90,6	3	34	43
5	25.03.2010	480,3	2	43	42
6	27.03.2010	120,0	1	48	52
7	29.03.2010	30,0	1	42	35
8	16.03.2011	30,2	1	42	55
9	01.04.2011	30,0	1	43	42
10	01.09.2011	88,9	3	32	40
11	02.09.2011	44,5	1	32	37
12	06.09.2011	29,7	1	31	40
13	14.09.2011	44,5	1	33	52
14	16.03.2012	1124,1	19	43	47
15	17.03.2012	90,3	2	43	56
16	18.03.2012	74,6	2	46	41
17	19.03.2012	59,7	2	47	60
18	01.04.2013	59,2	2	39	46
19	03.04.2013	148,0	2	37	34
20	05.04.2013	29,9	1	40	32
21	06.04.2013	488,1	3	40	42
22	07.04.2013	44,4	1	26	25
23	09.04.2013	430,1	6	32	35
24	10.04.2013	148,2	2	32	37
25	11.04.2013	148,8	4	35	38
26	15.04.2013	30,1	1	36	40
27	11.08.2013	30,2	1	30	34
28	14.08.2013	30,2	1	30	34
29	16.03.2014	29,9	1	44	46
30	19.03.2014	75,0	1	38	43
31	20.03.2014	60,3	2	41	49
32	21.03.2014	30,0	1	41	49
33	22.03.2014	270,1	5	44	56
34	23.03.2014	60,0	2	41	57
35	26.03.2014	30,0	1	41	54
36	27.03.2014	285,8	4	40	49

Copyright © FirEURisk Consortium. All rights reserved.

37	28.03.2014	30,0	1	45	54
38	01.04.2014	165,7	3	45	53
39	02.04.2014	166,1	4	48	54
40	03.04.2014	60,4	1	47	55
41	25.07.2014	59,9	1	32	34
42	26.07.2014	60,5	1	31	41
43	27.07.2014	211,5	2	32	37
44	28.07.2014	60,2	2	33	46
45	29.07.2014	44,8	1	34	44
46	26.08.2014	29,6	1	33	39
47	28.08.2014	29,6	1	31	27
48	21.09.2014	30,2	1	34	41
49	22.09.2014	105,2	3	29	36
50	23.09.2014	29,8	1	30	29
51	26.09.2014	60,1	1	36	51
52	27.09.2014	150,6	4	35	42
53	28.09.2014	30,2	1	35	42
54	29.09.2014	105,1	2	35	48
55	30.09.2014	164,9	4	34	34
56	02.10.2014	89,4	3	41	39
57	03.10.2014	30,3	1	42	53
58	04.10.2014	120,6	3	42	56
59	05.10.2014	255,5	2	38	47
60	07.10.2014	134,4	3	41	51
61	08.10.2014	297,7	2	40	48
62	09.10.2014	181,1	2	42	55
63	10.10.2014	208,8	6	44	56
64	11.10.2014	356,7	8	41	42
65	12.10.2014	535,2	5	41	47
66	13.10.2014	192,8	4	34	35
67	14.10.2014	596,8	8	42	50
68	15.10.2014	835,9	14	36	42
69	16.10.2014	343,9	7	41	49
70	17.10.2014	612,4	13	38	42
71	18.10.2014	30,2	1	43	54
72	19.10.2014	29,7	1	43	39
73	21.10.2014	89,0	2	37	45
74	22.10.2014	151,0	4	37	47
75	25.10.2014	29,6	1	44	62
76	28.10.2014	75,1	2	47	58
77	29.10.2014	45,1	1	44	53
78	17.03.2015	165,7	5	49	49
79	18.03.2015	30,0	1	47	53

Copyright © FirEURisk Consortium. All rights reserved.

80	31.03.2015	45,0	1	40	47
81	01.04.2015	616,8	9	45	52
82	02.04.2015	180,4	5	42	48
83	03.04.2015	240,9	6	48	47
84	04.04.2015	301,0	9	42	48
85	05.04.2015	120,3	4	40	43
86	06.04.2015	826,1	9	45	52
87	07.04.2015	481,7	13	45	50
88	08.04.2015	1021,1	17	49	54
89	09.04.2015	1067,6	16	52	58
90	10.04.2015	466,8	8	51	60
91	11.04.2015	735,9	8	48	55
92	12.04.2015	254,9	5	53	54
93	14.04.2015	149,9	3	49	50
94	15.04.2015	180,1	5	44	50
95	19.04.2015	60,2	2	47	44
96	21.04.2015	30,0	1	45	45
97	24.04.2015	90,0	3	41	49
98	25.04.2015	134,8	3	39	52
99	26.04.2015	1349,7	5	39	50
100	27.04.2015	1618,5	8	36	49
101	28.04.2015	1273,9	14	41	54
102	29.04.2015	1753,3	8	39	48
103	30.04.2015	1184,1	10	42	55
104	02.05.2015	59,9	1	33	32
105	04.05.2015	30,0	1	41	55
106	14.05.2015	44,4	1	36	32
107	17.05.2015	44,4	1	36	34
108	19.05.2015	29,6	1	36	29
109	23.05.2015	30,0	1	36	34
110	03.06.2015	29,6	1	34	48
111	09.06.2015	29,7	1	35	44
112	10.06.2015	29,7	1	36	51
113	11.06.2015	475,6	7	36	45
114	12.06.2015	638,9	4	37	51
115	13.06.2015	2375,4	4	37	57
116	14.06.2015	3162,1	9	35	51
117	15.06.2015	1009,2	16	32	45
118	16.06.2015	2078,8	15	31	43
119	18.06.2015	59,4	2	35	42
120	19.06.2015	104,0	3	35	48
121	22.06.2015	29,7	1	33	39
122	28.06.2015	89,8	3	35	43

Copyright © FirEUrisk Consortium. All rights reserved.

123	29.06.2015	180,7	5	34	50
124	30.06.2015	30,1	1	36	38
125	02.07.2015	150,9	2	33	50
126	03.07.2015	255,1	6	35	50
127	04.07.2015	30,2	1	35	54
128	05.07.2015	120,6	2	38	54
129	06.07.2015	44,8	1	37	35
130	07.07.2015	44,8	1	37	38
131	08.07.2015	89,7	1	38	36
132	10.07.2015	74,7	1	35	33
133	19.07.2015	45,3	1	36	36
134	21.07.2015	30,2	1	35	33
135	31.07.2015	88,9	1	37	48
136	04.08.2015	44,4	1	36	53
137	06.08.2015	74,0	1	37	38
138	08.08.2015	119,3	3	38	39
139	09.08.2015	180,3	3	38	44
140	10.08.2015	1409,1	3	39	37
141	11.08.2015	1423,4	6	38	34
142	12.08.2015	599,6	3	36	37
143	13.08.2015	374,3	6	37	51
144	14.08.2015	254,6	7	35	41
145	15.08.2015	329,8	7	38	47
146	16.08.2015	60,0	2	39	46
147	25.08.2015	44,4	1	39	56
148	26.08.2015	29,6	1	38	31
149	30.08.2015	89,3	1	37	51
150	31.08.2015	104,2	2	39	48
151	01.09.2015	134,0	4	38	46
152	03.09.2015	374,5	3	35	49
153	05.09.2015	120,5	1	34	53
154	06.09.2015	75,0	2	24	33
155	08.09.2015	44,7	1	34	45
156	09.09.2015	75,3	2	32	44
157	10.09.2015	60,0	1	33	55
158	11.09.2015	30,0	1	35	58
159	13.09.2015	29,8	1	32	40
160	04.10.2015	44,7	1	37	57
161	15.10.2015	30,2	1	35	30
162	18.10.2015	30,2	1	39	52
163	22.10.2015	30,2	1	27	22
164	23.10.2015	120,8	3	35	30
165	24.10.2015	679,4	3	32	22

Copyright © FirEURisk Consortium. All rights reserved.

166	26.10.2015	30,2	1	36	48
167	27.10.2015	60,4	1	38	48
168	30.10.2015	166,1	5	41	37
169	31.10.2015	90,6	3	42	40
170	01.11.2015	511,3	4	55	64
171	02.11.2015	29,9	1	47	60
172	06.11.2015	120,8	3	41	45
173	08.11.2015	44,8	1	32	37
174	12.07.2016	30,0	1	32	50
175	13.07.2016	45,0	1	33	47
176	14.07.2016	29,9	1	35	39
177	15.07.2016	90,1	1	32	53
178	18.07.2016	119,7	2	29	40
179	19.07.2016	59,8	1	30	36
180	23.07.2016	44,9	1	30	35
181	07.09.2016	45,1	1	38	56
182	08.09.2016	105,1	1	36	51
183	09.09.2016	90,3	1	35	43
184	10.09.2016	30,0	1	35	50
185	11.09.2016	60,1	2	37	47
186	13.09.2016	105,3	3	39	53
187	14.09.2016	45,1	1	38	62
188	17.09.2016	30,1	1	37	52
189	27.03.2017	74,1	1	44	47
190	09.04.2017	148,0	1	43	51
191	19.04.2017	29,6	1	44	44
192	16.08.2017	120,2	1	30	49
193	18.08.2017	75,1	1	35	51
194	20.08.2017	30,0	1	37	44
195	21.08.2017	90,4	1	34	37
196	22.08.2017	75,4	1	27	28
197	02.09.2017	177,4	2	32	45
198	03.09.2017	118,3	2	33	46
199	10.09.2017	44,3	1	33	47
200	24.03.2018	29,6	1	41	45
201	25.03.2018	118,3	2	43	45
202	26.03.2018	604,6	6	41	46
203	27.03.2018	687,7	11	38	40
204	28.03.2018	177,5	2	43	52
205	30.03.2018	648,9	8	31	32
206	31.03.2018	1745,1	8	29	34
207	04.04.2018	180,3	2	44	45
208	31.05.2018	29,9	1	30	41

Copyright © FirEURisk Consortium. All rights reserved.

209	03.08.2018	30,0	1	27	35
210	22.08.2018	59,3	1	31	40
211	23.08.2018	89,9	3	33	40
212	29.08.2018	44,6	1	28	46
213	31.08.2018	29,7	1	30	50
214	01.11.2018	180,2	2	32	38
215	01.04.2019	224,7	7	49	55
216	02.04.2019	255,4	5	47	51
217	03.04.2019	135,6	4	51	57
218	04.04.2019	629,7	9	50	56
219	05.04.2019	406,1	7	52	55
220	06.04.2019	663,2	8	50	54
221	07.04.2019	391,9	5	47	52
222	08.04.2019	211,0	4	44	53
223	09.04.2019	29,9	1	40	40
224	10.04.2019	45,2	1	41	46
225	11.04.2019	361,7	4	42	49
226	14.04.2019	60,2	2	44	49
227	23.04.2019	44,7	1	46	56
228	31.05.2019	29,8	1	26	26
229	05.06.2019	44,7	1	25	28
230	06.06.2019	44,7	1	26	33
231	09.06.2019	89,4	1	29	28
232	10.06.2019	29,8	1	28	39
233	11.06.2019	298,0	3	28	40
234	12.06.2019	29,8	1	30	37
235	14.06.2019	208,6	3	27	38
236	16.06.2019	59,6	1	30	44
237	27.06.2019	29,7	1	32	48
238	10.08.2019	90,7	1	30	38
239	12.08.2019	60,6	2	29	38
240	17.08.2019	75,7	1	28	60
241	19.08.2019	45,4	1	33	39
242	08.09.2019	30,1	1	34	42
243	11.09.2019	120,6	1	37	44
244	12.09.2019	163,9	2	37	40
245	19.09.2019	30,2	1	33	43
246	24.09.2019	30,2	1	39	45
247	25.09.2019	89,9	3	38	45
248	26.09.2019	60,4	1	27	32
249	27.09.2019	45,4	1	32	38
250	30.09.2019	104,2	2	37	46
251	02.10.2019	45,3	1	42	54

Copyright © FirEURisk Consortium. All rights reserved.

252	05.10.2019	29,8	1	37	48
253	06.10.2019	30,2	1	37	31
254	10.10.2019	60,4	1	37	57
255	12.10.2019	105,1	1	39	51
256	17.10.2019	30,0	1	40	49
257	21.10.2019	30,0	1	38	49
258	01.04.2020	630,5	16	47	47
259	02.04.2020	539,7	12	49	49
260	03.04.2020	2583,0	15	50	49
261	04.04.2020	4518,2	24	48	49
262	05.04.2020	585,8	9	48	51
263	06.04.2020	808,8	17	50	56
264	07.04.2020	1709,4	14	53	62
265	08.04.2020	4588,0	16	48	56
266	09.04.2020	5049,2	28	49	54
267	10.04.2020	5987,6	25	49	55
268	11.04.2020	4112,4	57	51	53
269	12.04.2020	3188,0	37	51	56
270	13.04.2020	3409,0	58	51	47
271	14.04.2020	2287,7	24	49	46
272	15.04.2020	4601,1	49	46	44
273	16.04.2020	5870,6	58	48	44
274	17.04.2020	5404,9	29	50	46
275	18.04.2020	2362,3	34	48	47
276	19.04.2020	1016,1	22	49	46
277	20.04.2020	898,0	18	45	45
278	21.04.2020	269,6	4	45	45
279	22.04.2020	59,9	2	48	53
280	23.04.2020	29,9	1	50	53
Total		119032,8	1331	38,6	48,4

According to the table, the average values of UDFHI in the burned areas for all seasons are 9.8% higher than for the entire area, which corresponds to a 25% excess. The ratio of the index values over the entire area and in the burned areas during different seasons of the year is also shown in Figure 56.

Copyright © FirEURisk Consortium. All rights reserved.

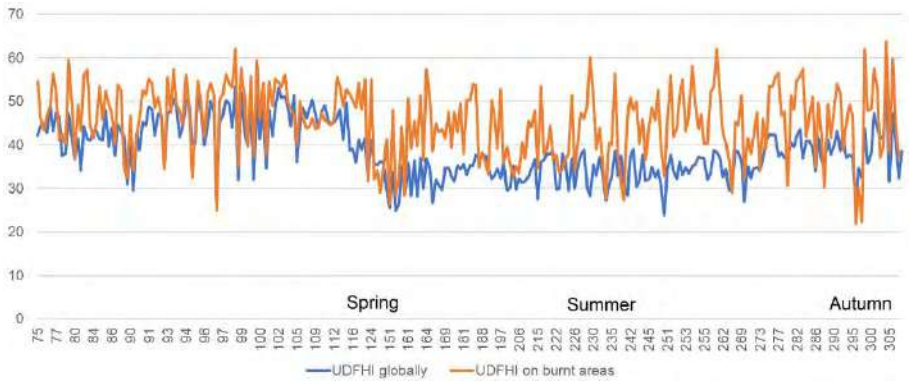


Figure 56 Comparison of UDFHI for the whole demonstration area and on burned areas over seasons during 11 year period.

In addition, the distribution of index values for the following ranges was estimated.

Table 38: Ranges of UDFHI

Number	Range of UDFHI values	Degree of fire danger
1	0-20	No hazard
2	20-40	Low Hazard
3	40-60	Medium hazard
4	>60	High hazard

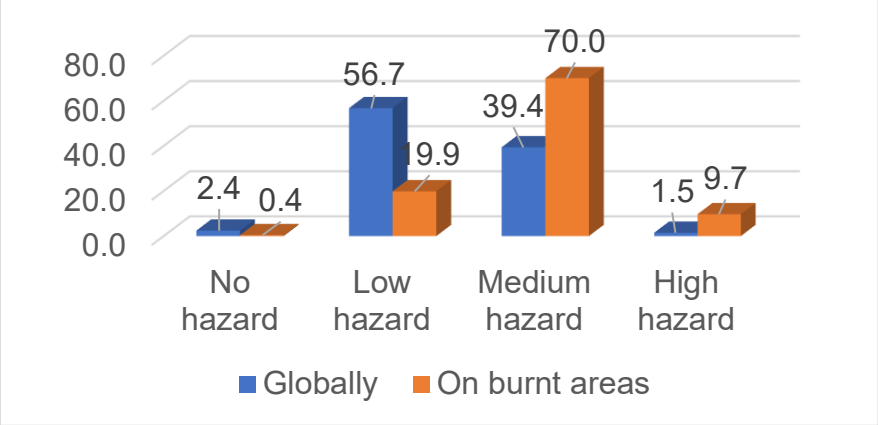


Figure 57: Distribution of the UDFHI on the entire area (left) and on burned areas (right) over seasons during 11 year period.

Copyright © FirEURisk Consortium. All rights reserved.

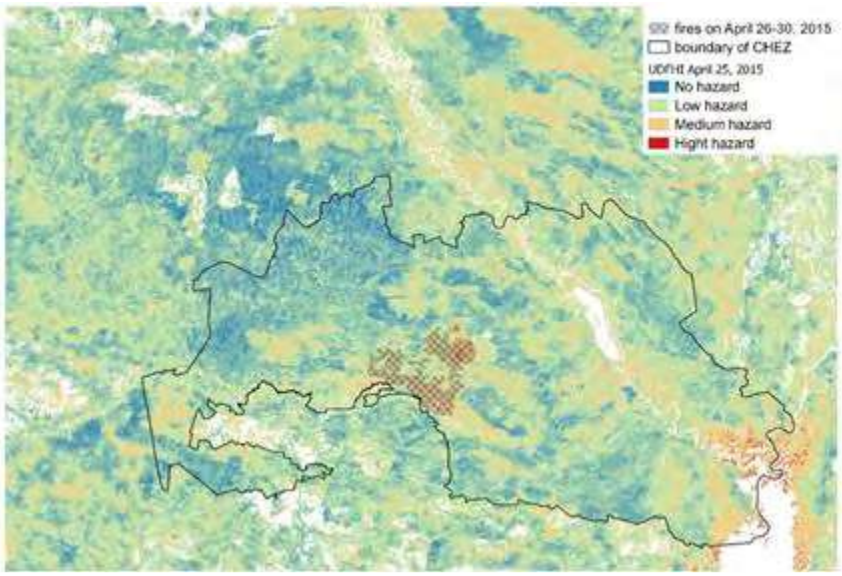


Figure 58: Map of UDFHI for April 25th, 2015 overlaid by fires during the following 5 days

On the figure besides UDFHI values polygons of fires happened from April 26 to 30, 2015 depicted by hatching. Even visually higher values of the index inside burned areas can be distinguished. On
fig. 7 numeric representation of the differences between values inside burned areas and the rest of the DA-15 is shown. Inside burned areas low hazard pixels are practically absent and part of medium hazard pixels almost 50 % more than on rest of the territory.

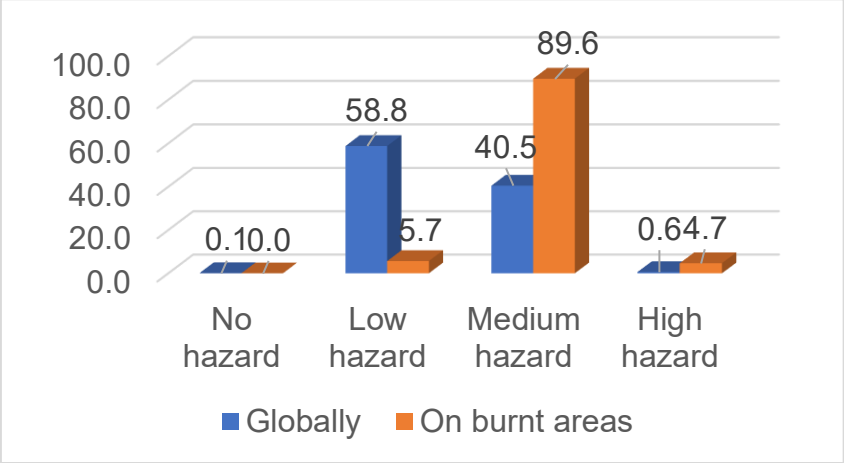


Figure 59: Distribution of the UDFHI on the entire area (left) and on burned areas (right) for the period from April 26 to 30, 2015.

In conclusion, completing the activity 1.1.1 of the project we estimated usability of the approach for estimating fire danger metric using remote sensing and meteorological data. Among a range of metrics Daily Fire Hazard Index was chosen and adapted to the peculiarities of the demonstration area. Despite the complexity and resource intensity of calculating this indicator, as well as the difficulties that arose during its validation, it was possible to obtain its values in the form of a series of images on an area of 16.5 thousand square km and over a time period of 11 years. The main criteria for estimating applicability of the index was comparing distribution of its values on the whole territory and inside burned areas in four ranges. As shown in the previous chapter count of pixels of medium and

Copyright © FirEURisk Consortium. All rights reserved.

high hazard ranges in burned areas 38.8 % more than on the whole area. This result is even more satisfying than 23% provided in (Laneve et al., 2020) for Sardinia in 2017.
However, it should be noted that the accuracy of determining the moisture content of dead fuel and extinction moisture content of different fuel types is still insufficient and requires further research.

8.4.1 Product Description: Fire danger index classification for Chernobyl Exclusion Zone

- **Format:** The Fire danger index classification for Chernobyl Exclusion Zone is a geospatial product in .tiff as is in qualitative units. The temporal coverage is from 2012 to 2022.
- **Resolution:** 1k and 500 m.
- **Description:** Calibration of fire danger index according to the last 10-year statistics of burned area gathered by MODIS in product MCD64A1, meteorological data and live-fuel moisture content.
- **Contact:** In case of doubts and/or suggestions, forward an email to Вадим Богомолов (ulabnit@gmail.com), Sergiy V. Zibtsev (sergiy.zibtsev@nubip.edu.ua).

Copyright © FirEUrisk Consortium. All rights reserved.

9. References

Albini, F. A.; Baughman, R. G. 1979. Estimating windspeeds for predicting wildland fire behavior. Res. Pap. INT-221. Ogden, Utah: U.S. Department of Agriculture, Forest Service, Inter- mountain Forest and Range Experiment Station. 12 p. - https://www.frames.gov/documents/behaveplus/publications/Albini_and_Baughman_1979_INT-RP-221_ocr.pdf

Alcasena, FJ, Ager, AA, Salis, M, Day, MA, Vega-Garcia, C (2018) Wildfire spread, hazard and exposure metric raster grids for central Catalonia. *Data in Brief* **17**, 1-5.

Allen, R. G., Pereira, L. S., Raes, D., & Smith, M. (1998). FAO Irrigation and Drainage Paper No. 56. Food and Agriculture Organization of the United Nations. https://www.researchgate.net/publication/345417517_FAO_Irrigation_and_Drainage_Paper_No_56

Andrews, Patricia L. 2012. Modeling wind adjustment factor and midflame wind speed for Rothermel's surface fire spread model. Gen. Tech. Rep. RMRS-GTR-266. Fort Collins, CO: U.S. Department of Agriculture, Forest Service, Rocky Mountain Research Station. 39 p. - https://gacc.nifc.gov/nwcc/content/products/fwx/publications/rmrs_gtr266.pdf

Andrews, Patricia L. 2014. Current status and future needs of the BehavePlus Fire Modeling System. International Journal of Wildland Fire 23(1):21-33.

Andrews, Patricia L. 2018. The Rothermel surface fire spread model and associated developments: A comprehensive explanation. Gen. Tech. Rep. RMRS-GTR-371. Fort Collins, CO: U.S. Department of Agriculture, Forest Service, Rocky Mountain Research Station - https://www.fs.usda.gov/research/treesearch/55928

Aragoneses Elena, Chuvieco Emilio and García Mariano (2022b), Product User Manual for the FirEURisk European fuel map, FiEURisk Internal Report, March 2022

Aragoneses Elena, Chuvieco Emilio, Garcia Mariano, Salis Michele, Ribeiro Luis Mario, and Vega Cristina (2022a), Definition of the fuel classification scheme, FiEURisk Internal Report, January 2022

Aragoneses, E, Chuvieco, E (2021) Generation and Mapping of Fuel Types for Fire Risk Assessment. *Fire* **4**, 59.

Aragoneses, E., M. García, M. Salis, L. M. Ribeiro, y E. Chuvieco. «Classification and mapping of European fuels using a hierarchical, multipurpose fuel classification system». Earth System Science Data 15, n.º 3 (2023): 1287-1315. https://doi.org/10.5194/essd-15-1287-2023.

Artes, T.; Oom, D.; de Rigo, D.; Durrant, T.; Maianti, P.; Libertà, G.; San-Miguel-Ayanz, J. A global wildfire dataset for the analysis of fire regimes and fire behaviour. *Sci. Data* **2019**, *6*.

Bugarić M., Alcasena F., Rodrigues Mimbrero M., Stipaničev D., Propagation potential - calculation methodology for Pilot Sites (PS), FirEURisk Report in WP 1.1.5, 2022

Burgan, R., Klaver, R., & Klaver, J. (1998). Fuel Models and Fire Potential From Satellite and Surface Observations. International Journal of Wildland Fire, 8(3), 159. https://doi.org/10.1071/WF9980159

Chuvieco Emilio, Viegas Domingos, Georgios Eftychidis (2022). Conceptual scheme for project integration, FiEURisk Internal Report, March 2022

Copernicus Climate Change Service (C3S) (2017): ERA5: Fifth generation of ECMWF atmospheric reanalyses of the global climate . Copernicus Climate Change Service Climate Data Store (CDS), date of access. https://cds.climate.copernicus.eu/cdsapp#!/home

Copyright © FirEURisk Consortium. All rights reserved.

Cunill Camprubí, À, González-Moreno, P, Resco de Dios, V (2022) Live Fuel Moisture Content Mapping in the Mediterranean Basin Using Random Forests and Combining MODIS Spectral and Thermal Data. Remote Sensing 14, 3162.

Diakakis, M.; Xanthopoulos, G.; Gregos, L. Analysis of Forest Fire Fatalities in Greece: 1977–2013. Int. J. Wildland Fire 2016, 25, 797–809.

Eftychidis, G. Mega-Fires in Greece (2007). In Encyclopedia of Natural Hazards; Bobrowsky, P.T., Ed.; Springer: Dordrecht, Netherlands, 2013; pp. 664–671. ISBN 978-1-4020-4399-4. Sustainability 2023, 15, 2498 14 of 16

Fernandes, A.P., Lopes, D., Sorte, S., Monteiro, A., Gama, C., Reis, J., Menezes, I., Osswald, T., Borrego, C., Almeida, M., Ribeiro, L.M., Viegas, D.X., Miranda, A.I., 2022. Smoke emissions from the extreme wildfire events in central Portugal in October 2017. Int. J. Wildl. Fire 1–13. https://doi.org/10.1071/WF21097

Finney, MA (2002) Fire growth using minimum travel time methods. Canadian Journal of Forest Research 32, 1420-1424.

Finney, MA PL Andrews, BW Butler (Eds) (2006) 'An overview of FlamMap fire modeling capabilities, Fuels Management-How to Measure Success. Proceedings RMRS-P-41.' Fort Collins, CO, 28–30 March. (USDA Forest Service, Rocky Mountain Research Station: Fort Collins, CO). Available at http://www.fs.fed.us/rm/pubs/rmrs_p041/rmrs_p041_213_220.pdf

Fosberg, M. A. (1977). Forecasting the 10-Hour Timelag Fuel Moisture. U.S. Department of Agriculture, Forest Service, Rocky Mountain Forest and Range Experiment Station, 187.

Haines, D.A. A lower atmospheric severity index for wildland fire. Natl. Weather Dig. 1988, 13, 23–27.

Hazeleger, W.; Severijns, C.; Semmler, T.; Ştefănescu, S.; Yang, S.; Wang, X.; Wyser, K.; Dutra, E.; Baldasano, J.M.; Bintanja, R.; et al. EC-Earth: A Seamless Earth-System Prediction Approach in Action. Bull Am Meteorol Soc 2010, 91, 1357–1364, doi:10.1175/2010BAMS2877.1.

Hersbach, H. et al. The ERA5 global reanalysis. Q. J. R. Meteorol. Soc. 2020, 146, 1999–2049.

Huemmrich K., The geosail model: a simple addition to the sail model to describe discontinuous canopy reflectance, Remote Sensing of Environment, 75 (2001), pp. 423–431

Idescat. (2022). Instituto de Estadística de Cataluña. Obtenido de Generalidad de Cataluña: https://www.idescat.cat/

IGN, 2018. Base Topográfica Nacional 1:25.000 (BTN25). Instituto Geográfico Nacional. Ministerio de Fomento, Gobierno de España, Madrid.

Krsnik, G, Busquets Olivé, E, Piqué Nicolau, M, Larrañaga, A, Cardil, A, García-Gonzalo, J, González Olabarría, JR (2020) Regional Level Data Server for Fire Hazard Evaluation and Fuel Treatments Planning. Remote Sensing 12, 4124.

Laneve, G., Pampanoni, V., & Uddien Shaik, R. (2020). The Daily Fire Hazard Index: A Fire Danger Rating Method for Mediterranean Areas. Remote Sensing, 12(15), 2356. https://doi.org/10.3390/rs12152356

Lang, N., Jetz, W., Schindler, K., & Wegner, J. D. (2022). A high-resolution canopy height model of the Earth. arXiv preprint arXiv:2204.08322 https://doi.org/10.48550/arXiv.2204.08322

López, A. S., San-Miguel-Ayanz, J., & Burgan, R. E. (2002). Integration of satellite sensor data, fuel type maps and meteorological observations for evaluation of forest fire risk at the pan-European scale. International Journal of Remote Sensing, 23(13), 2713–2719. https://doi.org/10.1080/01431160110107761 p. 102354.

Pampanoni V., G. Laneve and G. Santilli, Evaluating Sentinel-3 Viability for Vegetation Canopy Monitoring and Fuel Moisture Content Estimation, IGARSS 2022 - 2022 IEEE International Geoscience and

Copyright © FirEURisk Consortium. All rights reserved.

Remote Sensing Symposium, 17-22 July 2022, https://doi.org/10.1109/IGARSS46834.2022.9884150

Pettinari M. L. and Chuvieco E., Fire Behavior Simulation from Global Fuel and Climatic Information, Forests 2017, 8, 179 - https://www.mdpi.com/1999-4907/8/6/179

Pettinari, M. L. (2015): Global Fuelbed Dataset. Department of Geology, Geography and Environment, University of Alcala, Spain, PANGAEA - https://doi.pangaea.de/10.1594/PANGAEA.849808

Pettinari, M.L.; Chuvieco, E. Generation of a global fuel data set using the Fuel Characteristic Classification System. Biogeosciences 2016, 13, 2061–2076. - https://bg.copernicus.org/articles/13/2061/2016/

Politi, N.; Vlachogiannis, D.; Sfetsos, A.; Nastos, P.T. High Resolution Projections for Extreme Temperatures and Precipitation over Greece. Clim Dyn 2022, doi:10.1007/s00382-022-06590-w.

Politi, N.; Vlachogiannis, D.; Sfetsos, A.; Nastos, P.T. High-Resolution Dynamical Downscaling of ERA-Interim Temperature and Precipitation Using WRF Model for Greece. Clim. Dyn. 2021, 57, 799–825. https://doi.org/10.1007/S00382-021-05741-9.

Prichard, S.J., Kennedy, M.C., Wright, C.S., Cronan, J.B., Ottmar, R.D., 2017. Predicting forest floor and woody fuel consumption from prescribed burns in southern and western pine ecosystems of the United States. For. Ecol. Manage. 405, 328–338. https://doi.org/10.1016/j.foreco.2017.09.025

Prikaziuk E. and C. van der Tol, Global sensitivity analysis of the scope model in Sentinel-3 bands: thermal domain focus, Remote sensing, 11 (2019), p. 2424.

Probeck, M, Ruiz, I, Ramminger, G, Fourie, C, Maier, P, Ickerott, M, Storch, C, Homolka, A, Muller, SJ, Tiwari, H, Stumpf, A, Chun, S, Mattos, C, Lindmayer, A, Jahangir, F, Endara, P, Berndt, F, Dohr, M, Kapferer, W, Schleicher, C, Ralser, S, Innerbichler, F, Riffler, M, Siklar, M, Aifantopoulou, D, Paralykidis, S, Pinet, C, Jaffrain, G, di Federico, A, Corsi, M, Langanke, T, Dufourmont, H (2021) CLC+ Backbone: Set the Scene in Copernicus for the Coming Decade. 2076-2079.

Qin, X., Zhang, Z., Li, Z., & Yi, H. (2008). Forecasting method of nationak-level forest fire risk rating (Q. Tong, Ed.; p. 712317). https://doi.org/10.1117/12.816205

Quan X., M. Yebra, D. Riaño, B. He, G. Lai, and X. Liu, Global fuel moisture content mapping

Remote Sensing of Environment, 113 (2009), pp. 2403–2411.

Resco de Dios, V, Fellows, AW, Nolan, RH, Boer, MM, Bradstock, RA, Domingo, F, Goulden, ML (2015) A semi-mechanistic model for predicting the moisture content of fine litter. Agricultural and Forest Meteorology 203, 64-73.

Resco de Dios, V. et al. A semi-mechanistic model for predicting the moisture content of fine litter. Agric. For. Meteorol. 2015, 203, 64–73.

Riahi, K.; Rao, S.; Krey, V.; Cho, C.; Chirkov, V.; Fischer, G.; Kindermann, G.; Nakicenovic, N.; Rafaj, P. RCP 8.5-A Scenario of Comparatively High Greenhouse Gas Emissions. Clim. Chang. 2011, 109, 33–57. https://doi.org/10.1007/S10584-011-0149-Y/FIGURES/12.

Riccardi, C.L.; Ottmar, R.D.; Sandberg, D.V.; Andreu, A.; Elman, E.; Kopper, K.; Long, J. The fuelbed: A key element of the Fuel Characteristic Classification System. Can. J. For. Res. 2007, 37, 2394–2412. - https://www.frames.gov/documents/catalog/spa/riccardi_ottmar_sandberg_andreu_elman_kopper_long_inpress.pdf

Rodrigues, M, De la Riva, J (2014) An insight into machine-learning algorithms to model human-caused wildfire occurrence. Environmental Modelling and Software 57, 192-201.

Copyright © FirEURisk Consortium. All rights reserved.

Rodrigues, M.; Cunill Camprubí, À.; Balaguer-Romano, R.; Coco Megía, C.J.; Castañares, F.; Ruffault, J.; Fernandes, P.M.; Resco de Dios, V. Drivers and Implications of the Extreme 2022 Wildfire Season in Southwest Europe. Sci. Total Environ. 2023, 859, 160320.

Rothermel, Richard C. 1972. A mathematical model for predicting fire spread in wildland fuels. Res. Pap. INT-115. Ogden, UT: U.S. Department of Agriculture, Intermountain Forest and Range Experiment Station- https://www.fs.usda.gov/treesearch/pubs/32533

Rovithakis, A.; Grillakis, M.G.; Seiradakis, K.D.; Giannakopoulos, C.; Karali, A.; Field, R.; Lazaridis, M.; Voulgarakis, A. Future Climate Change Impact on Wildfire Danger over the Mediterranean: The Case of Greece. Environ. Res. Lett. 2022, 17, 045022. https://doi.org/10.1088/1748-9326/ac5f94.

Scott, J. H. (2012) Introduction to Wildfire Behavior Modeling, National Interagency Fuels, Fire & Vegetation Technology Transfer - http://pyrologix.com/wp-content/uploads/2014/04/Scott_20121.pdf

Scott, J. H.; Burgan, R. E. Standard fire behavior fuel models: a comprehensive set for use with Rothermel's surface fire spread model, Gen. Tech. Rep. RMRS-GTR-153. U.S. Department of Agriculture, 72 p. 2005. - https://www.fs.usda.gov/rm/pubs_series/rmrs/gtr/rmrs_gtr153.pdf

Scott, JH, Burgan, RE (2005) Standard fire behavior fuel models: a comprehensive set for use with Rothermel's surface fire spread model. USDA Forest Service, Rocky Mountain Research Station Gen. Tech. Rep. No. RMRS-GTR-153, Fort Collins, CO. Available at http://treesearch.fs.fed.us/pubs/9521.

Scott, Joe H. 2007. Nomographs for estimating surface fire behavior characteristics. Gen. Tech. Rep. RMRS-GTR-192. Fort Collins, CO: U.S. Department of Agriculture, Forest Service, Rocky Mountain Research Station. 119 p. - https://www.fs.usda.gov/research/treesearch/27177

Sexton, J. O., Song, X.-P., Feng, M., Noojipady, P., Anand, A., Huang, C., Kim, D.-H., Collins, K.M., Channan, S., DiMiceli, C., Townshend, J.R.G. (2013). Global, 30-m resolution continuous fields of tree cover: Landsat-based rescaling of MODIS Vegetation Continuous Fields with lidar-based estimates of error. International Journal of Digital Earth, 130321031236007. doi:10.1080/17538947.2013.786146.

Skamarock, W.C.; Skamarock, W.C.; Klemp, J.B.; Dudhia, J.; Gill, D.O.; Barker, D.M.; Wang, W.; Powers, J.G. A Description of the Advanced Research WRF Version 3. NCAR Technical Note -475+STR. 2008.

Stipaničev, D. & Bugarić, M (2023) Dead Fuel Moisture Content in Wildfire Propagation Potential Estimation for Split-Dalmatia County, to be presented on SplitTech 2023 – Wildfire Track, June 2023, Split, Croatia

Susan J. Prichard, David V. Sandberg, Roger D. Ottmar, Ellen Eberhardt, Anne Andreu, Paige Eagle, Kjell Swedin, Fuel Characteristic Classification System version 3.0: technical documentation, Gen. Tech. Rep. PNW-GTR-887. Portland, OR: U.S. Department of Agriculture, Forest Service, Pacific Northwest Research Station. 79 p., 2013 - https://www.fs.usda.gov/research/treesearch/45283

Tesfa, T. K., Leung, L. R., & Ghan, S. J. (2020). Exploring topography-based methods for downscaling subgrid precipitation for use in Earth System Models. Journal of Geophysical Research: Atmospheres, 125, e2019JD031456. https://doi.org/10.1029/2019JD031456

Turner, J.A and Lawson, B.D., Weather in the Canadian Forest Fire Danger rating System – A User guide to National standards and practices, Pacific Forest Research Center, BC-X-177, May 1978. - https://cfs.nrcan.gc.ca/pubwarehouse/pdfs/1843.pdf

Van Vuuren, D.P.; Edmonds, J.; Kainuma, M.; Riahi, K.; Thomson, A.; Hibbard, K.; Hurtt, G.C.; Kram, T.; Krey, V.; Lamarque, J.-F.; et al. The Representative Concentration Pathways: An Overview. Clim. Chang. 2011, 109, 5. https://doi.org/10.1007/s10584-011-0148-z.

Van Wagner, C.E.; Pickett, T.L. Equations and FORTRAN Program for the Canadian Forest Fire Weather Index System; 1985;

Copyright © FirEURisk Consortium. All rights reserved.

Varela, V.; Sfetsos, A.; Vlachogiannis, D.; Gounaris, N. Fire Weather Index (FWI) Classification for Fire Danger Assessment Applied in Greece. Tethys J. Weather. Clim. West. Mediterr. 2018, 15, 31–40. https://doi.org/10.3369/tethys.2018.15.03.

Vlachogiannis, D.; Sfetsos, A.; Markantonis, I.; Politi, N.; Karozis, S.; Gounaris, N. Quantifying the Occurrence of Multi-Hazards Due to Climate Change. Applied Sciences 2022, 3, doi:10.3390/app12031218.

Yebra M., E. Chuvieco, Linking ecological information and radiative transfer models to estimate

Urls:

Copernicus EMS: Copernicus Emergency Management Service | Copernicus EMS—Mapping. Available online: https://emergency.copernicus.eu/mapping/list-of-components/EMSR300 (accessed on 29 November 2022).

Mati wildfire: Deadly Fire at Mati Still Haunts Greece Three Years Later. Available online: https://greekreporter.com/2021/07/23/deadlywildfire-at-mati-still-haunts-greece-two-years-later/ (accessed on 29 November 2022).

North Evia wilfire: BBC News. Greece Wildfires: Evia Island Residents Forced to Evacuate—BBC News. Available online: https://www.bbc.com/news/world-europe-58141336 (accessed on 29 November 2022).

HNMS Climatology, Hellenic National Meteorological Service Available online: http://www.emy.gr/emy/en/climatology/climatology (accessed on 29 November 2022).

Copyright © FirEUrisk Consortium. All rights reserved.